The Total Synthesis of Parvineostemonine and Studies Toward the Synthesis of Pepluacetal

Doctoral thesis for obtaining the academic degree

Doctor of Natural Science (Dr.rer.nat.)

submitted by

Christa Gerlinger

at the

Universität Konstanz

Faculty of Sciences

Department of Chemistry

Konstanz, 2020

Date of the oral examination: 24 July 2020

1. Reviewer: Prof. Dr. Tanja Gaich

2. Reviewer: Prof. Dr. Andreas Marx

3. Reviewer: Prof. Dr. Rainer Winter

Meiner Familie und Marcel

“Leicht ist das Leben für keinen von uns. Doch was nützt das, man muß Ausdauer haben und vor allem Zutrauen zu sich selbst. Man muß daran glauben, für eine bestimmte Sache begabt zu sein, und diese Sache muss man erreichen, koste es was es wolle.“

Marie Curie

Parts of this thesis have been presented at scientific conferences:

TOCUS Stuttgart, 13.10.2017, Universität Stuttgart

Oral Presentation: „Enantiodivergent Total Synthesis of Parvineostemonine“

ACS-National Meeting & Exposition, 19.-23.08.2018, Boston

Oral Presentation: “Enantiodivergent Total Synthesis of Parvineostemonine”

ORCHEM Berlin, 10.-12.09.2018, Freie Universität Berlin

Poster Presentation: “Enantiodivergent Total Synthesis of Parvineostemonine”

Publications discussed in this thesis:

C. K. G. Gerlinger, S. Krüger, T. Gaich, Total Synthesis of Parvineostemonine by Structure Pattern Recognition: A Unified Approach to Stemona and Sarpagine Alkaloids, *Chem. Eur. J.* **2018**, *24*(16), 3994-3997.

H. Rebmann, **C. K. G. Gerlinger**, T. Gaich, Gram-Scale Total Syntheses of Sarpagine Alkaloids and non-Natural Derivatives, *Chem. Eur. J.* **2018**, *25*(11), 2704-2707. (Hot Paper)

C. K. G. Gerlinger, T. Gaich, Structure Pattern Based Total Synthesis, *Chem. Eur. J.* **2019**, *25*(46), 10782-10791.

Further Publications not discussed in this thesis:

T. Huber, T. A. Preuhs, **C. K. G. Gerlinger**, T. Magauer, Development of a ß-C-H Bromination Approach Towards the Synthesis of Jerantinine E, *J. Org. Chem*. **2017**, *82*, 7410-7419.

Abstract

I.

The enantiodivergent total synthesis of the *Stemona* alkaloid parvineostemonine (**V**) was accomplished in 11 isolated steps (13 chemical transformations) starting from bissulfoxide **I** and pyridinium betaine **II**. In this synthetic route a 3-oxidopyridinium [5+2] cycloaddition reaction enabled the construction of a regioisomeric mixture (**III** and **IV**). After separation of the regioisomers both enantiomers of the natural product (+)-parvineostemonine and (–)-parvineostemonine, can be accessed.

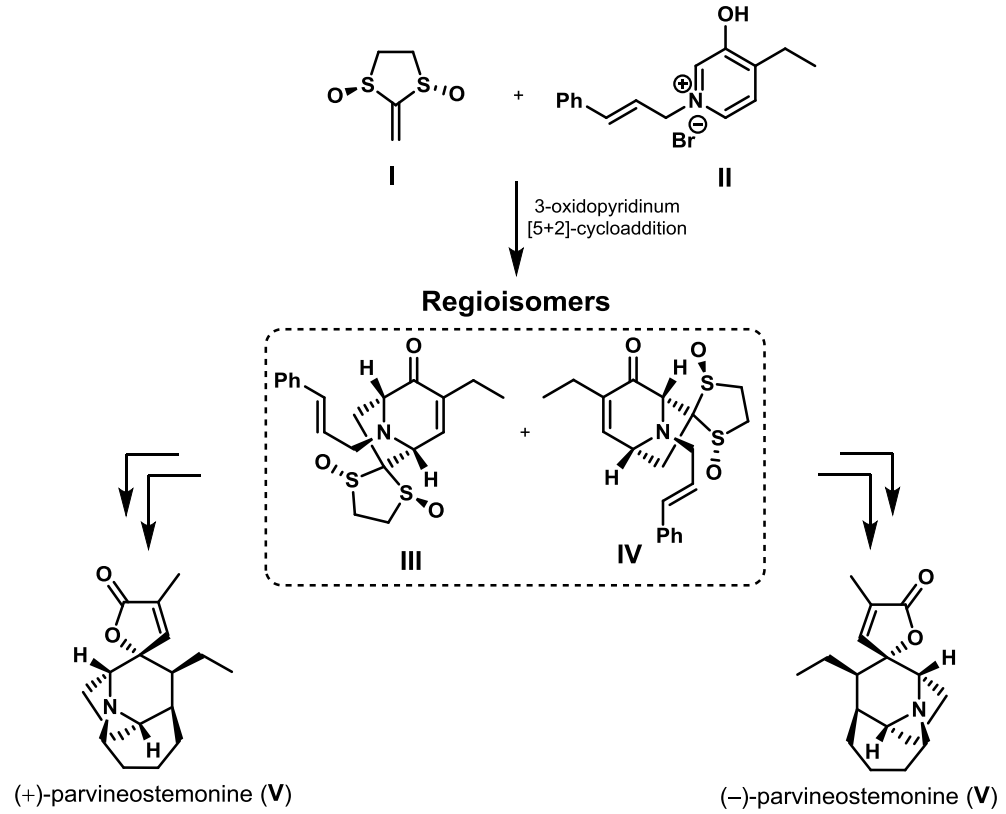

Scheme A. Enantiodivergent total synthesis of (+)-parvineostemonine (**V**) and (–)-parvineostemonine (**V**).

II.

Studies toward the total synthesis of the *Euphorbia peplus* diterpenoid pepluacetal (**XII**) are described in the second part of this thesis. The first elaborated route commences with the preparation of methyl ester **VII** which was further converted to olefin **IX** via stereoselective olefination with phosphonamide **VIII**. Subsequent nucleophilic 1,2-addition with cyclopentene

building block **X** realized the construction of highly functionalized key intermediate **XI**. Moreover, studies to advance precursor **XI** to the natural product are presented.

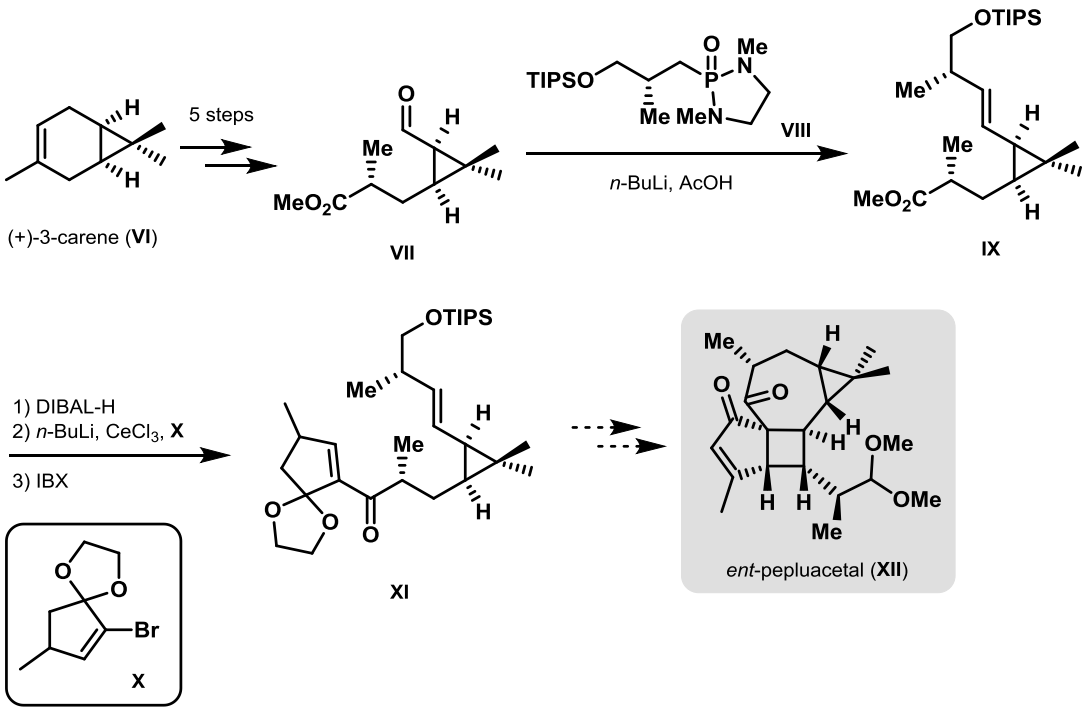

Scheme B. Synthesis of key intermediate XI.

The second synthetic approach toward the natural product pepluacetal (**XII**) started with the synthesis of vinyl triflate **XIII** and vinyl bromide **XV**. After elaboration of a robust synthesis of side chain **XVIII**, investigations to introduce **XVIII** are demonstrated. Furthermore, studies to advance key intermediates **XIV** and **XVI** to the natural product are presented.

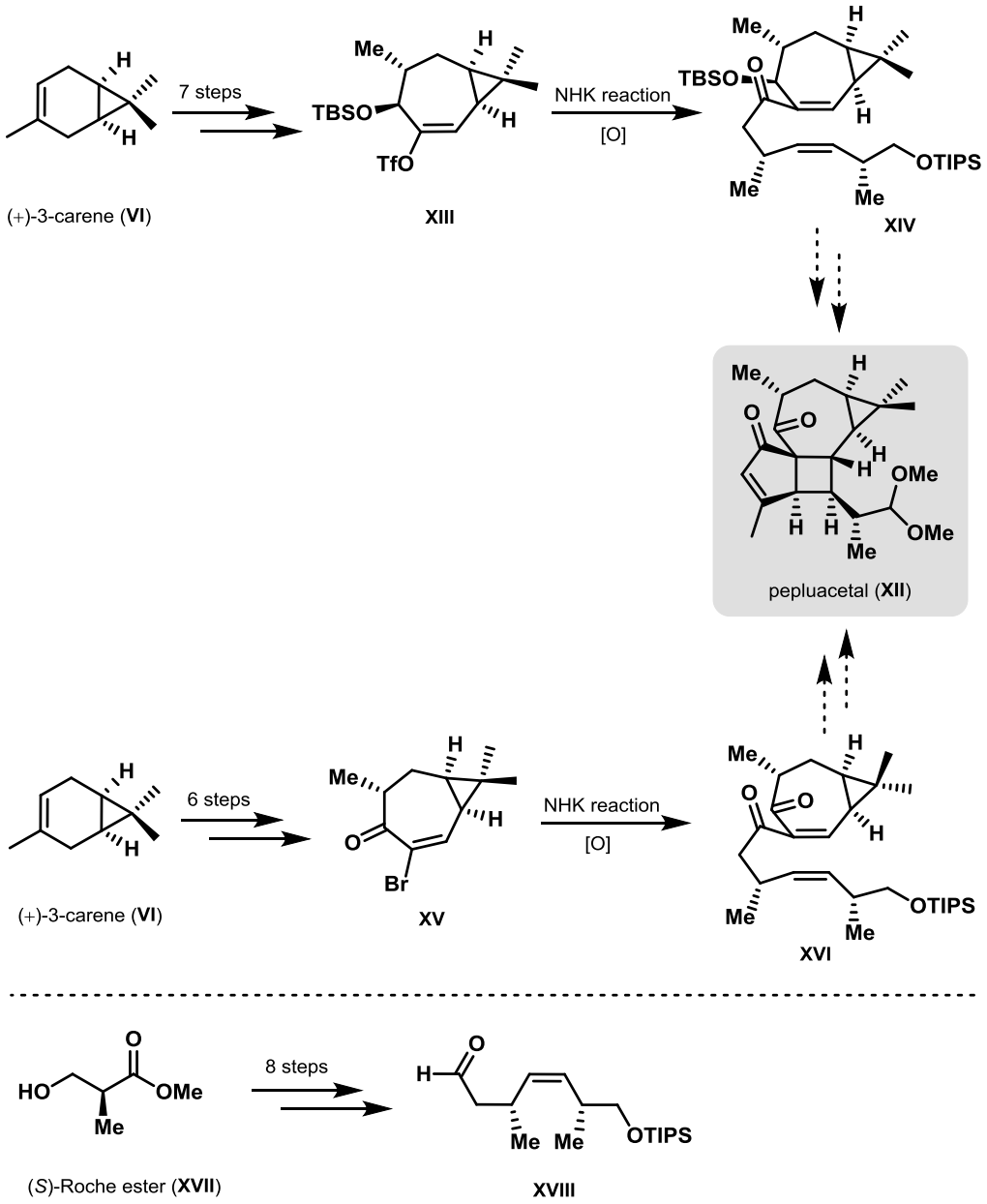

Scheme C. Synthesis of key intermediates XIV and XVI, and side chain XVIII.

Zusammenfassung

I.

Die enantiodivergente Totalsynthese des *Stemona* Alkaloids Parvineostemonine wurde ausgehend von Bissulfoxid **I** und Pyridinium Betain **II** in 11 isolierten Stufen (13 chemische Transformationen) durchgeführt. Eine 3-Oxidopyridinium [5+2] Cycloaddition ermöglichte den Aufbau einer Mischung aus den Regioisomeren **III** und **IV**. Nach Trennung der Regioisomere konnten beide Enantiomere des Naturstoffs, (+)-Parvineostemonine (**V**) und (–)-Parvineostemonine (**V**), hergestellt werden.

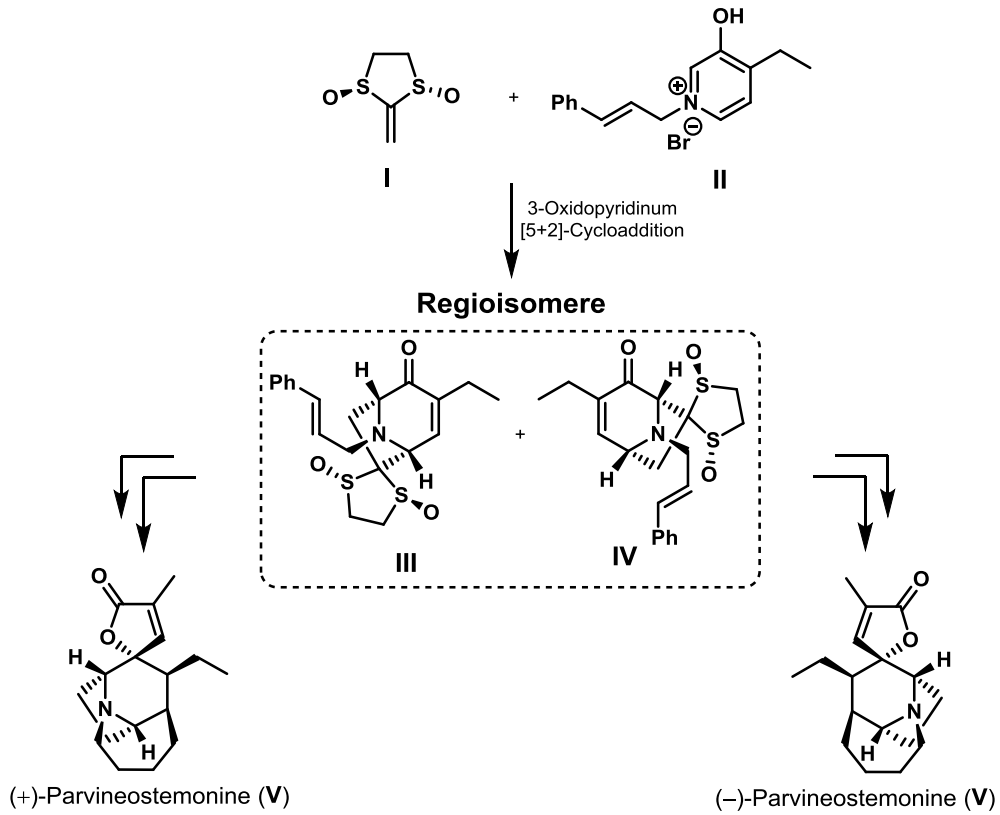

Schema A. Enantiodivergente Totalsynthese von (+)-Parvineostemonine (V) und (−)-Parvineostemonine (V).

II.

Im zweiten Teil dieser Doktorarbeit werden Studien zur Totalsynthese des *Euphorbia peplus* Diterpenoids Pepluacetal (**XII**) beschrieben. Die erste ausgearbeitete Route beginnt mit der Herstellung von Methylester **VII**, welcher anschließend mittels stereoselektiver Olefinierung mit Phosphonamide **VIII** zu Olefin **IX** umgesetzt wurde. Eine anschließende nukleophile 1,2-Addition mit Cyclopentene Baustein **X** realisierte den Aufbau des hochfunktionalisierten Schlüsselintermediates **XI**. Des Weiteren werden Studien zu dem Versuch, die Vorstufe **XI** in den Naturstoff umzuwandeln, präsentiert.

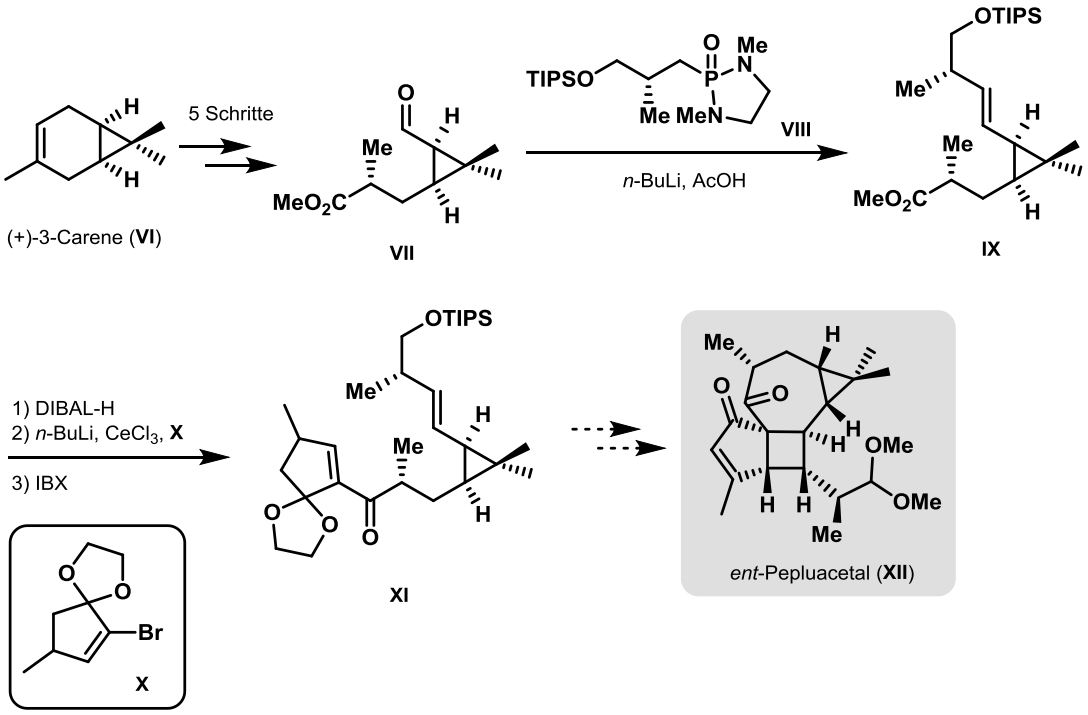

Schema B. Enantioselective Synthese des Schlüsselintermediates XI.

Die zweite synthetische Methode den Naturstoff Pepluacetal (**XII**) herzustellen beginnt mit der Synthese von Vinyltriflat **XVIII** und Vinylbromid **XV**. Nach dem Ausarbeiten einer robusten Synthese der Seitenkette **XVIII** werden Versuche diese einzubringen diskutiert. Des Weiteren werden Studien aufgezeigt, die Schlüsselintermediate **XIV** und **XVI** in den Naturstoff **XII** umzuwandeln.

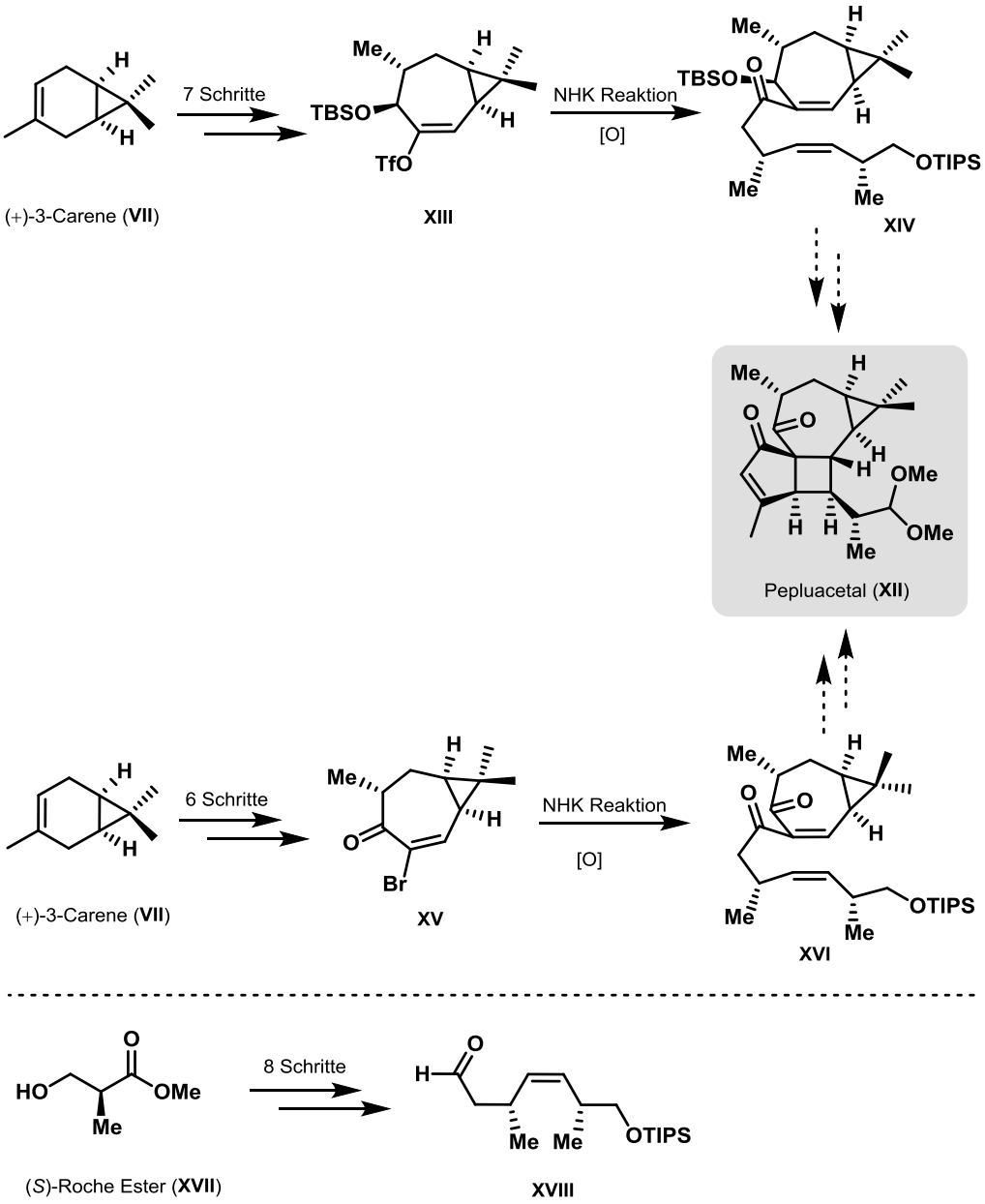

Schema C. Synthese der Schlüsselintermediate XIV und XVI, sowie der Seitenkette XVIII.

List of Abbreviations

°C	degrees Celsius
δ	chemical shift in ppm downfield relative to a standard
Ac	acetyl
ACN	1,1´-azobis(cyclohexanecarbonitrile)
AIBN	1,1′-azobis(isobutyronitrile)
Ar	undefined aryl substituent
ATR	attenuated total reflection (IR)
9-BBN	9-borabicyclo[3.3.1]nonane
Bn	benzyl
Bu	butyl
Bz	benzoyl
brsm	based on recovered starting material
Calcd	calculated
CAM	ceric ammonium molybdate(IV)
CAN	ceric ammonium nitrate
cat.	catalytic
CCDC	Cambridge Crystallographic Data Centre
CDI	Carbonyldiimidazole
cod	1,5-cyclooctadiene
COSY	correlation spectroscopy
dba	dibenzylideneacetone
DDQ	2,3-dichloro-5,6-dicyano-1,4-benzoquinone
DIBAl-H	diisobutylaluminium hydride
DIPA	*N*,*N*-diisopropylamine
DIPEA	*N*,*N*-diisopropylethylamine (Hünig's base)
DMAP	4-dimethylaminopyridine
DMF	dimethyl formamide
DMP	Dess−Martin Periodinan
DMPU	1,3-dimethyl-3,4,5,6-tetrahydro-2(1*H*)-pyrimidinone
DMSO	dimethyl sulfoxide
dppf	1,1’-bis(diphenylphosphino)ferrocene
d.r.	diastereomeric ratio
ee	enantiomeric excess
EI	electron ionization
equiv	equivalent(s)

Et	ethyl
ESI	electrospray ionization
e.g.	*exempli gratia* (for example)
g	gram
GGPP	geranylgeranyl diphosphate
h	hour(s)
HMBC	heteronuclear multiple bond correlation
HMDS	hexamethyldisilazide
HMPA	hexamethylphosphoramide
HPLC	high-pressure liquid chromatography
HR-MS	high resolution mass spectrometry
HSQC	heteronuclear single quantum correlation
Hz	Hertz
i-	*iso*
IC_{50}	half maximal inhibitory concentration
IR	infrared spectroscopy
IUPAC	International Union of Pure and Applied Chemistry
J	coupling constant
LDA	lithium diisopropylamide
m-CPBA	*meta*-chloroperbenzoic acid
Me	methyl
MIC	minimal inhibitory concentration
Min	minutes
mL	milliliter
mmol	millimole
MOM	methoxymethyl acetal
MMPP	Magnesium monoperoxyphthalat
MsCl	mesylsulfonyl chloride
NBS	*N*-bromosuccinimide
NMO	*N*-methylmorpholine-*N*-oxide
NMR	nuclear magnetic resonance
NOESY	nuclear Overhauser effect correlation spectroscopy
p	*para*
PCC	Pyridinium chlorochromate
PDC	Pyridinium dichromate
Pd/C	palladium on charcoal
PG	protecting group

Ph	phenyl
PIDA	phenyliodine(III) diacetate
PMB	*para*-methoxybenzyl
ppm	parts per million
Pr	propyl
py	pyridine
quant.	quantitative
Red-Al	sodium bis(2-methoxyethoxy)aluminium hydrid
R*f*	retardation factor (TLC)
ROESY	Rotating frame Overhauser enhancement spectroscopy
SPhos	2-dicyclohexylphosphino-2',6'-dimethoxybiphenyl
T	temperature
t	time
t-	*tert*
TBAF	tetrabutylammonium fluoride
TBS	*tert*-butyldimethylsilyl
TEBAC	Benzyltriethylammonium chloride
TEMPO	2,2,6,6-Tetramethylpiperidinyloxid
Tf	trifluoromethanesulfonyl
TFA	trifluoroacetic acid
TFAA	trifluoroacetic anhydride
THF	tetrahydrofuran
TIPS	triisopropylsilyl
TLC	thin layer chromatography
TMEDA	tetramethylethylenediamine
TMS	trimethylsilyl
TPAP	tetrapropylammonium perruthenate
Ts	tosyl
UV	ultraviolet
wt%	weight percent

Table of Contents

I The Parvineostemonine Project

1 Introduction

1.1. Natural Products

Natural products have been used in traditional medicine for thousands of years due to their unique effects on living organisms. These secondary metabolites play an important role in the discovery and development of new pharmaceutical drugs. From the 1940s to 2014, 49% of all approved anti-cancer agents worldwide were "*either natural products or directly derived therefrom*".[1] As a result, synthetic chemists are constantly searching for efficient and creative ways to synthesize natural products. However, their structural complexity poses a significant challenge resulting in lengthy and low-yielding routes with only few milligrams of the final target. To overcome the supply issue and also allow rapid derivatization, natural product synthesis remains one of the most powerful tools for improvement.

1.2 *Stemona* Alkaloids

Among natural products that have been marketed as drugs the class of alkaloids plays a very important role in new chemical entities. These structurally diverse compounds are produced by a variety of organisms interacting with several molecular targets and thus exhibiting a wide range of biological activities. Based on their unique structural features and intriguing biological activities, alkaloids are interesting and attractive targets for natural product synthesis and development of new pharmaceutical compounds. In 2001 it was found that nearly 50% of natural products derived drugs were based on alkaloids.[2]

Within the alkaloids, natural products belonging to the *Stemona* family are equally distinguished with a vast structural and biological diversity. This genus has been isolated from the monocotyledonous family *Stemonacea* together with *Stichoneuron* and *Croomia*, and is mainly distributed in the southeast of Asia. (–)-Tuberostemonine (**1**) (Figure 1) was the first *Stemona* alkaloid being isolated in 1934[3] and 85 years later over 200 additional congeners are reported and summarized in the most recent review by Greger et al.[4]

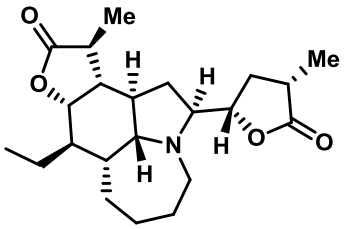

(–)-tuberostemonine (**1**)

Figure 1. First isolated *Stemona* alkaloid.

The biological activity of the *Stemona* alkaloids covers an unusually broad range which can be ascribed to their large structural diversity. Crude extracts from these plants have been used especially in traditional Chinese and Japanese medicine for respiratory treatments such as bronchitis, pertussis and tuberculosis.[5] But also applications as insecticides or antihelminthics, demonstrate the great field of application.[6] The therapeutic effect of the crude extracts of *Stemona* plants can be attributed to special components within this genus. Therefore, the hunt for therapeutically active members, the investigation of their biological activity and realization of their synthetic access is of high interest for academia and industry. An overview of different classification approaches, investigations on biosynthetic origins and biological activities of the *Stemona* alkaloid family will be discussed in the following.

1.2.1 Classifications

There have been many attempts to find a unified structural classification system for *Stemona* alkaloids, but due to their large diversity no general approach could be reported so far. The structural classifications that exist are either based on chemical perspectives (Pilli et al. 2010)[7] or biosynthetic considerations (Greger et al. 2006/2019[4], Wang and Chen 2014[8]).

Pilli and co-workers classified the *Stemona* alkaloids based on their structural features.[7] They characterized these alkaloids by the presence of a pyrrolo-[1,2-*a*]-azepine or a pyrido-[1,2-*a*]-azepine core (**2**) and organized them into eight groups (Figure 2). Stenine (I, **3**), stemoamide (II, **4**), tuberostemospironine (III, **5**), stemonamine (IV, **6**), parvistemoline (V, **7**) and stemofoline (VI, **8**) all containing the pyrrolo[1,2-*a*]azepine core, stemocurtisine (VII, **9**) bearing the pyrido-[1,2-*a*]-azepine skeleton and a miscellaneous group (VIII) including those alkaloids lacking the structural characteristics or being the only representatives of their group. Their review covered 97 members of the *Stemona* alkaloids between the years 1999 and 2009. Since then many new structures have been isolated and identified, and new classification systems have been published.

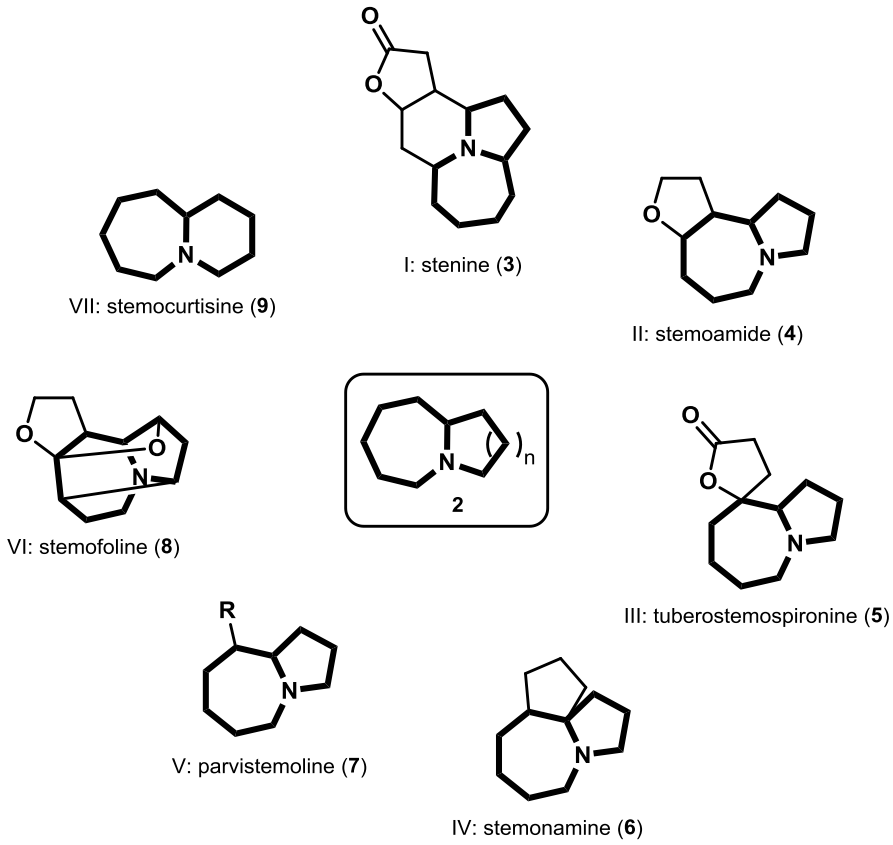

Figure 2. Classification of *Stemona* alkaloids by Pilli et al.[7]

In 2014, Wang and Chen divided the *Stemona* alkaloids into two main classes based on their biosynthetic origin from either L-ornithin or glutamic acid (see chapter 1.2.2).[8] These classes consist of the hemiterpenoid pyrrolidines (**10**-**13**) and the monoterpenoid pyrrolidines (**14**, **15**) (Figure 3) which are further subdivided into 14 types.

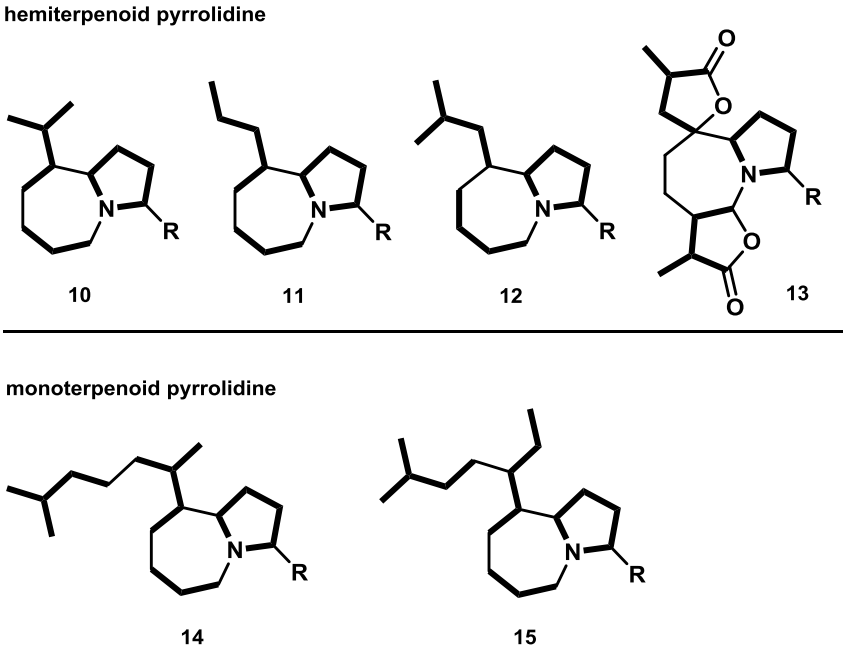

Figure 3. Classification of *Stemona* alkaloids by Wang and Chen.[8]

The division into different types is explained by the fact that these alkaloids consist of at least one monoterpene or hemiterpene unit, a pyrrolidine part and a linear carbon bond.[8]

Also based on biosynthetic considerations, Greger and co-workers published the most recent method in 2019 with an updated count of 215 *Stemona* alkaloids (Figure 4).[4] They reinvestigated their work from 2006[9] claiming the *Stemona* alkaloids being "*characterized by a pyrrolo-[1,2-a]-azepine core (ring A&B) usually linked with two α-methyl-γ-butyrolactone rings (C&D)*"[4]. Additionally supported by chemotaxonomic studies within the genus *Stemona*[10][11][12][13], they divided them into three skeletal types with different substitution patterns at C-9: the croomine-type (**16**), the stichoneurine-type (**18**) and the protostemonine-type (**19**).

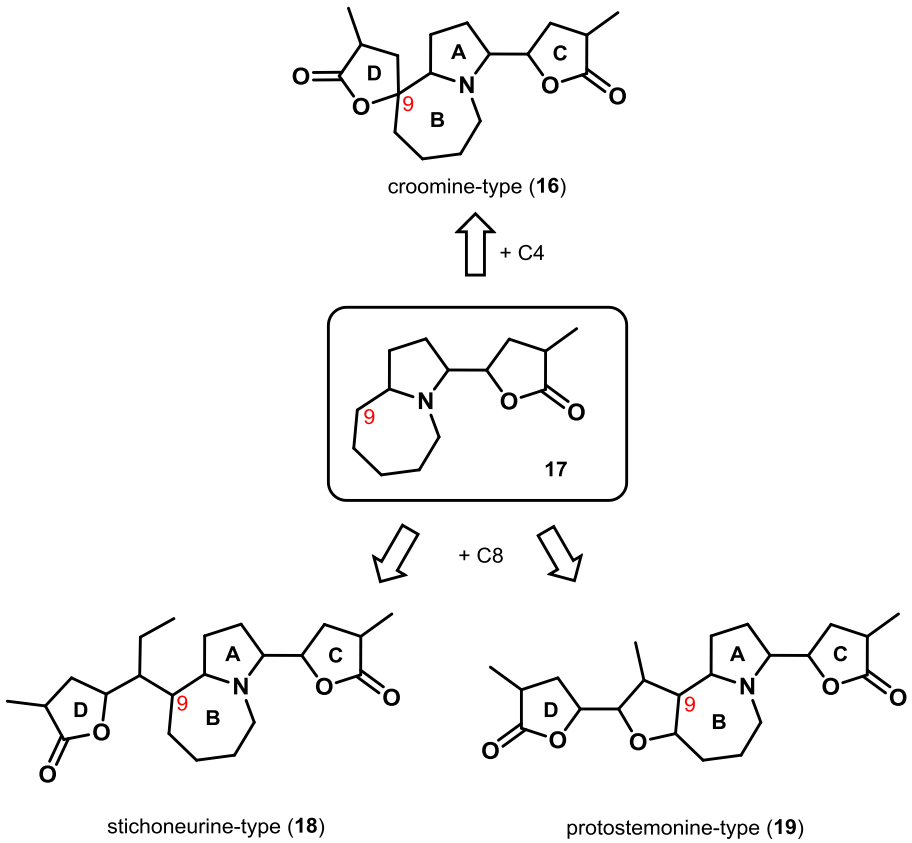

Figure 4. Classification of *Stemona* alkaloids by Greger et al.[4]

1.2.2 Biosynthesis

Until today there exist only few publications on biosynthetic investigations of *Stemona* alkaloids, which make a detailed biosynthetic discussion difficult. Therefore, this chapter only presents a short summary about so far proposed investigations.

In 2004, Seger and co-workers proposed a concept including the relationships between the pyrrolo-[1,2-*a*]-azepine skeleton and the pyrrolidine-type alkaloids.[14] Based on their classification system (see in chapter 1.2.1), they state pyrrolo-azepine core **24** as the smallest common structure for the majority of structure types of *Stemona* alkaloids. As shown in Scheme 1, they propose substructure **24** deriving from spermidine (**22**) (originating from L-ornithine (**20**) via putrescine (**21**)) and three isoprene units, with two of the isoprenoid carbon atoms incorporated into the seven-membered ring and one isoprene unit is used to build the α-methyl-γ-lactone side chain. Additionally, they propose cyclization and incorporation of the side chain proceeding via nucleophilic additions.

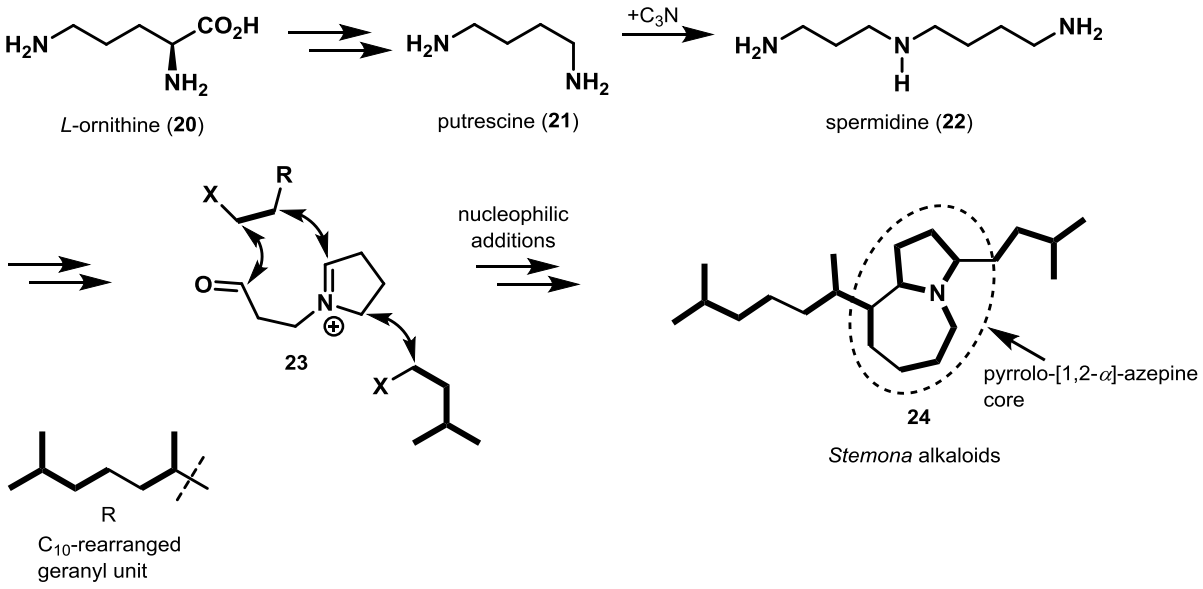

Scheme 1. Proposed biosynthetic pathway of *Stemona* alkaloids containing a pyrrolo-[1,2-*a*]-azepine by Seger and co-workers.

Five years later, the group of Greger and co-workers published a proposed biosynthesis of the *Stemona* alkaloid croomine (**29**) (Scheme 2).[15] According to the classification system of Greger croomine (**29**) is one of the three main skeletal types of the *Stemona* alkaloids, therefore the suggested biosynthetic pathway will be shortly discussed in the following. They proposed pandanamine (**28**) as common precursor due to the fact that this structure was indeed found during the isolation process of **29**. They propose pandanamine (**28**) deriving from intermediate **27** which in turn is build starting from spermidine (**22**). Following addition of leucine (**26**) to **22** and an oxidative process should form **27**. Decarboxylation, loss of ammonia and loss of water further give precursor pandanamine **28**. Ensuing cyclization processes should yield croomine (**29**).

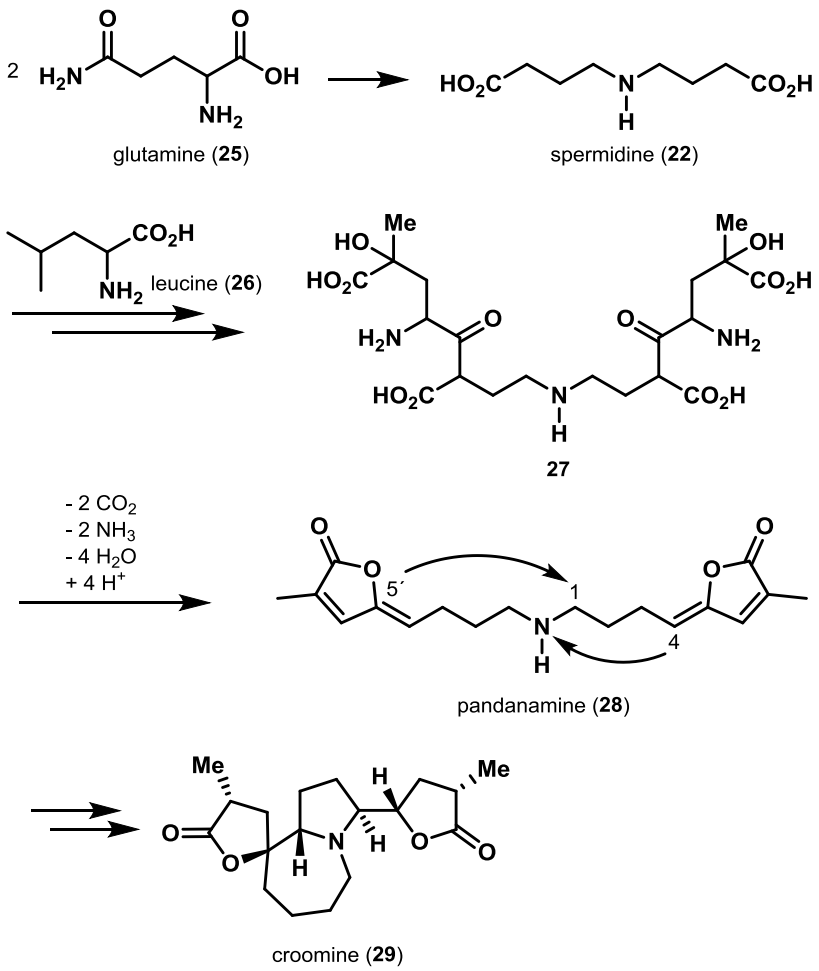

Scheme 2. Proposed biosynthetic pathway of croomine (29) by Greger and co-workers.

Scheme 3 represents the biosynthetic pathway for *Stemona* alkaloids containing a pyrido-[1,2-*a*]-azepine core, proposed by Pyne and co-workers.[16] They suggest that four equivalents of acetate form precursor **30** which undergoes condensation with diamine **31** (originating from putrescine (**21**) and spermidine (**22**)) to yield intermediate iminium ion **32**. Stereoselective reduction and oxidation of iminium ion **32** should obtain intermediate **34**, which could provide pyrido-[1,2-*a*]-azepine containing alkaloids after coupling with a geranyl unit (**33**).

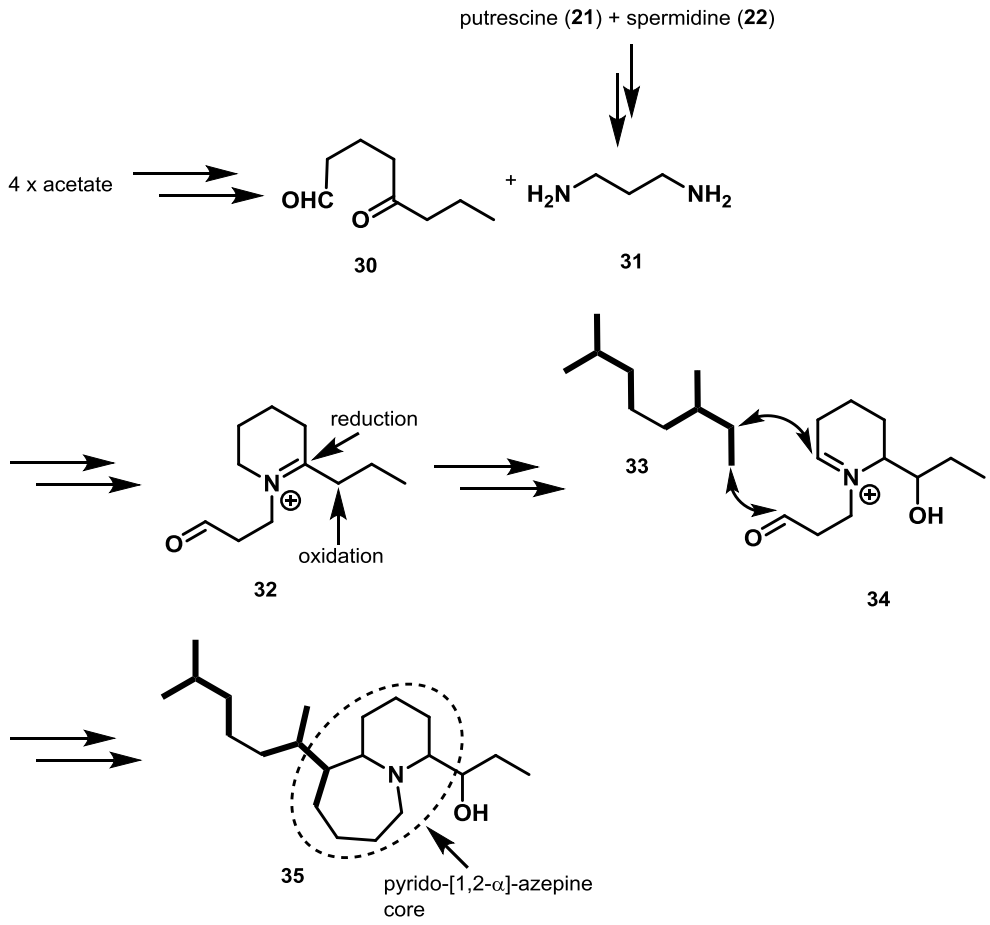

Scheme 3. Proposed biosynthetic pathway of *Stemona* alkaloids containing a pyrido-[1,2-*a*]-azepine core by Pyne and co-workers.

The most recent and detailed publication was released by Wang and Chen in 2014.[8] They based their consideration on the work by Seger and co-workers, dividing the *Stemona* alkaloids in three main structures consisting of a pyrrolo- or pyrido-[1,2-*a*]-azepine core, and a indolizidine core (Figure 5). These nuclei consist of three building blocks: 1) a pyrrolidine- or piperidine unit, 2) a C_3- or C_4- unit, and 3) either a C_2- or a C_1- unit deriving from the C_5-isoprene or C_{10}-geranyl unit and their rearranged derivates. The pyrrolidine moiety is supposed to derive from L-ornithine (**20**) as well as the C_4-unit. The piperidine ring may origin from the ring expansion of a pyrrolidine unit or the participation of a 4-α-methyl-μ-lactone moiety. The C_1-unit may be derived from a C_5-isoprene and a C_2-unit from malonyl-SCoA. The C_3-unit is proposed to arise from either glutamic acid (**40**) or 2-oxoglutaric acid (Figure 5).

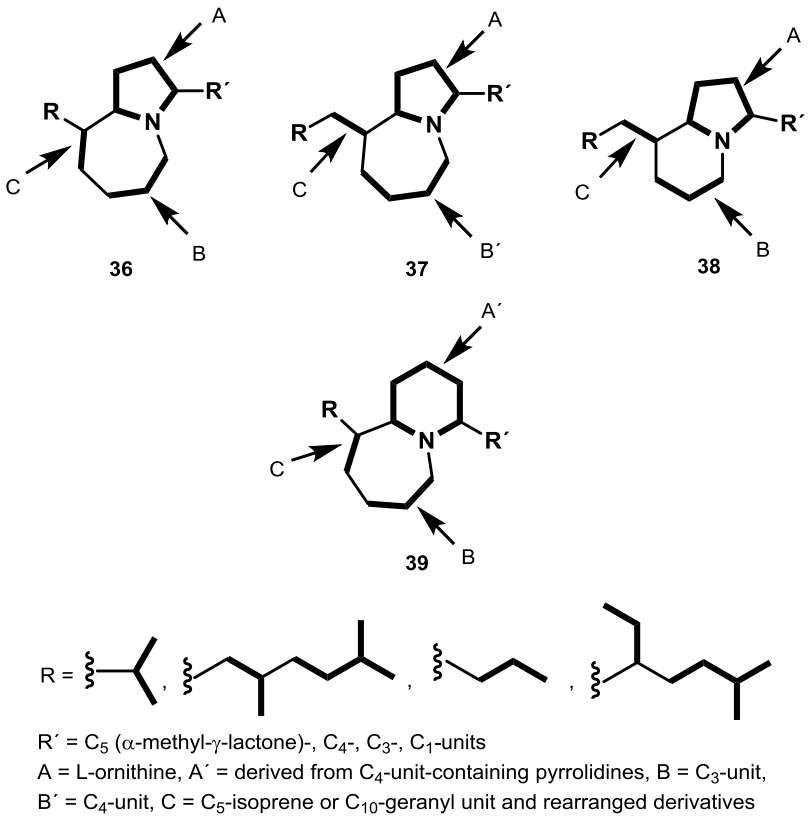

Figure 5. Proposed biosynthetic building blocks of *Stemona* alkaloids by Weng and Chen.

For the biosynthesis of *Stemona* alkaloids of structure **41** they propose a pathway via L-ornithine (**20**), glutamic acid (**40**) and hemi/mono-terpenes (Scheme 4a). For the construction of the indolizidine core **43** the building blocks may be originated from the same precursors, L-ornithine (**20**) and glutamic acid (**40**). The only difference lies in the participation of a C_1-unit (from a hemiterpene) in the construction of the piperidine ring (Scheme 4b). Alkaloids of structure **45** are supposed to derive from two equivalents of L-ornithine (**20**) and a hemiterpene (Scheme 4c). For the pyrido-[1,2-*a*]-azepine core, some skeletons may be derived from rearranged pyrrolo-[1,2-*a*]-azepine cores. The rest of these structures might originate from decarboxylation of the 4-α-methyl-γ-lactone moiety and following ring expansion (Scheme 4d).

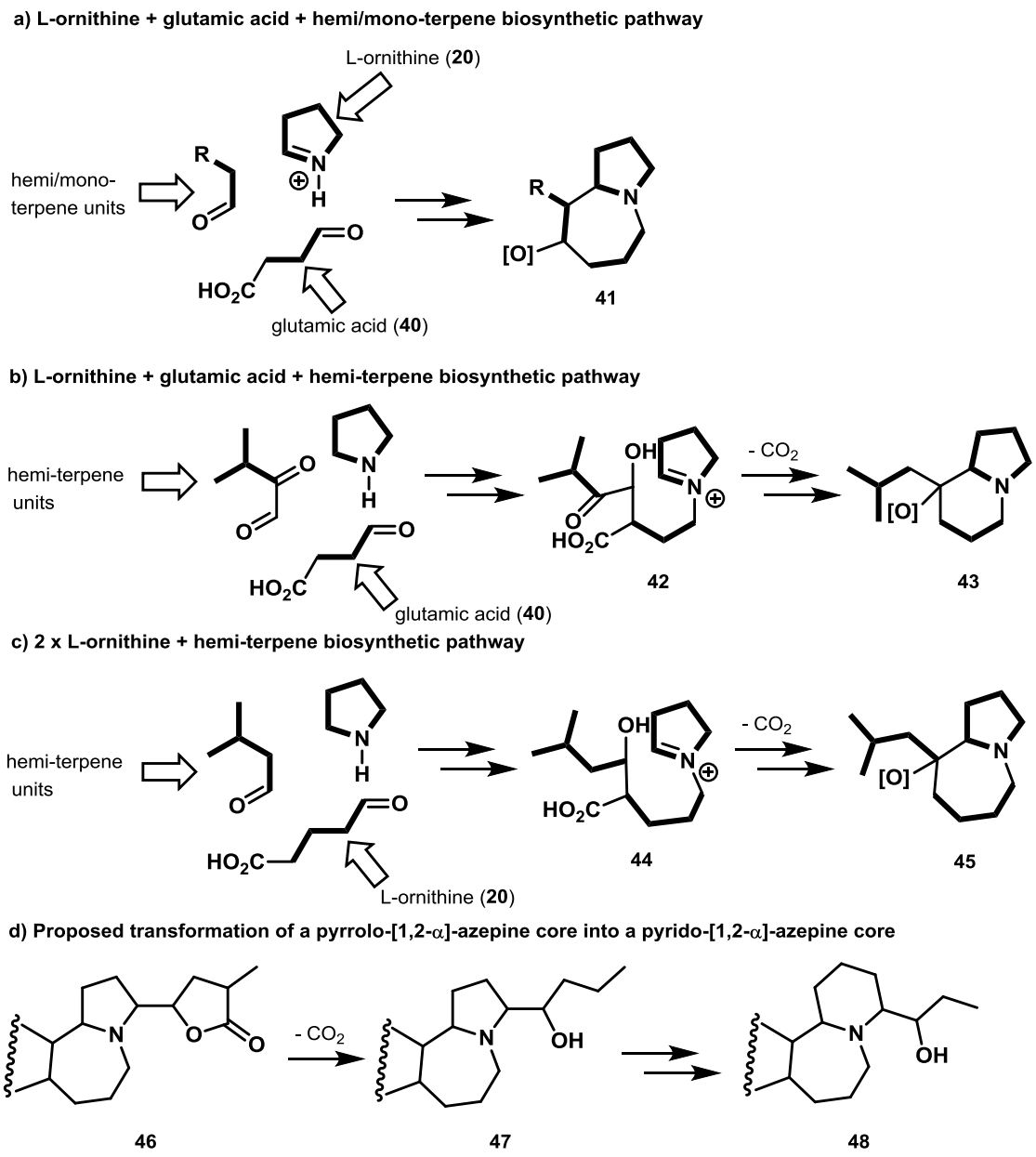

Scheme 4. Proposed biosynthesis of *Stemona* alkaloids core structures by Wang and Chen.

1.2.3 Bioactivity

The roots of several *Stemona* species are widely used as insecticides and for medicinal purpose. Especially the extensive use of *Stemona* roots as bio-insecticides is an important part among the bioactivities of this genus.[9] The insecticidal activity of various *Stemona* alkaloids was investigated e.g. **1** [17][18], **49**[17][19] and **50**[6][20] (Figure 6).

Antitussive activity was found in the roots of *Stemona tuberosa*, *S. japonica* and *S. sessilifolia* which are of special importance in traditional Chinese medicine (e.g. **51**, **52**) (Figure 6).[4] *Stemona tuberosa* additionally showed antitumoral activity.[21]

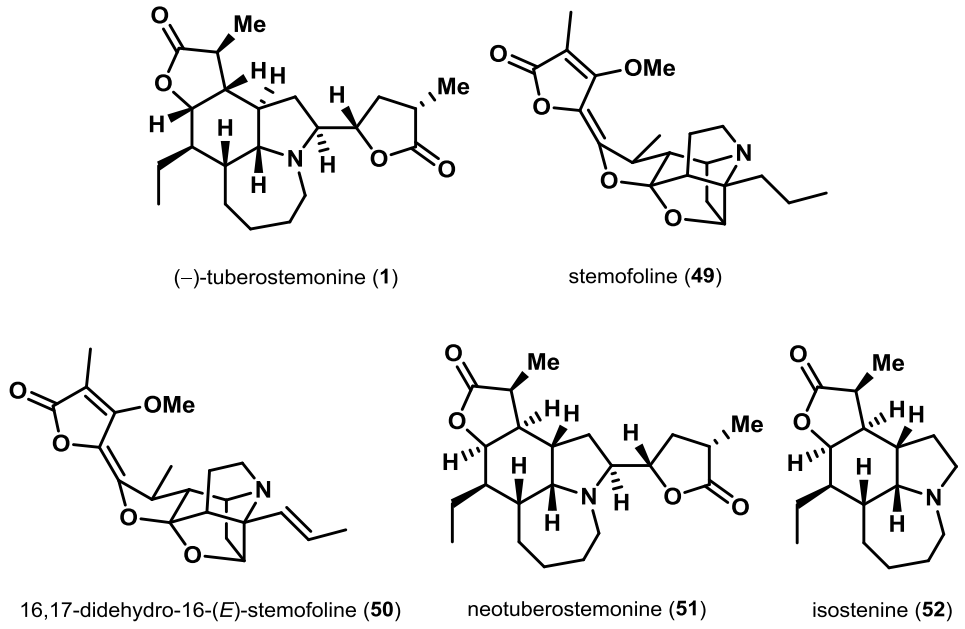

Figure 6. Biological active *Stemona* alkaloids.

1.3 *Stemona* Alkaloid Parvineostemonine

1.3.1 Isolation and Structural Characterization

Parvineostemonine (**53**) belongs to the family of *Stemona* alkaloids and was isolated in 2003 from the stems and leaves of the *Stemona parviflora* plant, collected in the Hainan province of China.[22] Ye and co-workers obtained parvineostemonine (**53**) as a slightly yellow amorphous solid which reacts positively to Dragendorff`s reagent. The structure was determined by UV, IR, HREIMS, 1D- and 2D-NMR spectra analysis. Additionally, the absolute configuration was confirmed by NOESY spectra analysis. Parvineostemonine (**53**) bears a unique spirotetracyclic structure (Figure 7). The central piperidine moiety (ring C) is fully substituted and contains five all-carbon contiguous stereogenic centers. The five-membered pyrrolidine moiety (ring B) is connected in a bridgehead fashion between C-3 and C-9 and seven-membered ring A also spans across the piperidine moiety introducing additional ring strain into the system. The butenolide moiety (ring D) is spiro-annulated to ring C.

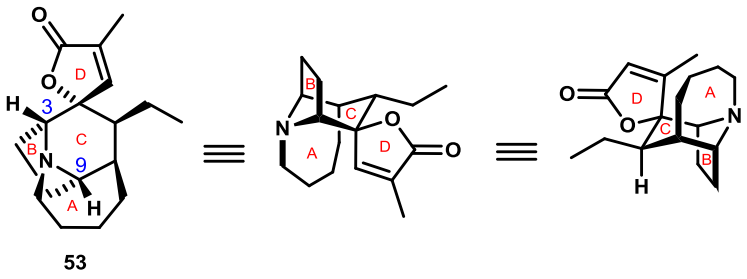

Figure 7. Different representations of the *Stemona* alkaloid parvineostemonine (53).

1.3.2 Literature known Approaches

Four years after the isolation of parvineostemonine (**53**), Li and co-workers published the first synthetic approach.[23] They investigated the construction of tropinone based alkaloids via a highly stereoselective [4+3] cycloaddition of *N*-substituted pyrroles with allenamide-derived nitrogen-stabilized chiral oxallyl cations (Scheme 5). This was realized by introducing electron-withdrawing groups to the pyrrole unit (**56**) and very slow addition of DMDO at low temperatures to favor the epoxidation of the allenamide (**54**) over the pyrrole-moiety (**56**).

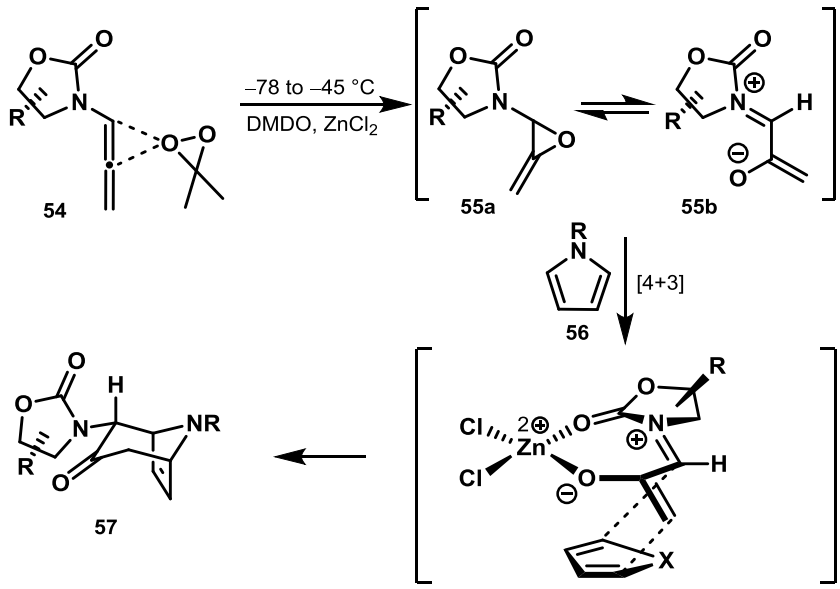

Scheme 5. Tropinone synthesis via [4+3] cycloaddition reaction by Li and co-workers.[23]

This method was applied in the construction of the *aza*-tricyclic core of parvineostemonine (**53**) (Scheme 6). With cycloadduct **60** in hand they first removed the remaining double bond via hydrogenation. Following removal of the Boc-group led to amine **61** in good yield. *N*-Allylation and subsequent allylation in α-position of the carbonyl gave diene **63**. Construction of the bridged seven-membered ring was then realized via ring-closing metathesis using Grubbs 1st generation catalyst. Unfortunately, from this point the group wasn't successful to advance intermediate **64** to the natural product.

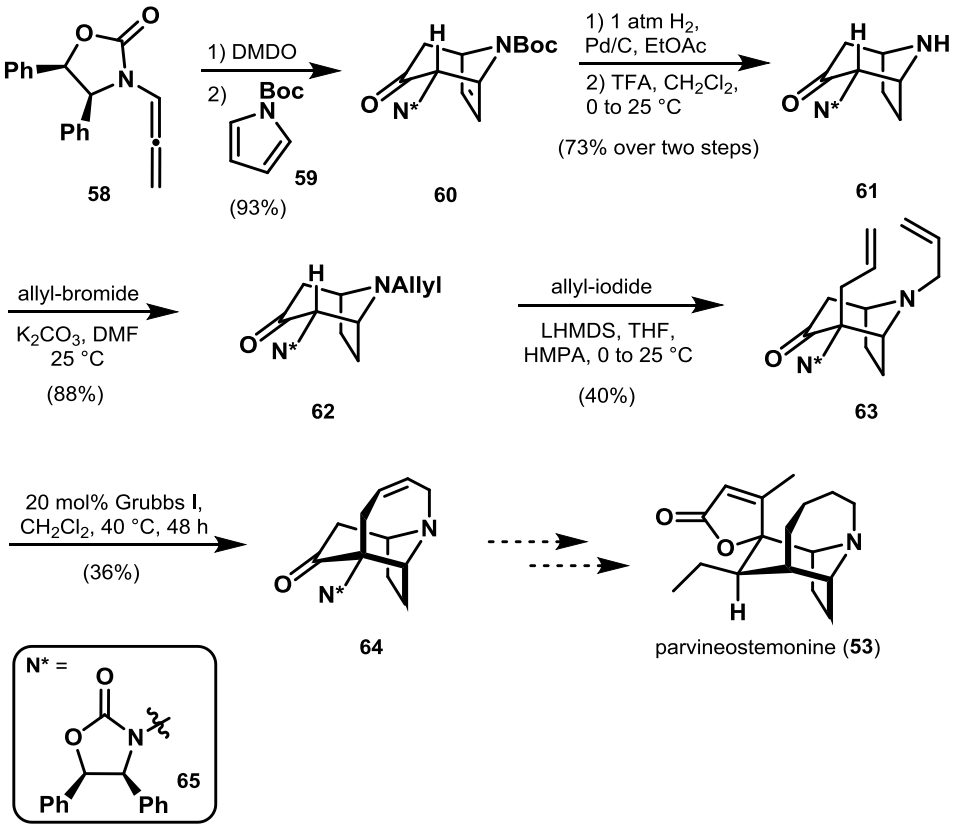

Scheme 6. Racemic approach towards parvineostemonine (53) by the Li group.[23]

The first completed total synthesis of parvineostemonine (**53**) was reported two years later in 2009 by Tu and co-workers (Scheme 7).[24] Their synthesis also commenced with a tropinone derivative as starter unit. After demethylation of tropinone **66** they obtained ammonium salt **67** which was further converted to amide **68** by treatment with 4-chlorobutyryl chloride. Subsequent α-hydroxylation, followed by hydrolyzation with hydrochloric acid gave α-hydroxy ketone **69** diastereoselectively. Dess-Martin Periodinan (DMP) oxidation and treatment with triflic anhydride afforded vinyl triflate **70**. Via Suzuki cross-coupling reaction they installed the ethyl side chain and following Finkelstein reaction to iodide **72** set the stage for the construction of caged tricyclic amide **73**. This key transformation was realized via radical-mediated 7-*exo*-trig cyclization using tributyltin hydride and 1,1′-azobis(cyclohexanecarbonitrile) (ACN) as an initiator. Beside amide **73**, the epimer of *epi*-**73** was obtained. Equilibration of *epi*-**73** to **73** was realized under basic conditions. The installation of the spiro-annelated butenolide was accomplished by reacting *epi*-**73** with ethyl (2-bromomethyl)acrylate and zinc powder in 78% yield diastereoselectively. After isomerization of the *exo*-cyclic double bond with $RhCl_3$-catalyst, lactone **77** was transformed into a thioamide and final reduction using Raney-Nickel afforded (±)-parvineostemonine (**53**) in high yield.

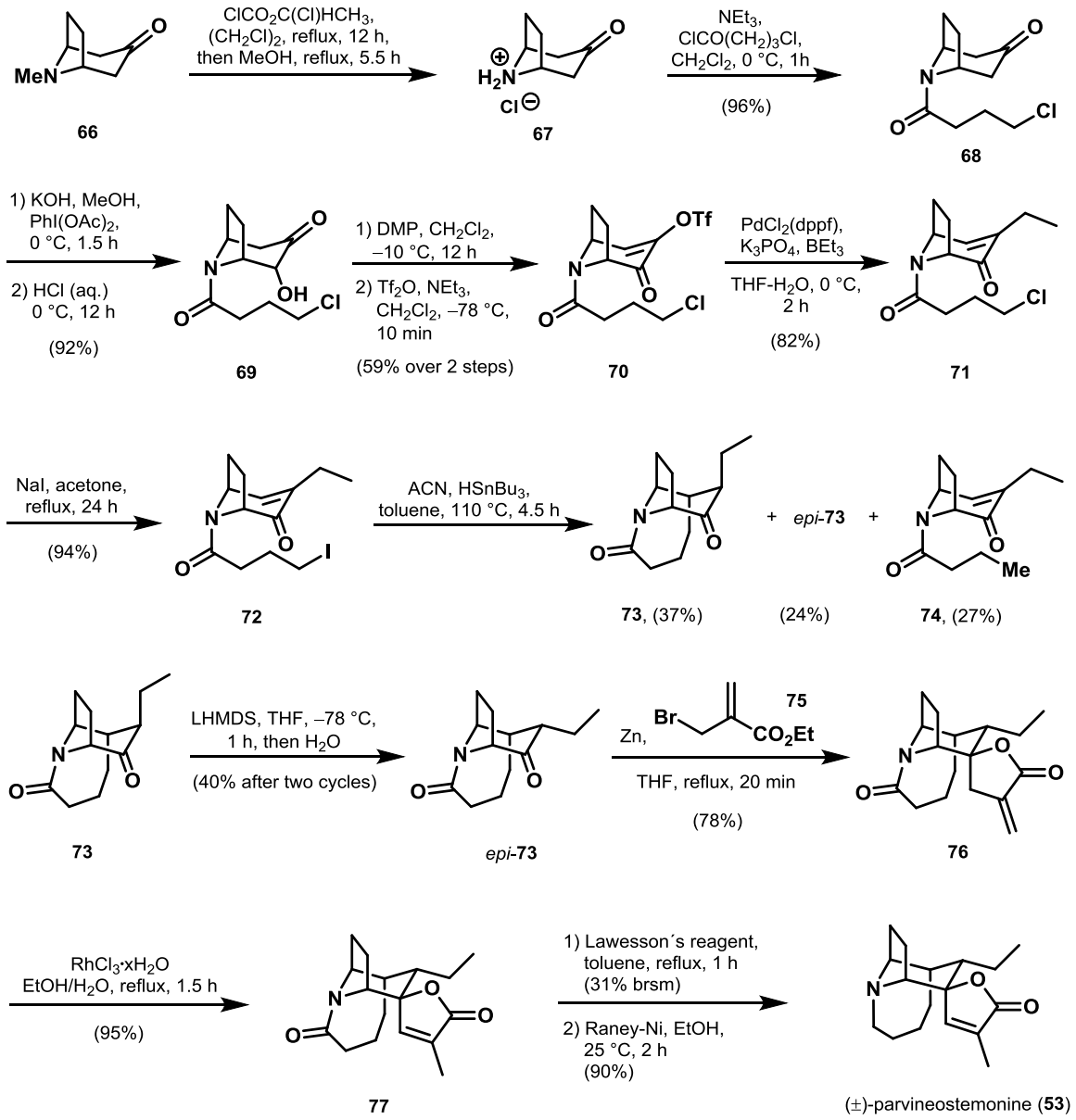

Scheme 7. Racemic total synthesis of parvineostemonine (53) by Tu and co-workers.[24]

1.4 The Concept of Structure Pattern Based Total Synthesis

The concept discussed herein represents a powerful approach to realize the challenges an organic chemist has to face when planning the total synthesis of natural products. As already stressed in the beginning syntheses of complex structures are often accompanied by inefficient amount of steps. Therefore the solution would be to change the chemist´s conventional mindset from a single target to following the concept of a synthesis based on structure patterns.[25]

As depicted in Figure 8 the conventional target-oriented syntheses (Figure 8a) follow one synthetic sequence and result in individual natural products. Nature however follows a different yet highly efficient strategy. It does not target a single molecule, but a complete family of natural products is created in a single biosynthetic sequence (Figure 8b). Inspired by nature's power to create such beautiful and complex molecular structures scientists are devoted to this field for decades and many elegant biomimetic syntheses have been accomplished since.[26][27][28] To pursue a biomimetic strategy a structural propinquity among the target structures and a common intermediate of all congeners are the two prerequisites that must be considered. However, nature´s pathways remain limited to specific structure types which confines biomimetic synthesis in structural diversification. Overcoming these limitations can be realized with a synthesis design based on "structure patterns" (Figure 8c). Compared to target-oriented syntheses where only individual natural products can be obtained, the discussed concept drastically shortens the number of steps required when accessing different natural product families. Additionally, compared to biomimetic syntheses also natural product families that are biogenetically unrelated to each other can be accessed.

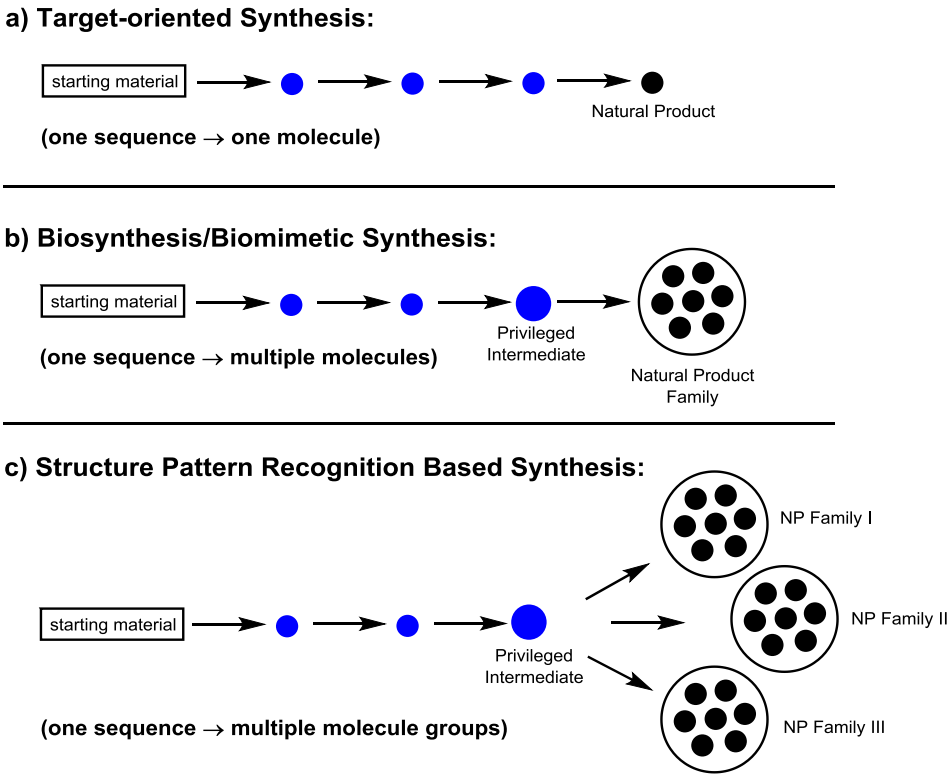

Figure 8. Comparison of strategic approaches in total synthesis.[29]

Realizing this concept, a common intermediate also "privileged intermediate" (PI) needs to be designed. The joint synthetic structure must be identified with suitable functionalization motifs which allow for a synthesis of a variety of natural products containing the privileged intermediate

as a substructure. The identification of one common intermediate present in different target structures drastically shortens the number of steps which required for individual syntheses.

Our group put this concept into practice by choosing target structures from three different natural product families (biogenetically related and unrelated to each other): the *Stemona*-, *Sarpagine*- and *Macroline* alkaloid family. Based on a database search we identified the common substructure which is depicted and highlighted in colors in Figure 9.

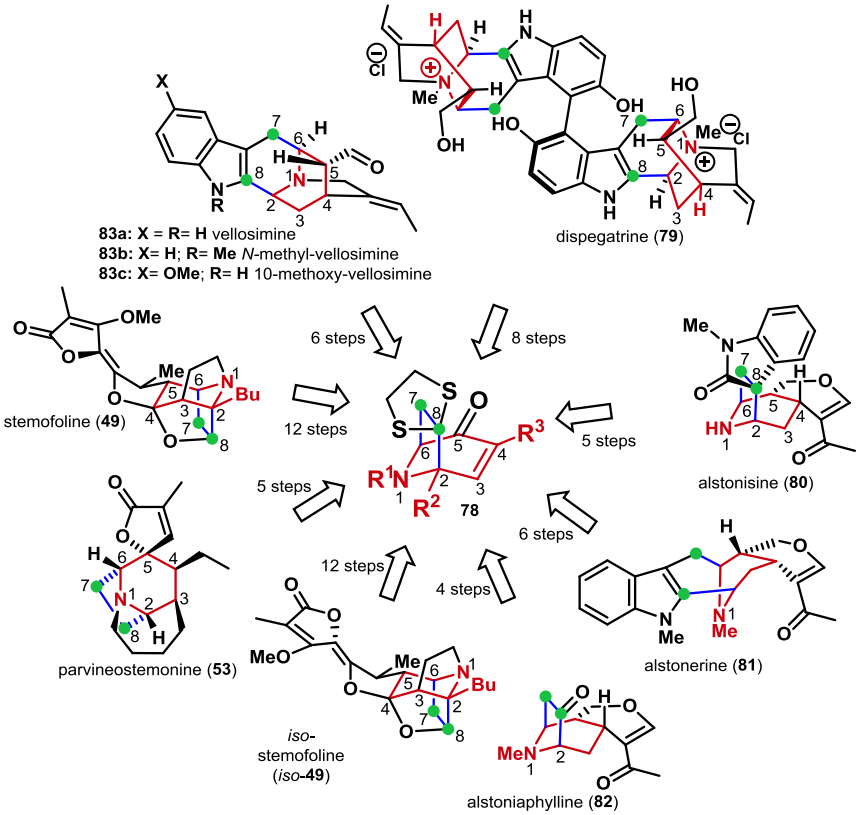

Figure 9. Natural products accessible through privileged intermediate 78.

Realization of this concept by our group was first accomplished in 2015 by achieving the total synthesis of three *Sarpagine* alkaloids: (+)-vellosimine (**83a**), (+)-*N*-methyl-vellosimine (**83b**) and (+)-10-methoxy-vellosimine (**83c**) (Scheme 8).[30] Further optimization of the reaction conditions enabled the synthesis of decagram quantities of key intermediates and in 2018 three additional *Sarpagine* alkaloids (+)-normacusine B (**90**), (+)-affinisine (**89**) and (+)-lochnerine (**88**), as well as ten non-natural derivatives could be achieved by our group.[31]

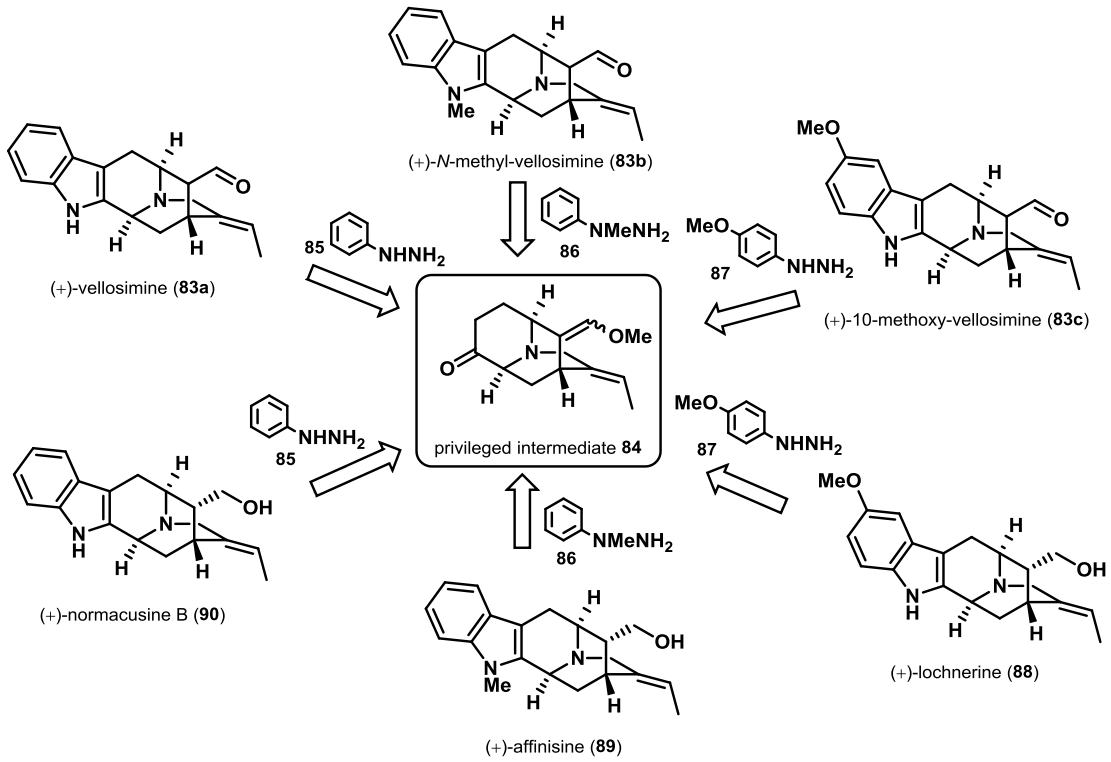

Scheme 8. *Sarpagine* alkaloids from common intermediate 84 completed by Gaich and co-workers in 2015-2018.[30][31]

The feasibility of this concept of a generalized approach was then proven with the accomplishment of the total synthesis of *Stemona* alkaloid parvineostemonine (**53**). This natural product also contains privileged intermediate **84**, previously used in the *Sarpagine* syntheses, and is biogenetically completely unrelated to the *Sarpagine* alkaloids (Scheme 9).[29]

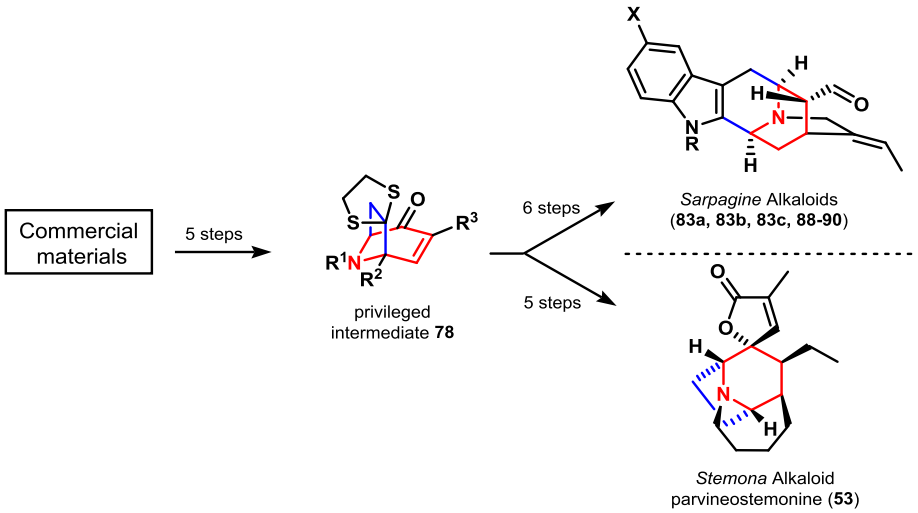

Scheme 9. Generalized approach towards *Sarpagine* and *Stemona* alkaloids.[29]

1.5 The 3-Oxidopyridinium [5+2] Cycloaddition Reaction

The design of privileged intermediate **78** was realized in our group by Dr. Sebastian Krüger in 2015 by developing a unified approach towards different *Sarpagine* alkaloids.[30] Identification of the common substructure gave a tricyclic system which was obtained from a 3-oxidopyridinium [5+2] cycloaddition between Aggarwal´s chiral ketene **92**[32] and 3-hydroxypyridinium salt **91**[33] (Scheme 10). This reaction was intensively studied before by Aggarwal and co-workers during their investigations of tropane skeleton constructions.[34] They reported that after the reaction of chiral bissulfoxide **92** with pyridinium betaine **91**, regioisomers **93** and **94** could be isolated with excellent diastereoselectivity. They rationalized this selectivity considering the possible transition state models depicted in Scheme 10. Transition state 1 (TS-1) delivers regioisomer **93** with two matching charge interactions compared to TS-2, being destabilized by steric repulsion and missing electrostatic attractions. Attractive interactions also occur in TS-3 delivering regioisomer **94**, in contrary to TS-4 where a combination of steric and electronic repulsion destabilizes the system and disfavors product formation. Investigations on the substitution pattern of betaine **91** in 2-position showed improved diastereoselectivity, whereas substituents in 6-position resulted in greater reversibility of the cycloaddition product.

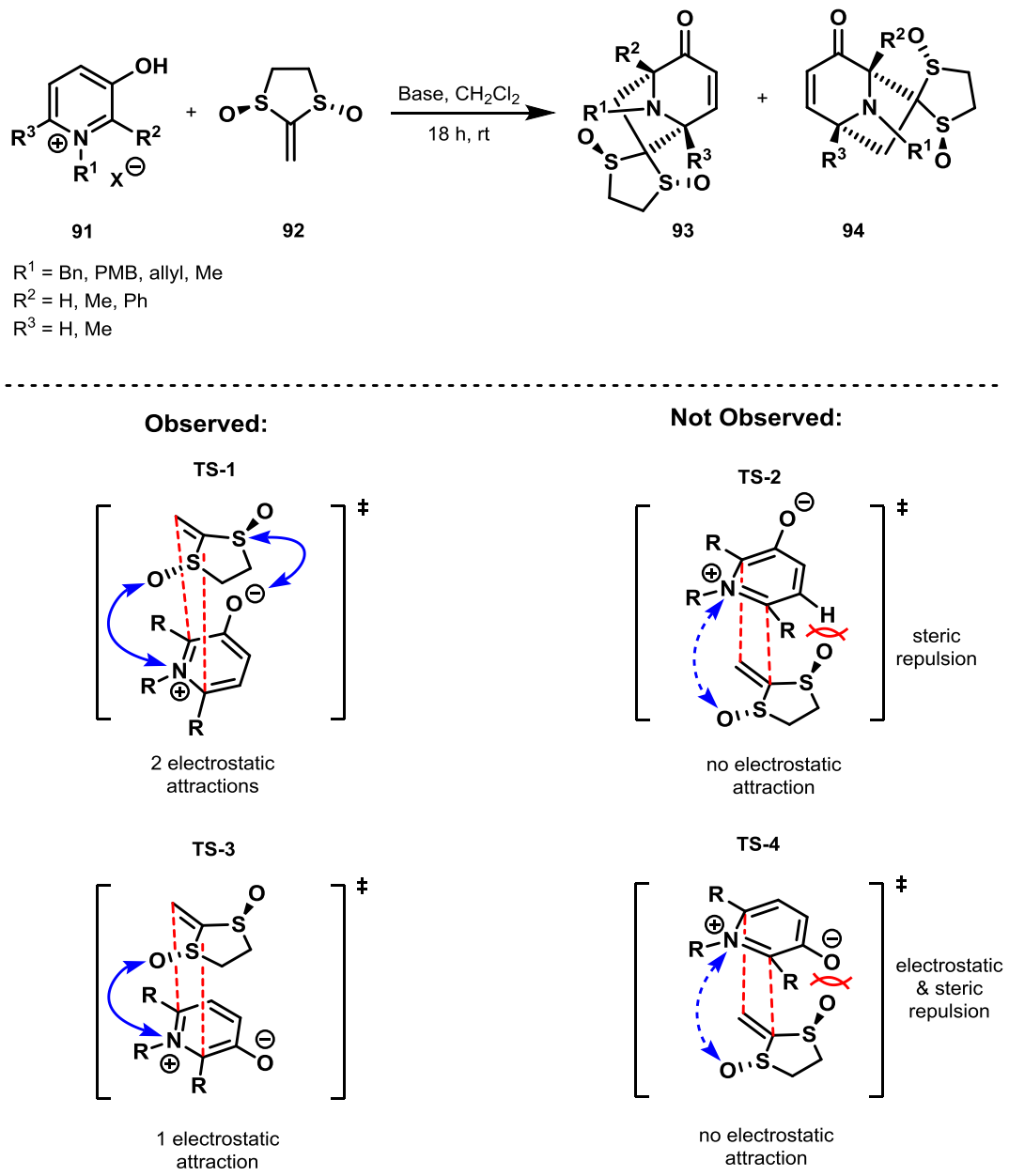

Scheme 10. Studies by Aggarwal and co-workers on the 3-oxidopyridinium [5+2] cycloaddition.[34]

Despite the fact that the described approach allows rapid and efficient access to tropane based structures, literature describes only few examples of 3-oxidopyridinium [5+2] cycloaddition reactions used in total synthesis. Some successful implementations of this strategy are illustrated in Scheme 11. The first example shows the 3-oxidopyridinium cycloaddition approach by Cha and co-workers for the construction of the tropane skeleton (**95**) of different sarain natural products in 1999.[35] Kozikowski used this strategy for the synthesis of various cocaine derivatives (**98**) reacting **100** and **101**.[33][36] Another application was reported in 1992 by Jung and co-workers.[37] In their total synthesis of racemic Bao Gong Teng A (**104**) they performed a [5+2] cycloaddition between acrylonitrile **102** and pyridinium betaine **103** to construct tropane skeleton **104**. Natural product **104** was also synthesized by Liebeskind and co-workers in 2006

via a molybdenum-mediated [5+2] cycloaddition between **105** and **106**.[38] In 2003, Stoltz and co-workers published the total synthesis of lemonomycin (**107**) via oxidopyrazinum cycloaddition between ketene **109** and betaine **108**.[39] The total synthesis of nominine (**110**) was accomplished by Gin and co-workers in 2006, with an intramolecular cycloaddition of oxidoisoquinoline betaine **111**.[40]

a) Cha 1999

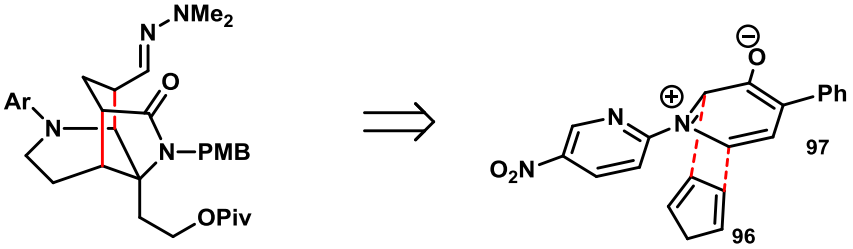

core structure of sarain derivatives (**95**)

b) Kozikowski 1996

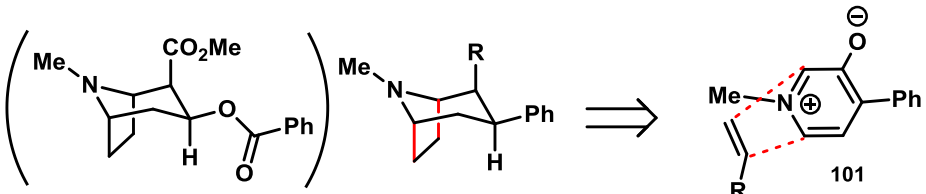

cocaine (**98**)

c) Jung 1992 and Liebeskind 2006

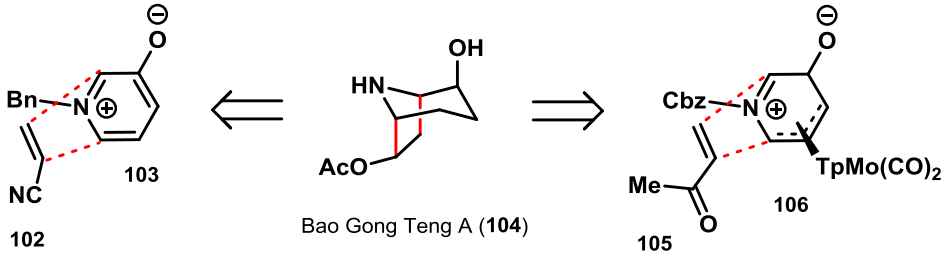

Bao Gong Teng A (**104**)

d) Stoltz 2003

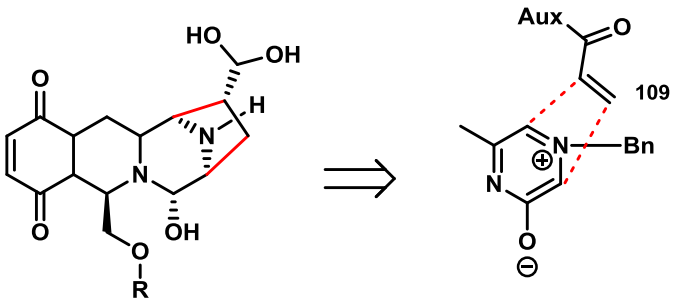

lemonomycin (**107**)

108

e) Gin 2006

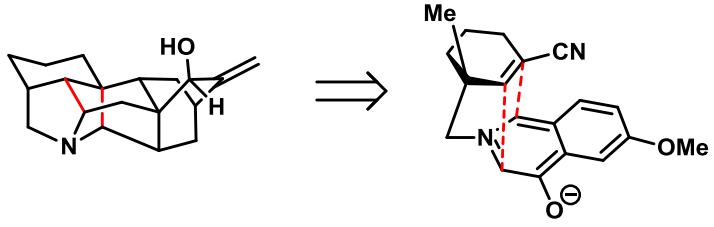

nominine (**110**)

111

Scheme 11. 3-Oxidopyrdinium [5+2] cycloaddition reactions used in total synthesis.

2 Results and Discussion

2.1 Enantiodivergence in Total Synthesis

With the concept of a structure pattern based synthesis the idea of the synthetic design of parvineostemonine (**53**) was defined. But given the fact that up to this date the absolute configuration of **53** remained unknown and still no detailed investigations into the biological activity were undertaken, having synthetic access to both enantiomers of the natural product was of utmost importance. Therefore, we pursued an enantiodivergent approach which would allow us to access both antipodes of the natural product. Various elegant enantiodivergent approaches based on symmetry elements in their common intermediate are described in literature. For example, Garg and Stoltz achieved the total synthesis of both enantiomers of dragmacidin F (**112**) from commercially available (±)-quinic acid (**113**) in 2004.[41] Furthermore, the efficient synthesis of the strong nerve-depolarizing agent (+)-anatoxin (**114**) and its unnatural antipode (–)-anatoxin (**114**) has been accomplished from L-glutamic acid (**115**) by the group of Rapoport in 1990.[42]

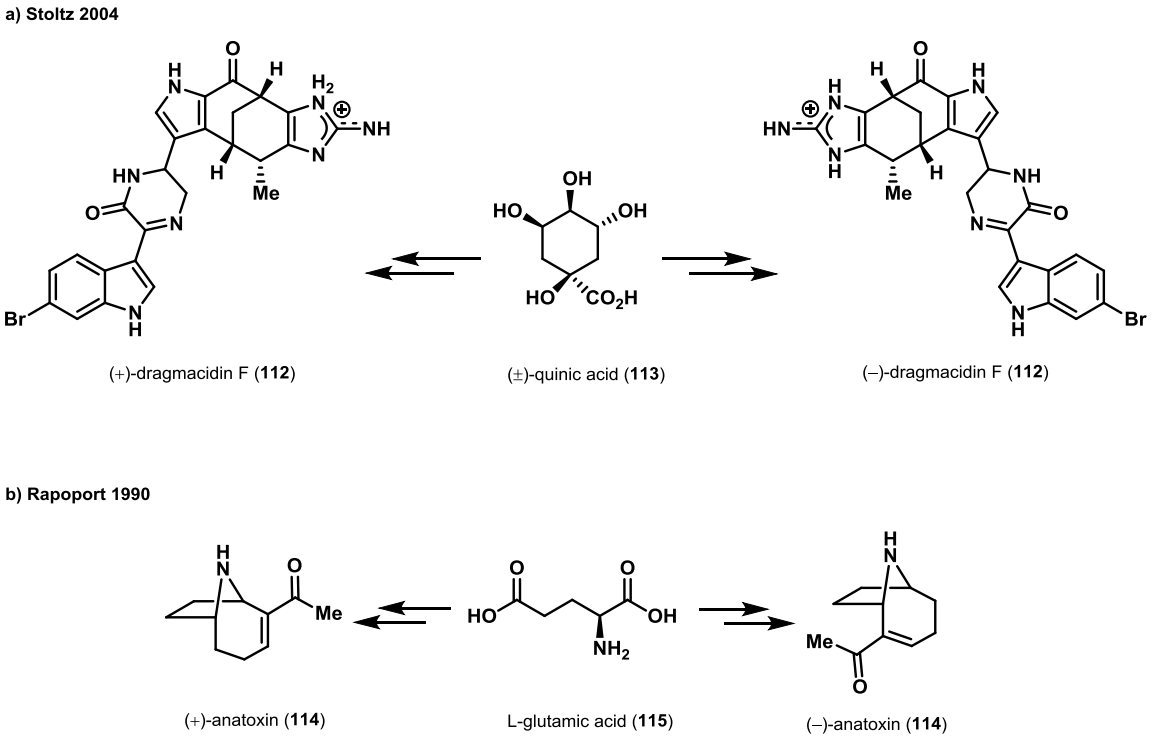

Scheme 12. Enantiodivergent approaches by Stoltz and Rapoport.[41][42]

By combining two efficient and powerful concepts, namely structure pattern based and enantiodivergent total synthesis, the synthetic access to both enantiomers of parvineostemonine (**53**) was designed and will be discussed in detail in the following chapter.

2.2 Total Synthesis of Parvineostemonine

Earlier studies on the total synthesis of parvineostemonine (**53**) were performed by Dr. Sebastian Krüger and are described in detail in his work.[43] The following represents the optimization and conclusion of the third-generation approach towards the natural product (Scheme 13).[29] Our retrosynthetic planning started with the introduction of the butenolide moiety to enantiomeric ketones (–)-**116** and (+)-**116** via nucleophilic 1,2-addition followed by *in situ* oxidation and lactonization. Ketones (–)-**116** and (+)-**116** were envisioned to be constructed via ring-closing metathesis starting from regioisomeric olefins **117** and **120**. At this point, in a forward sense removal of the dithiolane moiety (highlighted in red in Scheme 13) was envisioned to convert the two regioisomers **117** and **120** into their respective enantiomers (–)-**116** and (+)-**116**, representing the enantiodivergent step of the synthesis. Bisolefins **117** and **120** should be obtained via conjugate addition of an allyl moiety starting from compounds **118** and **119**. Regioisomers **118** and **119** in turn were planned to be constructed via the 3-oxidopyridinium [5+2] cycloaddition reaction between literature known bissulfoxide **92** and pyridinium betaine **121**.

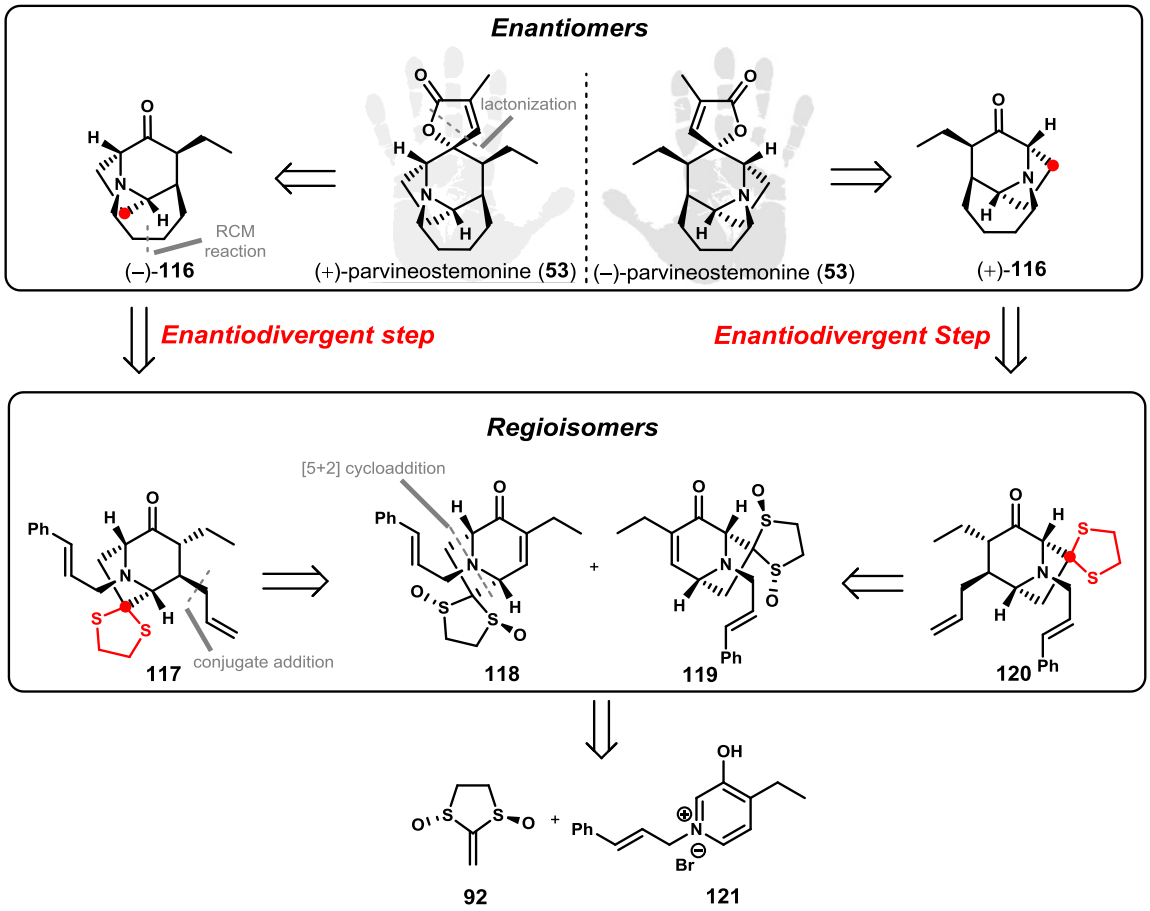

Scheme 13. Retrosynthetic planning of both enantiomers of parvineostemonine (53).

Our synthetic route commenced with the preparation of Aggarwal´s bissulfoxide **92** in four steps from commercially available acetal **122** (Scheme 14).[32] Acid catalyzed transthioketalization afforded dithiolane **124** in high yield. Oxidation of **124** gave bissulfoxide **125** with excellent enantioselectivity (>98% ee) but low yield. Doubling the amount of equivalents of the reagents afforded **125** in 45-60% yield on decagram scale. Amination using dimethylamine was achieved in quantitative yield and subsequent Hoffmann elimination yielded chiral olefin **92** which was used crude in the 3-oxidopyridinium [5+2] cycloaddition reaction.

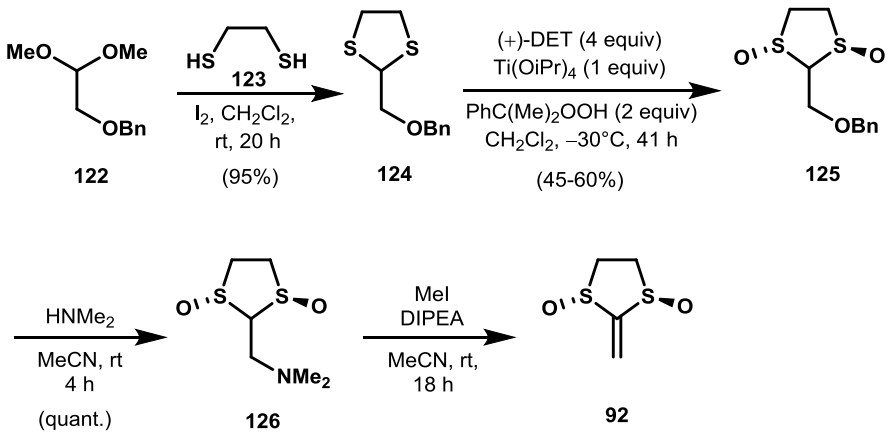

Scheme 14. Synthesis of bissulfoxide 92 from acetal 122.

For the synthesis of oxidopyridinium salt **121** we followed the literature procedure of Kozikowski and co-workers starting with benzyl protection of commercially available 3-hydroxypyridine (**127**) (Scheme 15).[33] After copper-mediated introduction of the ethyl side chain, the resulting dihydropyridine intermediate was rearomatized using *o*-chloranil to give **129** in 65% yield over two steps. Removal of the benzyl protecting group by hydrogenation afforded phenol **130** in 95% yield, which was then treated with cinnamyl bromide (**131**) to yield the desired betaine **121** in 71% yield.[43]

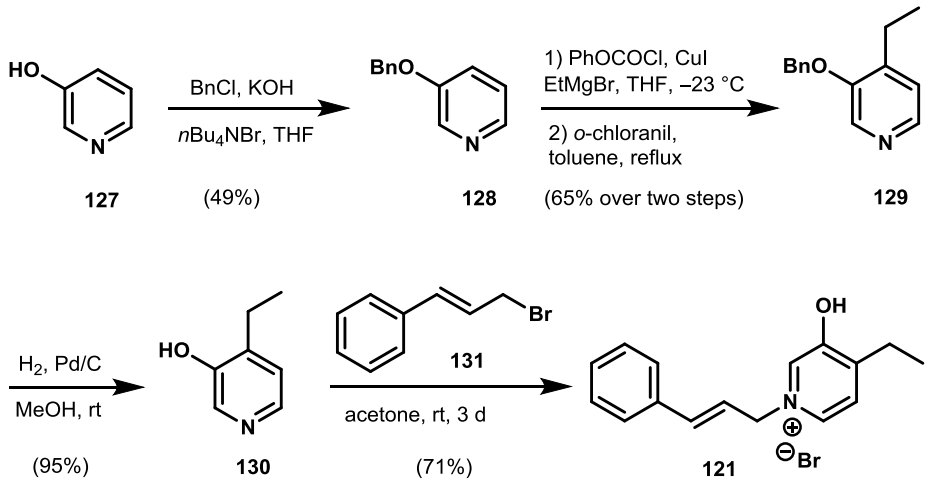

Scheme 15. Synthesis of oxidopyridinium betaine 121 from 3-hydroxypyridine (127).[43]

With the required coupling partners in hand, the 3-oxidopyridinium [5+2] cycloaddition reaction could be investigated (Scheme 16).[43] Under basic conditions bissulfoxide **92** and pyridinium salt **121** afforded regioisomeric cycloaddition products **118** and **119** in excellent yield (detected by ^{1}H-NMR analysis). With a ratio of 5.6:1 (**118**:**119**) a significant increase in regioselectivity could be observed compared to the studies by Aggarwal and coworkers discussed in chapter 1.5.[34] Due to the position of the ethyl side chain we expected very small to no influence at all in

the course of the cycloaddition reaction. Detailed analysis of the two possible transition states in this reaction led us to propose that for TS-1 no destabilization occurs.[43] However, for TS-2 an additional steric clash between the sulfur-lone pair and the ethyl side chain in betaine **121** may cause additional destabilization and leads to a greater regioselectivity compared to original studies. Since Aggarwal only investigated betaine substitutions in the 2- and 6-position, this result found by our group was new and unexpected.[43]

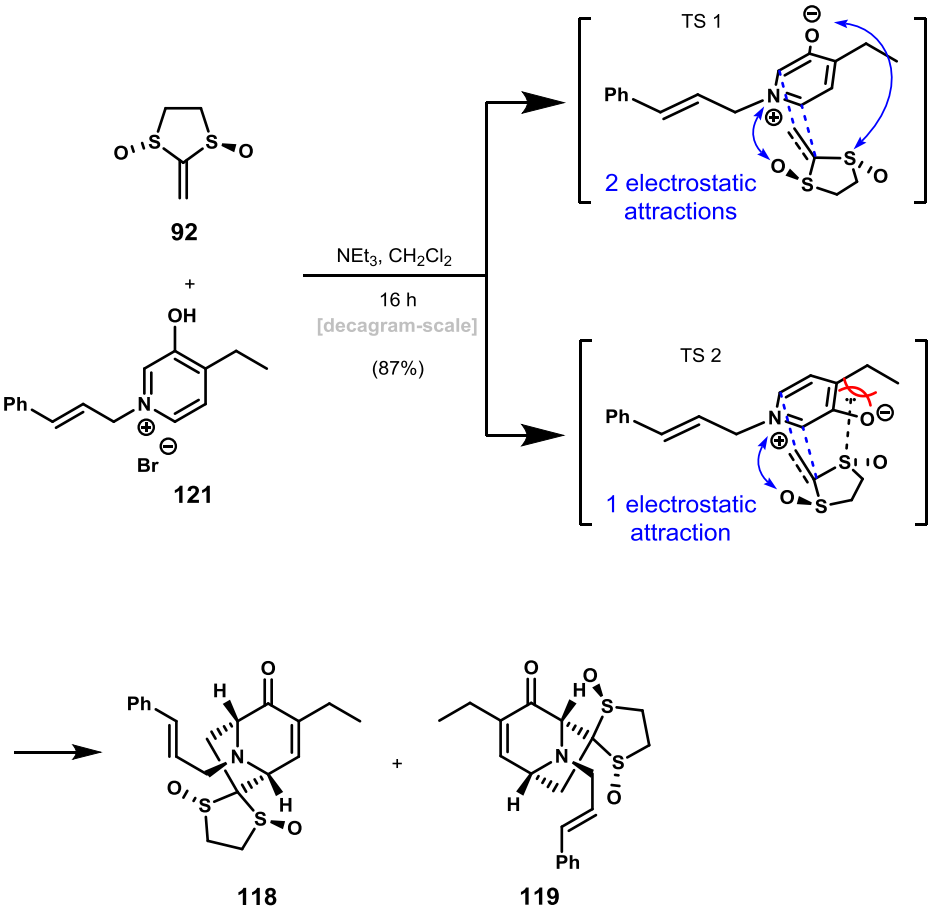

Scheme 16. [5+2] cycloaddition reaction between bissulfoxide 92 and betaine 121.

The regioisomeric mixture of **118** and **119** could not be separated until reduction of the bissulfoxide moiety to the corresponding dithiolane (Scheme 17). This was achieved using trifluoroacetic acid and sodium iodide in acetonitrile at temperatures between –10 and –5 °C and afforded regioisomers **132** and **133** in high yield. From this point onwards, regioisomers **132** and **133** were carried on separately and the same reaction conditions were applied for both compounds.

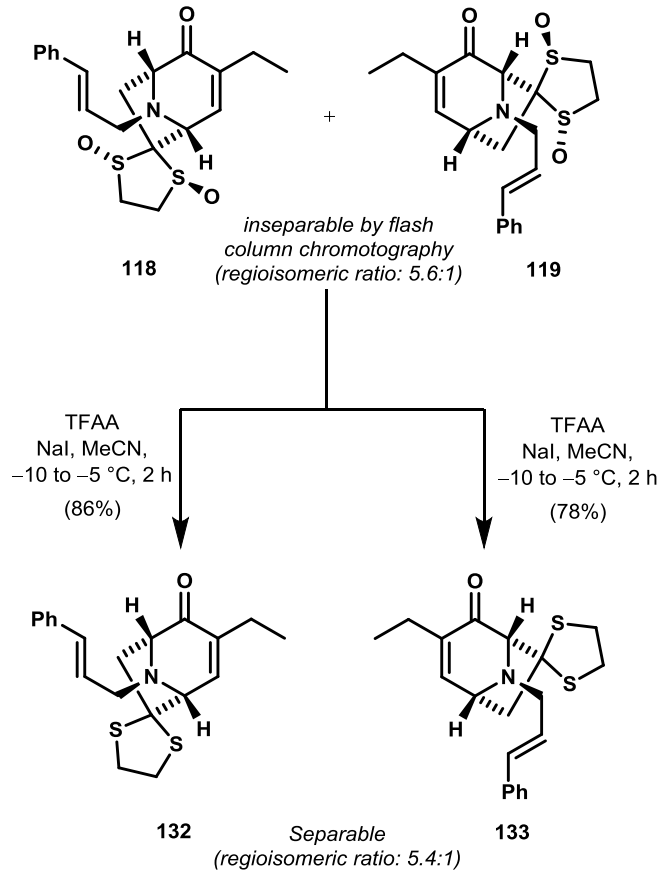

Scheme 17. Reduction of bissulfoxides 118 and 119 to dithiolanes 132 and 133.

Our next task was the introduction of the allyl moiety, which was realized following the Lipshutz protocol proceeding in high yields for both isomers (**132**: 83%, **133**: 78%) (Scheme 18).[44] As expected, the attack from the allyl copper species proceeded from the opposite side of bridgeheaded ring B. However, upon quenching the resulting enolate the newly formed stereocenter at C10 gave exclusively *trans* orientation between the ethyl- and the allyl-side chain. This result was unexpected since this orientation implied an axial orientation of the ethyl group. Initial attempts to invert the stereocenter proved unsuccessful and were therefore postponed to a later stage of the synthesis.[43] The seven-membered ring was constructed via ring closing metathesis using Grubbs 2nd generation catalyst under refluxing conditions, forming regioisomers **134** and **136** in good overall yield. Single crystal X-ray analysis of regioisomer **134** confirmed the relative stereochemistry and therefore the *trans* orientation of the two side chains. With olefins **134** and **136** in hand the stage was set to perform the enantiodivergent step in the synthesis. This transformation was realized with the removal of the dithiolane moiety, transforming regioisomers **134** and **136** into their respective enantiomers (+)-**135** and (–)-**135**. Using Raney Nickel, the desulfurization proceeded together with reduction of the double bond.[29]

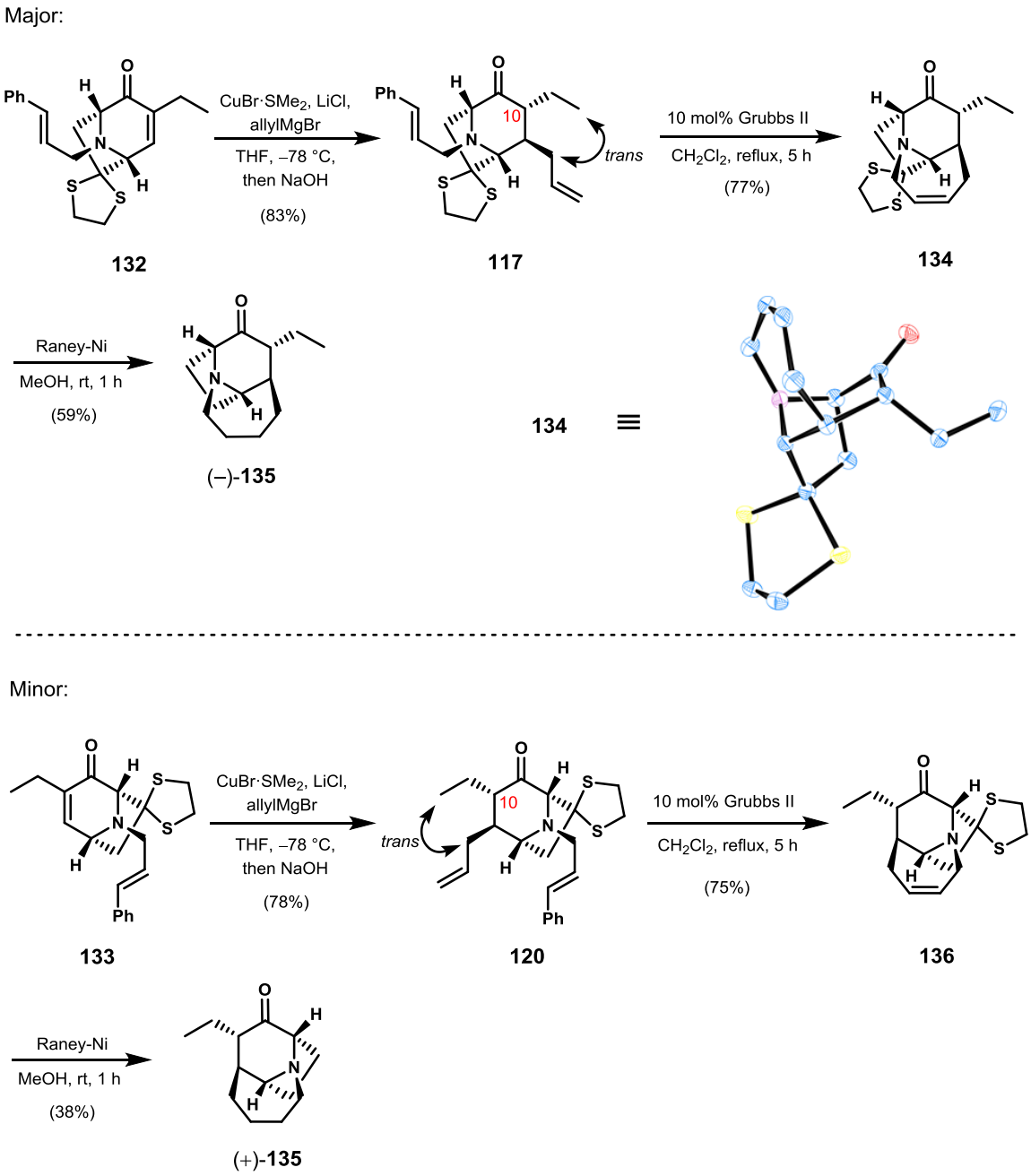

Scheme 18. Synthesis of enantiomers (–)-135 and (+)-135.[29]

For the following investigations only enantiomer (–)-**135** will be discussed. For enantiomer (+)-**135** the same reaction conditions were applied.

At this stage of the synthesis attempts to convert the stereocenter at C10 were investigated and are summarized in Table 1. Kinetic conditions which were conducted in earlier studies using KHMDS at –78 °C gave very inconsistent selectivity (1:1 to 6:1, **135**:**116**).[43] Therefore, we changed our approach to invert the stereocenter under thermodynamic conditions. We started by using KO*t*Bu as a base and stirring the reaction for 18 h to 48 h at ambient temperature resulting in a consistent ratio of 1.2:1 (**116**:**135**) (Table 1, entry 1). Using a mixture of NaOH and

pyrrolidine decreased the ratio of the desired ketone **116** to 3:1 (**135**:**116**) (Table 1, entry 2). Switching to DBU produced 86% of **116** based on recovered starting material and upon eight iterative circles (Table 1, entry 7).[29]

Table 1. Epimerisation attempts of the stereocenter at C10.

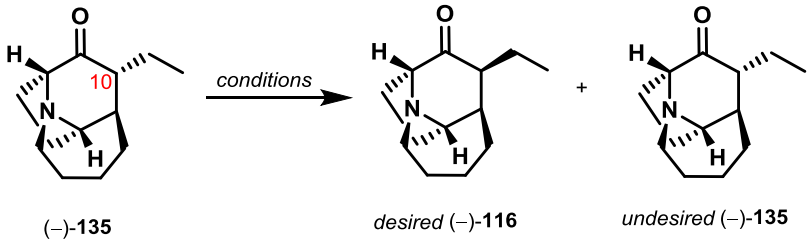

(–)-**135** *desired* (–)-**116** *undesired* (–)-**135**

Entry[a]	Base	Equivalents of Base	T [°C]	t [h]	Yield[c]
1	KO*t*Bu[b]	2 to 4	0 to 25	18 to 48	72% (1.2:1, **135**:**116**)
2	NaOH/pyrrolidine	1 to 1.3	0 to 25	7	74% (3:1, **135**:**116**)
3	DBU	2	25	24	86% (1.5:1, **135**:**116**)
4	DBU	2	25	48	83% (1.2:1, **135**:**116**)
5	DBU	2	45	48	85% (1.5:1, **135**:**116**)
6	DBU	3	25	96	85% (1.1:1, **135**:**116**)
7	DBU	4	25	96	86% (1:1, **135**:**116**)

[a] all reactions were conducted in dry THF as solvent. [b]tBuOH/THF (1:1, 0.1 M) was used as a solvent [c]the listed yields were calculated based on recovered starting material.

Next, installation of the butenolide moiety was investigated. The initial idea was inspired by the synthesis of Tu and co-workers who introduced the last missing carbon cycle via a Refomatzky-type reaction followed by [Rh]-catalyzed isomerization of the *exo*-double bond as discussed in section 1.3.2 (Scheme 15).[24]

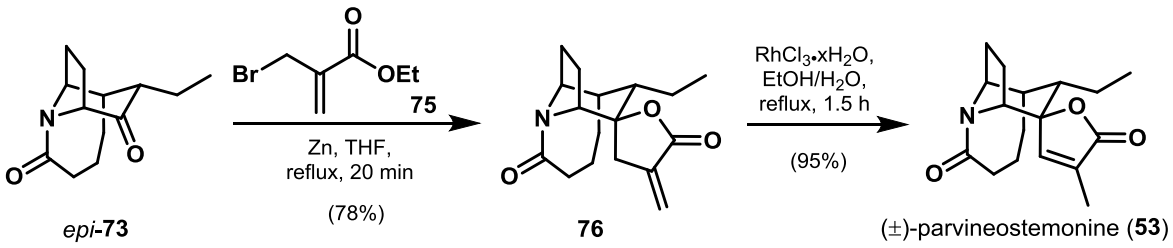

epi-**73** **76** (±)-parvineostemonine (**53**)

Scheme 19. Spiroannelation in the total synthesis of parvineostemonine (53) by Tu and co-workers.[24]

Earlier studies by Dr. S. Krüger gave desired tetracycle **137** when applying the same reaction conditions.[43] However, this step was only conducted once on very small scale and when repeating these conditions no product formation could be observed (Table 2, entry 1). The best result with 6% could be achieved increasing the amount of equivalents of zinc and ethyl 2-(bromomethly)acrylate (**75**) and refluxing the reaction for two hours (entry 3). Extended reaction times only led to decomposition (entry 4). Attempts to increase the reactivity of the nulceophilic species by addition of dibromoethane gave no conversion (entry 5). Same results were obtained when using magnesium instead of zinc as metal source (entry 6). Using Lewis acids such as $BF_3{\cdot}OEt_2$ to further activate the carbonyl moiety in (–)-**116** remained fruitless (entry 7). Activation of the zinc powder by the procedure described by Knochel afforded only trace amounts of product (entry 8).[45] A samarium mediated process to install the missing butenolide moiety only gave a complex mixture of products that could not be identified (entry 9).

Table 2. Attempts to introduce the butenolide moiety to ketone (–)-116.

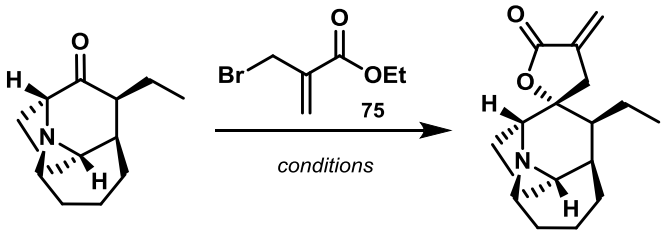

(–)-**116** (–)-**137**

Entry[a]	Conditions (equiv.)	Additive (equiv.)	T [°C]	t [h]	Observation
1[b]	Zn (2.6), **75** (1.3)	-	70	0.4	no conversion
2[c]	Zn (5), **75** (3)	-	70	1	no conversion
3	Zn (10), **75** (5)	-	70	2	**137** (6%)
4	Zn (10), **75** (5)	-	70	12	decomposition
5	Zn (10), **75** (5)	$C_2H_4Br_2$ (0.1)	70	12	no conversion
6	Mg (10), **75** (5)	$C_2H_4Br_2$ (0.1)	70	12	no conversion
7	Zn (10), **75** (5)	$BF_3{\cdot}OEt_2$ (0.1)	–78 to 0	3	no conversion
8[d]	Zn (5), **75** (3)	LiCl (1.2), TMS-Cl (0.1), $C_2H_4Br_2$ (0.5)	25	0.4	traces of **137**
9	SmI_2 (6), **75** (10)	*t*BuOH (6)	0 to 25	1	complex mixture

[a]all reactions were conducted in dry THF as solvent. [b]a freshly prepared stock solution of Zn and **75** in THF was added to neat ketone (–)-**116**. [c]neat **75** was added to a refluxing solution of ketone (–)-**116** and Zn in dry THF. [d]Zn was activated according to the literature procedure by Knochel and coworkers.[45]

In conclusion, all attempts to introduce the missing butenolide moiety using Reformatzky-, Grignard- or radical-conditions proved unsuccessful. We assumed that the lack in reactivity can

result from different coordination properties of a tertiary amine compared to an amide functionality which is present in the ketone used by Tu and co-workers. Therefore, the use of stronger nucleophiles and conditions to suppress coordination to the tertiary amine were investigated next. To determine the reactivity of ketone (–)-**116** different lithium- and Grignard-reagents were tested for nucleophilic 1,2-addition (Scheme 20). In both cases full conversion of starting material could be observed.

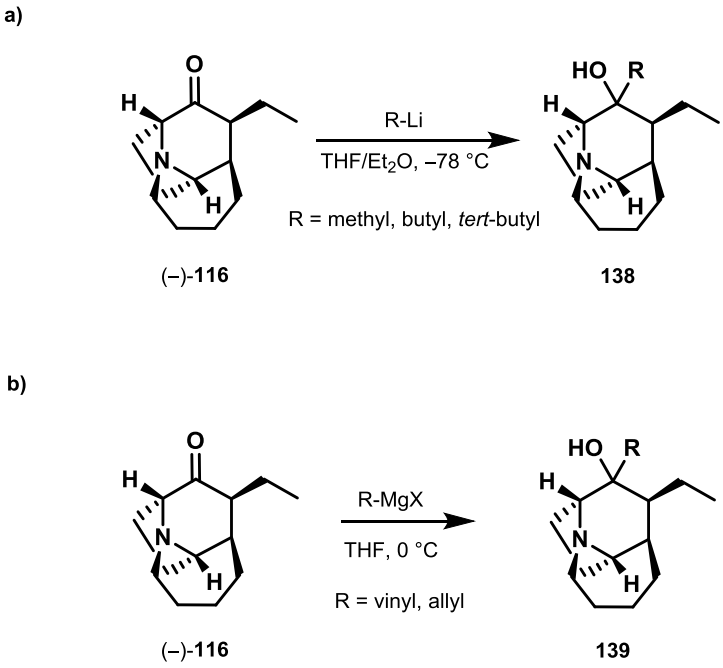

Scheme 20. Nucleophilic addition to ketone (–)-116.

Motivated by these results we further investigated the nucleophilic 1,2-addition to ketone (–)-**116**. With vinyl iodide **140** the appropriate nucleophile for butenolide installation was found and examined (Table 3). Halogen-lithium exchange with *n*-BuLi and *t*-BuLi at different temperatures gave very inconsistent results between 20-30% isolated yield (entry 1-3). Using a Knochel Grignard species gave no conversion (entry 4).[46] Difficulties in this step may be associated with the formation of an instable di-anion, therefore attempts to increase the reactivity of the lithium bases by the addition of tetramethylenediamine (TMEDA) were undertaken and gave the best results between 35% and 41% yield (entry 5).

Table 3. Nucleophilic addition of 140 to ketone 116.

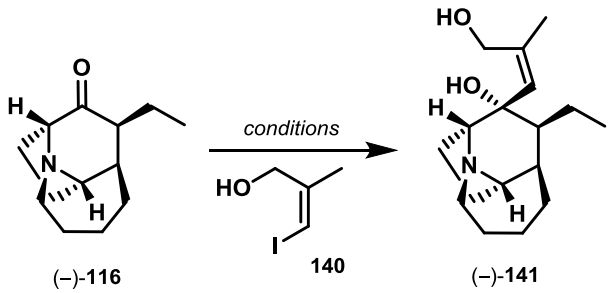

(–)-**116** (–)-**141**

Entry	Conditions (equiv.)	Additive (equiv.)	T [°C]	Yield
1[a]	**140** (1.3), *t*-BuLi (3)	-	–78 to 0	20% (**116**: 60%)
2[a]	**140** (10), *t*-BuLi (8)	-	–78 to 0	23% (**116**: 37%)
3[b]	**140** (20), *n*-BuLi (18)	-	–78 to 0	25-30% (**116**: 31%)
4[b]	**140** (1), *i*-PrMgCl·LiCl (1.1)	-	–78 to –45	0% (no conversion)
5[c]	**140** (20), *n*-BuLi (18)	TMEDA	–78 to 0	35-41% (**116**: 20%)

[a]dry diethyl ether was used as solvent. [b]dry THF was used as solvent. [c]TMEDA was freshly distilled.

We next employed the oxidative ring formation of diol **141** to the natural product (+)-parvineostemonine (**53**) (Table 4). Investigation of different oxidation conditions gave either lactol **142** or decomposition of starting material (entry 1-3). However, using an excess of Jones reagent, (+)-parvineostemonine (**53**) could be obtained in excellent yield (entry 4.)

Table 4. Oxidation conditions of diol 141.

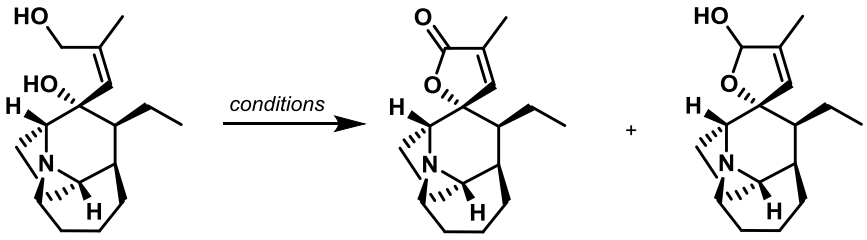

(–)-**141** (+)-parvineostemonine (**53**) (–)-**142**

Entry	Conditions (equiv.)	Solvent	T [°C]	t [h]	Observation
1	IBX (4)	DMSO	25	1	decomposition
2	PDC (6)	DCM	0 to 25	12	traces of **142**
3	TPAP (0.05), NMO (4)	MeCN	0	1	**142** (89%) and **53** (5%)
4	Jones reagent (5)	acetone	0	0.5	**53** (90%)

Circumventing difficulties with the di-anion formation and consequently low yields in the nucleophilic 1,2-addition, an attachment of a protecting group to allylic alcohol **140** should stabilize the system.[47] Intrigued from the results with Jones reagent, a *tert*-butylsilyl-group was installed, which should be cleaved simultaneously under the acidic conditions during the oxidation step (Scheme 21).[29]

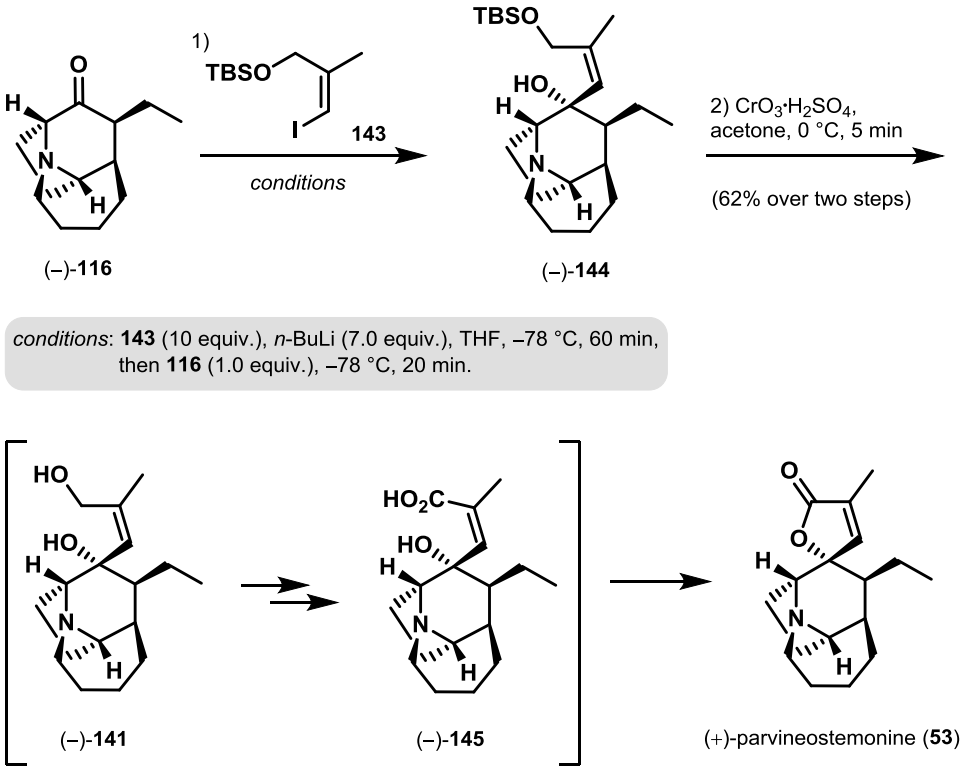

Scheme 21. Addition of TBS-protected vinyl iodide 143 to ketone (–)-116 and following Jones oxidation.[29]

With TBS-protected vinyl iodide **143** in hand, the addition to ketone (–)-**116** and following Jones oxidation was investigated. Nucleophilic 1,2-addition was performed using optimized conditions noted in Scheme 21. Next, crude tertiary alcohol **144** was treated with an excess of Jones reagent (7.0 equiv., 1.5 M in acetone) at low temperature. Under these conditions (+)-parvineostemonine (53) was completed in 62% yield over the last two steps.[29]

3 Summary

The first enantioselective total synthesis of both enantiomers of the *Stemona* alkaloid parvineostemonine (**53**) is described in the first part of this thesis (Scheme 22).[29] Pursuing initial studies in our group this approach was embedded in the concept of a "structure pattern based total synthesis".[30] The synthesis of a common intermediate enabled access to different *Sarpagine* alkaloids and with the accomplishment of synthesizing biogenetically unrelated *Stemona* alkaloid parvineostemonine (**53**) the potential of structure pattern based recognition as a strategic approach for total synthesis was proven.[25] Additionally, the total synthesis was realized via an enantiodivergent approach enabling access to both enantiomers of the natural product (+)-**53** and (–)-**53**. Therefore the absolute configuration could be elucidated for the first time, revealing (+)-**53** as the natural occurring enantiomer of parvineostemonine.[29]

Starting from Aggarwal´s chiral bissulfoxide **92** and pyridinium salt **121** the 3-oxidopyridinium [5+2] cycloaddition reaction successfully constructed the regioisomeric mixture of **118** and **119**, representing the privileged intermediate. In three further steps the regioisomers were separated and the seven-membered ring could be installed via ring-closing metathesis. The enantiodivergent step of the synthesis results from the reduction of the double bond which converts, together with removal of the dithiolane moiety, the regioisomers **134** and **136** into their respective enantiomers (–)-**116** and (+)-**116**. Epimerization of the ethyl side chain followed by installation of the spiro-annulated butenolide moiety successfully completed the first enantiodivergent total synthesis of the *Stemona* alkaloid parvineostemonine (**53**).

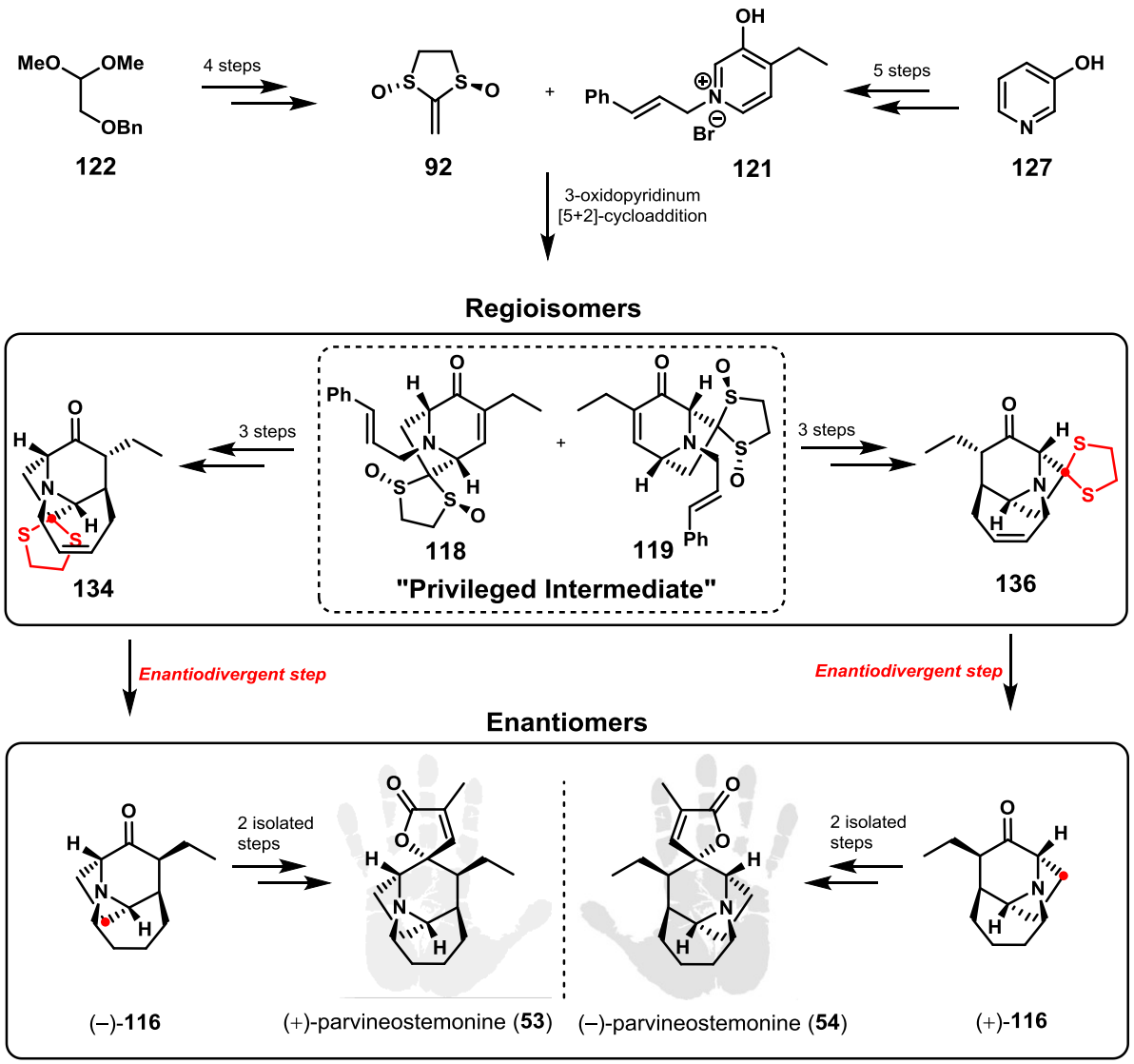

Scheme 22. Enantiodivergent total synthesis of (+)-parvineostemonine (53) and (–)-parvineostemonine (53).

In summary, the synthesis has been accomplished in 11 isolated steps (13 of total steps from commercial materials). Through intense optimization of the reaction conditions we were able to design a robust route yielding decagram amounts of key intermediates as well as reasonable amounts of both enantiomers of parvineostemonine (**53**), which additionally offers the opportunity to start investigations in biological activities.

II The Pepluacetal Project

1 Introduction

1.1 *Euphorbia* Diterpenes

Euphorbiaceae is one of the largest families of flowering plants consisting of over 300 genera and 8000 species.[48] The genus *Euphorbia* is one of the six largest genera (*Astragalus*, *Bulbophyllum*, *Psychotria*, *Carex*, *Begonia, and Euphorbia*) of this family, which is further subdivided into many subgenera and species. Lately, Hohmann and co-workers summarized 78 different *Euphorbia* species until 2014.[48] The members of this family are widely distributed all around the world, some being located in tropical climate while others can be found in rainforests as herbs and trees.[49] Their morphology ranges from small, annual and perennial herbaceous plants to woody shrubs, lianas, trees and even large desert succulents.[50] The production of milky irritant latex specifically characterizes members of this genus. Due to their great structural diversity resulting from various macrocyclic and polycyclic skeletons, they possess a wide range of therapeutically relevant biological activities. Therefore, these diterpenes are a main focus of natural product drug discovery for many years.

However, this genus is not only of pharmaceutical relevance but it also consists of representatives of big economic importance like *Euphorbia tetragonal* and *Euphorbia triangularis* (inferior rubber), *Euphorbia antisyphylitica* (candellila wax), and *Euphorbia resinifera* ("euphorbium").[51] This implicates that *Euphorbia* represents a complex genus with a lot of research potential in many different areas.

1.1.1 Biosynthesis and Classification

In the biosynthesis of *Euphorbia* diterpenes geranylgeranyl pyrophosphate (GGPP, **151**) represents the C_{20}-precursor for the formation of the different skeletal types.[52] GGPP (**151**) originates from the monomeric C_5-units isopentenyl pyrophosphate (IPP, **147**) and dimethylallyl pyrophosphate (DMAPP, **146**), both deriving from the mevalonate pathway in most cases (Scheme 23).[53] The opposite reactivity of DMAPP (**146**) and IPP (**147**) allows for coupling to form the monoterpene precursor geranyl pyrophosphate (GPP, **149**). Further assembly of IPP (**147**) and GPP (**149**) units gives access to farnesyl pyrophosphate (FPP, **150**) as sesquiterpene precursor and geranylgeranyl pyrophosphate as diterpene precursor (GGPP, **151**).[53]

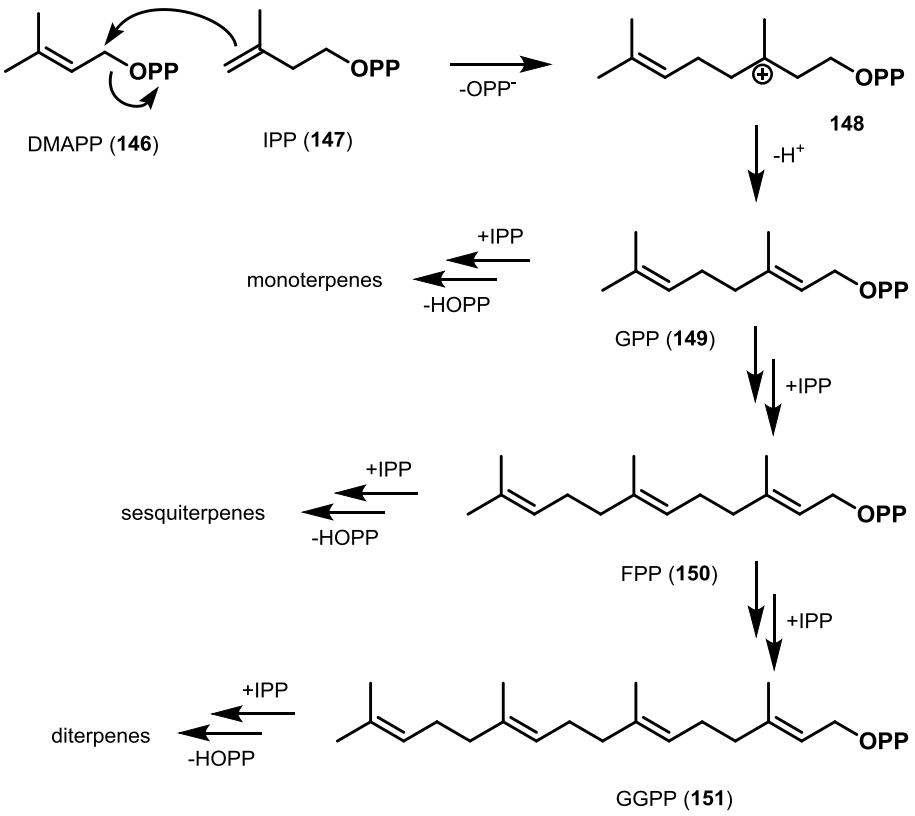

Scheme 23. Biosynthesis of terpene skeletons from DMAPP (146) and IPP (147).

Cyclization reactions from GGPP toward complex polycyclic carbon skeletons like 14-membered macrocylic cation **153** are realized by type I cyclizations (Scheme 24). Abstraction of a proton forms natural product cembrene A (**154**) inlcuding a cembrane skeleton, which in turn represents the basic skeleton for the formation of different skeletal types found in the genus *Euphorbia*. The cyclization to the bicyclic casbene skeleton **155** is realized by casbene synthase.[54] Beyond casbene structure **155**, the biosynthetic pathway remains speculative.[55] Cyclization between C6 and C10 delivers the lathyrane skeleton **156** as a proposed intermediate in the biosynthesis of *Euphorbia* diterpene structures such as jatropholane (**157**) and tigliane (**158**), as well as crotofolane (**159**), ingenane (**160**) and daphnane (**161**).[56][52]

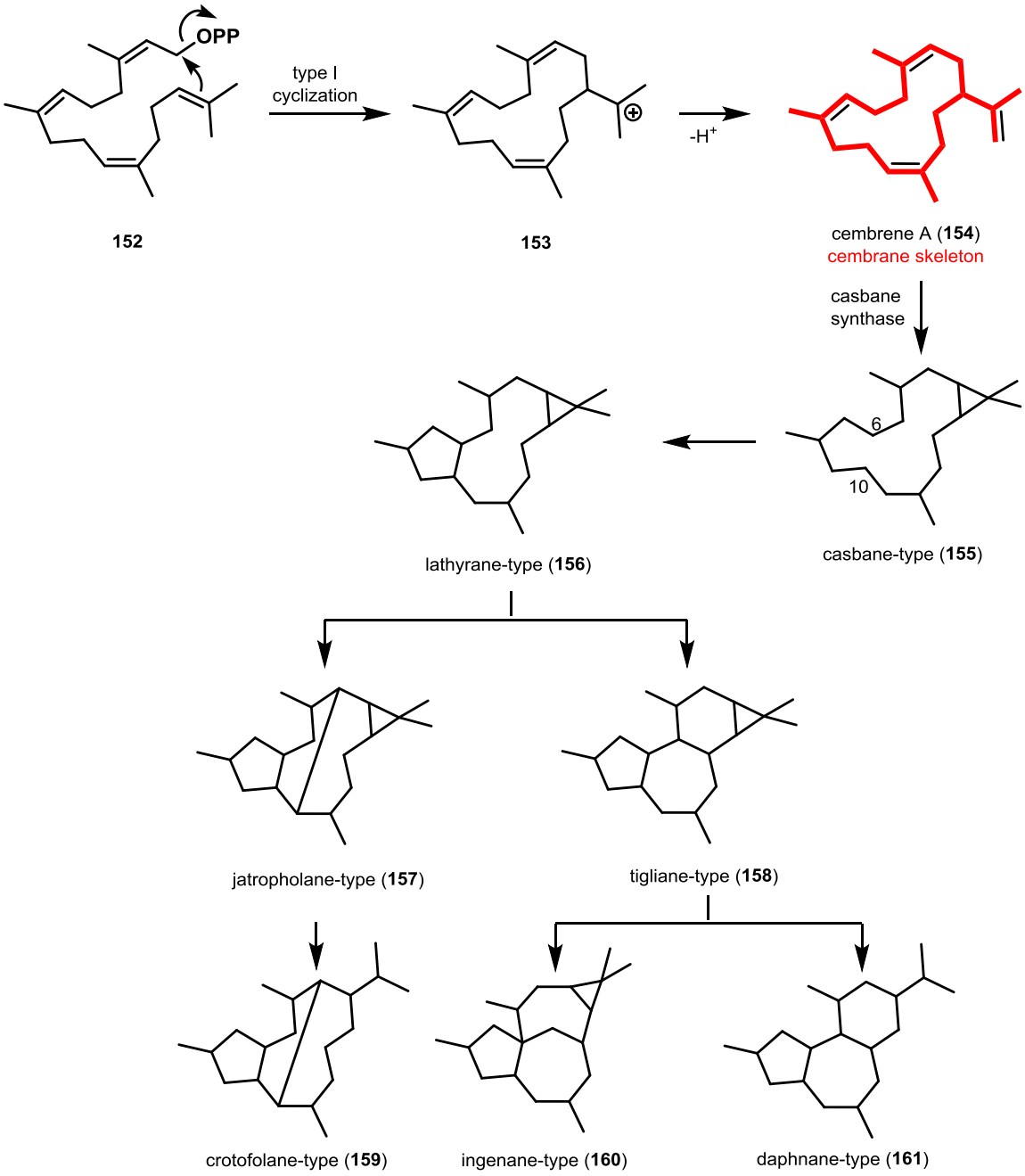

Scheme 24. Biosynthesis of the cembrane skeleton and further classes of diterpene structures found in the genus *Euphorbia*.

1.1.2 Bioactivity

The biological research on compounds isolated from the *Euphorbia* genus has been intensively promoted over the last decades. The fact that structural diversity is often linked with biological functionality is well reflected by various representatives. This species features a huge structural abundance with wide-ranging biological activities. These include antitumor activity (e.g. **162**, **162a**)[57][58], in particular anti-proliferative activity (e.g. **163**)[59], as well as tumor promoting

effects (e.g. **164**)[60], multi-drug-resistance (e.g. **165**)[61], antimicrobial (e.g. **163**,)[59] and anti-inflammatory (e.g. **166**)[62] activity, cytotoxic (e.g. **167**)[63] as well as immunomodulatory (e.g. **167**)[48] and also pesticidal activity (e.g. **168**)[64].

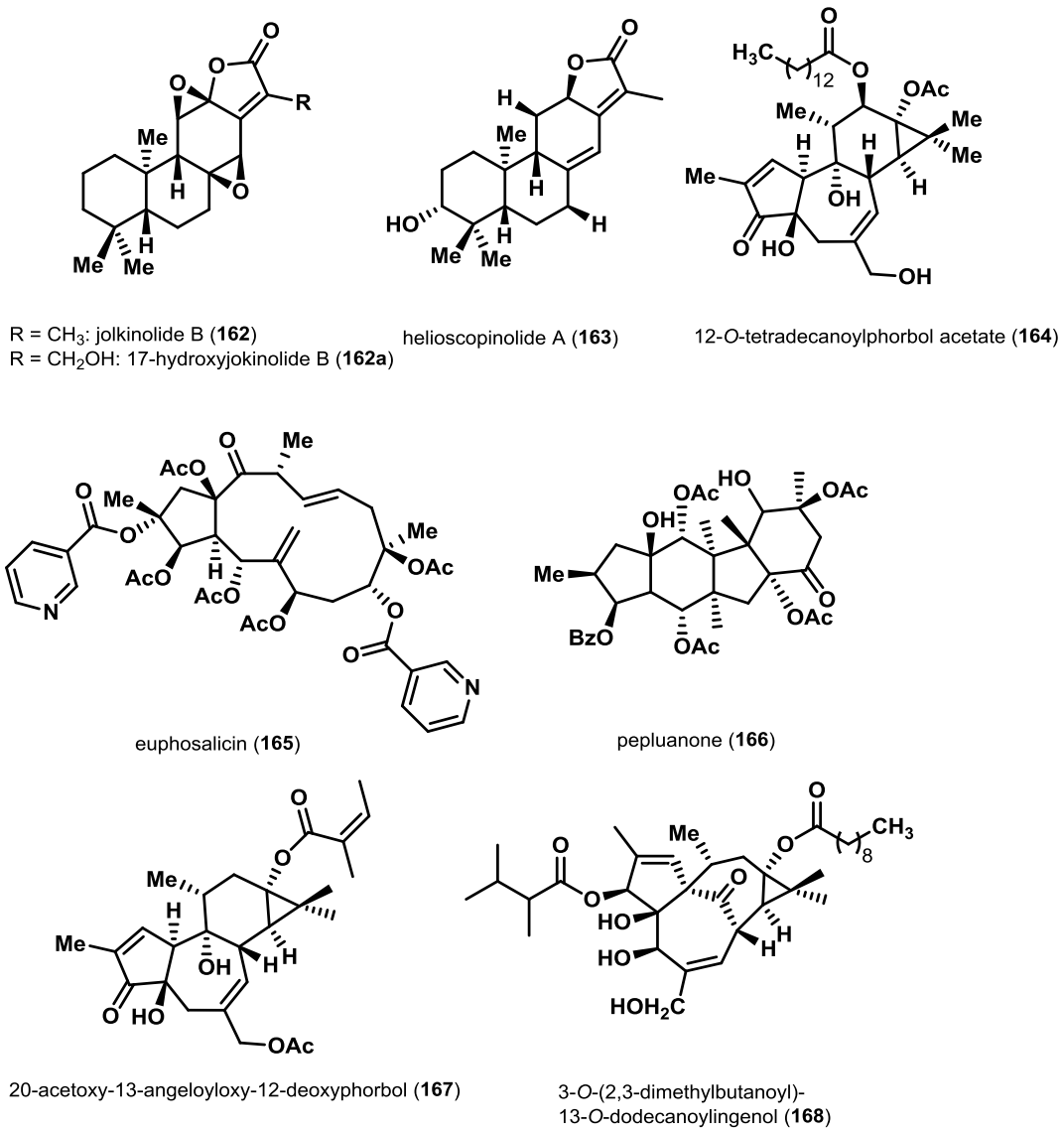

Figure 10. Selected biologically active *Euphorbia* diterpenoids.

The by far most famous *Euphorbia* diterpenoid in the pharmaceutical field is ingenol mebutate (**169**), also known as ingenol-3-angelate or under its LEO Pharma trade name Picato (Figure 11). Numerous clinical studies have been performed with this compound and it is currently a well-established drug for the treatment of skin cancer.[48]

Other highly promising targets are prostratin (**170**) and resiniferatoxin (**171**) (Figure 11). The latter is of considerable interest due to its ability to activate latent viral reservoirs and to protect healthy cells from infection; therefore, it currently serves as a lead compound for the treatment of

latent HIV infections.[65] Resiniferatoxin (**171**) is an ultrapotent vanilloid receptor agonist.[66] By activating a Ca^{2+} cation channel expressed in a subpopulation of primary afferent sensory neurons, it has already been investigated in phase II and III clinical evaluation for the therapy of long-lasting analgesia.[66]

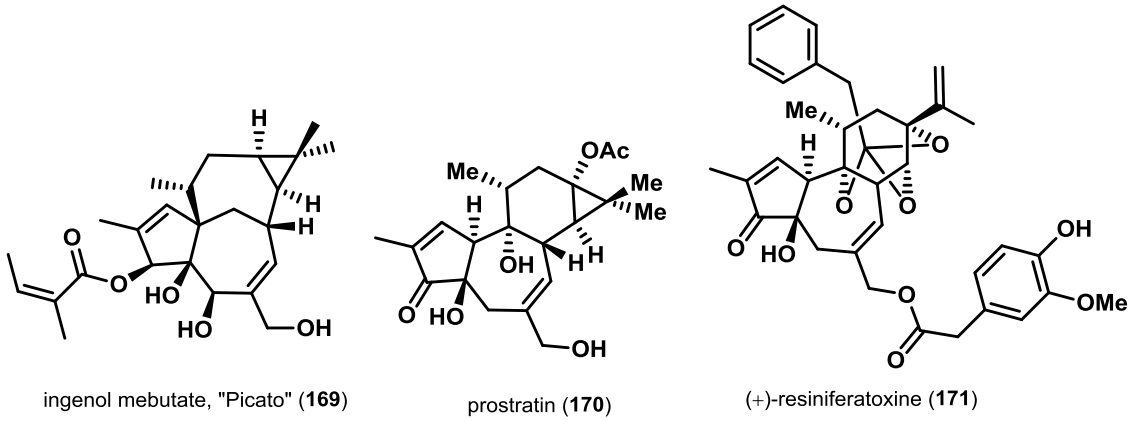

Figure 11. Selected structures of *Euphorbia* diterpenoids used in clinical studies.

These examples demonstrate that the field of *Euphorbia* diterpenoid natural products is highly interesting for pharmaceutical industry. However, the sustainable harvesting of significant amounts of the source organism still remains a major challenge. Therefore, the development of efficient synthetic routes for total synthesis will not only deliver sufficient amounts for clinical trials, but also establishes the possibility for the discovery of possible active synthetic intermediates. Selected examples of efficient and elegant total syntheses of *Euphorbia* diterpenoids will be showcased in the following chapter.

1.1.3 *Euphorbia* Diterpenoids in Natural Product Synthesis

Many total syntheses of a variety of structurally complex *Euphorbia* diterpenoids have been accomplished over the last decades. Due to their highly promising bioactivities and interesting structures, ingenol and its derivatives represent one of the most investigated targets in the synthesis of such diterpenoids. The challenging constitution of these complex skeletons is reflected by the natural product ingenol (**182**).[66] Since its isolation in 1968[67], four total syntheses[55][29][68][69], one formal synthesis[70] and several approaches[71] have been reported.

Among them, the enantioselective synthesis of (–)-ingenol (**183**) by Baran and co-workers in 2013 still remains the most concise synthesis so far.[55] This biosynthetically inspired synthesis was completed in merely 14 steps starting from commercially available (+)-3-carene (**172**) (Scheme 25). Chlorination and ozonolysis of **172** afforded ketone **173**. Subsequent installation of the methyl group and coupling with **174** was realized performing a one-pot protocol. This

consisted of reductive enolate formation-methylation and a second deprotonation followed by addition of the formed enolate to compound **174**, yielding **175** in 44% as a single diastereomer. **175** was further treated with ethynylmagnesium bromide (**176**) followed by silyl protection of the two hydroxyl groups to afford **177**, setting the basis for the envisioned allenic Pauson–Khand-type reaction. The latter proceeded smoothly in 72% yield. The addition of methylmagnesium bromide to ketone **178** delivered the corresponding carbinol stereoselectively. Treatment with OsO_4 and protection of the resulting diol with *N*,*N*-carbonyldiimidazole (CDI) afforded carbonate **179** in 68% stereoselectively. Treatment of **179** with $BF_3{\cdot}OEt_2$ implemented the bio-inspired key pinacol rearrangement, establishing the strained *in*/*out* stereochemistry of ingenane-structures. Allylic oxidation and *in situ* protection of the hydroxyl group followed by cleavage of the TBS group accomplished the formation of **181**. Finally, dehydration was performed using Martin´s sulfurane and regioselective hydroxylation with SeO_2 triggered the transformation into (–)-ingenol (**182**). The total synthesis was completed in 1.2% overall yield and showcases an efficient and powerful example of a biomimetically inspired total synthesis.

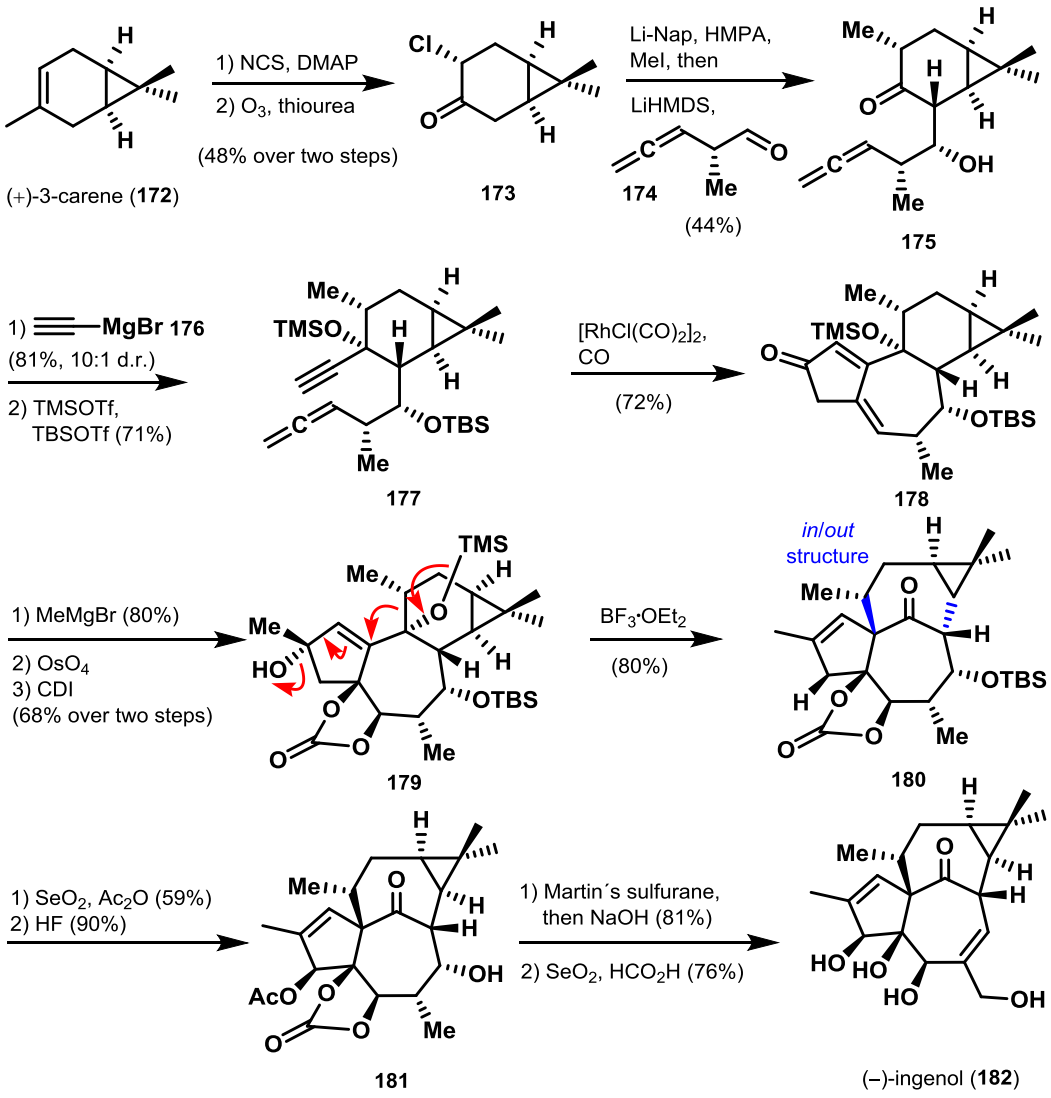

Scheme 25. Baran´s total synthesis of (–)-ingenol (182).[55]

Further interesting *Euphorbia* compounds can be found among the jatrophone-type diterpenoids. Featuring significant inhibitory effects against a variety of cell lines including lung carcinoma, lymphocytic leukemia and intramolecular carcinsarcoma, these compounds have been highly interesting targets for total synthesis. For instance, the group of Smith III investigated the synthesis of these skeletal types and accomplished the first total synthesis of a jatrophone natural product - normethyljatrophone (**194**) - in 1981.[72]

As first building block, aldehyde **185** was prepared starting from 3,3-dimethyl-4-pentynoic acid (**183**) in 55% yield following a four-step sequence. Therefore, the generated dianion from **183** was treated with an excess of propanal followed by TBS protection of the resultant alcohol yielding **184**. A reduction-oxidation sequence then furnished aldehyde **185**. The second coupling partner cyclopentene **187** was constructed following a five-step sequence starting from α-(hydroxymethyl)cyclopentenone (**186**) previously established by the same group.

Construction of spiro-furanone carbocycle **188** was accomplished by aldol condensation of **185** and **187**, followed by oxidation to install the aldehyde moiety and subsequent acid-catalyzed deprotection and cyclization-dehydration in 68% overall yield. The envisioned key aldol cyclization was be realized by Mukaiyama aldol condensation of an acetal with a silyl enol ether. Therefore, the aldehyde group in **188** was converted into an acetal, followed by the formation of a silyl enol ether from the lower carbonyl group in **190**. Treatment of intermediate **191** with $TiCl_4$ resulted in a diastereomeric mixture (2:1) with **192** as the major product. Elimination was found to be possible with both isomers yielding **193** after very slow isomerization to the more stable (*Z*)-isomer. The final steps included a selective *cis*-hydrogenation using $PdSO_4$/pyridine yielding the undesired (*Z*)-double bond, which was isomerized to yield normethyljatrophone (**194**) in 71% yield over two steps.

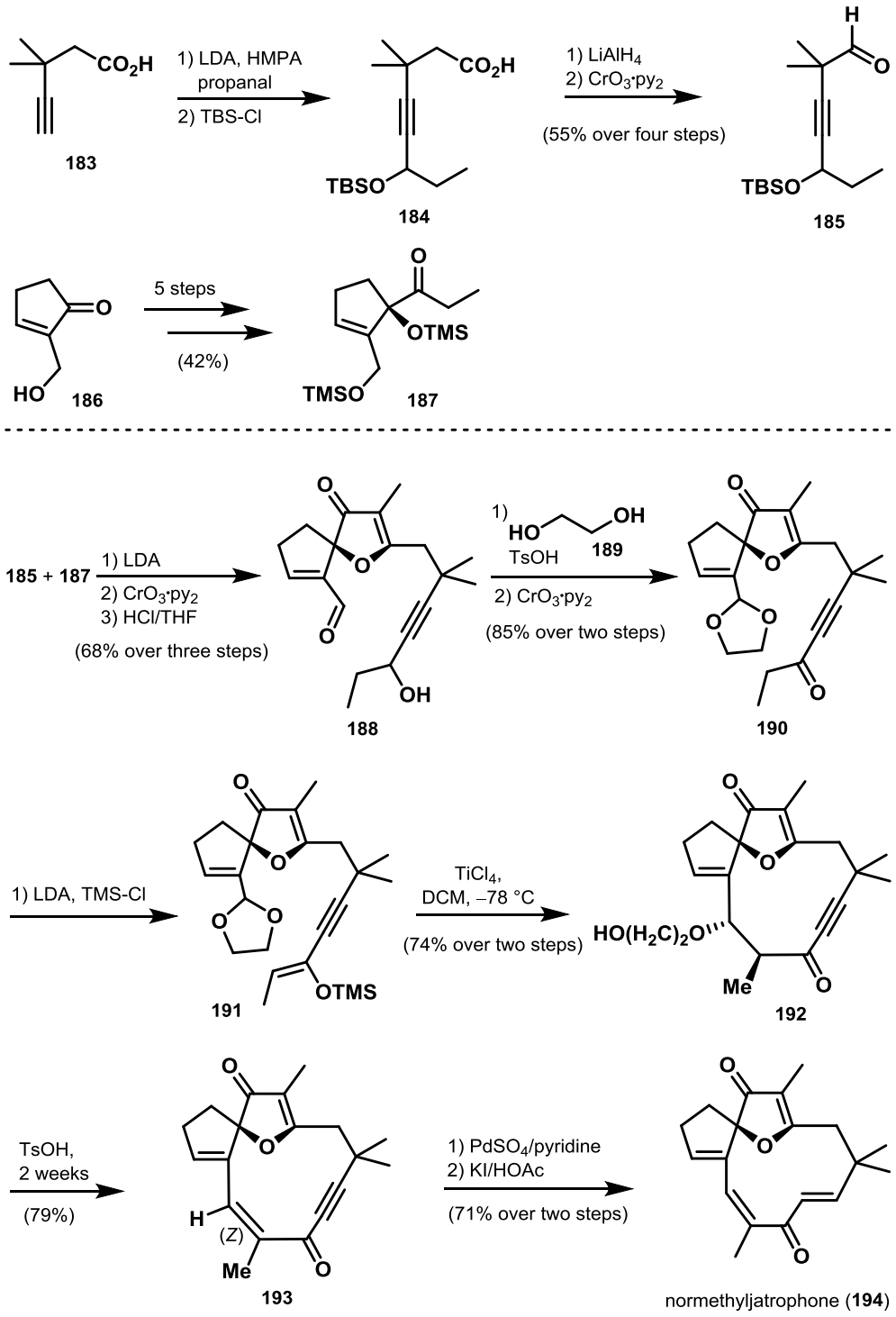

Scheme 26. Total synthesis of normethyljatrophone (194) by Smith III.[72]

As mentioned in Chapter 1.1.1 (Biosynthesis and Classification), the lathyrane skeleton is assumed to be the biosynthetic precursor of various *Euphorbia* diterpenoids. Therefore, synthetic investigations on this core structure seemed to be particularly attractive. The first total synthesis of a lathyrane-based carbon skeleton was realized with the synthetic accomplishment of the diterpenoid (–)-bertyadionol (**207**), also performed by the group of Smith III and co-workers.[73]

They completed the total synthesis in 18 steps starting from (–)-*cis*-chrysanthemic acid (**195**) (Scheme 27). Arndt–Eistert homologation afforded methyl ester **196**. Subsequent allylic oxidation and dithioacetal formation then gave access to **197**. Condensation of **197** with lithioethyl diethylphosphonate **198** yielded **199** in a 1:1 mixture of diastereomers and an overall yield of 35% over four steps. Subsequently, the formed dianion of **199** was mixed with compound **200** to afford enone **201** after acidic workup. Acetylation and reduction yielded a 1:1 mixture of alcohol **202**. 2-Tetrahydropyranyl (THP) ether formation followed by deprotection of the acetate moiety and Collins oxidation delivered enal **203**. For the construction of the marcocycle, **203** was treated with sodium hydride yielding enone **204**. Installation of a benzoate group was realized following a four-step sequence obtaining **205**. After installation of the methyl group, the benzoate moiety was removed under basic conditions. Finally, the dithioketal was oxidized to a monosulfoxide and subsequent hydrolysis completed the total synthesis of (–)-bertyadionol (**207**) in 23% over the last two steps.

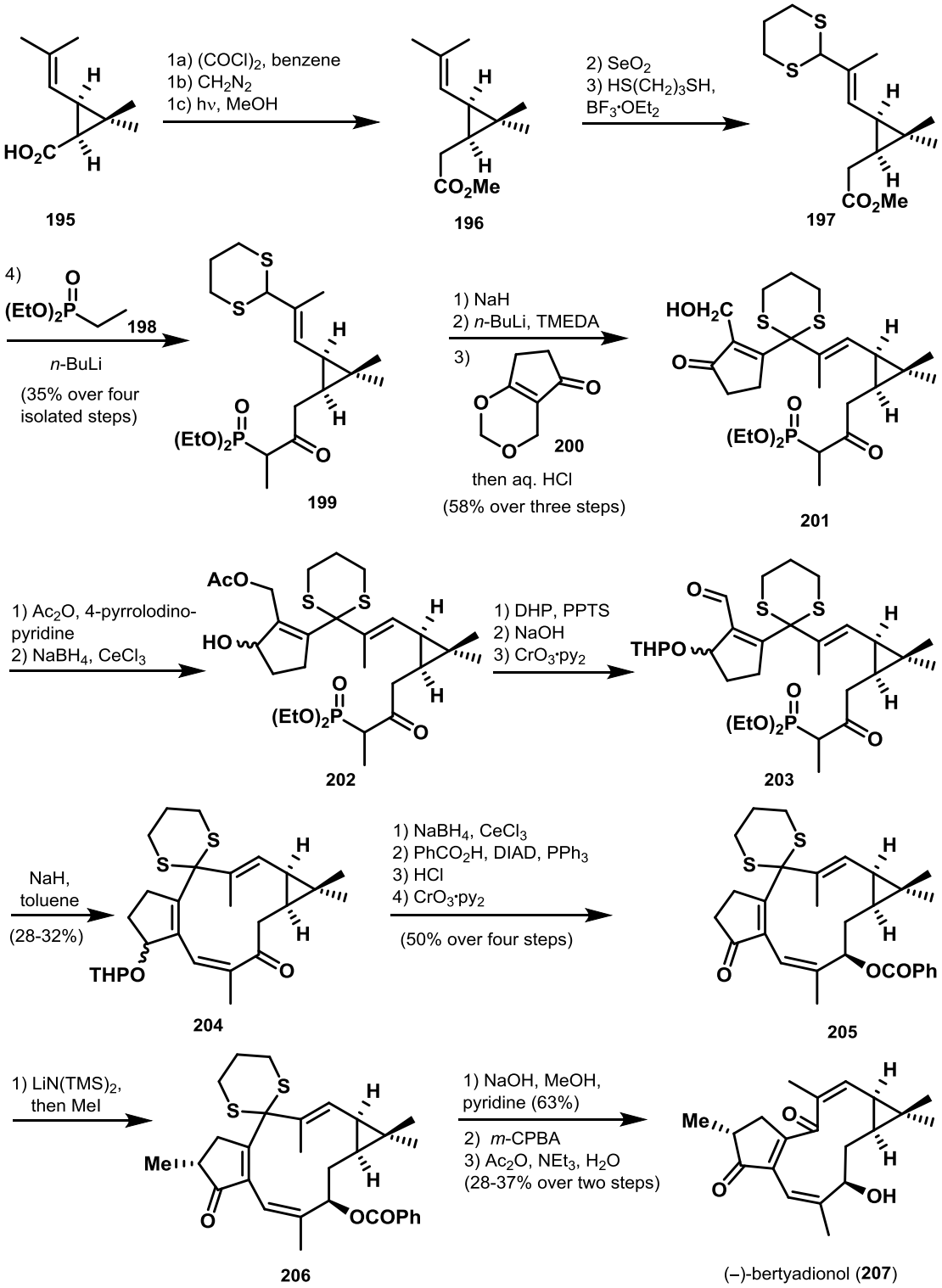

Scheme 27. Total synthesis of (–)-bertyadionol (207) by Smith III.[73]

1.2 *Euphorbia peplus* Diterpenoid Pepluacetal

Euphorbia peplus, also known as petty spurge, radium weed, cancer weed or milkweed, is a species of the genus *Euphorbia*. This annual growing plant is originally native to Europe, North Africa and West Asia, and a significant variety of natural products have been isolated from this species.[74] Among them, the natural product pepluacetal (**208**) was isolated recently and chosen as synthetic target for the second part of this thesis. Detailed information and characteristics of **208** will be discussed in the following.

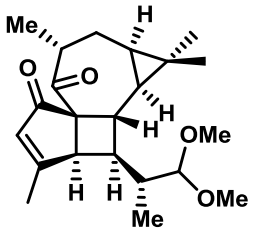

pepluacetal (**208**)

Figure 12. Structure of *Euphorbia peplus* diterpenoid pepluacetal (208).

1.2.1 Isolation, Biosynthesis and Bioactivity

Figure 13. Image of the *Euphorbia peplus* plant.[75]

Diterpenoid pepluacetal (**208**) was isolated in 2016 from *Euphorbia peplus* (Figure 13).[76] The natural product was isolated from 25 kg of air-dried powder of the plant, which was extracted, separated by flash column chromatography on silica gel and further purified by semi-preparative HPLC (2.3 mg).[76]

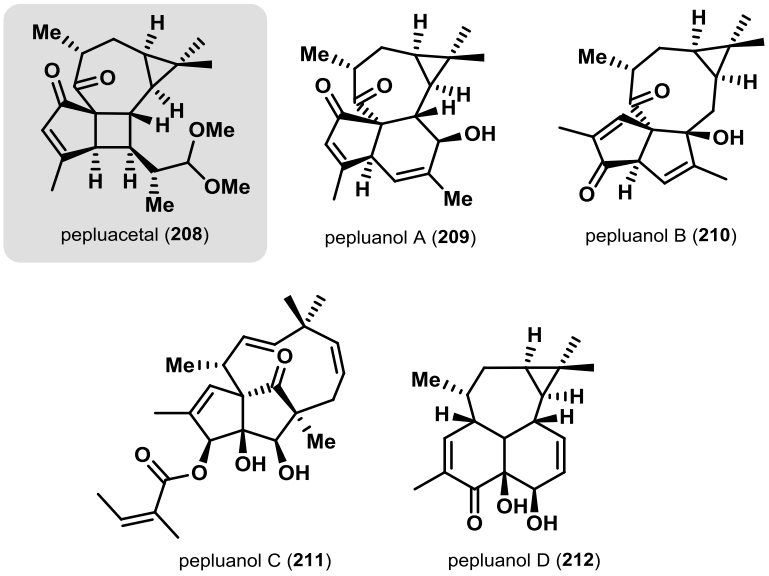

Figure 14. *E. peplus* diterpenoids pepluacetal (208) and pepluanol A-D (209-212).

Pepluacetal (**208**) was isolated together with pepluanol A (**209**) and B (**210**), and two years later pepluanol C (**211**) and D (**212**) were isolated by the same group (Figure 14).[77] In the *Euphorbia* family roughly 25 different carbon skeletons are reported so far, however pepluacetal (**208**) and the pepluanols A-D (**209 - 212**) represent completely new structural classes. Except for pepluanol C (**211**) they all consist of a tetracyclic ring system and share the cyclopropane ring with an attached gem-dimethyl group. Pepluacetal (**208**) additionally features a four-membered cycle (Figure 15). Furthermore, pepluacetal (**208**) exhibits an unprecedented 5/4/7/3 ring system and seven contiguous stereogenic centers with one being quaternary.

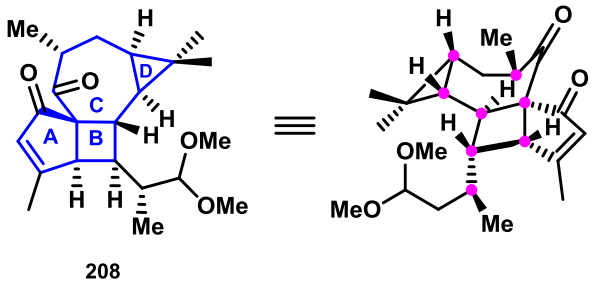

Figure 15. Different representations of pepluacetal (208).

The biosynthesis of pepluacetal (**208**), pepluanol A (**209**) and pepluanol B (**210**) was proposed by Qiu and co-workers and starts from lathyrane skeleton **213** (Scheme 28).[76] The authors suggest that pepluanol B (**210**) and intermediate **214** are formed after cyclization and oxidation of **213**. Intermediate **214** is assumed to be further converted into diketone **215** by oxidative rearrangement. Following conjugate addition of water should afford **216**, which is proposed to

undergo an acid catalyzed 1,2-methyl shift to obtain pepluanol A (**209**). Proceeding from **209** the authors suggest an isomerization of the double bond into conjugation, forming intermediate **217** followed by an intramolecular conjugate addition and acetal formation with methanol to finally obtain pepluacetal (**208**).

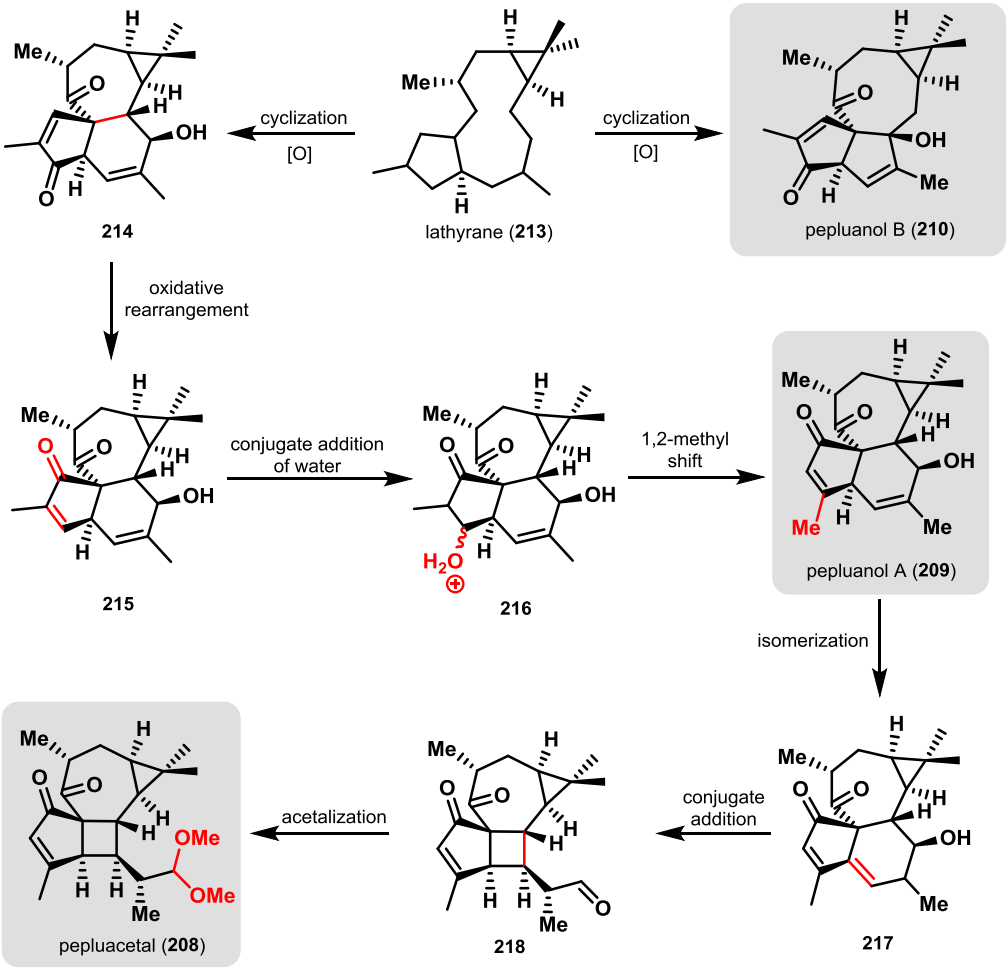

Scheme 28. Proposed mechanism of the biosynthesis of pepluacetal (208), pepluanol A (209) and pepluanol B (210).

Isolated pepluacetal (**209**) forms colorless crystals; therefore the absolute configuration could be determined by single crystal X-ray analysis (Figure 16), which was further consistent with the sequential correlations in the ROESY spectrum.

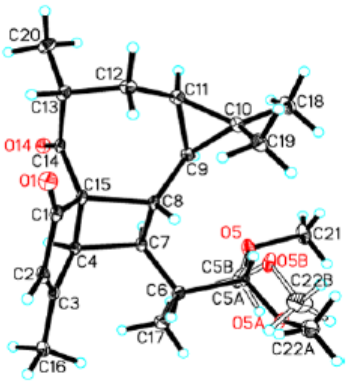

Figure 16. Single crystal X-ray structure of pepluacetal (208).[76]

Plants of *Euphorbia peplus* are traditionally used for the treatment of asthma and psoriasis.[78] This fact suggested the group of Qiu to investigate the activity of compounds **208 - 212** to affect the $K_v1.3$ channel, which is the predominant K^+ channel in the activated effector memory T_{EM} cells.[76] Therefore, $K_v1.3$ inhibitors can be used as T_{EM} cell-specific immunosuppressants for autoimmune disorders without suppressing the native immune response. It was found that all five natural products (pepluacetal (**208**), pepluanol A-D (**209-212**)) exhibit inhibitory effects against this channel. In their experiment, pepluanol B (**210**) showed the strongest effect with an IC_{50} value of 9.50 µM, whereas pepluanol A (**209**) and pepluacetal (**208**) inhibit $K_v1.3$ by a ratio of 24.9±8.6% and 46.0±9.1% at a concentration of 30 µM, respectively.[76] For pepluanol C (**211**), an inhibitory ratio of 31.6±8.3%, and for pepluanol D (**212**), a ratio of 30.5±2.8% was found.[77] The implication of these results is that the genus *Euphorbia* is not only a pool of new diterpenoid structures, but also a source of promising $K_v1.3$ inhibitors.

1.2.2 Total Synthesis of Pepluanol A

Among the recently isolated structures presented in the previous chapter, the total synthesis of pepluanol A (**209**) was accomplished only one year after its structural elucidation. The group of Ding and co-workers established an efficient diastereoselective total synthesis comprising 15 steps starting from literature known enone **219** (Scheme 29).[79]

Iodination of enone **219** and following Pd-catalyzed Negishi cross-coupling with homoallylzinc bromide **220** gave cycloheptenone **221** in good yield. Diels–Alder cycloaddition between **221** and Rawal diene **222** achieved the construction of the bicyclic ring in **209**. Acidic quenching of the reaction mixture allowed for the formation of cis-[6,7]-bicyclic diketone **223** in 83% yield as single diastereomer. After successful regioselective enol-triflation, the methyl moiety was installed via Cu-catalyzed cross-coupling yielding **224** in 72% over two steps. Inversion of the stereochemistry at C13 proceeded smoothly together with the removal of the benzoyl group and subsequent regioselective epoxidation of the double bond afforded **225**. After dehydration of hemiketal **225**, the terminal alkene was cleaved by Lemieux–Johnson oxidative cleavage, setting the stage for reductive annulation. The latter delivered tricyclic diol **227** as a 1:1 mixture of diastereomers in high yields. The structures could be confirmed by single crystal X-ray analysis. Installation of the missing cyclopropane moiety was further accomplished using *in situ* generated dibromocarbene. Due to the preferred boat transition state, installation of the cyclopropane proceeded exclusively from the convex face of the molecule and afforded tetracycle **228** in 44% yield after reductive bis-methylation. After regioselective oxidation of the alcohol at C3, Saegusa–Ito oxidation and silylation of the hydroxyl group at C7 afforded enone **229**. Pepluanol A (**209**) was finally accomplished after regioselective Grignard-addition of a methyl group, followed by Dauben–Michno oxidation and acid-induced desilylation in 59% yield over the last two steps.

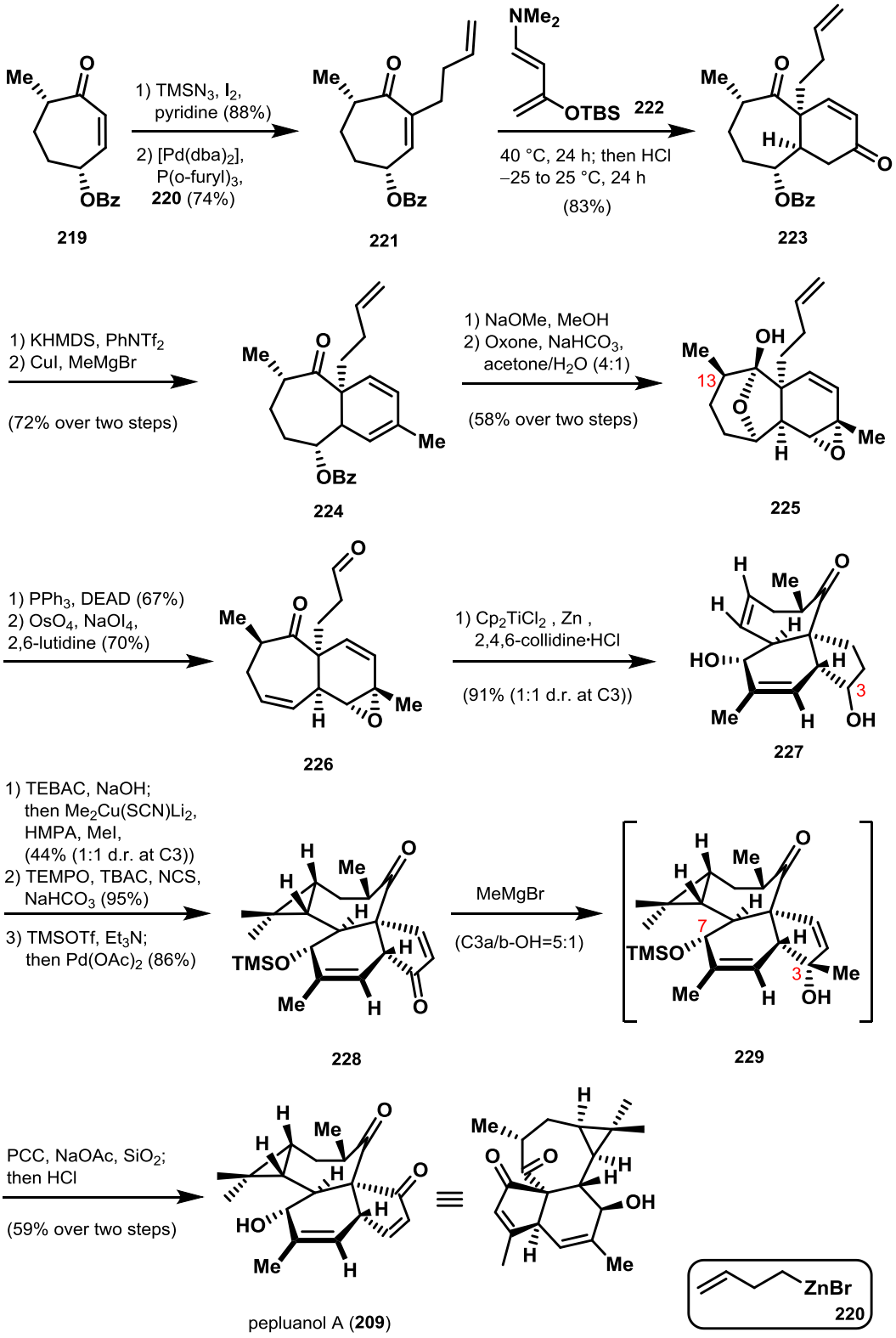

Scheme 29. Diastereoselective total synthesis of pepluanol A (209) by Ding and co-workers.[79]

1.3 The [2+2] Photocycloaddition Reaction

Within natural product synthesis photochemical reactions are particularly fascinating because of their unconventional nature. The absorption of light by a molecule enables reaction pathways that cannot be accessed by conventional methods. Consequently, remarkable transformations occur leading the starter unit to an entirely different outcome. Among photoinduced chemical reactions, the [2+2] photocycloaddition of olefins had by far the most impact on natural product synthesis.[80] Since this reaction was chosen by us as key step toward our total synthesis of pepluacetal (**208**), the following section provides a historical and mechanistical introduction and describes selected examples in natural product synthesis.

1.3.1 Historical Aspects

The first photochemical reaction was described by Liebermann in 1877.[81] Exposure of the natural product thymoquinone to sunlight led to dimerization product **230**, describing a formal [2+2] photodimerization reaction for the first time (Figure 17). 1908 was the year that marks the so-called intramolecular enone [2+2] photocycloaddition.[82] A noteworthy example is the synthesis of carvonecamphor (**231**) by exposing (+)-carvone to sunlight.[83][84] Barely 60 years later, intermolecular [2+2] photocycloaddition reactions were investigated for the first time. Early structures obtained by this chemistry were reported by the group of Schneck[85] with the synthesis of *rac*-**232**, and Eaton and co-workers[86] with the synthetic studies toward *rac*-**233**.

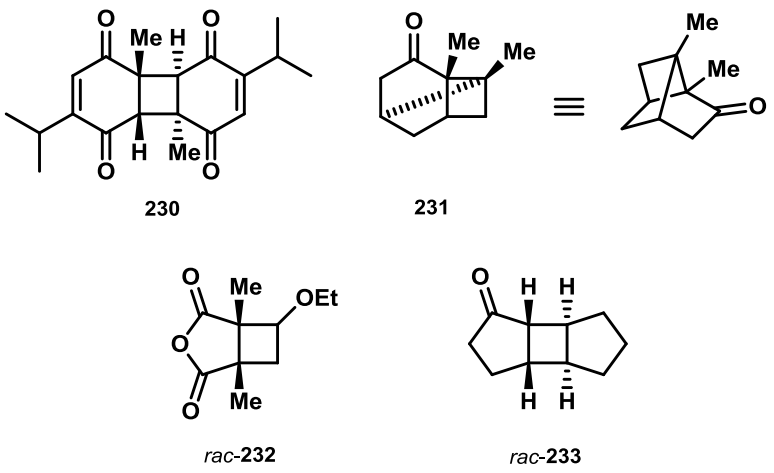

Figure 17. Selected historically relevant [2+2] photocyclization products.

1.3.2 Mechanistical Aspects

The basic reaction includes the direct excitation of an olefin (**234**) from its ground state S_0 to its first excited singlet state S_1 (Scheme 30). Subsequent reactions are either the addition to another olefin or a dimerization process.[82]

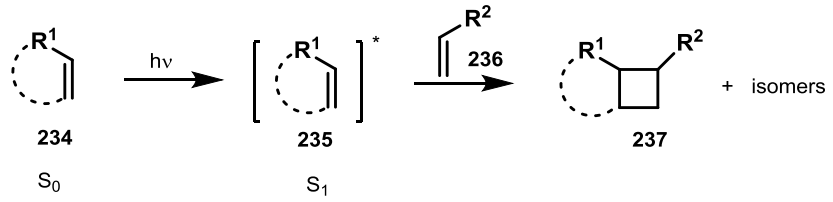

Scheme 30. Photoinduced [2+2] cycloaddition of an olefin 234 via its first excited singlet state 235.

To allow for a successful intermolecular [2+2] photocycloaddition, a long-lived excited state is desired to facilitate the attack of another olefin.[82] For this purpose conjugated enones are most suitable. With these substrates, direct excitation to the corresponding S_1 state is possible. From the S_1 state, intersystem crossing (ISC) to the respective triplet state is rapid and photochemical reactions can occur from the lowest-lying triplet state T_1, which is in most cases of $\pi\pi^*$ character (Scheme 31). The long lifetime of the T_1 state allows for an intermolecular attack of another olefin to generate a 1,4-diradical intermediate (**240**), from which final products are formed after ISC to S_1.[82]

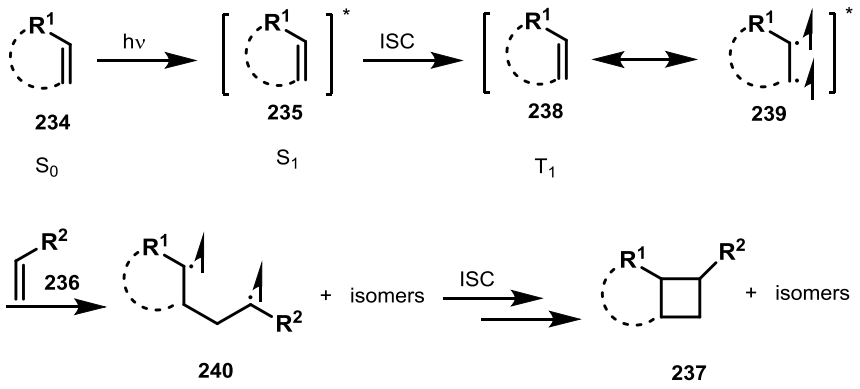

Scheme 31. Photoinduced [2+2] cycloaddition of an olefin 234 via its first excited triplet state T_1 238.

However, the direct excitation not always enables the population of the triplet state of an olefin. But this energy transfer can be induced by another photoexcited molecule, a so-called triplet sensitizer (Scheme 32). These compounds are characterized by low-lying S_1 and high-lying T_1 states with preferably high ISC rates. Energy transfer from the T_1 state of these sensitizers to an olefin is possible. Typically, aromatic or aliphatic ketones are used as sensitizers, such as acetone (often used as solvent), benzophenone or acetophenone.[82]

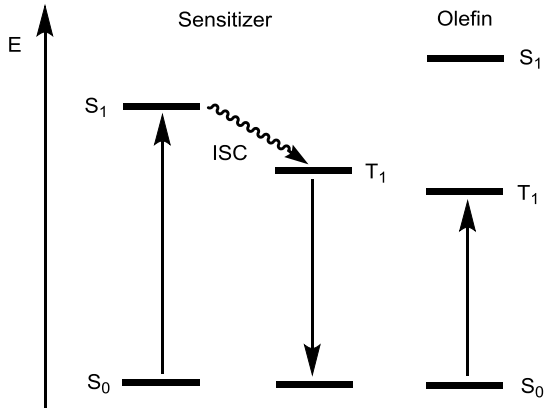

Scheme 32. Sensitization of an olefin via triplet energy transfer.

Photoinduced [2+2] cycloaddition reactions also occur in an intramolecular fashion, however with several limitations. The S_1 state of non-conjugated alkenes is higher, therefore higher energies are required for excitation, which is often not possible with conventional photochemical equipment.[87] Additionally, their triplet energies are higher compared to conjugated alkenes, which makes photocycloaddition between simple alkenes via direct irradiation or sensitization difficult. Other limitations are possible rotations around the C-C double bond in the case of a S_1 state with $\pi\pi^*$ character, which leads to efficient loss of energy. Additionally, the S_1 state of non-conjugated alkenes is often short-lived, which leads to competing photophysical pathways such as fluorescence and internal conversion (IC).

However, in the presence of transition metals a direct excitation is possible (Scheme 33). Additionally, the UV absorption maxima increase in the presence of a catalyst enabling [2+2] photocycloadditions. Among several reported transition metals used as catalysts in photochemical reactions[88], copper(I) salts have been found to be most efficient.[87] Especially their ability to catalyze with very high diastereoselectivity has established Cu(I) salts as the catalysts of choice. Among the copper(I) salts, Cu(OTf) has been found to be most efficient.[87] Due to the nature of its counterion, which does not coordinate to the olefin and therefore does not compete with the metal, Cu(OTf) or $Cu(OTf)_2$ are today the most commonly used catalysts for photoinduced [2+2] cycloaddition reactions with non-conjugated alkenes.

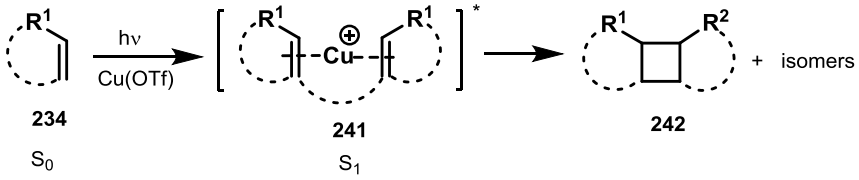

Scheme 33. Copper(I) catalyzed [2+2] photocycloaddition of olefins.

1.3.3 [2+2] Cycloaddition in Natural Product Synthesis

This chapter represents approaches toward the construction of similar structures compared to the core framework of pepluacetal (**208**) (highlighted in red in Figure 18).

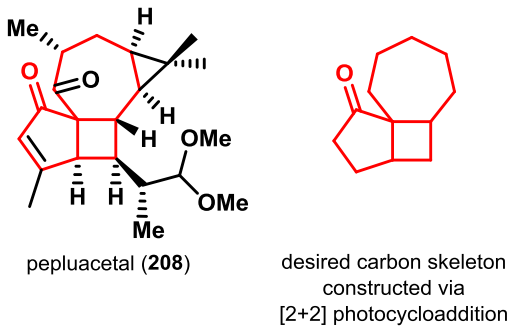

Figure 18. Envisioned carbon structure of pepluacetal (208) constructed via [2+2] photocyclization.

The construction of a similar core as pepluacetal was reported by Piva and co-workers covering investigations of an intramolecular [2+2] photocycloaddition of α,β-unsaturated oxoesters and oxoamides (Scheme 34, a)).[89] The authors were able to obtain cycloadducts like **244** by irradiation of the corresponding oxoesters **243** with very high selectivity.

In the total synthesis of tricyclic sequiterpene isocomene (**247**), the group of Pirrung also constructed a four/five-membered cyclic system in the course of a [2+2] photocycloaddition

(Scheme 34, b)).[90] In a single step, irradiation of **245** gave desired tricycle **246** including the construction of three contiguous, quaternary stereogenic centers.

For the construction of the natural product *epi*-precapnelladiene (**250**), Birch and Pattenden also investigated the construction of a four/five-membered cyclic system with the establishment of intermediate **249** starting from cyclohexenone **248** (Scheme 34, c)).[91]

Examples of Cu(I) catalyzed [2+2] photocycloadditions are well demonstrated by the total syntheses of (±)-kelsoene (**253**) by Bach and co-workers (Scheme 34, d))[92] and approaches toward the construction of the core of bielschowskysin (**256**) by the group of Ghosh (Scheme 34, e)).[93]

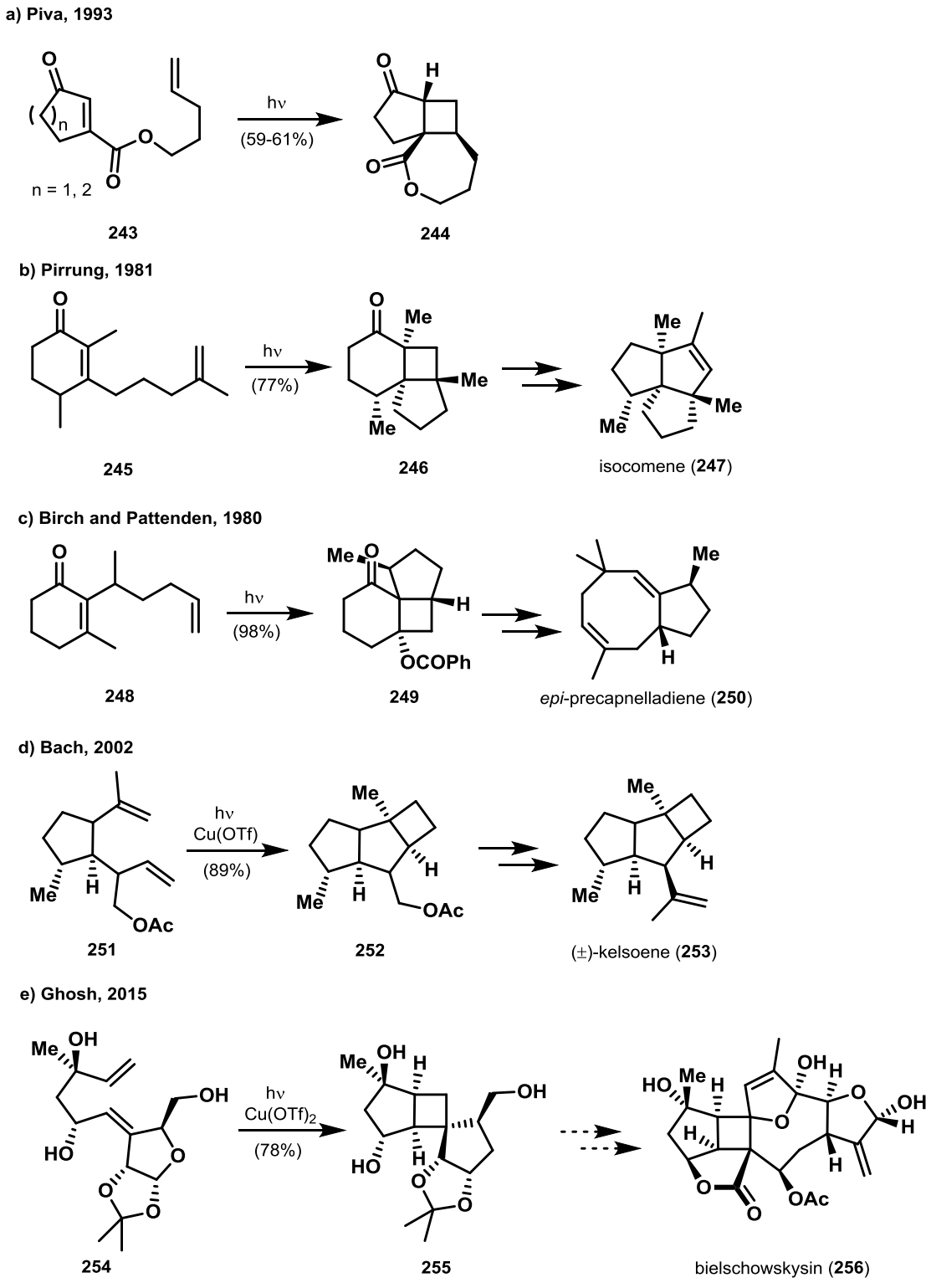

Scheme 34. Selected examples of [2+2] photocycloadditions in natural product synthesis.

2 Results and Discussion

Pepluacetal (**208**) represents a unique and highly complex target for total synthesis. The primary challenge lies in the successful construction of the sterically demanding tetracyclic carbon skeleton (containing a seven-, five-, four- and three-membered ring). We envisioned two distinct synthetic strategies to access pepluacetal (**208**) (Figure 19). In both approaches the central cyclobutane was foreseen to arise from a late-stage transannular [2+2] photocyclization. Cyclopentene derivative **257** would thus serve as a key intermediate and in the forward sense allow constructing the seven- and four-membered rings of pepluacetal (**208**) via a photoinduced [2+2] cycloaddition (Figure 19, strategy A). Alternatively, in strategy B, **258** which contains the seven-membered ring would serve as the cycloaddition precursor to forge the five- and four-membered ring system of the natural product.

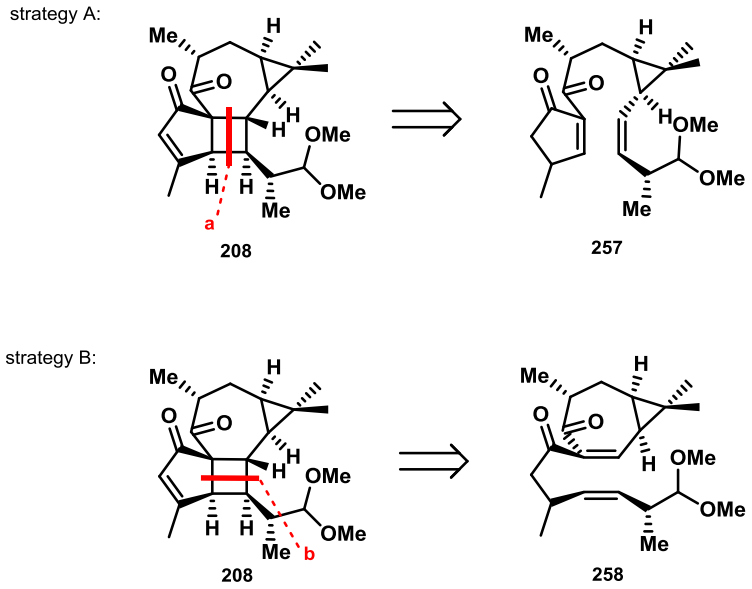

Figure 19. Retrosynthetic bond disconnections for the cyclobutane ring in pepluacetal (208).

2.1 First-generation Approach: Strategy A

In strategy A it was envisioned to commence the synthetic route from commercially available (+)-3-carene (**172**) targeting the total synthesis of the enantiomer of the natural product pepluacetal (**208**), due to the commercial availability of only one enantiomer of starting material **172**.

As outlined in the retrosynthetic analysis (Scheme 35), the key step of the synthesis was envisioned to be the photoinduced [2+2] cycloaddition reaction of **259** to construct the full carbon skeleton of the natural product. Cycloaddition precursor **259** could be derived from cyclopentene building block **261** and aldehyde **260** via a nucleophilic 1,2-addition in the forward sense. The

synthesis of **261** could be executed based on a known literature procedure, including a Nazarov-type cyclization between crotonyl chloride **262** and vinyltrimethylsilane **263**, followed by selective bromination and acetalization. With respect to the preparation of aldehyde **260**, selective installation of the *trans*-oriented double bond, which is required for the [2+2] photocyclization, was essential. **260** was thus traced back to methyl ester **264** and the appropriate olefination reagent **266.** In the forward sense, a diastereoselective olefination reaction between these building blocks would then give rise to desired (*E*)-alkene **260**. Olefination reagent **266** was planned to be prepared starting from (*R*)-Roche ester **267**. Methyl ester **264** was traced back to silyl enol ether **265**, which in turn could be obtained from cheap and readily available (+)-3-carene (**172**).

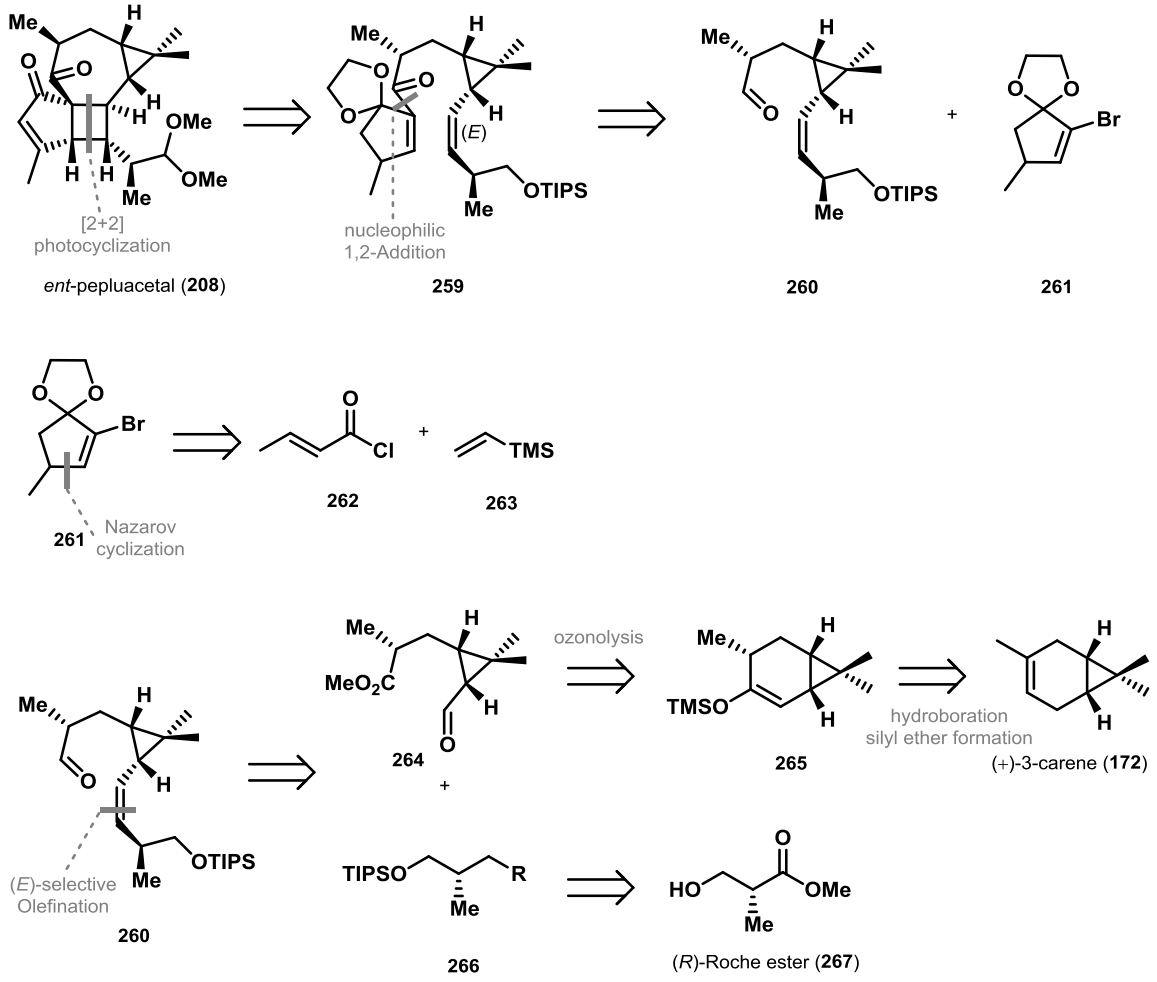

Scheme 35. Initial retrosynthetic analysis of *ent*-pepluacetal (208).

Cyclopentene building block **261** was synthesized in three steps (Scheme 36). Starting from crotonyl chloride (**262**) and vinyltrimethylsilane (**263**), cyclopentene **261** was prepared via a Nazarov-type cyclization in 70% yield.[94] Subsequent bromination in α-position and protection of the carbonyl group as the corresponding acetal gave vinyl bromide **261** in 62% over two steps.[95]

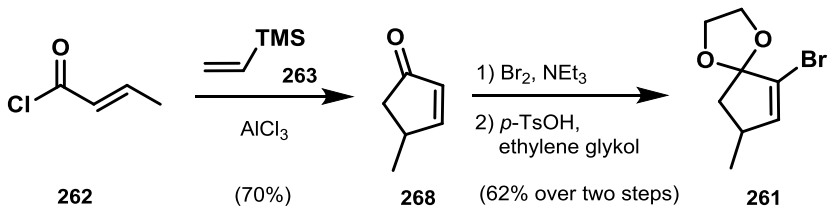

Scheme 36. Synthesis of cyclopentene building block 261.

The synthesis of methyl ester **264** was carried out according to a literature procedure that was optimized (Scheme 37).[96] Following hydroboration of (+)-3-carene (**172**), and further oxidation of the intermediate secondary alcohol, ketone **270** was obtained in 82% yield. Bicycle **270** was then converted into silyl enol ether **265**. Applying the literature reported reaction conditions using lithium diisopropylamide, we observed exclusive formation of the undesired and thermodynamically more stable silyl enol ether. Fortunately, use of sterically more demanding lithium tetramethylpiperidine (TMP) selectively gave silyl ether **265** as the desired kinetic product. Next, ozonolysis of the formed double bond was carried out to yield an intermediate carboxylic acid. Isolation and purification of the acid was initially performed using an acid-base wash of the crude reaction mixture to remove side products of the ozonolysis reaction. However, this workup proved to be challenging and due to the high polarity of the carboxylic acid led to low recovery of the desired product. Additionally, the instability of the intermediate carboxylic acid resulted in low yields for the ozonolysis reaction. Finally, it was discovered that treatment of the crude acid with trimethylsilyldiazomethane was more practical and allowed isolation of methyl ester **264** in 14% over three steps.

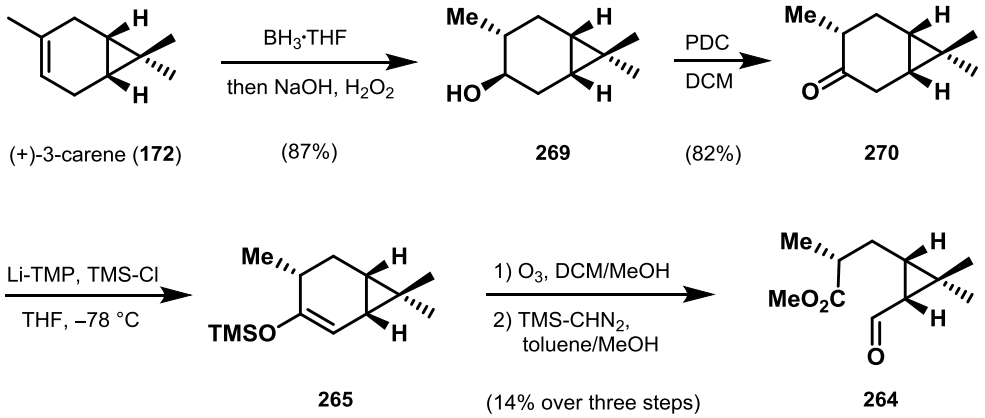

Scheme 37. Synthesis of methyl ester 264 using an optimized literature known procedure.

In order to achieve a successful [2+2] cycloaddition reaction, the geometry of the double bond in the precursor is required to be (*E*). Based on a literature survey focusing on methods for (*E*)-selective olefinations, we began our investigations with Horner-Wadsworth-Emmons (HWE) reaction conditions. On these grounds, phosphonium ester **274** was foreseen to be synthesized in

four steps starting from commercially available (*R*)-Roche ester (**267**) (Scheme 38).[97] The primary hydroxy group in **267** was converted into the corresponding triisopropylsilyl (TIPS) ether **271** in 97% yield. The TIPS group was chosen as protecting group due to its stability toward a variety of conditions. TIPS-protected Roche-ester **271** was next reduced to the corresponding alcohol **272** using DIBAL-H. Subsequently, **272** was converted into alkyl iodide **273** via Appel reaction which occurred in high yield. Unfortunately, a variety of investigated reaction conditions aiming at the preparation of phosphonium ester **274** proved to be unsuccessful and led to decomposition of starting material.

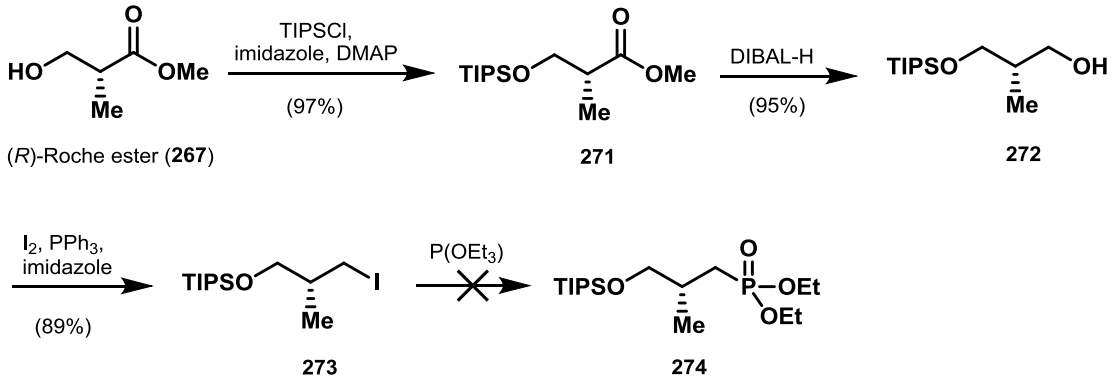

Scheme 38. Unsuccessful preparation of phosphonate 274 starting from (*R*)-Roche ester 267.

Next, we investigated the Silvestre Julia modification of the Wittig reaction.[98] Therefore sulfonium oxide **278** was prepared from TBS-protected alcohol **275** in two steps (Scheme 39).[99]* Mitsunobu reaction afforded sulfide **276** which, following oxidation with hydrogen peroxide and ammonium heptamolybdate tetrahydrate at elevated temperature, gave rise to the Silvestre Julia reagent **277** in high yield.

*Optimization of the synthetic steps shown in Scheme 39 was carried out by B.Sc. Valentin Bruder.

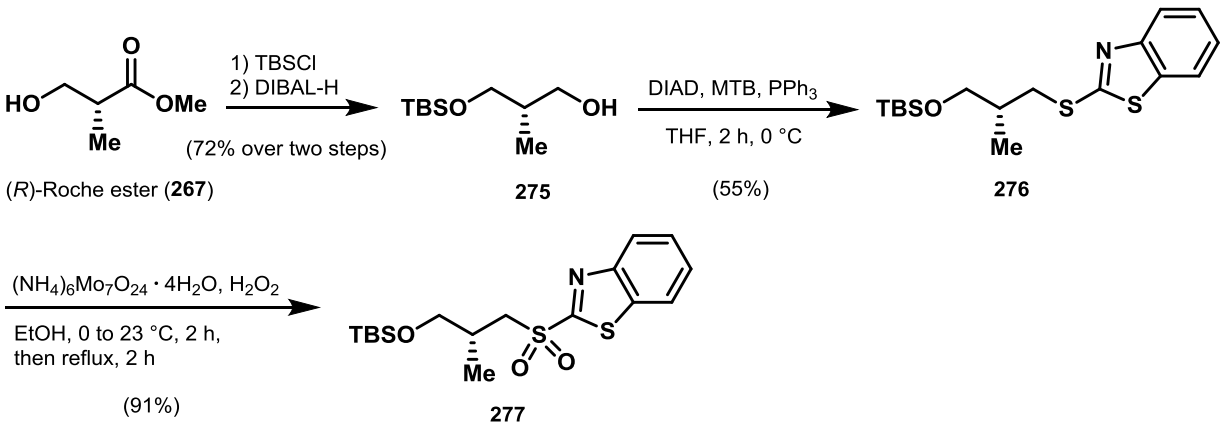

Scheme 39. Synthesis of Silvestre Julia reagent 277.

With reagent **277** in hand, selective olefination of methyl ester **264** was investigated next (Table 5). Following a survey of various reaction conditions, it was observed that mixtures of (*E*)- and (*Z*)-isomers **278** and **279** were formed in moderate yields. Importantly, it was established that the (*E/Z*)-ratio was influenced by the base counter ion as well as the choice of solvent. As such, lithium counter ion gave the highest (*E*)-selectivity (3:1), while potassium was less selective (1.25:1) (entry 2, 4).

These results are not in line with numerous studies reported in the literature[100] but are in agreement with the results found by Liu and Jacobsen in their synthetic studies on the natural product (+)-ambrutucin.[101] Aiming to further increase the (*E)*-selectivity in this transformation, different solvent systems with NaHMDS were investigated. Since literature reports indicate that an increased (*E*)-selectivity may occur with polar and coordinating solvents, dimethoxy ethane (DME) and dimethyl formamide (DMF) were examined (entry 5, 6). However, while an improved yield was obtained in the case of DME, the selectivity was not favorably influenced by this modification. Since dimerization of sulfone reagent **277** was detected under some reaction conditions, we applied the Barbier procedure and changed the order of reagent addition. On these grounds, a premixed solution of aldehyde **264** and sulfone **277** in THF was treated with LiHMDS at low temperature (entry 7).[102] Disappointingly, only a slightly improved (*E*)-selectivity at the cost of a decreased yield was observed.

Table 5. Investigation of Julia olefination of methyl ester 264 with reagent 277.[**]

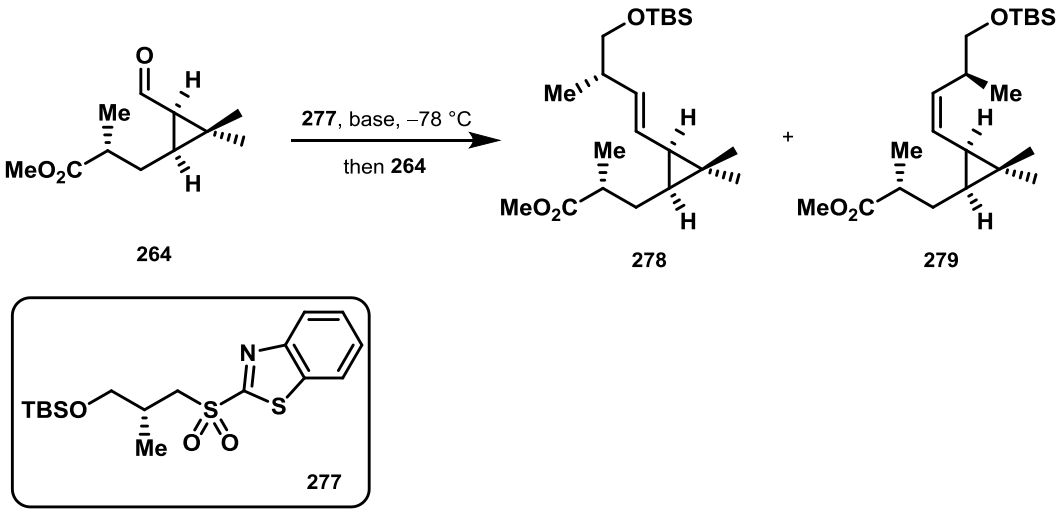

Entry	Base (equiv)	Solvent	Ratio	Yield[a]
1	LDA	THF	3:1	52%
2	LiHMDS	THF	3:1	49%
3	NaHMDS	THF	2.8:1	39%
4	KHMDS	THF	1.25:1	47%
5	NaHMDS	DMF	5.25:1	27%
6	NaHMDS	DME	4:1	57%
7	LiHMDS	THF	4:1	43%

[a]isolated yields of a mixture of both double bond isomers.

Isomers **278** and **279** proved to be inseparable by standard silica gel flash column chromatography or reverse phase HPLC, thus requiring us to develop an olefination protocol which would occur with near perfect (*E*)-selectivity. Therefore, various further stereoselective olefination methodologies were examined. The Schlosser modification represents a variant of the classic Wittig olefination.[103] This reaction allows for the selective formation of (*E*)-alkenes with non-stabilized yildes using an excess of lithium salts. Therefore a mixture of alkyl iodide **273** and triphenylphosphine in MeCN was heated at 82 °C for 24 h to furnish phosphonium salt **280** in satisfying yield after recrystallization (Scheme 40).

[**]Experiments listed in Table 5 were carried out by B.Sc. Valentin Bruder.

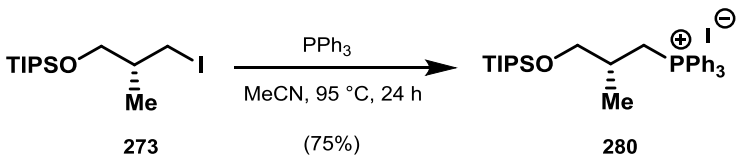

Scheme 40. Synthesis of phosphonium salt 280.

Unfortunately, investigating the standard Schlosser olefination conditions only of starting material was observed (Table 6, entry 1). The addition of lithium salts can induce improved stereocontrol in this reaction and is believed to promote the ring opening of the oxaphosphetane intermediate.[104][105] However, addition of LiBr also was non-productive and resulted in decomposition of **264** (entry 2). Alternatively, use of KHMDS and quenching the reaction with a large excess of MeOH was investigated (entry 3). The group of Kim and co-workers reported high diastereoselectivities for the olefination with non-stabilized ylides applying this procedure.[106] Unfortunately, no desired product was formed under these reaction conditions and decomposition of starting material was observed.

Table 6. Attempts for (*E*)-selective olefination with phosphonium salt 280 applying Schlosser conditions.

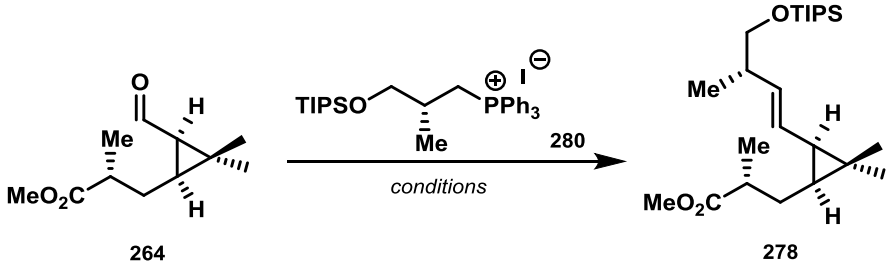

Entry	Conditions (equiv)	Additives	Solvent	Observation
1	PhLi (4), KO*t*-Bu (2.5), HCl	-	THF/Et_2O	decomposition
2	PhLi (4), KO*t*-Bu (2.5), HCl	LiBr	THF/Et_2O	decomposition
3	KHMDS (1.3)	MeOH	THF	decomposition

When performing the olefination reaction under standard Wittig conditions using KHMDS a 1:10 ratio of (*E*:*Z*)-double bond isomers was obtained in satisfying yields of 65% (Scheme 41). We decided to also investigate isomerization of (*Z*)-isomer **279** to the presumably more stable (*E*) double bond isomer **278**. However, both heating the reaction mixture at reflux and radical conditions using diphenyldiselenide resulted in no conversion of (*Z*)-alkene **279**.

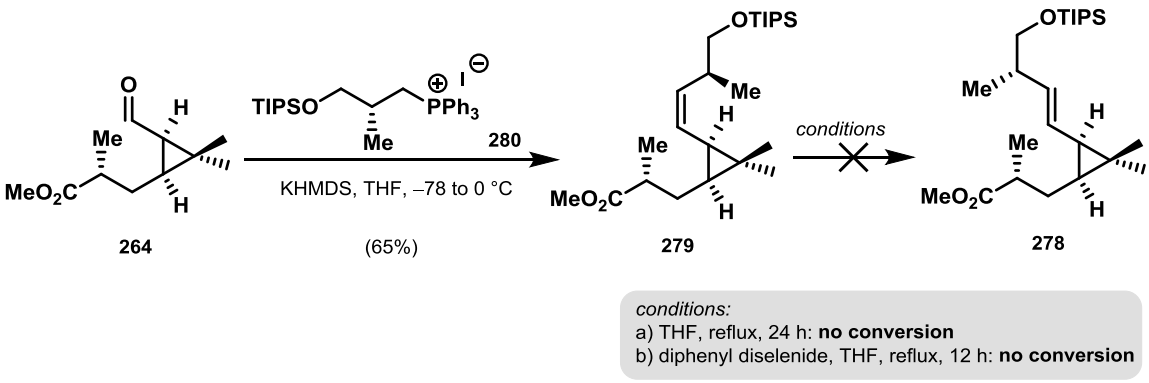

Scheme 41. Attempts for isomerization of the double bond in 279.

Next, we investigated an olefin cross-metathesis approach using Grubbs 2nd generation catalyst (Scheme 42). Therefore, we followed the work from Danoldson and Lukesh who investigated a similar substrate to ours.[107] Methyl ester **264** and TIPS-protected Roche ester **282** were both subjected the Wittig olefination to give alkenes **281**[108] and **283**[109], respectively. Treatment of a mixture of olefins **281** and **283** with Grubbs 2nd generation catalyst gave rise to a complex mixture of unidentified products and only trace amounts of desired olefin **278**.

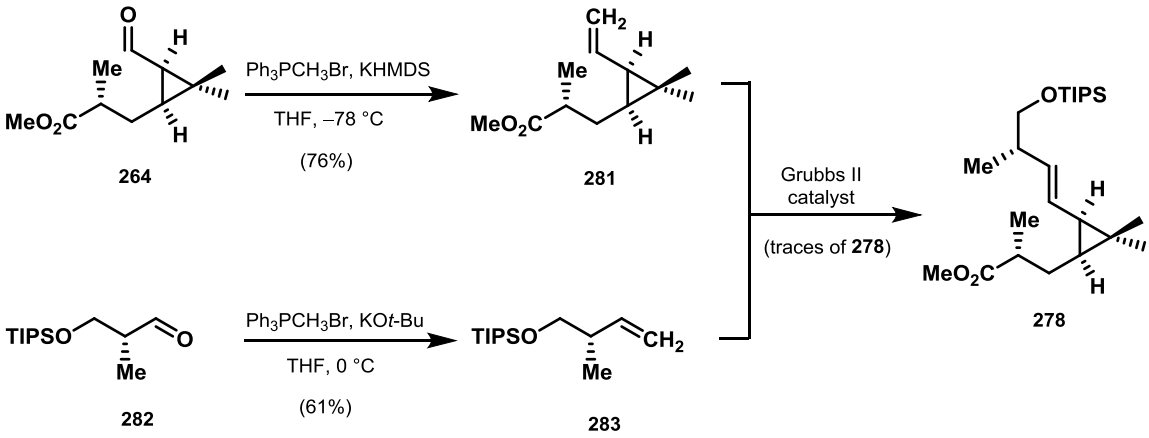

Scheme 42. Synthetic attempts of olefin 278 via cross-metathesis using Grubbs 2nd generation catalyst.

A further strategy for *trans*-selective olefinations was reported by Corey and Kwiatkowski in 1966.[110] They developed a procedure for the formation of olefins from phosphonic acid bisamides and carbonyl compounds. Ever since then cyclic phosphonamide reagents have proven to be an efficient method for diastereoselective olefination reactions. Mechanistically this reaction proceeds via the intermediates depicted in Scheme 43.[111] Deprotonation of phosphonamide **284** with *n*-BuLi and following treatment of the so-formed anion with a carbonyl compound (**285**) results in formation of the corresponding alkene **288** via the intermediacy of **286** and **287**. Upon treatment of oxaphosphetane oxide **287** with acetic acid at –78 °C, olefin **288** is formed with high *trans*-selectivity.

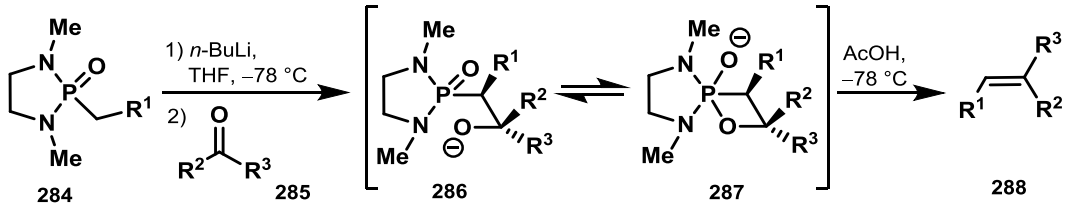

Scheme 43. Mechanism for olefinations with phosphonamide anions.

Hanessian and co-workers employed this type of phosphonamide in their studies on the total synthesis of the antifungal natural product (+)-ambruticine (**292**) (Scheme 44).[112] Using reagent **289** and ketone **290**, they prepared olefin **291** as a 6:1 mixture of separable (*E*/*Z*)-isomers. These results inspired us to investigate a related approach for the challenging (*E*)-selective olefination of aldehyde **264**.

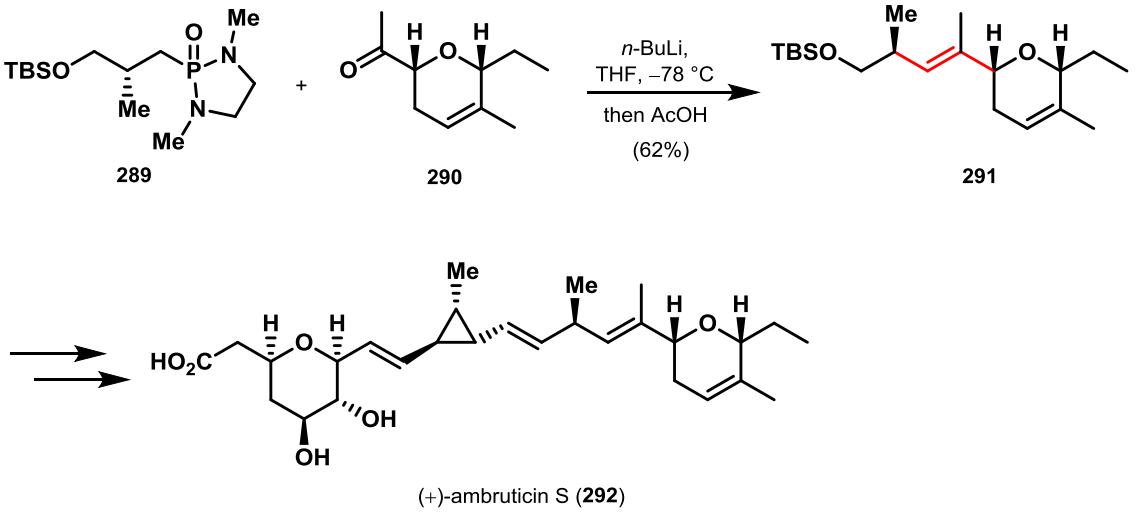

Scheme 44. Stereoselective olefination in the total synthesis of (+)-ambruticin S (292).[112]

Thus, phosphonium oxide **295** was prepared from *N*,*N*′-dimethylethylenediamine (**293**) in a single step.[112] Alkylation of **294** with alkyl iodide **273** proceeded smoothly and gave rise to phosphonamide **295** in 68% yield over two steps (Scheme 45).

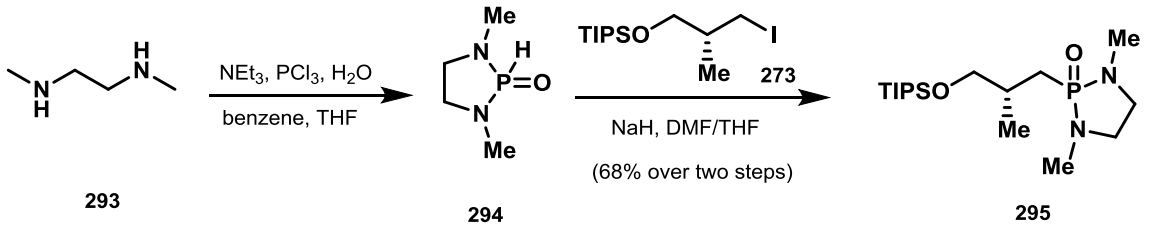

Scheme 45. Synthesis of phosphonamide 295.

With phosphonamide **295** in hand, *trans*-selective olefination of methyl ester **264** was investigated and optimization attempts are summarized in Table 7. Gratifyingly, deprotonation of **295** at low temperature followed by the addition of aldehyde **264** and quenching the reaction with AcOH furnished olefin **278** as a single (*E*)-isomer, albeit in 25% yield (entry 1). Unfortunately, various optimization attempts aimed at improving the yield by prolonging the reaction time or conducting the reaction at higher temperature merely resulted in a slight increase in yield (entry 2).

Initial studies by Corey and co-workers reported the intermediate ß-hydroxy phosphonamides as highly stable and readily isolable compounds.[113] Since in our system full conversion of starting material was observed by analysis by thin layer chromatography, we hypothesiyed that incomplete elimination might be causing the low yields. However, contrary to the results by Corey, we weren't able to isolate a ß-hydroxy phosphonamide species. Attempts to further react the crude reaction mixture by heating to reflux in dry benzene or toluene, as described in original studies, merely resulted in decomposition (entry 3).[113] Also further addition of base, aimed at improving the elimination, resulted in a significant decrease in yield (entry 4, 5).

Table 7. (*E*)-selective olefination attempts with phosphonamide 295.

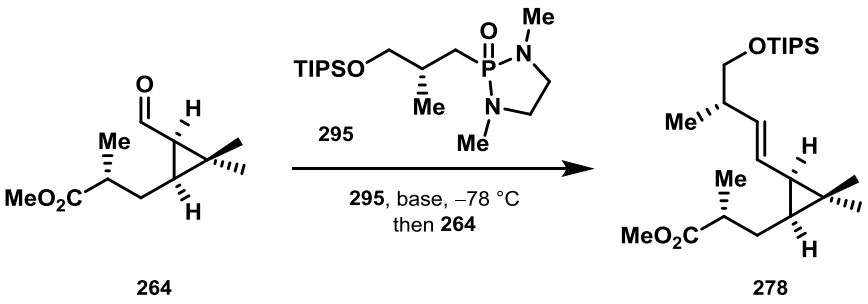

Entry	Conditions (equiv.)	T [°C]	t [h]	Yield
1	**295** (2.22), *n*-BuLi (1.88), AcOH	–78 to 0	1	25%
2	**295** (2.22), *n*-BuLi (1.88), AcOH	–78 to 23	2-15	32-34%
3[a]	**295** (2.22), *n*-BuLi (1.88), AcOH	–78 to 70	12	0% (decomposition)
4[a]	**295** (2.22), *n*-BuLi (3.76), AcOH	–78 to 23	15	14%
5[a]	**295** (4.44), *n*-BuLi (3.76), AcOH	–78 to 23	15	12%

[a]optimization of this step was carried out by B.Sc. Valentin Bruder.

Despite the low yields, the phosphonamide anion olefination method represented the only approach resulting in the desired near-perfect (*E*)-selectivity. Since separation of the double bond isomers could not be achieved by standard silica gel column chromatography we decided to continue our synthetic route using this methodology.

In order to perform the envisioned nucleophilic addition with cyclopentene building block **261**, methyl ester **278** was converted to aldehyde **260**. Therefore, methyl ester **278** was reduced to alcohol **296** in high yields using DIBAL-H at low temperature (Table 8).While treatment of alcohol **296** with activated MnO_2 resulted in no desired product formation (Table 8, entry 1), the use of chromium based oxidative reagents such as PDC (entry 2), Ley-Griffith oxidation conditions or DMP resulted in complete decomposition of starting material (entry 3, 4). Eventually it was discovered that oxidation with IBX in DMSO at low temperature furnished aldehyde **260** in good yield (entry 5).

Table 8. Oxidation conditions for alcohol 296.

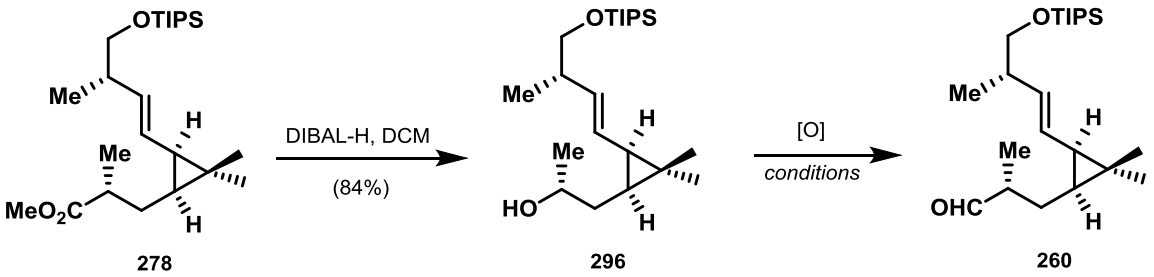

278 296 260

Entry	Conditions	Yield
1	MnO_2	0% (no conversion)
2	PDC	0% (decomposition)
3	TPAP, NMO, 4 Å MS	0% (decomposition)
4	DMP, $NaHCO_3$	0% (decomposition)
5	IBX, DMSO	79% (**260**)

With both vinyl bromide **261** and aldehyde **260** in hand, bromine-lithium exchange in the former compound and subsequent nucleophilic addition to **260** was investigated (Table 9). Generation of the lithiated species was initially attempted using *t*-BuLi. However, analysis by thin layer chromatography revealed low conversion of starting material even after prolonged reaction times and elevated temperature (entry 1). Attempts to improve the reactivity of *t*-BuLi by addition of HMPA resulted in a similar reaction outcome (entry 2). Fortunately, use of sterically less encumbered *n*-BuLi enabled the addition of **261** to aldehyde **260** for the first time (entry 3). A further improvement was achieved by transmetalation from lithium to cerium, using $CeCl_3$, affording addition product **297** in satisfying 66% yield (entry 4). Alcohol **297** was obtained as a 1:1 mixture of diastereomers which proved to be inseparable via standard silica gel column chromatography or reverse phase HPLC.

Table 9. Optimization of conditions for nucleophilic addition.

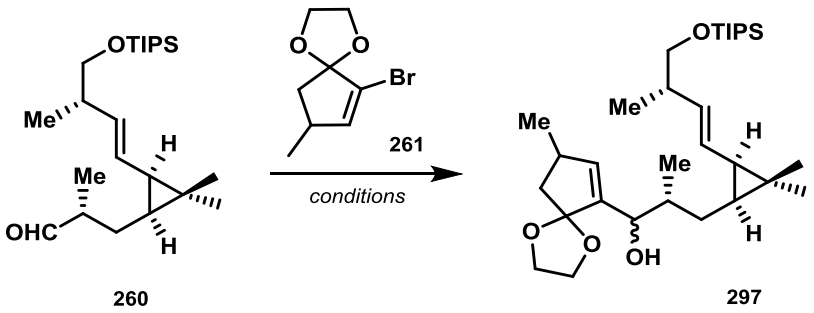

Entry	Conditions	Yield
1	*t*-BuLi	traces (**297**)
2	*t*-BuLi, HMPA	traces (**297**)
3	*n*-BuLi	37% (**297**)
4	*n*-BuLi, $CeCl_3$	66% (**297**)

As the substrate for the subsequent [2+2] photocyclization we prepared ketone **259**. Oxidation of the diastereomeric mixture of alcohol **297** was achieved using IBX at low temperature to furnish the key intermediate **259** in 50% yield (Scheme 46). At this stage of the synthesis we had successfully introduced the five-membered ring A and installed all carbon atoms that are present in the tetracyclic enantiomer of pepluacetal (**208**).

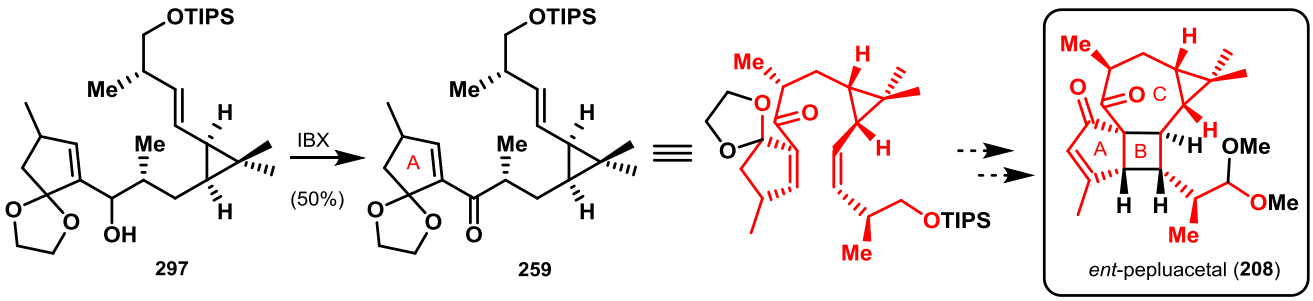

Scheme 46. Synthesis of key intermediate 259.

With key intermediate **259** in hand the envisioned [2+2] photocyclization for the construction of the full carbon skeleton was next investigated. The absorption spectrum of ketone **259** gave a maximum at 249 nm wavelength and additional maxima at 278 nm and 336 nm wavelengths. Based on careful evaluation of this spectroscopic data we proceeded to investigate the intramolecular [2+2] photocyclization of key intermediate **259** to construct the four- and seven-membered carbon cycles (Table 10). In this respect, different solvent systems with appropriate absorbing regions were examined (entry 1-6). Disappointingly, most reaction conditions investigated resulted in non-specific decomposition of the starting material **259**. In solvent

systems such as diethyl ether and THF (entry 3, 4) trace formation of reduced ketone **299** were detected by ^{1}H-NMR analysis which we assumed formed via hydride addition during workup of the crude reaction mixture. The use of triplet sensitizers, such as acetone, which was employed as the reaction solvent also resulted in decomposition (entry 6). Since UV-spectroscopic analysis had indicated an additional smaller absorption maximum at 336 nm, irradiation at 365 nm using MeCN and triplet sensitizers such as benzophenone and acetophenone were also investigated. However, either no conversion (entry 7) or decomposition (entry 8) of starting material took place under these conditions.

Due to the promising catalytic activity of Cu(II) salts in [2+2] photocyclization reactions (see section 1.3.2), $Cu(OTf)_2$ was employed as catalyst (entry 9-12). Disappointingly, use of this additive in the attempted cyclization at different wavelengths and reaction temperatures resulted in formation of traces of reduced ketone **299** or decomposition of the starting material. Performing the transformation at low temperature, led to no improvement and resulted in a similar reaction outcome (entry 9-12).

Table 10. Attempts for intramolecular [2+2] photocycloaddition.

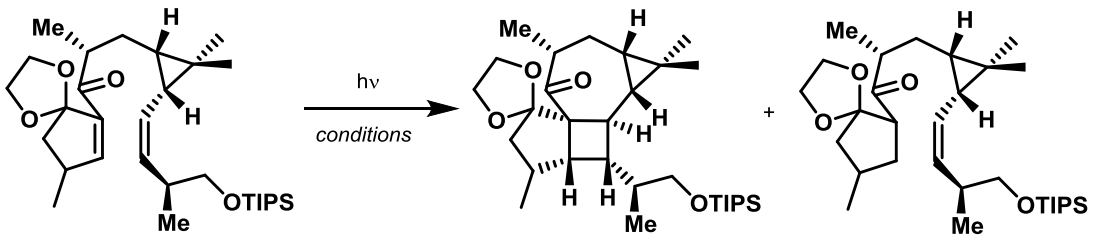

259 298 299

Entry[a]	Wavelength [nm]	Conditions	T [°C]	Observation
1	254	MeCN	23	decomposition
2	254	DCM	23	decomposition
3	254	Et_2O	0 to 23	**299**: traces, rest:decomposition
4	254	THF	23	**299**: traces, rest:decomposition
5	254	Benzene	23	no conversion
6	254	Acetone	0 to 23	decomposition
7	365	MeCN, Benzophenone	23	no conversion
8	365	MeCN, acetophenone	23	no conversion
9	254	Et_2O, $Cu(OTf)_2$	–78 to 23	**299**, rest decomposition
10	254	THF, $Cu(OTf)_2$	–78 to 23	**299**, rest decomposition
11	254	MeCN, $Cu(OTf)_2$	–78 to 23	decomposition
12	254	DCM, $Cu(OTf)_2$	–78 to 23	decomposition

[a]all reactions were carried out in dry and degassed solvents.

To our disappointment, we were unable to realize the envisioned intramolecular [2+2] photocyclization, despite extensive screening of various reaction conditions.

In summary, the presented strategy suffered from several synthetic drawbacks and had proven to be an unsatisfactory route (Scheme 47).The preparation of methyl ester **264** was inefficient and while the following olefination reaction could be achieved with high (*E*)-selectivity, this transformation resulted in 32% yield at best and further improvements remained unsuccessful. Finally, ketone **259** failed to undergo the desired key cyclization.

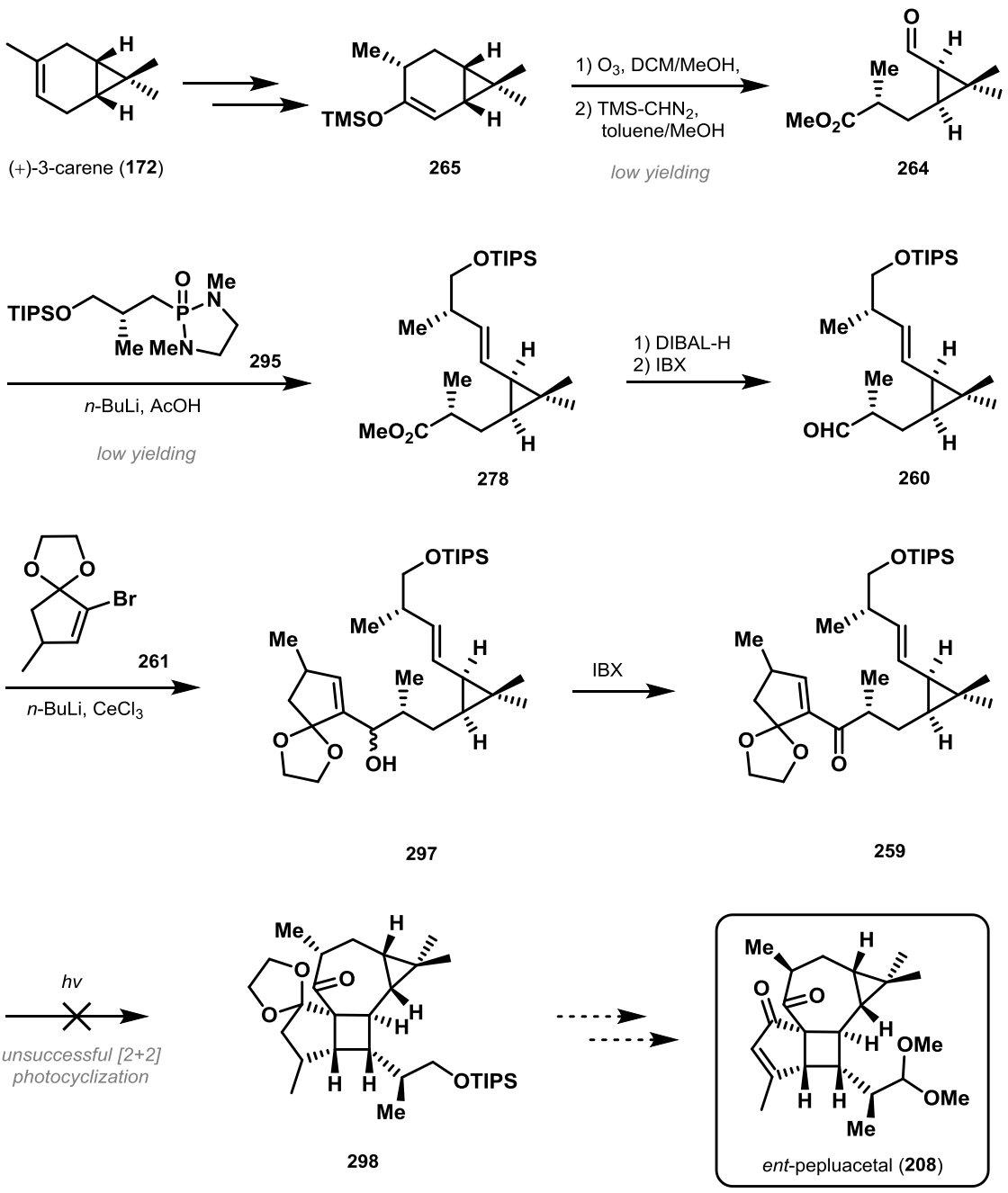

Scheme 47. Drawbacks of the synthetic route presented in chapter 2.1.

Despite the unsuccessful results, several synthetic achievements were made during our first approach towards pepluacetal (**208**). The olefination with phosphonamide **295** accomplished an olefination with excellent stereoselectivity and after nucleophilic addition with cyclopentene unit **261** we were able to construct a highly functionalized and complex intermediate (**259**) in only five synthetic steps from literature known methyl ester **264**.

However, we had to abandon this strategy and pursue an alternative route toward pepluacetal (**208**) which will be discussed in detail in the following chapter.

2.2 Second-generation Approach: Strategy B

Since previous attempts of the intramolecular [2+2] photocyclization to build the core structure of pepluacetal (**208**) had proven unsuccessful, an alternative route was investigated in parallel to the synthetic studies presented in chapter 2.1. In this approach the general idea was to construct the five- and the four-membered ring during the course of the [2+2] cycloaddition reaction. In this synthetic route, the focus lay on the construction of key intermediate **301** as the new photocyclization precursor. The second-generation retrosynthetic analysis is depicted in Scheme 48, and pursued the synthesis of the naturally occurring enantiomer of pepluacetal (**208**).

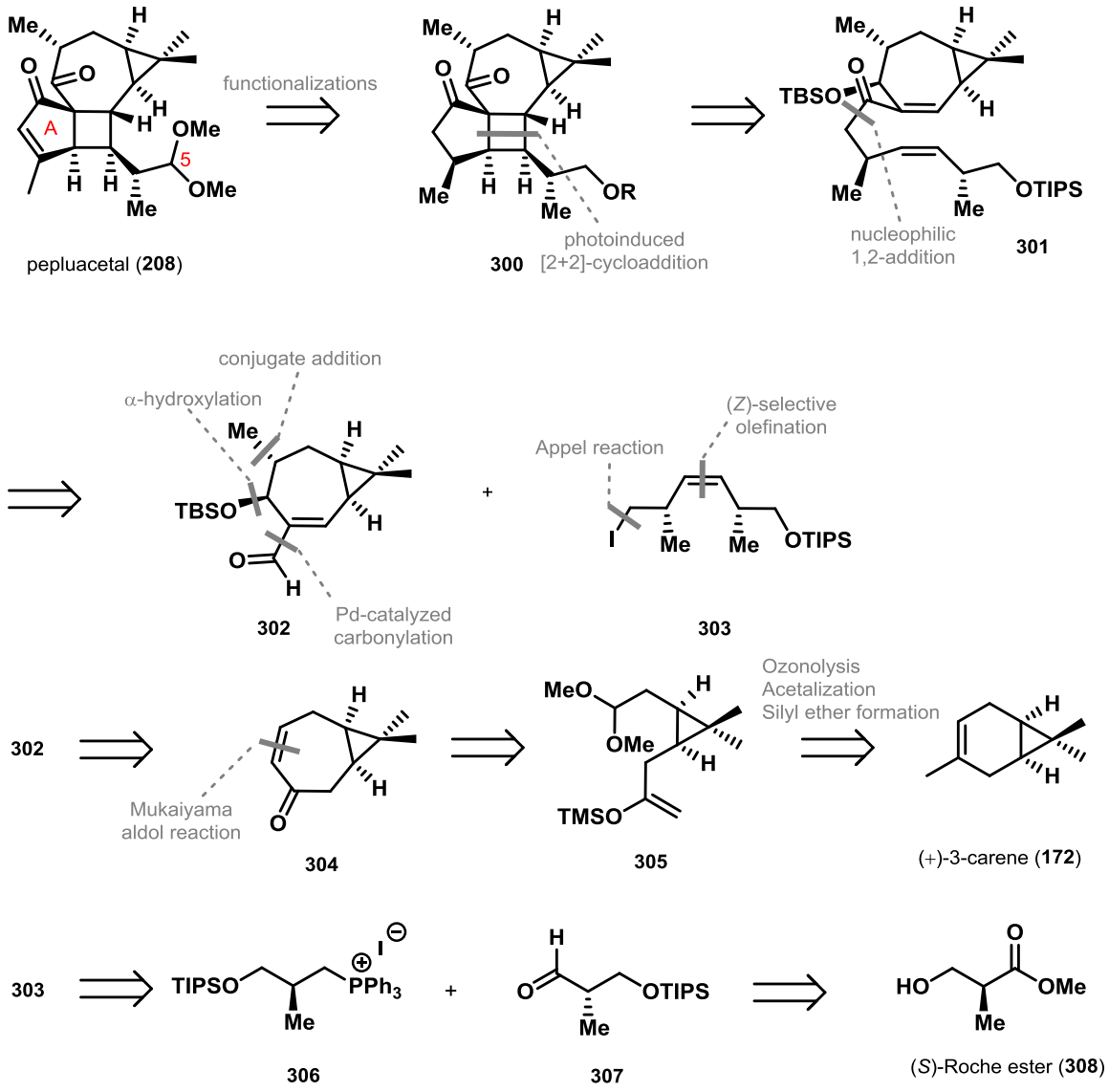

Scheme 48. Second-generation retrosynthetic analysis of pepluacetal (208).

The unsaturation in ring A as well as functionalization at C5 were envisioned to be introduced at a late stage of the synthesis, via Saegusa-Ito-oxidation and selective acetalization starting from

compound **300**. To assemble the unique tetracyclic carbon skeleton of pepluacetal (**208**) we envisioned an intramolecular [2+2] photocyclization of key intermediate **301**. Our plans for the preparation of cyclization precursor **301** were based on nucleophilic addition of olefin **303** to aldehyde **302**. In turn, aldehyde **302** was envisioned to be derived from literature known enone **304** via a synthetic sequence consisting of conjugate addition, α-hydroxylation and Pd-catalyzed carbonylation. Unsaturated ketone **304** was traced back to commercially available (+)-3-carene (**172**) based on a known literature procedure. With respect to alkyl iodide **303** the (*Z*)-oriented double bond was foreseen to be constructed via stereoselective olefination between phosphonium salt **306** and aldehyde **307**. These two building blocks could readily be derived from commercially available (*S*)-Roche-ester (**308**).

At the outset of our studies, unsaturated ketone **304** was synthesized in five steps based on a literature procedure (Scheme 49).[96] Starting from (+)-3-carene (**172**), keto-acetal **310** was prepared via ozonolysis of **172** followed by selective acetalization of the aldehyde moiety in **309**. Enol-ether formation then gave **305** together with small amounts of the thermodynamic product. Lewis acid catalyzed intramolecular Mukaiyama aldol reaction of the crude reaction mixture afforded seven-membered ketone **311** in 52% yield. Finally, β-elimination converted **311** to desired enone **304**.

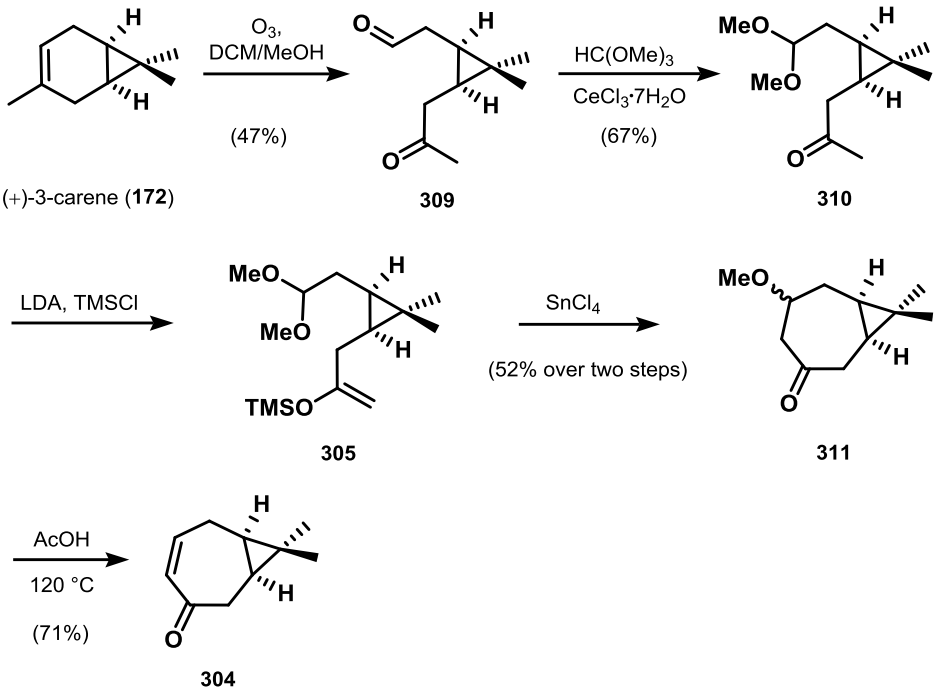

Scheme 49. Synthesis of literature known enone 304.[96]

With enone **304** in hand, conjugate addition to introduce the methyl moiety and subsequent α-hydroxylation were examined. The 1,4-addition was realized by following a modified

procedure of the Kharasch addition developed by Reetz and co-workers.[114][115] Their investigations highlighted that the use of CuX_3Li_2 instead of $CuBr{\cdot}SMe_2$ was beneficial and in some cases had efficient catalyzing effects on the reaction. Notably, the original Kharasch reaction conditions did not afford any desired product with our substrate, while the modified procedure by Reetz furnished desired silyl enol ether **312** in high yields and as a single diastereomer.

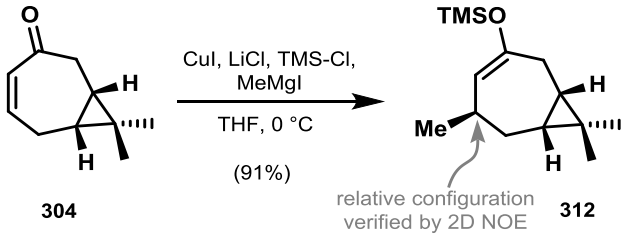

Scheme 50. Synthesis of silyl ether 312 via CuI_3-Li_2-catalyzed conjugate addition.

Next, the synthesis of α-hydroxy ketone **313** required careful optimization of the reaction conditions (Table 11). We started our investigations with standard conditions using *m*-CPBA buffered with $NaHCO_3$ which resulted in no conversion of enol ether **312** (entry 1).[116] In the absence of $NaHCO_3$, 16% and 19% of desired hydroxy ketone **313** together with 30% of hydrolyzed enol ether **314** could be obtained in different solvent systems (entry 2, 3).[117][118] Use of less acidic peroxy acid magnesium bis(monoperoxyphthalate) (MMPP) also resulted in hydrolysis of enol ether **312** (entry 4).[119] Similar results were obtained using reagents such as $Pb(OAc)_2$ (entry 5), ceric ammonium nitrate (CAN) (entry 6), OsO_4 together with *N*-methlymorpholine-*N*-oxide (NMO) (entry 7) or ReO_3Me together with H_2O_2 and pyridine (entry 8)[120].

Intrigued by the result obtained with *in situ* prepared dimethlydioxirane (DMDO) which gave a mixture of starting material and desired hydroxy ketone **313** (entry 9), full conversion of silyl enol ether **312** was then achieved using freshly prepared DMDO and stirring at low temperature for 24 h (entry 10).[121]

Table 11. Attempts for α-hydroxylation of enol ether 312.

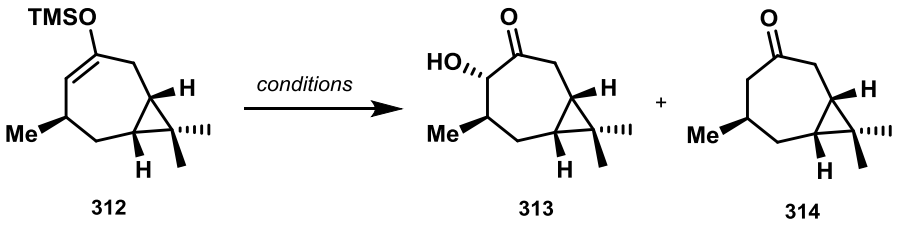

Entry	Conditions	T [°C]	Observation
1	*m*-CPBA, $NaHCO_3$, DCM	–30	no conversion
2	*m*-CPBA, hexanes	–30 to –15	**313** (19%), rest: **314**
3	*m*-CPBA, toluene	–30 to –15	**313** (16%), rest: **314**
4	MMPP, H_2O, DCM	23	**314**
5	$Pb(OAc)_2$ (dry)	0 to 23	**314** (10%)
6	CAN	0 to 23	**314**
7	OsO_4, NMO	–5 to 0	**314**
8	ReO_3Me, H_2O_2, pyr.	0	**314**
9	DMDO (*in situ*)	0	**313** (28%), **312** (40%)
10	DMDO, acetone	–78	**313** (75%)

In order to perform the envisioned Pd-catalyzed carbonylation, hydroxy ketone **313** had to be converted into vinyl triflate **316** (Scheme 51). Therefore, **313** was converted to the corresponding silyl ether **315** which was further transformed into vinyl triflate **316** by trapping the enolate derived from **315** with Comins` reagent.[122]

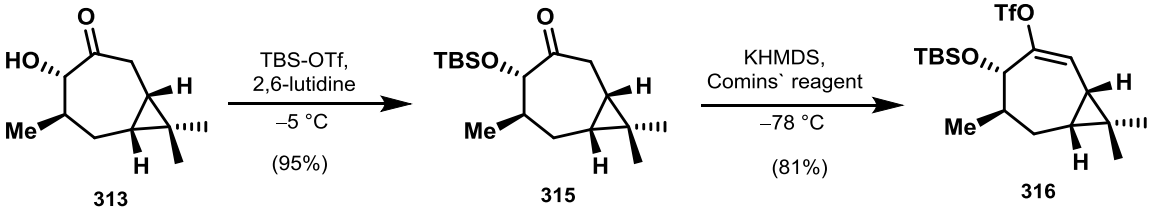

Scheme 51. Preparation of vinyl trilflate 316.

Next, the Pd-catalyzed carbonylation was examined. Different conditions to directly furnish either aldehyde **318**, methyl ester **319** or Weinreb amide **317** were investigated (Table 12). The first strategy was applied for the synthesis of aldehyde **318**. Following the Stille procedure for palladium-catalyzed formylation, only traces of product **318** were obtained (entry 1).[123] Methyl

ester **319** was prepared using tetrakis(triphenylphosphane)palladium(0) ($Pd(PPh_3)_4$) as Pd-source and LiCl additive (entry 3).[124] However, very variable yields between 23-50% were obtained. While initial attempts to synthesize Weinreb amide **317** resulted in no conversion of starting material or only traces of product (entry 4, 5)[125], use of the same reaction conditions as for preparation of methyl ester **319** and using *N*,*O*-dimethylhydroxylamine as the nucleophile enabled the synthesis of Weinreb amide **317** in good yield (entry 6).

Table 12. Investigations of the Pd-catalyzed CO-insertion.

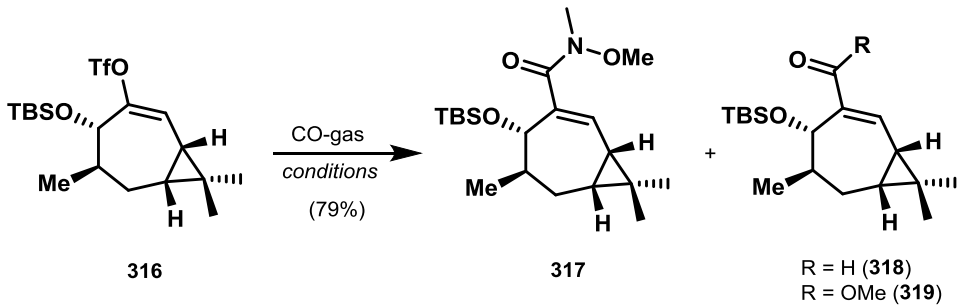

Entry	Conditions	Solvent	T [°C]	Observation
1	$Pd(PPh_3)_4$, LiCl, $HSnBu_3$	THF	23	traces of **318**
2	$PdCl_2(PPh_3)_2$, NEt_3	MeOH/DMF	55	no conversion
3	$Pd(PPh_3)_4$, LiCl, NEt_3	MeOH/DMF	23 to reflux	**319** (23-50%)
4	$Pd(OAc)_2$, XantPhos, Na_2CO_3, HN(OMe)Me	THF	23 to reflux	no conversion
5	$Pd(PPh_3)_4$, NEt_3, HN(OMe)Me	THF	23 to reflux	traces of **317**
6	$Pd(PPh_3)_4$, NEt_3, LiCl, HN(OMe)Me	DMF	55	**317** (79%)

In summary, the optimized procedure for the preparation of Weinreb amide **317** gave the most favorable result in this Pd-catalyzed carbonylation reaction, and additionally allowed direct examination of the subsequent nucleophilic addition without further reduction/oxidation steps.

2.2.1 Synthetic Investigations of the Side Chain

In order to perform the nucleophilic addition to establish key intermediate **301**, the synthesis of side chain **320** was investigated next (Scheme 52). Introduction of the correct stereochemistry at C6 required the use of (*S*)-Roche ester (**308**) as the starting material. To achieve a successful [2+2] photocycloaddition reaction, the geometry of the double bond in this strategy is required to be (*Z*).

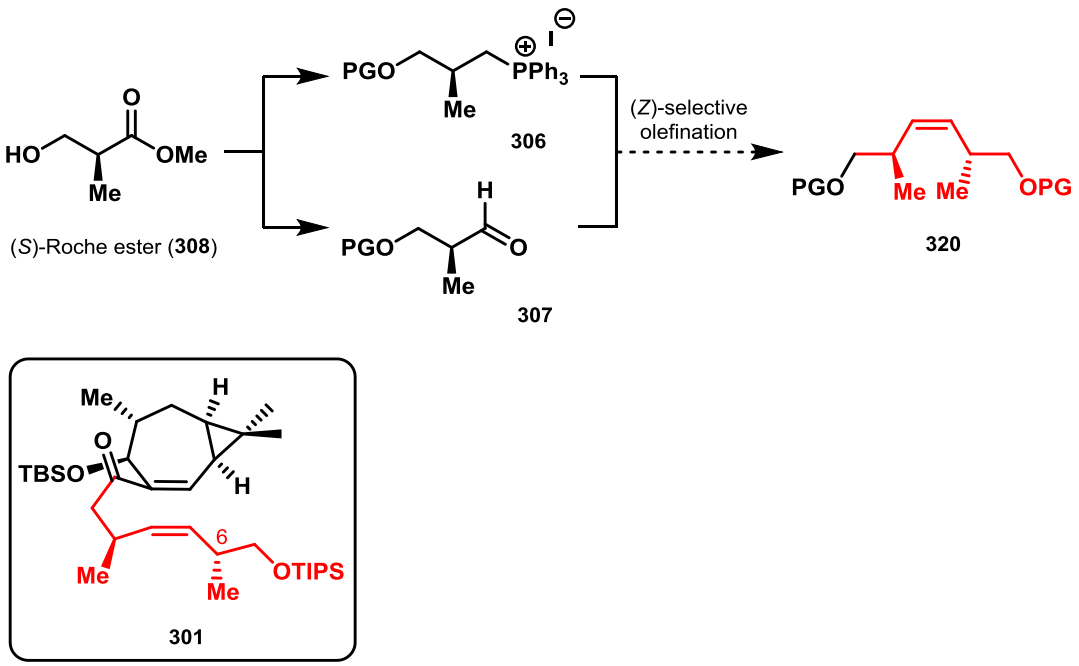

Scheme 52. Envisioned synthesis of side chain 320.

The synthesis started with the protection of the primary hydroxyl group in (*S*)-Roche ester (**308**) (Scheme 53). Therefore methoxymethyl (MOM), TBS, TIPS and tosyl were considered as protecting groups which exhibit varying steric and electronic properties and have distinct stabilities toward a variety of reaction conditions. All protections proceeded smoothly following literature known procedures.[99][126][127][128]

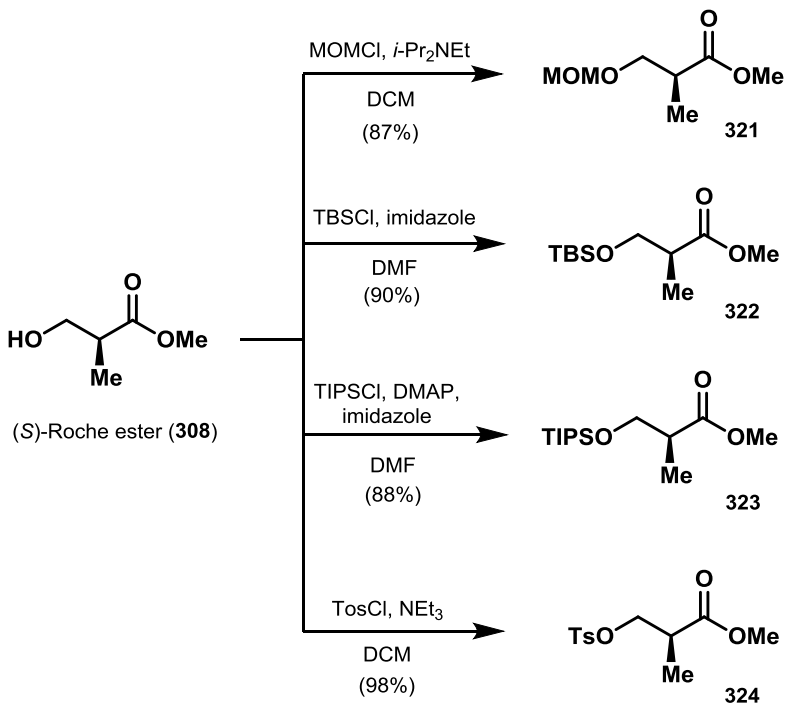

Scheme 53. Different protecting groups for (*S*)-Roche-ester (308).

As outlined in Scheme 54, preparation of the two building blocks for (*E*)-selective olefination then was pursued with methyl esters **321-324** which were first reduced to alcohols **325-328** and then oxidized to aldehydes **329-332** using Parikh-Doering-oxidation conditions. Since only the TIPS-protecting group was tolerated in the preparation of the phosphonium salt, only **334** was further converted to **305**.

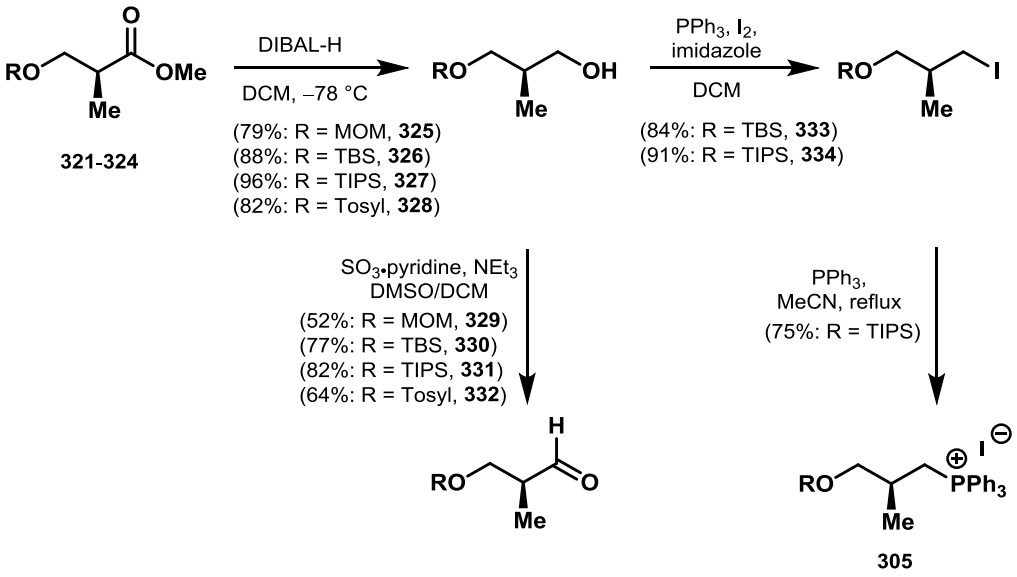

Scheme 54. Preparation of coupling elements for (*Z*)-selective olefination.

Having successfully synthesized aldehydes **329-332** and phosphonium salt **305**, the synthesis of olefins **335-338** was examined next (Table 13). Treatment of phosphonium salt **305** with base led to formation of an unstabilized yilde that was expected to lead to (*Z*)-selective olefination with aldehydes **329-332**. Therefore, the lithium-, sodium- and potassium salts of the hexamethlydisilizane bases were investigated. Addition of aldehydes **329-332** to the *in situ* formed ylide led to decomposition of the starting material (entry 1, 3, 4). While addition of TBS-protected aldehyde **330** to ylide **305**, generated with NaHMDS, resulted in formation of trace amounts of desired olefin **336** (entry 2), treatment of phosphonium salt **305** with phenyl lithium resulted in decomposition (entry 5). Employing KO*t*-Bu as the base in this transformation resulted in no conversion of starting material (entry 6).

Table 13. Attempts for (*Z*)-selective olefination with aldehydes 329-332 and phosphonium salt 305.

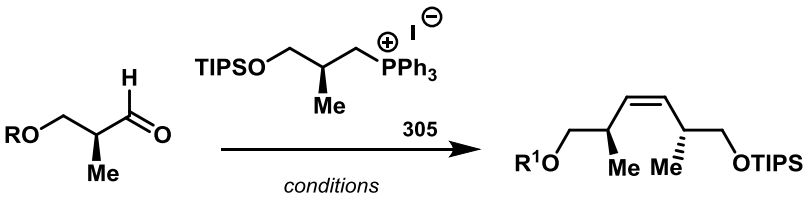

329 (R = MOM)
330 (R = TBS)
331 (R = TIPS)
332 (R = Tosyl)

335 (R = MOM)
336 (R = TBS)
337 (R = TIPS)
338 (R = Tosyl)

Entry	Conditions	T [°C]	Observation
1	LiHMDS	–78 to 0	decomposition
2	NaHMDS	–78 to 0	traces product for **336**
3	KHMDS	–78 to 0	decomposition
4	KHMDS, 18-crown-6	–78 to 0	decomposition
5	PhLi	–78 to 0	decomposition
6	KO*t*-Bu	0	no conversion

This reaction outcome was surprising, as the simple Wittig olefination of Roche esters has been reported in the literature.[108] Our substrates, aldehydes **329-332**, appeared to be highly unstable under the basic reaction conditions and decomposed readily.

Next, we decided to investigate an intermolecular regioselective olefin cross metathesis reaction with olefins **339** (TBS) and **340** (TIPS) (Scheme 55). Among others, Grubbs and co-workers developed different ruthenium-based catalysts capable of producing (*Z*)-olefins with high stereoselectivity.[129] Ruthenium-catalyst **341** is one in this series showing about 95% (*Z*)-selectivity.[130] For examination of this catalyst with our substrate, olefins **339** and **340** were prepared following olefination.[108] Unfortunately, the attempted cross-metathesis of olefins **339** and **340** resulted in formation of a complex mixture of inseparable and unidentified products and no desired alkene could be isolated.

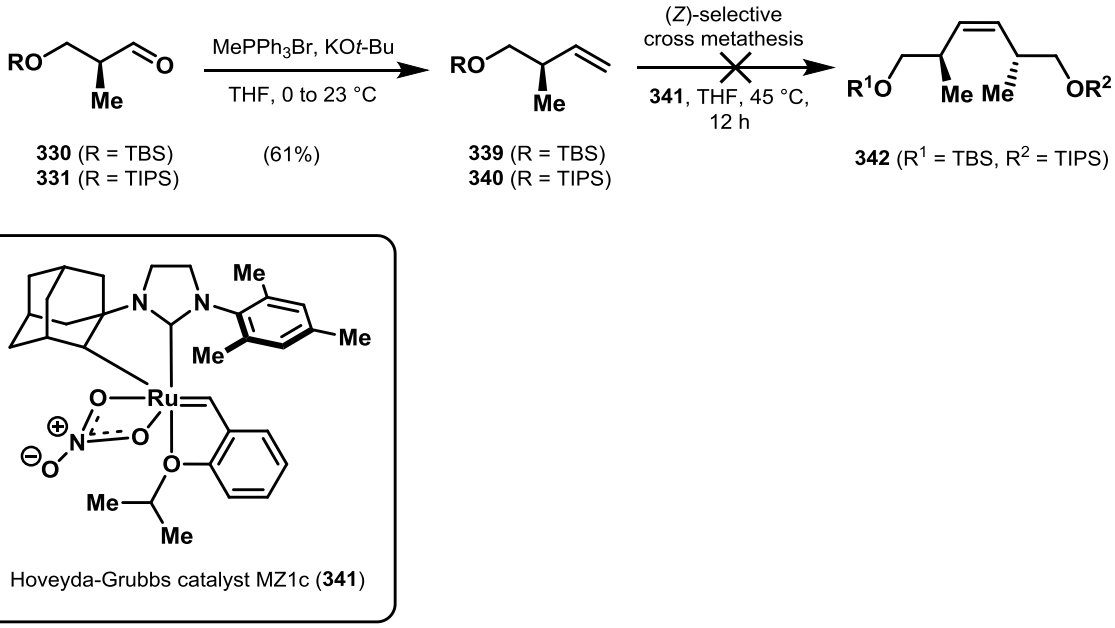

Scheme 55. Synthesis of olefins 339 and 340 and unsuccessful cross metathesis reaction.

Given the difficulties encountered with the preparation of olefin **320** we decided to successively introduce the side chain pieces and perform the convergent olefination at a later stage of the total synthesis. In this respect, we aimed to prepare aldehyde **345** which subsequently could undergo olefination with phosphonium salt **306** (Scheme 56).

The synthesis of aldehyde **345** started with the addition of alkyl iodide **334** to Weinreb ketone **317** (Scheme 56). Initial attempts at the addition of the lithium species derived from alkyl iodide **334** resulted in no product formation (Scheme 56, conditions a)). Investigations to activate the carbonyl moiety for the 1,2-addition were then explored by adding lanthanide(III) salts as Lewis-acid. Use of $CeCl_3$ led to no improvement and starting material remained, most likely due to the poor solubility of this reagent in organic solvents (Scheme 56, conditions b)). The activity of the catalyst strongly depends on its solubility and in this respect Knochel and co-workers have reported the beneficial effects of LiCl.[131] Therefore, they investigated the preparation of THF-soluble lanthanide catalysts for the addition of various organometallic reagents to carbonyl compounds. To increase the reactivity of amide **317** we examined the use of a commercially available 0.6 M solution of $LaCl_3$•2LiCl in THF. Fortunately, using these reaction conditions α,β-unsaturated ketone **343** was obtained in 71% yield. Global removal of the TBS-groups was realized using tetrabutylammonium fluoride (TBAF), and was followed by global oxidation using an excess of DMP which completed the synthesis of aldehyde **345** as the key precursor for the olefination reaction.

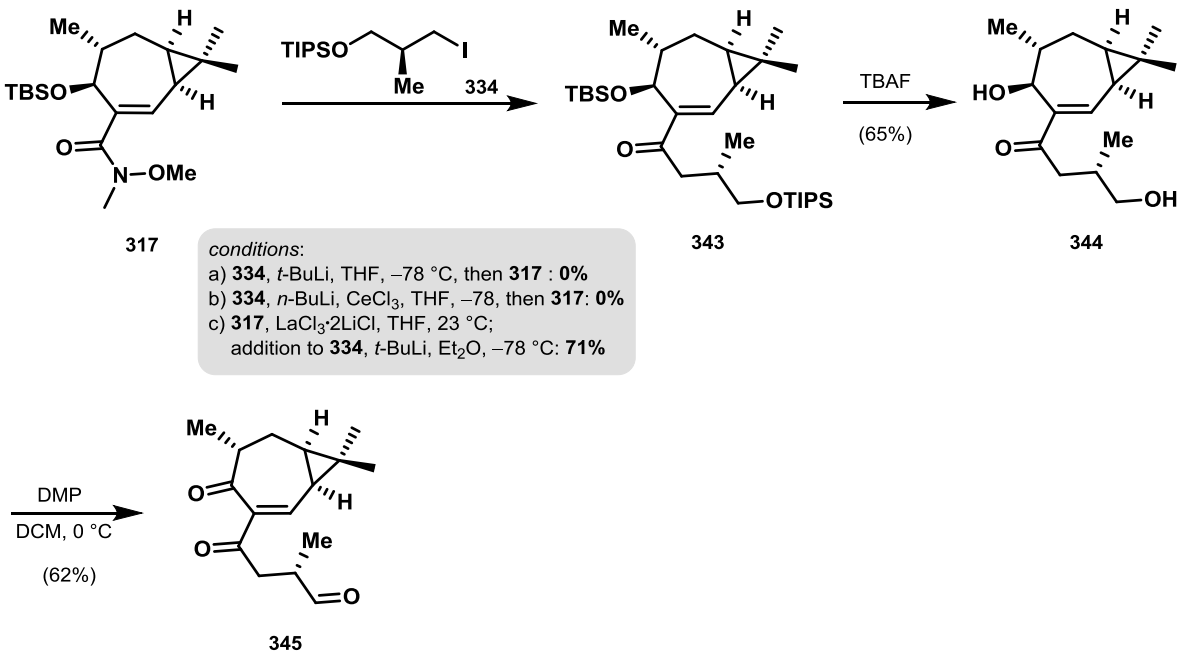

Scheme 56. Synthesis of aldehyde 345.

Olefination attempts with aldehyde **345** are summarized in Table 14. Unfortunately, decomposition of **345** occurred under all investigated conditions and no formation of key intermediate **346** was observed. It was hypothesized that the highly activated enone system, as is present in aldehyde **345**, hampered a successful reaction outcome.

Table 14. Olefination attempts of aldehyde 345.

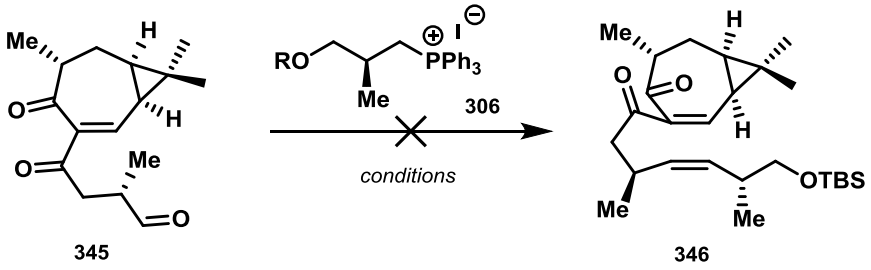

Entry	Conditions	T [°C]	Observation
1	LiHMDS	–78 to 0	decomposition
2	NaHMDS	–78 to 0	decomposition
3	KHMDS	–78 to 0	decomposition
4	KHMDS, 18-crown-6	–78 to 0	decomposition
5	PhLi	–78 to 0	decomposition
6	KO*t*Bu	0	decomposition

At this stage, we abandoned these investigations to further explore a new synthesis of the side chain. We reasoned that a higher substitution of the aldehyde chain might lead to an enhanced stability under basic olefination conditions. Additionally, we decided to pursue new strategies to introduce the side chain which will be discussed in detail in the following chapter. Together, this led to the design of a new synthetic approach which is depicted in Scheme 57.

The following synthesis was accomplished and optimized by M. Sc. Po Yuan. Starting from alkyl iodide **334**, introduction of the 1,3-dithiane moiety **347** was realized using *n*-BuLi and subsequent treatment of silyl ether **348** with TBAF gave alcohol **349** in 77% yield over two steps. Parikh-Doering oxidation of alcohol **349** furnished aldehyde **350**, which eventually proved to be sufficiently stable for the ensuing diastereoselective olefination. Ylide formation was accomplished with *n*-BuLi at low temperature (–70 °C), and addition of this reactant to aldehyde **350** resulted in the formation of olefin **351** as a single double bond isomer and in excellent yield. Finally, removal of the dithiane moiety gave aldehyde **352**.

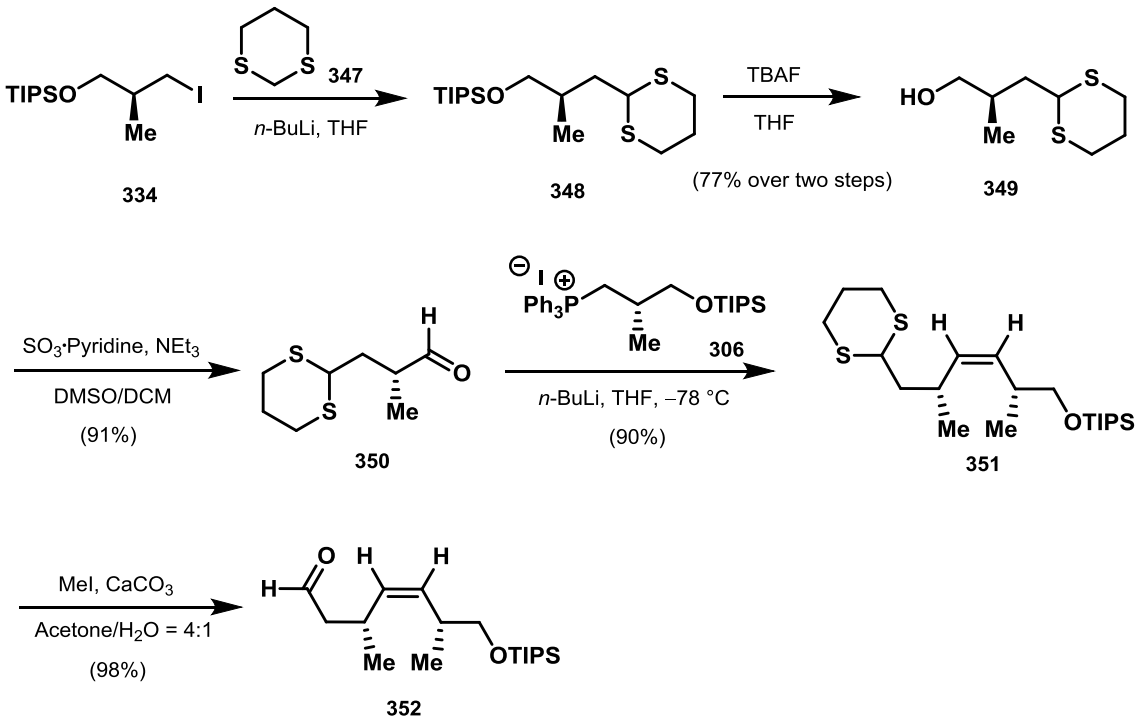

Scheme 57. Synthesis of side chain 352.

Introduction attempts of the new developed side chain **352** will be discussed in detail in the following chapter.

2.2.2 Side Chain Introduction – First Approach

With olefins **351** and **352** in hand, we envisioned three different strategies for their introduction of (Scheme 58). First, a nucleophilic addition of deprotonated dithiane **351** to ketone **315** followed by dehydration and removal of the dithiane moiety. Second, a Shapiro reaction between hydrazone **355** and aldehyde **352** and third, coupling of a vinylic organometallic species **357** with aldehyde **352**.

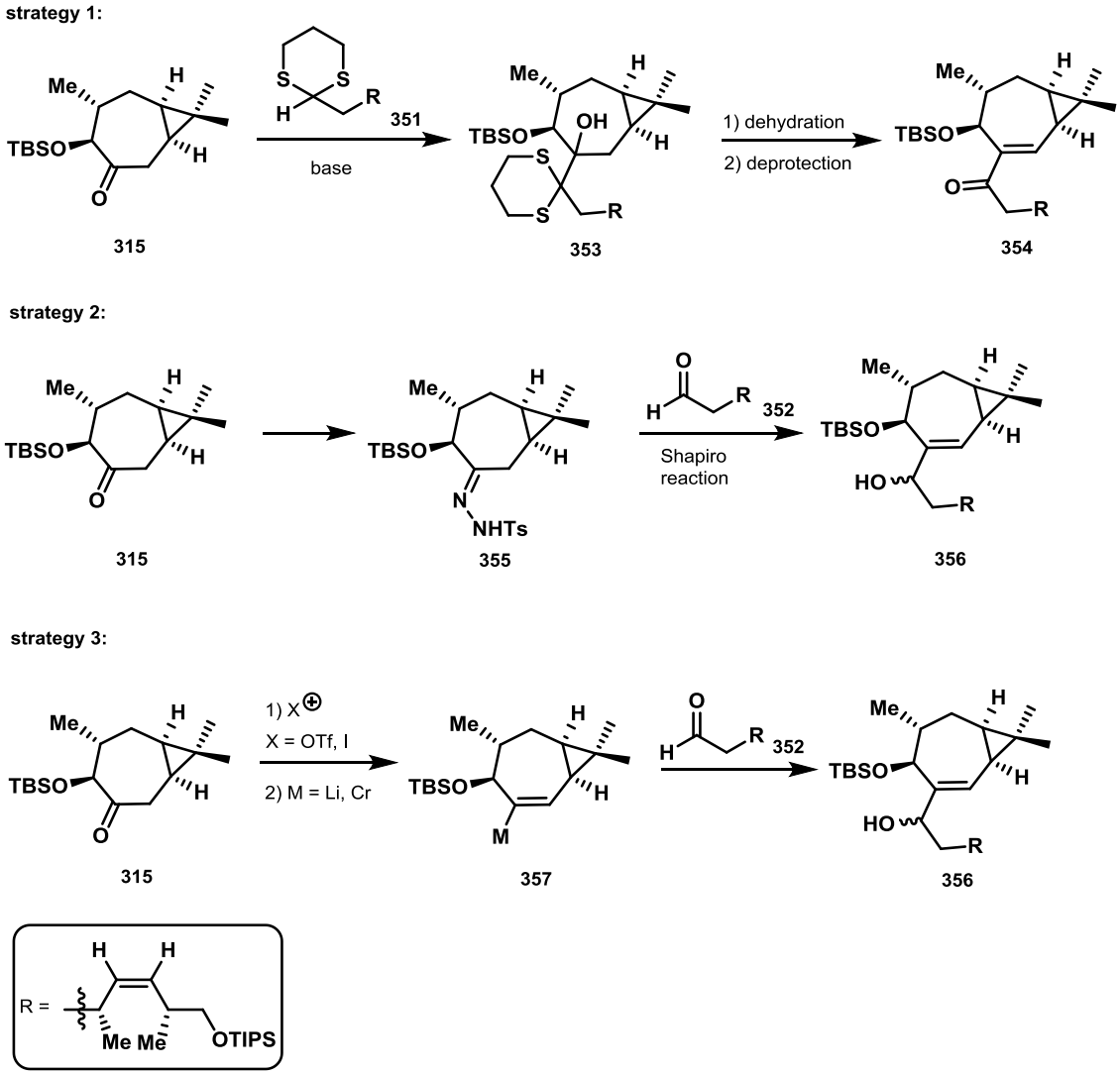

Scheme 58. Different strategies for the introduction of the side chains 351 and 352.

Nucleophilic addition between ketone **315** and dithiane **351** was examined first (Scheme 59).* Treatment of lithiated **351** with **315** resulted in no product formation. Since addition to ketone **315** with dithiane **351** proved unsuccessful we examined whether the deprotonation of **351** occurs at all. Thus, the crude reaction mixture of **351** was treated with an excess of deuterium oxide. NMR studies revealed that deuterium incorporation took place which led us to reason that ketone **315** might be too sterically hindered for the addition of nucleophiles like dithiane **351**.

*Optimization of the synthetic steps shown in Scheme 58, strategy 1 was carried out by M.Sc. Po Yuan.

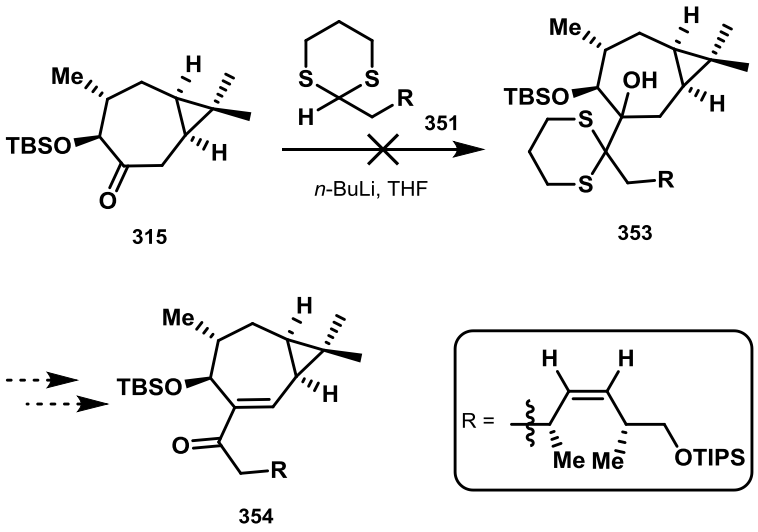

Scheme 59. Unsuccessful addition of deprotonated dithiane 351 to ketone 315.

Our next synthetic strategy was based on the introduction of aldehyde **352** via a Shapiro reaction.[132] Therefore, ketone **315** was converted into hydrazone **355** by treatment with tosyl-hydrazine in methanol at ambient temperature (Scheme 60).

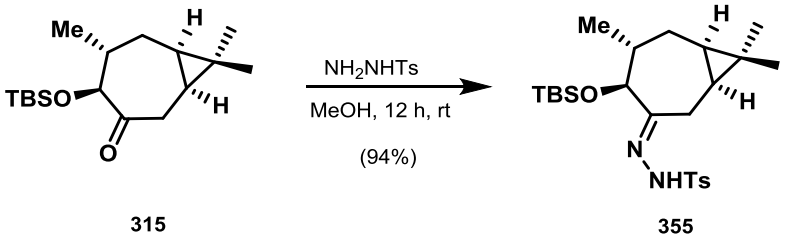

Scheme 60. Synthesis of hydrazones 355.

Hydrazone **355** was then subjected to Shapiro reaction conditions to install aldehyde **352** (Table 15). Treatment of hydrazone **355** with two equivalents of base at –78 °C gave the distinct color change from colorless to dark red.[133] The resulting reaction mixture was stirred for one hour while warming to –10 °C, which was accompanied by the typical color change to bright yellow. The latter observation usually indicates the loss of nitrogen and consequently the generation of the vinyl lithium species.[133] Following addition of aldehyde **352** and monitoring of the resulting reaction mixture by thin layer chromatography, low conversion of starting material and one newly formed product could be detected. Isolation of the product (15-20% yield) and careful NMR-analysis indicated that addition product **358** had formed, highlighting that an unsuccessful conversion to the vinyl lithium species had occurred (entry 1, 2). This result was unexpected based on the higher acidity of the hydrogen at the hydrazone compared to the hydrogen at C8 position.

Changing the reaction conditions by using more equivalents of base, addition of TMEDA and employing another solvent system also resulted in no conversion of starting material even after prolonged reaction times (entry 3). Heating the reaction mixture to ambient temperature again gave no conversion and further heating led to decomposition of **355**. Eventually it was discovered that the use of an excess of *sec*-BuLi and aldehyde **352** resulted in formation of trace amounts of desired addition product **356** (entry 4).

Table 15. Investigations of the Shapiro reaction between hydrazone 355 and aldehyde 352.

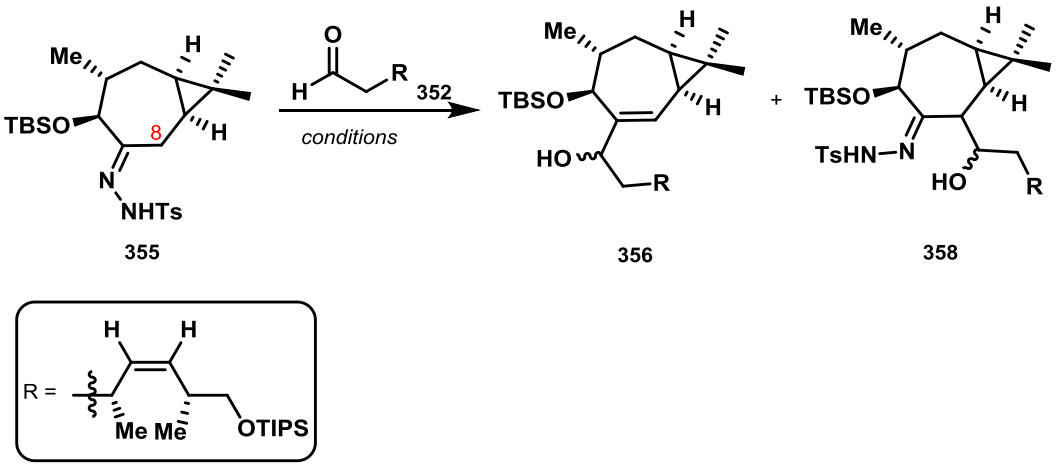

Entry	Conditions (equiv)	Solvent	T [°C]	t [h]	Observation
1	*n*-BuLi (2), **352** (1)	THF	–78 to –10	1	**358** (15%), rest: **355**
2	*n*-BuLi (4), **352** (1)	THF	–78 to 0	3	**358** (20%), rest: **355**
3	*n*-BuLi (4.9), **352** (4), TMEDA (10)	hexanes	–78 to 23	5-12	no conversion, starts to decompose
4	*sec*-BuLi (4.5), **352** (2)	THF	–78 to 0	12	traces of **356**, rest: **355**

Given the unsatisfactory results in the previous strategies to introduce the side chain, reductive coupling between vinyl triflate **316** with aldehyde **352** using Nozaki-Hiyama-Kishi (NHK) reaction conditions was next investigated (Table 16).[134][135] Treatment of vinyl triflate **316** and aldehyde **352** with an excess of chromium(II) chloride and catalytic amounts of nickel(II) chloride resulted in no conversion of starting material (entry 1). Since the low reactivity of the triflate was assumed to hamper the reaction, addition of a large excess of chromium(II) chloride and stoichiometric amounts of nickel(II) chloride were examined (entry 3). However a 1:1 mixture of both isomers of alcohol **356** were obtained in merely 17% yield. The use of 4-*tert*-butyl pyridine as an additive has been described to generally enhance the reaction rate by aiding dissolution of solid chromium(II) salts and by suppressing homo coupling reactions. With the

addition of 4-*tert*-butyl pyridine, especially vinyl triflates have been found to show good reactivity in NHK reactions.[136] However, using 4-*tert*-butyl pyridine as an additive also led to no conversion in the NHK reaction between vinyl triflate **316** and aldehyde **352** (entry 4).

Table 16. Investigations of the NHK-coupling between vinyl triflate 316 and aldehyde 352.

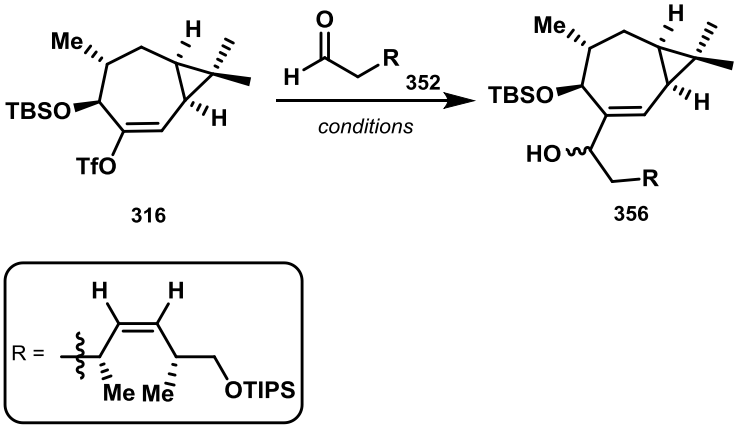

Entry[a]	Conditions (equiv)	T [°C]	t [h]	Observation
1	$CrCl_2$ (4), $NiCl_2$ (0.1), DMF	25	12	no conversion
2	$CrCl_2$ (4), $NiCl_2$ (0.1), DMF	50	12	no conversion
3	$CrCl_2$ (100), $NiCl_2$ (1), DMF/THF	25-50	24	**356** (17%, 1:1)
4	$CrCl_2$ (4), $NiCl_2$ (0.1), 4-*t*-Bu-pyridine (25), DMF	25-50	24	no conversion

[a]all reaction were performed using freshly degassed solvents.

Since we assumed that the low reactivity of the triflate was the main problem for the unsuccessful NHK reaction, our next investigations focused on the conversion of the vinyl triflate moiety into a vinyl halide or vinyl stannane.

A methodology for the synthesis of alkenyl halides from vinyl triflates was recently developed by Reisman and co-workers, that enables a nickel-catalyzed halogenation of alkenyl triflates under mild reaction conditions.[137] Side chain **352** should then later be introduced by addition of the generated vinyl lithium species derived from **359** or **360** to aldehyde **352** (Scheme 61). However, investigation of the reported reaction conditions by Reisman and co-workers resulted in no conversion of starting material **316**.

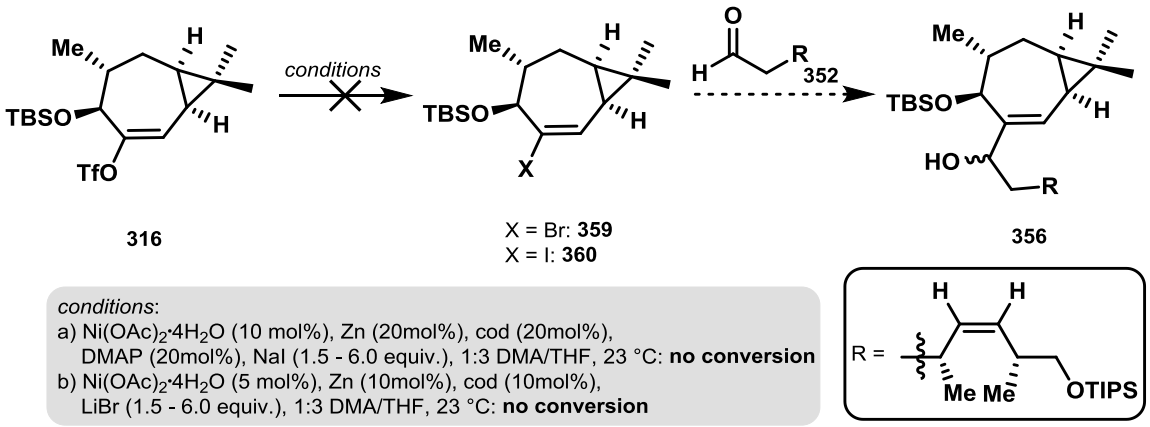

Scheme 61. Attempted nickel-catalyzed halogenation of vinyl triflate 316.

In parallel we examined the transformation of vinyl triflate **316** to vinyl stannane **361** via a palladium-catalyzed cross-coupling with hexamethlyditin and $Pd(PPh_3)_4$ (Scheme 62).[138] Unfortunately, application of these reaction conditions only resulted in a complex mixture of unidentified products.

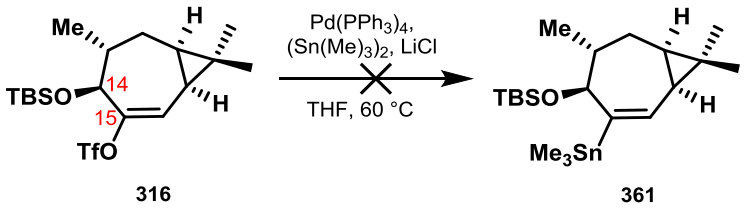

Scheme 62. Attempted stannylation of vinyl triflate 316.

In conclusion, all investigated strategies for introduction of the side chain to ketone **315** proved to be unsuccessful. While it was assumed that the low reactivity of the triflate might have hampered a successful reaction outcome, conversion to a corresponding vinyl species was unsuccessful in our hands. Furthermore, we anticipated that the *tert*-butyl silyl moiety might sterically interfere with the reaction. However, examining different protecting groups such as MOM, tosyl and TBDPS showed no difference in reactivity, leading to assume that any substitution in this position (C14, Scheme 62) might lead to a steric demand interfering with functionalizations at C15 as described above. At this stage we revisited potential strategies for the introduction of the side chain which will be discussed in detail in the following chapter.

2.2.3 Side Chain Introduction – Second Approach

As use of ketone **315** had not allowed the synthesis of key intermediate **346** our next synthetic approach was based on investigations using a less functionalized seven-membered ring system. Therefore, it was decided to prepare ketone derivative **362**, which lacks the OTBS-moiety, and to reinvestigate the previous strategies: Shapiro reaction with a hydrazone (**363**) (Scheme 63, strategy 1) and coupling of an organometallic species (**365**) with aldehyde **352** (Scheme 63, strategy 2).

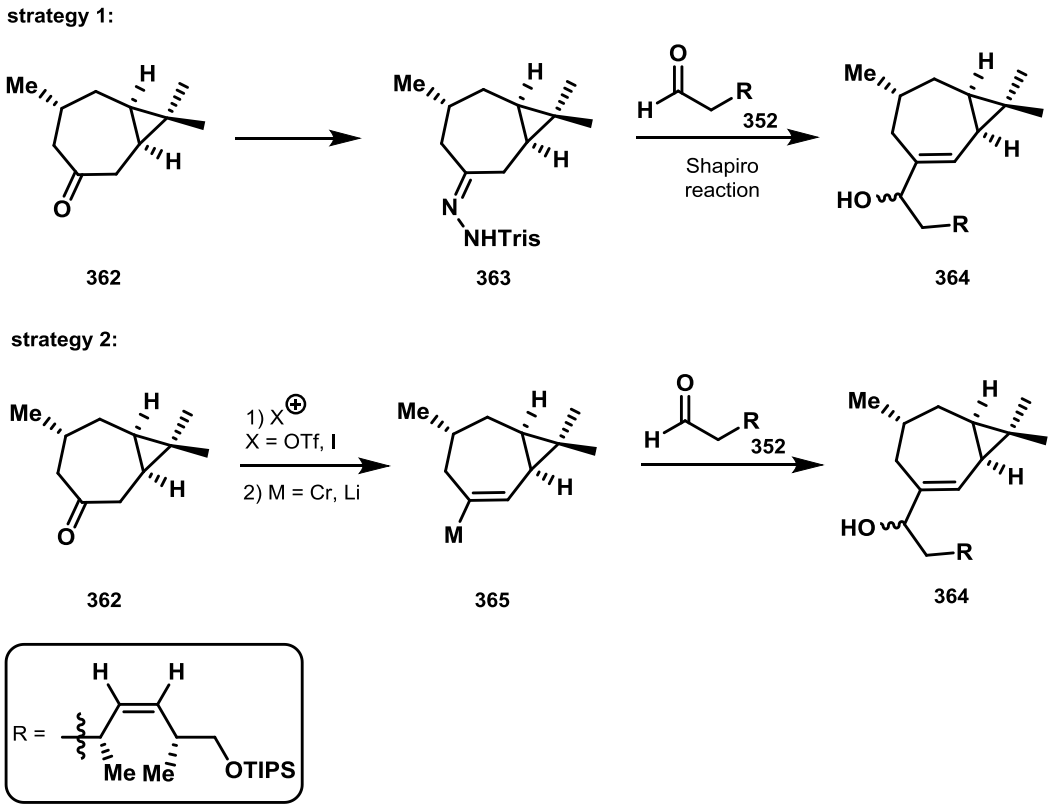

Scheme 63. Envisioned investigations of introduction of side chain 352 with ketone 362.

With the isomers of alcohol **364** we planned to advance to the tetra-cyclic carbon skeleton via two different routes (Scheme 64). First, the missing carbonyl functionality should be introduced via oxidation at C14, followed by intramolecular [2+2] photocyclization for the construction of tetracycle **367** (Scheme 64, a)). Alternatively, the key step should be performed first with alcohols **364** and subsequent oxidation at C14 (Scheme 64, b)).

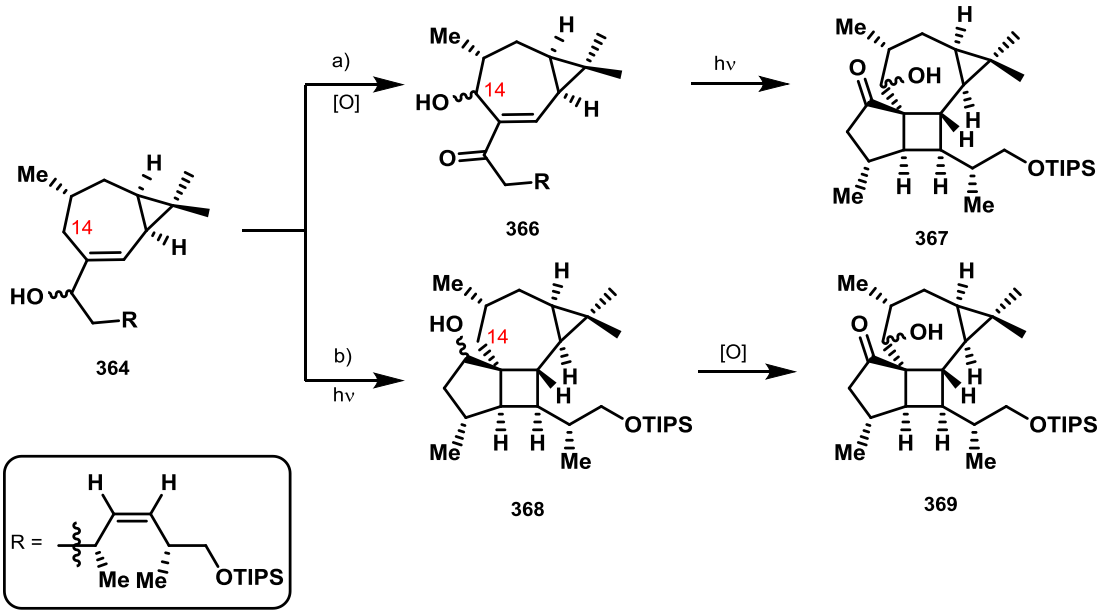

Scheme 64. Envisioned end game for the construction of the carbon skeleton of pepluacetal (208).

The synthesis of ketone **362** was achieved following similar reaction conditions for the preparation of silyl enol ether **312**, followed by an acidic workup. Using these conditions ketone **362** was obtained in 69% yield. Next, ketone **362** was converted into hydrazone **363**, this time with a 2,4,6-triisopropylbenzenesulfonyl (Tris) rest, and consequently subjected to the Shapiro reaction (Scheme 65).

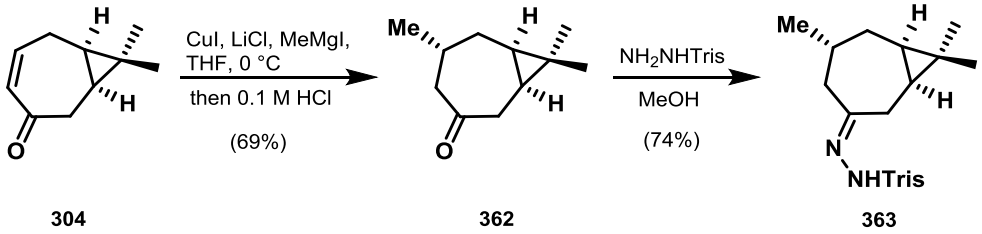

Scheme 65. Synthesis of hydrazone 363.

Gratifyingly, treatment of **363** with *n*-BuLi, followed by addition of **352** gave key intermediate **364** (Table 17, entry 1). However, repeating the same reaction gave inconsistent yields of 22-43% of isolated product together with inseparable impurities and olefin **370**, indicating that addition of the intermediate vinyl lithium species to aldehyde **352** had not occurred (Table 17, entry 2-4).

Table 17. Investigations of Shapiro reaction with hydrazone 363.

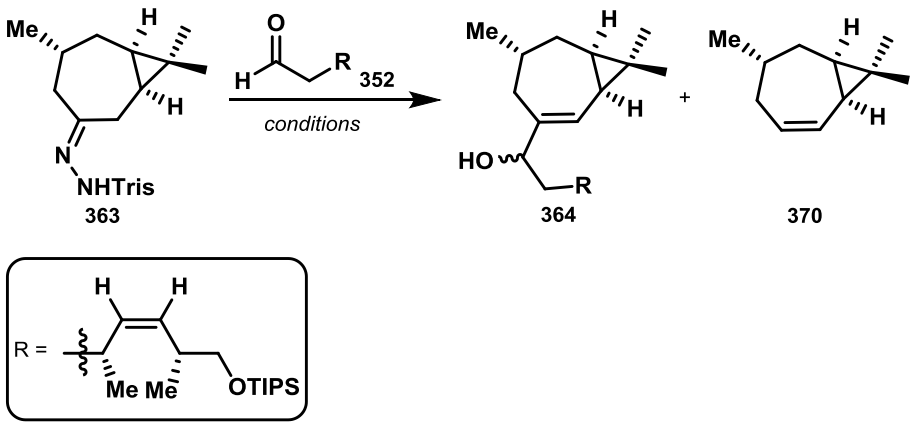

Entry	Conditions (equiv.)	Solvent	T [°C]	t [h]	Observation
1	*n*-BuLi (2), **352** (1)	THF	–78 to –10	1	**364** (22-43%)
2	*n*-BuLi (4), **352** (2)	THF	–78 to –10	3-12	**364** with impurities, **370**
3	*n*-BuLi (2), **352** (1), TMEDA (10)	hexanes	–78 to 23	12	**364** with impurities, **370**
4	*sec*-BuLi (2), **352** (1)	THF	–78 to –10	12	**364** with impurities, **370**

Given the difficulties encountered with the Shapiro reaction, we decided to reinvestigate the synthesis of vinyl iodide **372** as well as the NHK reaction. Starting from ketone **362**, vinyl triflate **371** was prepared by addition of Comins` reagent at ambient temperature, followed by cooling the resulting reaction mixture to –78 °C and treatment with KHMDS to generate the enolate which was trapped instantly by the triflation reagent. Surprisingly, vinyl triflate **371** was obtained as a single regioisomer. With **371** in hand, we applied the methodology for the synthesis of vinyl halides by Reisman and co-workers[137] (Scheme 66), and successfully obtained vinyl iodide **372**. Vinyl halide **372** was found to be highly volatile and could not be isolated without significant amount of residual solvent. Therefore, the subsequent generation of the organolithium species derived from **372** and subsequent 1,2-addition to aldehyde **352** proved to be problematic and gave alcohol **364** in inconsistent yields.

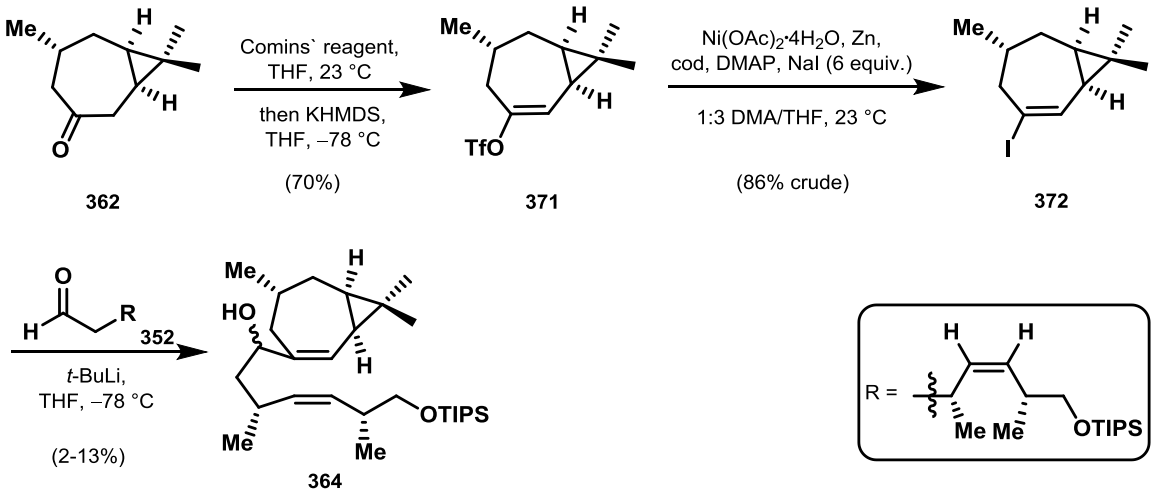

Scheme 66. Synthesis of key intermediate 364 via 1,2-addition of vinyl iodide 371 and aldehyde 352.

Based on the difficulties encountered with the isolation of vinyl iodide **372**, we decided to investigate the NHK reaction of triflate **371** and side chain **352** (Scheme 67). Applying the same reaction conditions as described before, the NHK reaction between vinyl triflate **371** and aldehyde **352** resulted in formation of the desired product in 65% yield. With the construction of a 1:1 mixture of both isomers of allylic alcohol **364** we were again able to introduce all carbon atoms that are present in the natural product pepluacetal (**208**).

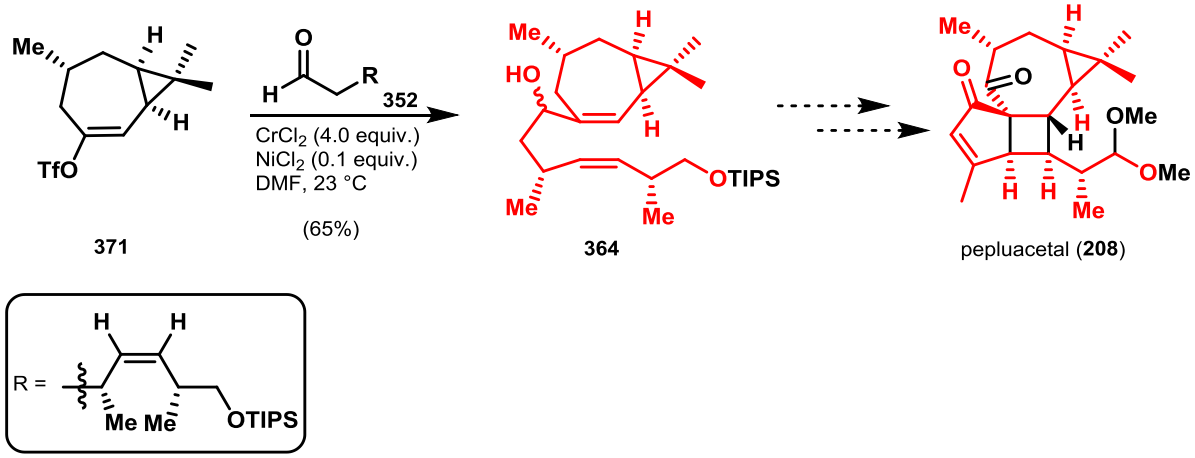

Scheme 67. NHK investigations with vinyl triflate 371.

Cyclization precursor **364** should be accessible by oxidation of alcohol **364** at C14. Therefore, different oxidation conditions were next investigated (Table 18). SeO_2 constitutes the most commonly used reagent in allylic oxidations and was investigated first. Although an excess of reagent was used in order to enable the second oxidation, only ketone **373** was obtained (entry 1). Addition of *tert*-butylhydroperoxide (*t*-BuOOH) and stirring at ambient temperature for several

hours, or addition of potassium dihydrogenphosphate and refluxing the resulting reaction mixture in toluene at 110 °C also merely resulted in the formation of ketone **373** (entry 2, 3). The same result was encountered using SeO_2 in refluxing dioxane (entry 4). Chromium based oxidants were implemented next; however, ketone **373** was the only formed product (entry 5, 6, 7). Manganese dioxide gave no conversion (entry 8). Lastly, we examined iridium-catalyzed silylation and subsequent oxidation of the generated oxasilolane, based on a methodology developed by Hartwig and co-workers (entry 9).[139] However, formation of the oxasilolane species was unsuccessful in our hands.

Table 18. Attempts to oxidize C14.

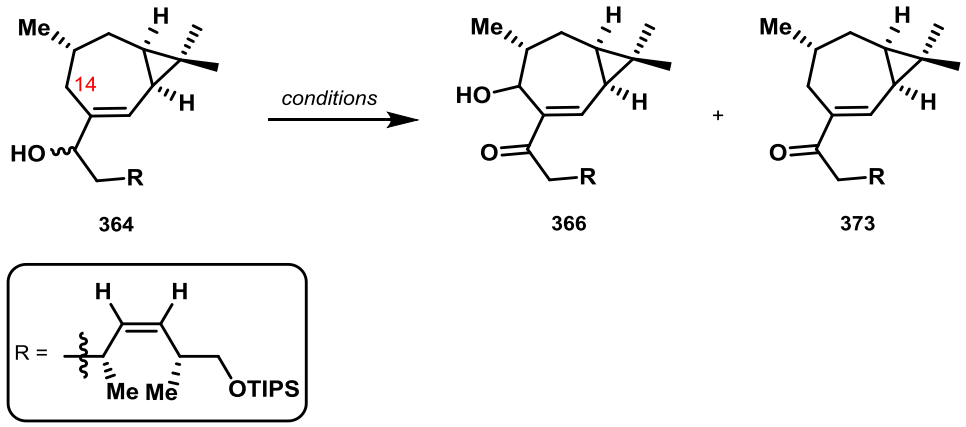

Entry	Conditions	Solvent	T [°C]	Observation
1	SeO_2	THF	23	**373**
2	SeO_2, *t*-BuOOH	THF/DCM	0 to 23	**373**
3	SeO_2, KH_2PO_4,	toluene	110	**373**
4	SeO_2	dioxane	23 to 101	**373**
5	CrO_3	DCM	0 to 23	**373**
6	Jones reagent	acetone	0 to 23	**373** (starts to decompose)
7	CrO_3, 3,5-Dimethlypyrazole	DCM	0 to 23	**373**
8	MnO_2	DCM	0 to 23	no conversion
9	$[Ir(OMe)(cod)_2]$, Et_2SiH_2, then [Ir]/Me_4Phen, norbornene	THF	120	no conversion

Since oxidation proved to be unsuccessful at this stage, we decided to investigate the transannular [2+2] photocyclization, and therefore postpone oxidation of C14 to a later stage of the total synthesis. Starting from the mixture of both isomers of alcohol **364** different conditions for

photocyclization were examined (Table 20). UV-spectroscopic analysis of **364** showed maximum absorption at 252 nm and an additional maximum at 332 nm. Irradiation of a solution of **364** in acetonitrile, DCM or acetone with a UV-lamp at 254 nm 1,4 reduction and delivered ketone **374** (entry 1, 2, 3). Replacement of the solvent with toluene resulted in no conversion of starting material (entry 4). Changing the irradiation wavelength from 254 nm to 365 nm with addition of photosensitizer benzophenone was equally unfruitful, resulting in no starting material conversion even after prolonged reaction times (entry 7, 8).

Table 19. Attempts for intramolecular [2+2] photocyclization with both isomers of alcohol 364.

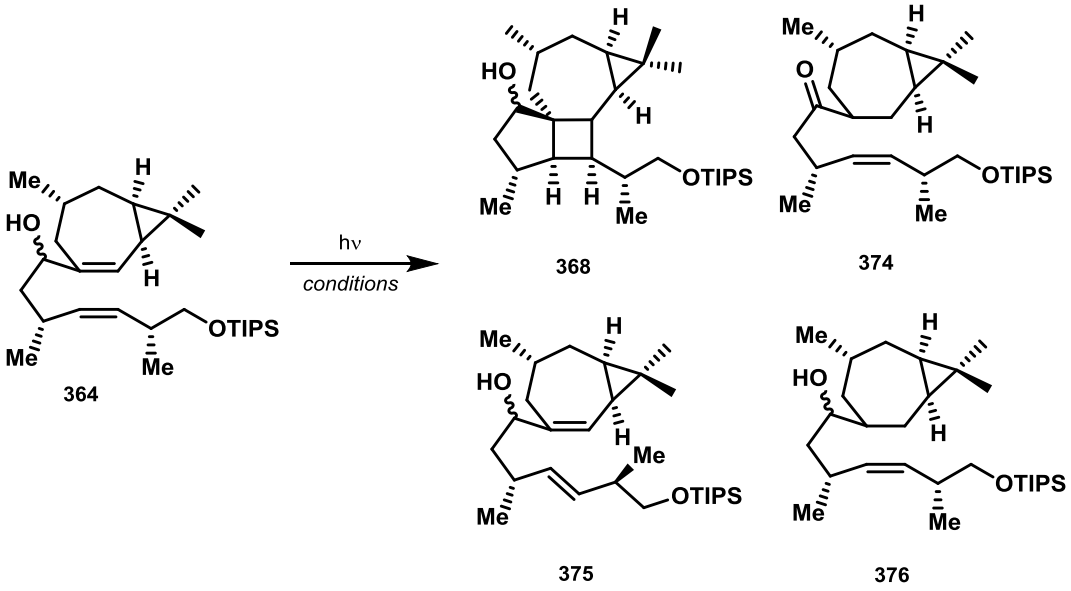

Entry[a]	Wavelength [nm]	Conditions (equiv)	T [°C]	t [h]	Observation
1	254	MeCN	23	18	**374**
2	254	DCM	0 to 23	12	**374**
3	254	acetone	0 to 23	24	**364**+**374**
4	254	toluene	23	48	no conversion
5	254	Et_2O, $Cu(OTf)_2$ (0.2)	–78	5	**364**+**375**
6	254	Et_2O, $Cu(OTf)_2$ (0.2)	23	1	**375**
7	365	MeCN, benzophenone (1)	23	48	no conversion
8	365	Et_2O,benzophenone (1)	23	48	no conversion

[a]all reactions were performed in dry and degassed solvents.

Interestingly, irradiation of a mixture containing $Cu(OTf)_2$ as an additive in Et_2O resulted in photoisomerization of the double bond (entry 5, 6). Since intramolecular [2+2] photocyclization

of 1,6-dienes likely follow a stepwise mechanism, it is not surprising that intermediates are formed that can undergo isomerization.

In parallel to the investigations of the [2+2] cycloaddition with alcohol **364**, we examined our key step with ketone **373** (Table 20). Since for ketone **373** the maximum absorption wavelength was determined to be at 253 nm, UV-lamp sources with 254 nm were investigated first. Performing the reaction at low temperatures in DCM resulted in low conversion of starting material **373** and trace isomerization of the double bond **378** and **379** (entry 1). Running the same reaction at higher temperature, gave a mixture consisting of starting material **373** and small amounts of unsaturated ketone **378** and reduced ketone **379** where photoisomerization of the double bond also had taken place (entry 2). An increased amount of isomerization product **378** was obtained when the reaction mixture was warmed to ambient temperature (entry 3). While photocycloaddition in the presence of $Cu(OTf)_2$ at –78 °C also led to photoisomerization, decomposition of the starting material took place upon warming to 0 °C and irradiating the reaction mixture for 12 h (entry 4). Using photosensitizer acetone as solvent resulted in complete decomposition of starting material (entry 5). Irradiation with 365 nm wavelength in acetonitrile with and without benzophenone as triplet sensitizer gave no conversion (entry 6, 7).

Table 20. Attempts for photoinduced [2+2] cycloaddition with ketone 373.

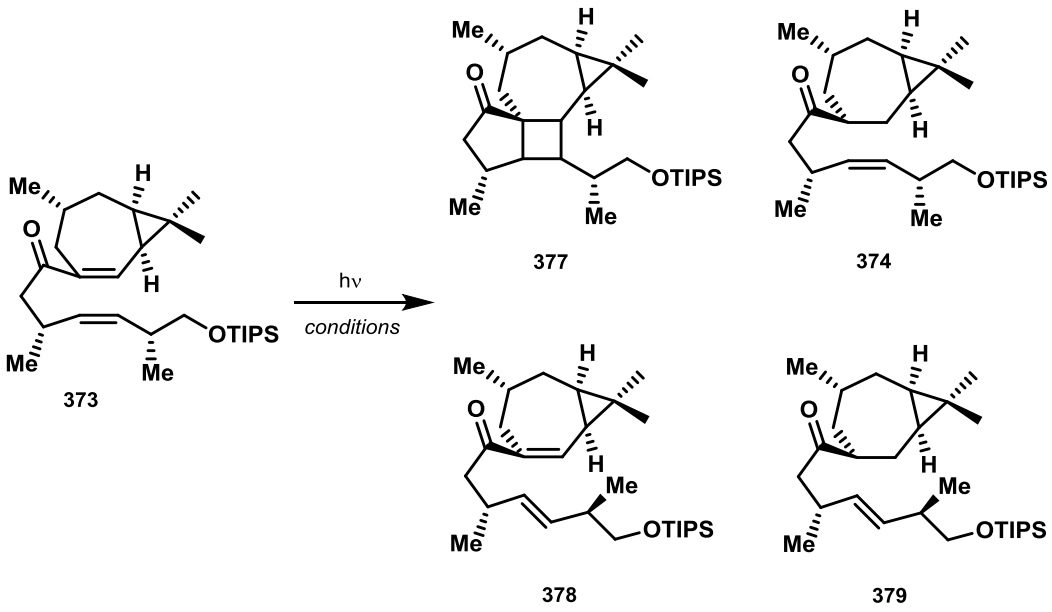

Entry[a]	Wavelength [nm]	Solvent, Additive (equiv.)	T [°C]	t [h]	Observation
1	254	DCM	–78	1	Mainly **373**, **378**, **379**
2	254	DCM	0	1.5	**373**, **378**, **379**
3	254	DCM	23	12	**378**
4	254	Et_2O, $Cu(OTf)_2$ (0.13)	–60 to 0	1-12	**378**, **374** starts to decompose
5	254	acetone	0	12	decomposition
6	365	MeCN	0	18	no conversion
7	365	MeCN, benzophenone	23	48	no conversion

[a]all reactions were performed in dry and degassed solvents.

Unfortunately, extensive screening of reaction conditions for this late-stage transannular [2+2] photocyclization with alcohol **364** and ketone **373** were unsuccessful and either photoisomerization of the double bond, 1,4-reduction, no conversion or decomposition of starting material was observed. At this point, it remained unclear what caused the unsuccessful reaction, possibly an unfavorable conformation of the starting material could explain the obtained results.

Since neither oxidation of C14 nor photoinduced [2+2] cycloaddition had proven successful, we had to abandon this strategy. Rather we were motivated to gain access to a key intermediate, with the correct oxidation state at C14, and investigate the photocycloaddition on this more advanced substrate.

2.3 Third generation approach: Strategy B

The previous presented synthetic studies directed toward the construction of key intermediate **377** revealed that the intramolecular [2+2] photocyclization was found to be challenging. Therefore, a new synthesis of seven-membered ring C was designed and examined by M.Sc. Po Yuan in parallel to the previous presented approaches. This strategy is only presented for completeness of the synthetic investigations toward the total synthesis of pepluacetal (**208**) and will not be discussed in detail.

In this approach, the construction of the challenging carbon skeleton of pepluacetal (**208**) should also be realized via late-stage transannular [2+2] cycloaddition starting from key intermediate **380** (Scheme 68). Introduction of the side chain was planned to be accomplished via a NHK reaction between vinyl bromide **381** and aldehyde **352** that had proven successful on the related system. Enone **381** in turn was planned to be derived from silyl ether **383** by performing a cyclopropanation followed by ring opening to construct the seven-membered cycle. The synthesis of silyl ether **383** was envisioned to start from ketone **384**, which in turn could be obtained following a known literature sequence again starting with (+)-3-carene (**172**). The advantage of this route lies in the construction of key intermediate **380** that contains all functionalities that are present in the natural product, and that doesn't require additional late-stage oxidation steps.

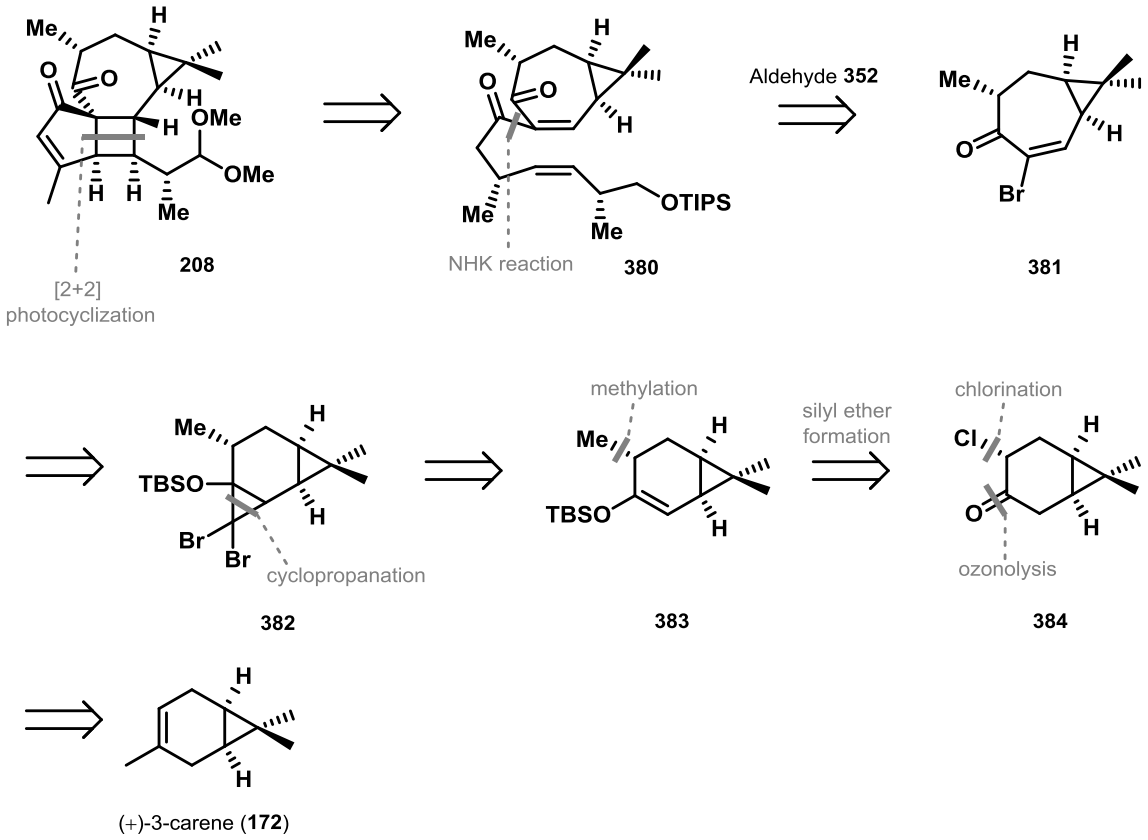

Scheme 68. Third-generation retrosynthesis of pepluacetal (208).

Following the retrosynthetic plan, ketone **381** was synthesized in three steps based on a procedure developed by Baran and co-workers (Scheme 69).[55] Formation of the silyl ether was realized using KHMDS and TBSOTf and gave silyl enol ether **383** in 90% yield. Construction of **382** was then accomplished by cyclopropanation[140] and subsequent ring opening under acidic conditions[141] yielding **381** after optimization of the reaction conditions. Performing the envisioned NKH reaction between vinyl bromide **381** and aldehyde **352** gave key intermediate **380** in 68% yield. After oxidation of the allylic alcohol the photoinduced cyclization was investigated next. Unfortunately, attempts to construct the sterically demanding core structure **388** of pepluacetal (**208**) also proved to be challenging with diketone **380** and the desired product could not be isolated. However, the key step in this approach was only conducted using the reaction conditions depicted in Scheme 69. Therefore, future studies should focus on in-depth investigations of the photocyclization of diketone **380** and alcohol **387** both in the presence and absence of catalysts.

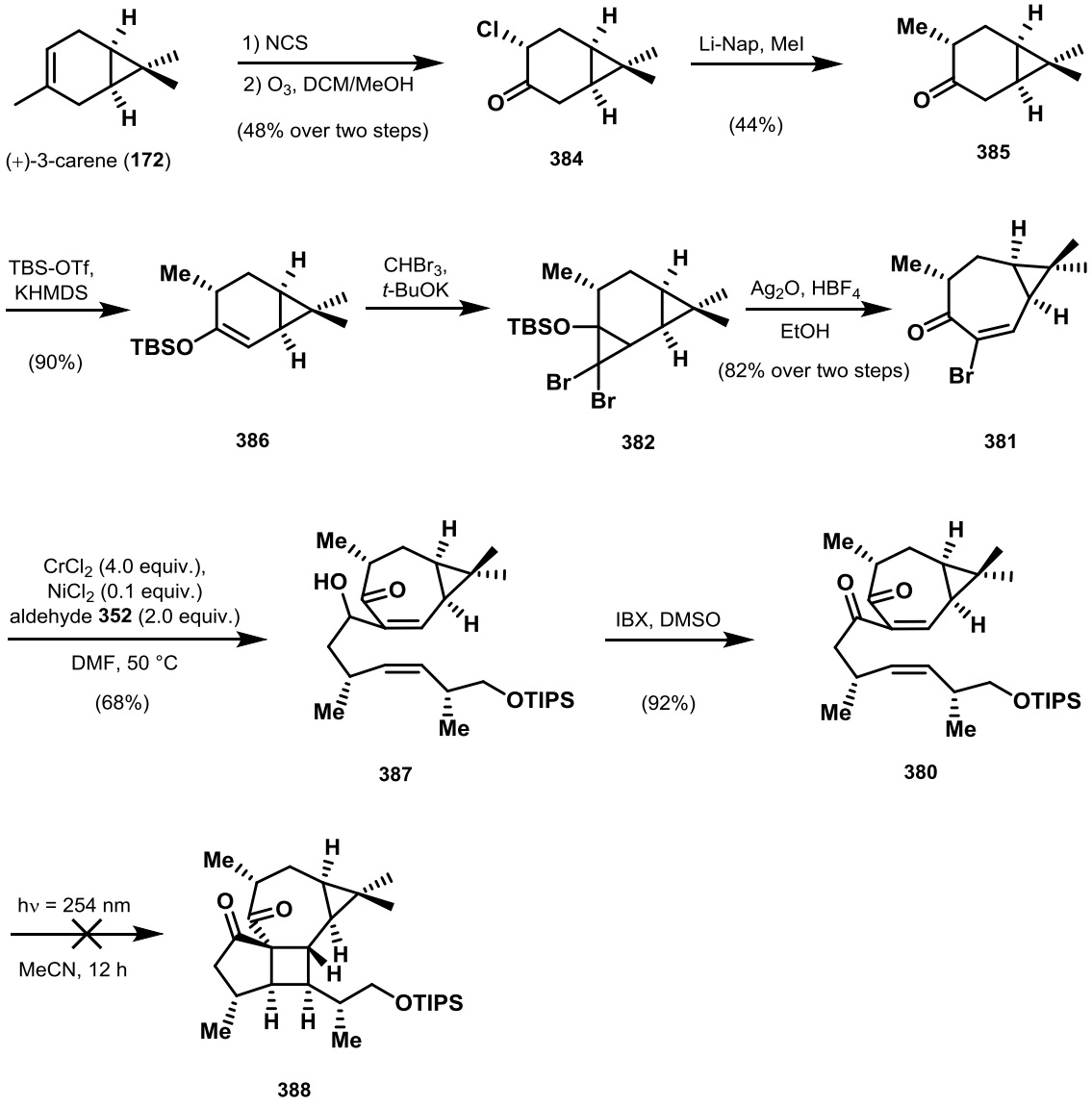

Scheme 69. Synthesis of key intermediate 380 and unsuccessful photocyclization.

3 Summary and Outlook

Progress toward the total synthesis of the *Euphorbia* diterpenoid pepluacetal (**208**) was discussed in the second part of this thesis.

In our first approach, we aimed to synthesize the challenging carbon core structure by late-stage transannular [2+2] photocyclization (Scheme 70). Therefore, a versatile route for the synthesis of key intermediate **259** was developed. The elaborated route commences with the preparation of methyl ester **264** in a five-step sequence starting from (+)-3-carene (**172**). Methyl ester **264** was then converted to alkene **278** via (*E*)-selective olefination with phosphonamide **295**, which was prepared starting from (*R*)-Roche ester. Aldehyde **260** was successfully obtained in two further steps. Cyclopentene building block **261** was synthesized following a three-step sequence. Next, the two building blocks **260** and **261** were coupled via nucleophilic 1,2-addition.

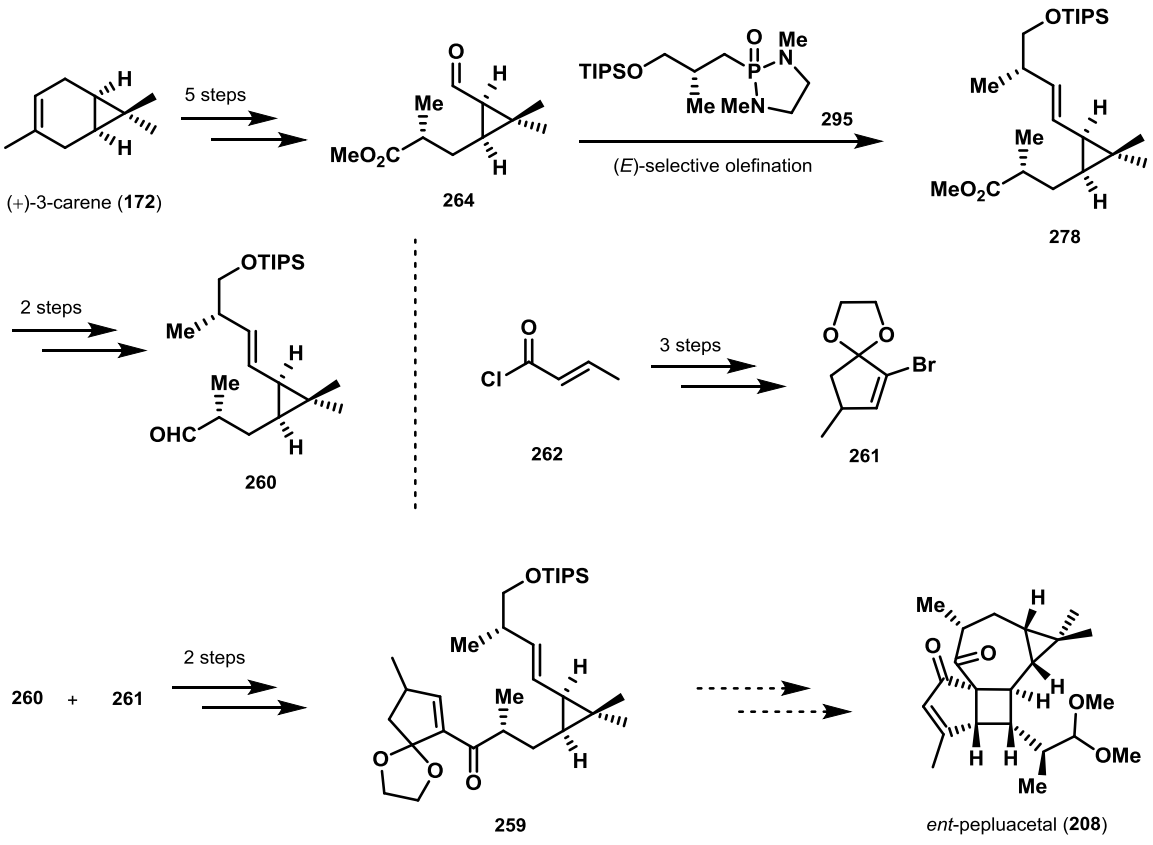

Scheme 70. Enantioselective synthesis of key intermediate 259.

With the established route toward key intermediate **259** in hand, we extensively investigated various conditions for an intramolecular [2+2] photocyclization toward the natural product. However, the construction of the sterically demanding scaffold of pepluacetal (**208**) remained unsuccessful following this approach.

An alternative approach commenced with literature known building block **304** which was synthesized in five steps also starting from (+)-3-carene (**172**) (Scheme 71). In four further steps enone **304** was converted to vinyl triflate **316** which was the starting point for investigating the introduction of side chain **352**. A robust synthesis of side chain **352** was developed following a five-step sequence starting from **308**.

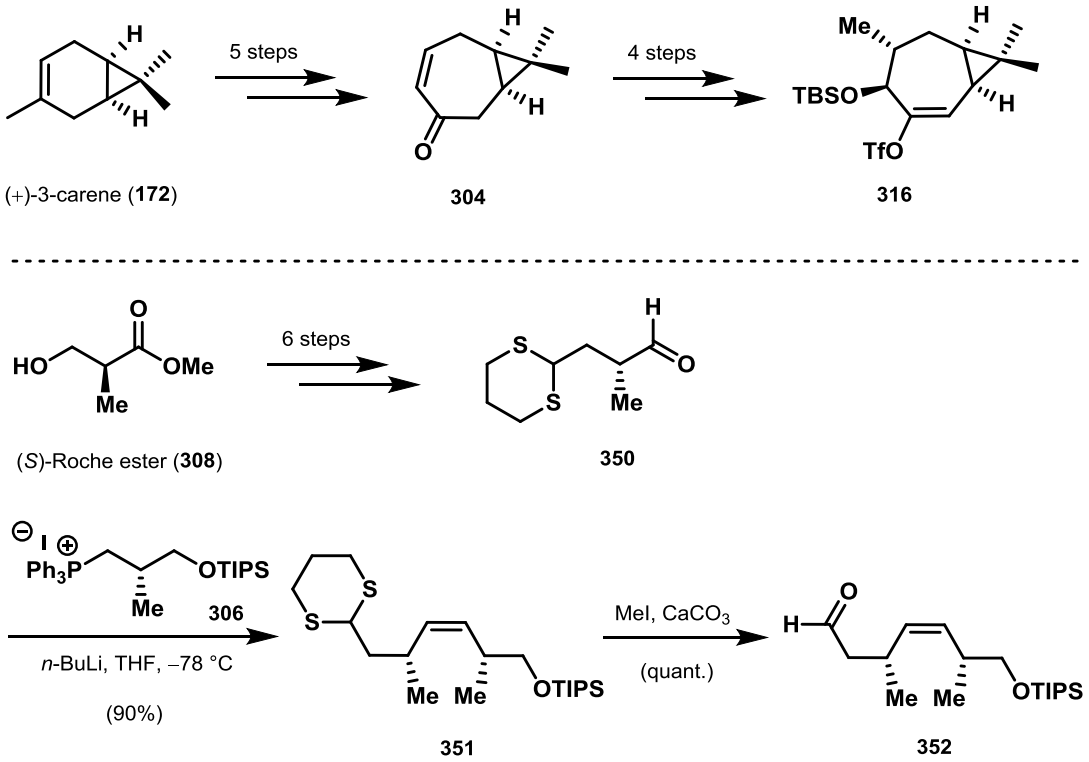

Scheme 71. Synthesis of vinyl triflate 316 and side chain 352.

Since introduction of the side chain **352** proved to be unsuccessful using ketone **316**, vinyl triflate **371** was prepared (Scheme 72). Gratifyingly, the NHK reaction of **371** and **352** enabled the successful construction of key intermediates **364** and **373**. However, extensive studies of various reaction conditions for the ensuing photocyclization proved to be unsuccessful also with the key intermediates alcohol **364** and ketone **373** as the substrates.

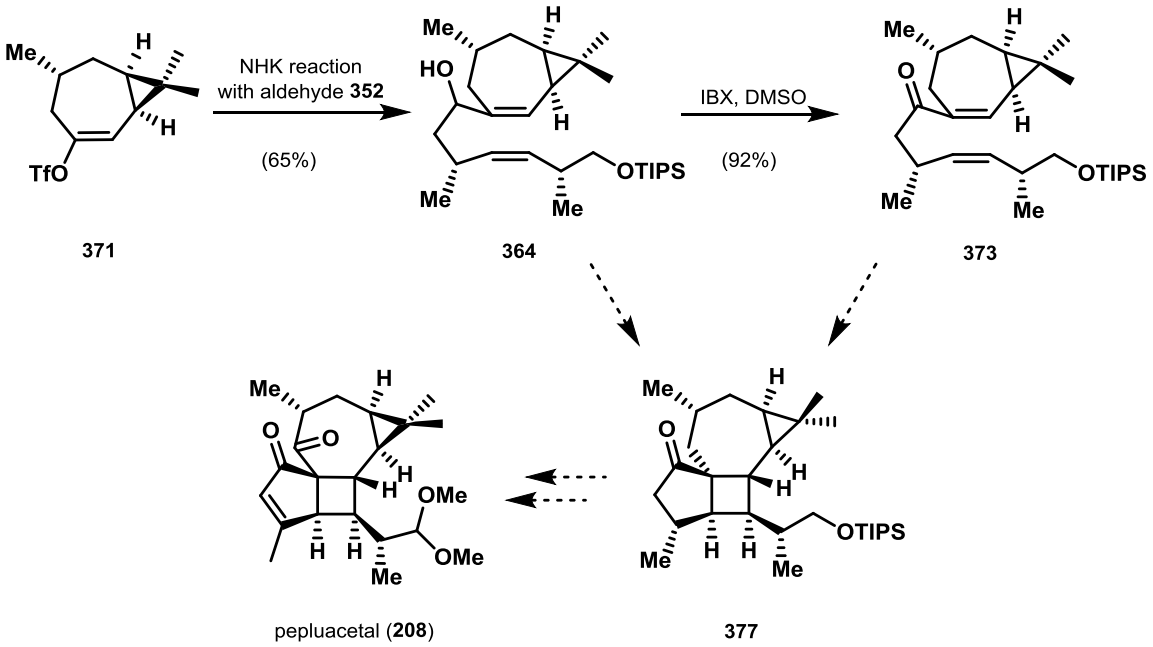

Scheme 72. Enantioselective synthesis of key intermediates alcohol 364 and ketone 373.

In a third synthetic approach developed by M.Sc. Po Yuan key intermediate **380** was prepared following a seven-step sequence (Scheme 73). The strategy commenced with the preparation of ketone **384** starting from (+)-3-carene (**172**) in three, literature known steps. The seven-membered ring C was constructed in three further steps proceeding via cyclopropanation and acid catalyzed ring opening. NHK reaction eventually furnished **380** after oxidation of the secondary alcohol.

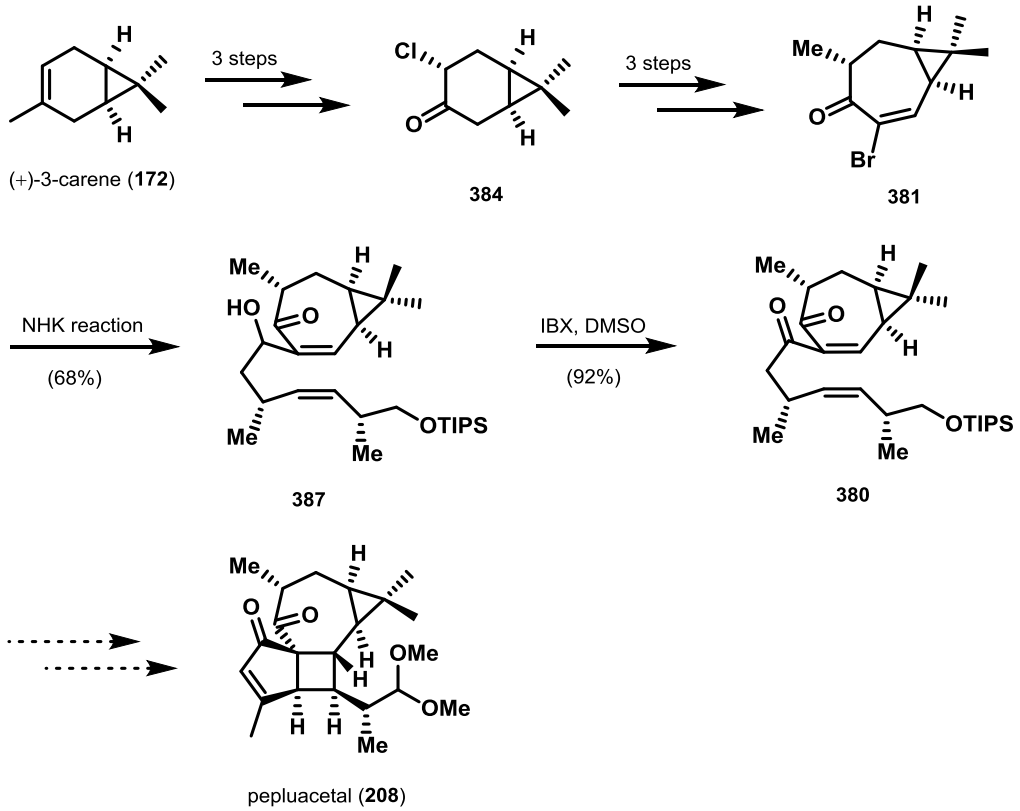

Scheme 73. Synthesis of diketone 380 as precursor for the total synthesis of pepluacetal (208).

With key intermediate **380** the envisioned [2+2] photocyclization to construct the tetracyclic skeleton of pepluacetal (**208**) proved to be challenging and could not be realized so far. Therefore, future studies will focus on in-depth investigations of this synthetic step.

Overall, the pursued strategies presented in this thesis highlight important results toward the total synthesis of the natural product pepluacetal (**208**). The developed routes not only include optimized functionalization procedures on highly complex substrates, but also disclosed unexpected challenges regarding sterics and electronics which will enable a better understanding of these structurally unique systems in the future. Further studies focusing on the completion of the total synthesis of pepluacetal (**208**) are currently under investigation in the Gaich laboratories.

III Experimental Part

1 General Details

All reactions were performed in glassware fitted with rubber septa under a positive pressure of nitrogen, unless otherwise noted. Air- and moisture-sensitive liquids were transferred via syringe or stainless-steel cannula through rubber septa. Solids were added under inert gas or were dissolved in appropriate solvents. Low temperature-reactions were carried out in a Dewar vessel filled with a cooling agent: acetone/dry ice (−78 °C), H_2O/ice (0 °C). Reaction temperatures above 24 °C were conducted in a heated oil bath. The reactions were magnetically stirred and monitored by NMR spectroscopy or analytical thin-layer chromatography (TLC), using plates precoated with silica gel (0.25 mm, 60 Å pore size, *Merck*) impregnated with a fluorescent indicator (254 nm). TLC plates were visualized by exposure to ultraviolet light (UV), were stained by submersion in aqueous basic potassium permanganate solution ($KMnO_4$), aqueous acidic ceric ammonium molybdate solution (CAM), or an aqueous acidic *p*-anisaldehyde solution and were developed by heating with a heat gun. Flash-column chromatography on silica gel was employed on silica gel (60 Å, 40–63 μm, *Merck KGaA*). Flash column chromatography on silica gel using triethylamine pretreated silica gel was performed by preparing the silica gel slurry with triethylamine (7.5% v/v in corresponding eluent mixture) and flushing the column with the eluent prior to loading the compound on the column. The yields refer to chromatographically and spectroscopically (^{1}H and ^{13}C NMR) pure material unless stated otherwise.

1.1 Solvents and Reagents

Triethylamine (Et_3N), diisopropylamine (DIPA) and *N*,*N*-diisopropylethylamine (DIPEA) were distilled under nitrogen atmosphere from calcium hydride prior to use. Benzene, toluene, 1,4-dioxane, dimethylformamide (DMF), dimethyl sulfoxide (DMSO), dichloromethane (CH_2Cl_2), acetonitrile (MeCN), ethanol (EtOH), tetrahydrofuran (THF), diethyl ether (Et_2O) and methanol (MeOH) were purchased from *Acros Organics* as 'extra dry' reagents and used as received. All other reagents and solvents were purchased from chemical suppliers (*Sigma-Aldrich, Acros Organics, Alfa Aesar, Strem Chemicals, TCI Europe, carbolution, ABCR*) and were used as received. Solvents for extraction, crystallization and flash column chromatography on silica gel were purchased in technical grade and distilled under reduced pressure prior to use. Lithium chloride and lithium bromide were dried at 100 °C under vacuum (0.1 mmHg) for 12 h and stored in a drying oven at 130 °C (760 mmHg); the hot, dried solid was flame dried under vacuum (0.1 mmHg) for 4–5 min immediately prior to use. 4 Å molecular sieves were washed (methanol, acetone, dichloromethane) and then dried at 100 °C under vacuum (0.1 mmHg) for 12 h and

stored in a drying oven at 130 °C (760 mmHg); the molecular sieves were flame dried under vacuum (0.1 mmHg) for 4–5 min immediately prior to use.

1.2 NMR Spectroscopy

NMR spectra were recorded on a 400 MHz spectrometer (Avance III 400), a 600 MHz spectrometer (Acance III 600) with and without cryoplatform or an 800 MHz spectrometer (Avance NEO) with cryoplatform from Bruker. All NMR spectra were measured in CDCl3 solution. Proton chemical shifts are expressed in parts per million (ppm, δ scale) and are referenced to residual protium in the NMR solvent ($CHCl_3$: δ 7.26, C_6HD_5: 7.16). Carbon chemical shifts are expressed in parts per million (δ scale, assigned carbon atom) and are referenced to the carbon resonance of the NMR solvent ($CDCl_3$: δ 77.16, C_6D_6: 128.06). ^{1}H NMR spectroscopic data are reported as follows: Chemical shift in ppm (multiplicity, coupling constants *J* (Hz), integration intensity, assigned proton) (e.g. "5.21 (t, *J* = 7.3 Hz, 1H, H-9)"). The multiplicities are abbreviated with s (singlet), br s (broad singlet), d (doublet), t (triplet), q (quartet), p (pentet), se (sextet), h (heptet) and m (multiplet). In case of combined multiplicities, the multiplicity with the larger coupling constant is stated first. Except for multiplets, the chemical shift of all signals, as well for centrosymmetric multiplets, is reported as the center of the resonance range. Furthermore, the numbering of the proton and carbon atoms does not correspond to the IUPAC nomenclature. ^{13}C NMR spectroscopic data are reported as follows: Chemical shift in ppm In addition to ^{1}H and ^{13}C NMR measurements, 2D NMR techniques such as homonuclear correlation spectroscopy (COSY), heteronuclear single quantum coherence (HSQC) and heteronuclear multiple bond coherence (HMBC) were used to assist signal assignment. For further elucidation of 3D structures of the products, nuclear Overhauser enhancement spectroscopy (NOESY) was conducted. All raw FID files were processed and the spectra analyzed using the program *MestReNova 9.0.1* from *Mestrelab Research S. L*.

1.3 Mass Spectrometry

High resolution mass spectra were measured on an LTQ Orbitrap Velos spectrometer from Thermo Fisher Scientific (Velos Pro) with or without loop-mode injection from a Waters (RP18) HPLC system or a Micromass LCT spectrometer via loop-mode injection from a Waters (Alliance 2695) HPLC system. Ionization was achieved by ESI, modes of ionization, calculated and found mass are given.

1.4 IR Spectroscopy

IR spectra were measured on a PerkinElmer Spectrum 100 FT-IR spectrometer. Data are represented in frequency of absorption (cm^{-1}). Samples were prepared as a neat film or a film by evaporation of a solution.

1.5 Optical Rotation

Optical rotation values were recorded on a JascoP-2000 Digital Polarimeter using the sodium D line (589 nm). The specific rotation is calculated as follows:

$$[\alpha]_{\lambda}^{\varphi} = \frac{\alpha}{\beta \cdot d}$$

α: recorded optical rotation

β: concentration of the analyte in 10 mg/mL

d: length of the cuvette in dm

φ: measuring temperature in °C

λ: wave length in nm

The respective concentration and the solvent are denoted in the analytical part of the experimental description.

1.6 UV-Vis Spectroscopy

The data collections were performed either on an *Oxford Diffraction* Xcalibur diffractometer, on a *Bruker* D8Quest diffractometer or on a *Bruker* D8Venture at 100 K or at 173 K using MoKα-radiation (λ = 0.71073 Å, graphite monochromator). The CrysAlisPro software (version 1.171.33.41) was applied for the integration, scaling and multi-scan absorption correction of the data. The structures were solved by direct methods with SIR97 and refined by least-squares methods against *F*2 with SHELXL-97. All non-hydrogen atoms were refined anisotropically. The hydrogen atoms were placed in ideal geometry riding on their parent atoms. Further details are summarized in the tables at the different sections.

1.7 X-ray Analysis

X-ray diffraction analysis of single crystals was performed at 100 k on a STOE IPDS-II diffractometer equipped with a graphite-monochromated radiation source (λ = 0.71073 Å) and an image plate detection system. A crystal mounted on a fine glass fiber with silicon grease was employed.

2 Experimental Procedures

2.1 The Parvineostemonine Project

1-Cinnamyl-4-ethyl-3-hydroxypyridin-1-ium bromide (121)

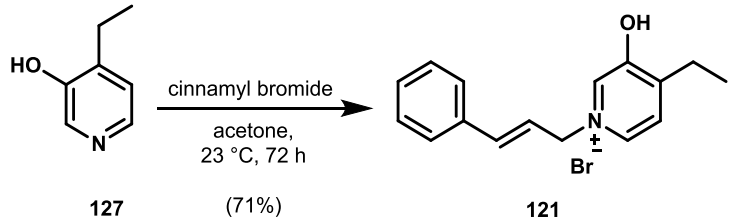

127 (71%) 121

4-Ethylpyridin-3-ol **127** (6.34 g, 51.5 mmol, 1 equiv) was dissolved in acetone (60.0 mL), followed by the addition of cinnamyl bromide (10.1 g, 51.4 mmol, 1 equiv) in acetone (60.0 mL). The resulting solution was stirred for three days at room temperature. The precipitate was filtered off to obtain 11.8 g (71%) of the desired product **121**.

^{1}H NMR (400 MHz, MeOD): δ = 8.45 (dd, *J*=6.1, 1.4 Hz, 1H), 8.30 (d, *J*=1.4 Hz, 1H), 7.83 (d, *J*=6.1 Hz, 1H), 7.54–7.46 (m, 2H), 7.39–7.26 (m, 3H), 6.99 (d, *J*=15.7 Hz, 1H), 6.53 (dt, *J*=15.8, 7.1 Hz, 1H), 5.30 (d, *J*=7.2 Hz, 2H), 2.88 (q, *J*=7.5 Hz, 2H), 1.31 (t, *J*=7.5 Hz, 3H) ppm. **^{13}C NMR** (100 MHz, MeOD): δ = 156.7, 152.6, 139.7, 136.9, 136.7, 130.0, 129.9, 128.5, 128.1, 122.0, 63.7, 24.2, 12.4 ppm.

IR (Diamond-ATR, neat) $\tilde{\nu}_{max}$**:** 3339, 3026, 2974, 2936, 1626, 1582, 1528, 1474, 1373, 1310, 1281, 1134, 1059, 976, 878, 841 cm^{-1}.

Melting Point: 123-125 °C.

HRMS (ESI, *m/z*): calcd for $(C_{16}H_{18}NO)^+$: 240.1383, found: 240.1388.

(1*R*,5*R*)-8-cinnamyl-3-ethyl-8-azaspiro[bicyclo[3.2.1]oct[3]ene-6,2'-[1,3]dithiolan]-2-one 1',3'-dioxide (118) and (1*R*,5*R*)-8-cinnamyl-3-ethyl-8-azaspiro[bicyclo[3.2.1]oct[2]ene-6,2'-[1,3]dithiolan]-4-one 1',3'-dioxide (119)

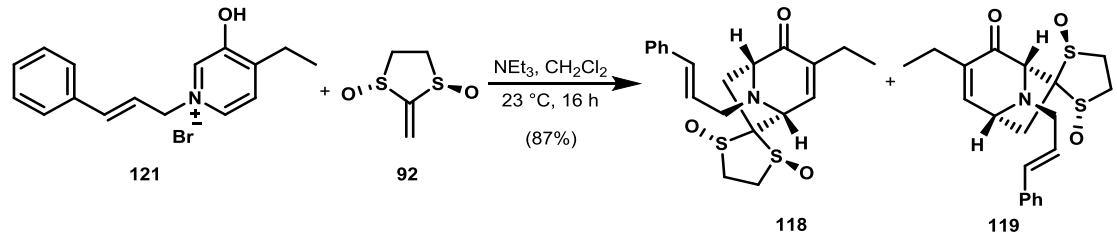

Bissulfoxide **92** (445 mg, 2.97 mmol, 1.6 equiv) was dispersed in dichloromethane (18 mL) under an inert atmosphere, followed by the addition of solid pyridinium salt **121** (590 mg, 1.84 mmol, 1 equiv) and triethylamine (0.28 mL, 2.02 mmol, 1.1 equiv). The reaction vessel was wrapped in aluminium foil and the reaction mixture was stirred at ambient temperature for 24 h. The remaining solvent was then removed under reduced pressure and the crude remains were purified by flash column chromatography on silica gel (100% acetone) to yield 626 mg (87%) of regioisomeric tricycles **118** and **119** (5.6:1 ratio **118**:**119**) as a yellow foam. The mixture of regioisomers was used directly in the next step as separation could not be achieved.

Major regioisomer (**118**):

TLC (100% acetone): R_f = mixture of regioisomers: 0.78 (UV, $KMnO_4$).

^{1}H-NMR (400 MHz, $CDCl_3$): δ = 7.36–7.31 (m, 2H), 7.30–7.23 (m, 2H), 7.22–7.16 (m, 1H), 6.62 (dt, *J* = 5.1, 1.4 Hz, 1H), 6.47 (d, *J* = 16.0 Hz, 1H), 6.12 (dt, *J* = 16.0, 6.2 Hz, 1H), 4.29 (d, *J* = 5.1 Hz, 1H), 3.91–3.82 (m, 2H), 3.54–3.46 (m, 2H), 3.42–3.31 (m, 3H), 2.45 (d, *J* = 15.4 Hz, 1H), 2.30 (q, *J* = 7.5 Hz, 2H), 2.20 (dd, *J* = 15.5, 7.7 Hz, 1H), 1.07 (t, *J* = 7.3 Hz, 3H) ppm.

IR (Diamond-ATR, neat, mixture of regioisomers) $\tilde{\nu}_{max}$**:** 2968, 2932, 2832, 1684, 1599, 1495, 1449, 1373, 1234, 1138, 1092, 1065, 1040, 968, 835 cm^{-1}.

HRMS (mixture of regioisomers) (ESI, *m/z*): calcd for $(C_{20}H_{23}NO_3S_2)^+[M+H]^+$: 390.1198; found: 390.1201.

Minor regioisomer (**119**):

TLC (100% acetone): R_f = mixture of regioisomers: 0.78 (UV, $KMnO_4$).

^{1}H NMR (400 MHz, $CDCl_3$): δ = 7.36–7.31 (m, 2H), 7.30–7.23 (m, 2H), 7.22–7.16 (m, 1H), 6.77 (td, *J* = 5.5, 1.4 Hz, 1H), 6.49–6.45 (m, 1H), 6.17–6.09 (m, 1H), 4.15 (br.s, 1H), 4.06 (t, *J* =

5.5 Hz, 1H), 3.69–3.62 (m, 1H), 3.91–3.32 (m, 6H), 2.62 (d, *J* = 14.3 Hz, 1H), 2.43–2.37 (m, 1H), 2.29–2.24 (m, 2H), 1.08–1.04 (m, 3H) ppm.

(1*R*,5*R*)-8-cinnamyl-3-ethyl-8-azaspiro[bicyclo[3.2.1]oct[3]ene-6,2'-[1,3]dithiolan]-2-one (132) and (1*R*,5*R*)-8-cinnamyl-3-ethyl-8-azaspiro[bicyclo[3.2.1]oct[2]ene-6,2'-[1,3]dithiolan]-4-one (133)

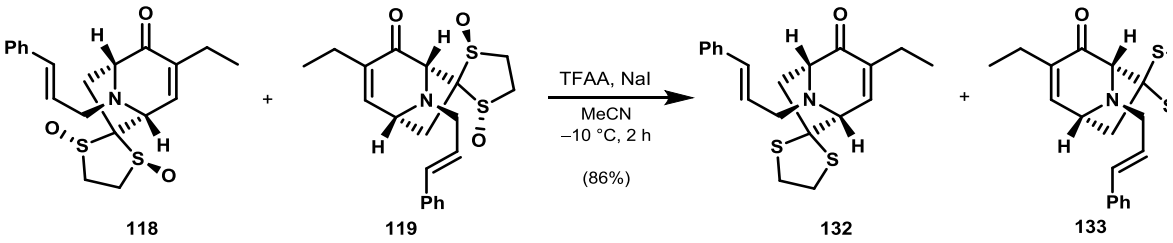

118 119 132 133

To a solution of regiosiomeric mixture of bissulfoxides **118/119** (5.6:1 mixture of major/minor by NMR, 1.00 g, 2.56 mmol, 1 equiv) in acetonitrile (52.0 mL) sodium iodide (1.92 g, 12.8 mmol, 5 equiv) was added. The resulting reaction mixture was cooled to –10 °C and stirred 20 min and trifluoroacetic anhydride (1.08 mL, 7.70 mmol, 3 equiv) was added dropwise. The reaction was stirred at –10 °C for 2 h before adding first a saturated sodium thiosulfate solution, then 2 M sodium hydroxide solution to quench the reaction. The mixture was diluted with dichloromethane and transferred to a separation funnel. The phases were separated, and the aqueous layer was extracted two more times with dichloromethane. The combined organic layers were dried over magnesium sulfate and the solvent was removed under reduced pressure. The crude mixture was purified by flash column chromatography on silica gel (10% ethyl acetate in petroleum ether) to give 668 mg (73%, isolated major regioisomer **132**) and 128 mg (13%, isolated minor regioisomer **133**) as yellow solid.

Major regioisomer **132**:

TLC (16% ethyl acetate in petroleum ether): R_f = 0.50 (UV, $KMnO_4$).

^{1}H NMR (400 MHz, $CDCl_3$): δ = 7.40–7.38 (m, 2H), 7.34–7.28 (m, 2H), 7.26–7.20 (m, 1H), 6.64 (dt, *J* = 5.1, 1.4 Hz, 1H), 6.53 (d, *J* = 16.0 Hz, 1H), 6.26–6.15 (m, 1H), 3.85 (d, *J* = 5.1 Hz, 1H), 3.65 (d, *J* = 8.2 Hz, 1H), 3.49–3.37 (m, 3H), 3.35–3.31 (m, 1H), 3.29–3.20 (m, 2H), 3.10 (dd, *J* = 14.7, 7.9 Hz, 1H), 2.37–2.22 (m, 2H), 1.09 (t, *J* = 7.5 Hz, 3H) ppm. **^{13}C NMR** (100 MHz, $CDCl_3$): δ = 198.9, 140.1, 139.9, 136.9, 132.5, 128.6, 127.7, 126.5, 126.4, 71.2, 69.8, 68.1, 50.9, 45.6, 40.5, 40.4, 21.1, 12.6 ppm.

IR (Diamond-ATR, neat) $\tilde{\nu}_{max}$**:** 3024, 2963, 2922, 2872, 2827, 1680, 1597, 1578, 1495, 1447, 1371, 1335, 1304, 1277, 1206, 1070, 966, 934, 910, 891, 854 cm^{-1}.

$[\boldsymbol{\alpha}]_{\boldsymbol{D}}^{\boldsymbol{20}}$: –59.0 (c = 0.61; $CHCl_3$).

HRMS (mixture of regioisomers) (ESI, *m/z*): calcd for $(C_{20}H_{23}NOS_2)^+$ $[M+H]^+$: 358.1299; found: 358.1299.

Minor regioisomer **133**:

TLC (16% ethyl acetate in petroleum ether): R_f = 0.30 (UV, $KMnO_4$).

^{1}H NMR (400 MHz, $CDCl_3$): δ = 7.40–7.35 (m, 2H), 7.34–7.28 (m, 2H), 7.25–7.21 (m, 1H), 6.59 (dt, *J*=5.2, 1.5 Hz, 1H), 6.51 (d, *J*=16.0 Hz, 1H), 6.22 (dt, *J*=15.7, 6.5 Hz, 1H), 3.87 (t, *J*=5.8 Hz, 1H), 3.74 (d, *J*=0.7 Hz, 1H), 3.52–3.32 (m, 4H), 3.29–3.21 (m, 1H), 3.20–3.12 (m, 1H), 2.93 (dd, *J*=13.5, 6.3 Hz, 1H), 2.40 (d, *J*=13.7 Hz, 1H), 2.26 (q, *J*=7.1 Hz, 2H), 1.09 (t, *J*=7.3 Hz, 3H) ppm. **^{13}C NMR** (100 MHz, $CDCl_3$): δ = 195.8, 141.1, 140.3, 136.9, 133.1, 128.7, 127.8, 126.6, 126.2, 83.9, 65.4, 58.6, 52.1, 45.3, 41.0, 39.0, 21.2, 12.3 ppm.

IR (Diamond-ATR, neat) $\tilde{\nu}_{max}$**:** 3024, 2963, 2930, 1682, 1494, 1449, 1371, 1275, 1221, 1134, 1053, 1011, 968, 881 cm^{-1}.

HRMS (mixture of regioisomers) (ESI, *m/z*): calcd for $(C_{20}H_{23}NOS_2)^+$ $[M+H]^+$: 358.1299; found: 358.1299.

$[\boldsymbol{\alpha}]_{\boldsymbol{D}}^{\boldsymbol{20}}$: –116 (c = 0.61; $CHCl_3$).

(1*R*,3*R*,4*R*,5*R*)-4-allyl-8-cinnamyl-3-ethyl-8-azaspiro[bicyclo[3.2.1]octane-6,2'-[1,3]dithiolan]-2-one (117)

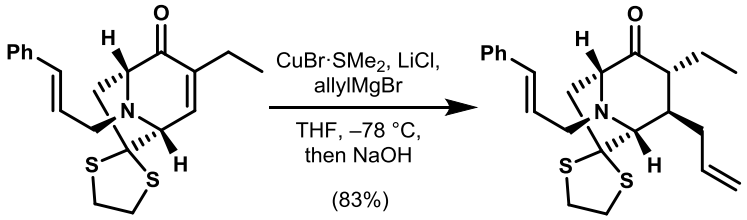

132 117

$CuBr{\cdot}SMe_2$ (240 mg, 1.16 mmol, 1 equiv) and dry lithium chloride (133 mg, 1.35 mmol, 1.8 equiv) were placed into a flame dried Schlenk flask and treated as described by Lipshutz et al.[44] Tetrahydrofuran (3.75 mL) was added and the resulting reaction mixture was cooled to –78 °C. Allylmagnesium bromide solution (1.0 M in diethyl ether, 1.60 mL, 1.35 mmol, 1.8 equiv) was added to the solution, followed by immediate dropwise addition of Michael acceptor **132** (286 mg, 749 µmol, 0.9 equiv). The reaction mixture was stirred for 10 min, before the addition of 2 M sodium hydroxide solution at –78 °C quenched the reaction. The mixture was allowed to stir for 1 h at ambient temperature, before the mixture was transferred to a separation funnel. Ethyl acetate was added, as well as neat sodium chloride, and the aqueous phase was extracted with ethyl acetate. The combined organic layers were then washed with saturated aqueous sodium chloride solution, followed by drying over magnesium sulfate. The solvent was removed under reduced pressure and the obtained crude oil was purified *via* flash column chromatography on silica gel (10% ethyl acetate in petroleum ether) to yield 250 mg (83%) of **117** as a clear oil.

TLC (10% ethyl acetate in petroleum ether): $R_f = 0.41$ (UV, $KMnO_4$).

^{1}H NMR (400 MHz, $CDCl_3$): δ = 7.43–7.35 (m, 2H), 7.35–7.28 (m, 2H), 7.25–7.20 (m, 1H), 6.59 (d, *J* = 16.0 Hz, 1H), 6.23 (dt, *J* = 15.8, 6.6 Hz, 1H), 5.78 (dddd, *J* = 16.5, 10.8, 8.5, 5.1 Hz, 1H), 5.08–4.91 (m, 2H), 3.61–3.38 (m, 5H), 3.33–3.24 (m, 1H), 3.24–3.17 (m, 2H), 2.96 (dd, *J* = 14.7, 7.8 Hz, 1H), 2.44–2.33 (m, 2H), 2.30–2.18 (m, 1H), 2.18–2.11 (m, 2H), 1.72–1.59 (m, 2H), 0.96 (t, *J* = 7.5 Hz, 3H) ppm. **^{13}C NMR** (100 MHz, $CDCl_3$): δ = 213.9, 137.0, 136.6, 133.2, 128.7 (2C), 127.7, 127.1, 126.5 (2C), 117.8, 74.5, 71.2, 70.1, 54.6, 50.7, 48.5, 40.8, 40.5, 40.3, 39.2, 21.4, 12.3 ppm.

IR (Diamond-ATR, neat) $\tilde{\nu}_{max}$**:** 3024, 2961, 2924, 2874, 1715, 1639, 1597, 1495, 1449, 1375, 1342, 1275, 1148, 1105, 1047, 966, 912 cm^{-1}.

HRMS (ESI, *m/z*): calcd for $(C_{23}H_{29}NOS_2)^+$ $[M+H]^+$: 400.1769; found: 400.1766.

$[\boldsymbol{\alpha}]_{\boldsymbol{D}}^{\boldsymbol{20}}$: –44.0 (c = 0.83; $CHCl_3$).

(3*R*,4*S*,9*R*,9a*R*,10*R*)-10-ethyl-2,3,5,8,9,9a-hexahydrospiro[9,3-ethanopyrrolo[1,2-*a*]azepine-1,2'-[1,3]dithiolan]-11-one (134)

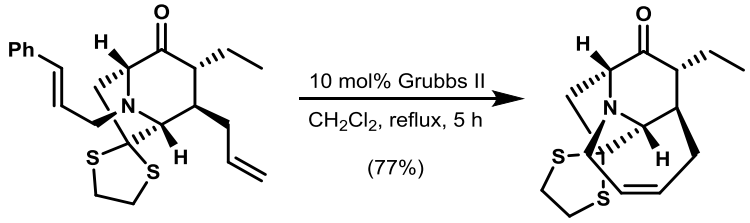

117 **134**

Bisolefin **117** (202 mg, 505 µmol, 1 equiv) was dissolved in degassed dichloromethane (35.0 mL) and Grubbs II catalyst (43 mg, 51.0 µmol, 0.1 equiv) was added in dichloromethane (15.0 mL). The reaction mixture was heated to reflux for 5 h. The solvent was then evaporated and the crude remains were subjected to flash column chromatography on silica gel (11% ethyl acetate in petroleum ether) to obtain 110 mg (77%) of olefin **134** as a white solid.

TLC (16% ethyl acetate in petroleum ether): $R_f = 0.50$ ($KMnO_4$).

^{1}H NMR (400 MHz, $CDCl_3$): δ = 5.70 – 5.56 (m, 2H), 3.98–3.89 (m, 1H), 3.64 – 3.55 (m, 1H), 3.45 – 3.27 (m, 5H), 3.24 – 3.17 (m, 1H), 3.01 – 2.89 (m, 2H), 2.36 – 2.24 (m, 3H), 2.00 – 1.93 (m, 1H), 1.83 – 1.70 (m, 2H), 1.00 (t, *J*=7.2 Hz, 3H) ppm. **^{13}C NMR** (100 MHz, $CDCl_3$): δ = 214.7, 130.6, 129.1, 76.2, 71.8, 67.8, 52.2, 49.3, 45.6, 41.1, 39.8, 38.9, 37.6, 28.7, 12.8 ppm.

IR (Diamond-ATR, neat) $\tilde{\nu}_{max}$**:** 2961, 2920, 1705, 1449, 1423, 1277, 1244, 1163, 1136, 972 cm^{-1}.

$[\boldsymbol{\alpha}]_{\boldsymbol{D}}^{\boldsymbol{20}}$: –164 (c = 0.18; $CHCl_3$).

HRMS (ESI, *m/z*): calcd for $(C_{15}H_{21}NOS_2)^+$ $[M+H]^+$: 296.1143; found: 296.1145.

(3*R*,4*R*,9*R*,9a*S*,10*R*)-10-ethyloctahydro-1H-9,3-ethanopyrrolo[1,2-*a*]azepin-11-one ((–)-135)

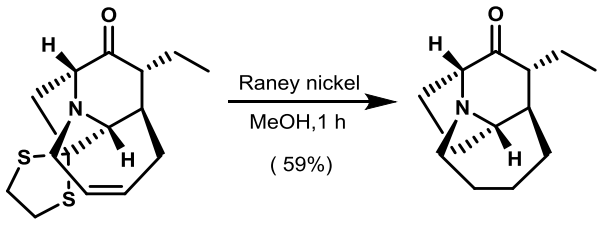

134 (–)-**135**

An aqueous dispersion of Raney nickel in water (4 pipettes) was washed three times with methanol, and the waste solvent was discarded. Dithiolane **134** (20.0 mg, 67.7 µmol) was added

in methanol (2.00 mL), and the reaction mixture was stirred for 1 h at ambient temperature. Raney nickel was then filtered off, and the solvent was removed under reduced pressure. The crude oil was subjected to flash column chromatography on silica gel (4% methanol in dichloromethane) to give 8.20 mg (59%) of amine (–)-**135** as clear oil.

TLC (4% methanol in dichloromethane): $R_f = 0.50$ ($KMnO_4$).

^{1}H NMR (400 MHz, $CDCl_3$): δ = 3.50 (d, *J*=7.2 Hz, 1H), 3.47 – 3.41 (m, 1H), 3.37 (d, *J*=7.9 Hz, 1H), 2.45 (td, *J*=12.0, 2.1 Hz, 1H), 2.28 – 2.17 (m, 1H), 2.17–2.06 (m, 1H), 2.00 – 1.90 (m, 3H), 1.84 – 1.52 (m, 8H), 1.51 – 1.38 (m, 1H), 0.91 (t, *J*=7.5 Hz, 3H) ppm. **^{13}C NMR** (125 MHz, $CDCl_3$): δ = 217.1, 70.1, 59.2, 51.2, 49.0, 45.3, 34.5, 31.0, 27.5, 27.1, 26.5, 26.4, 11.8 ppm.

IR (Diamond-ATR, neat) $\tilde{\nu}_{max}$**:** 2924, 1705, 1456, 1377, 1281, 1159, 1148, 1134, 986, 816, 799 cm^{-1}.

HRMS (ESI, *m/z*): calcd for $(C_{13}H_{21}NO)^+$ $[M+H]^+$: 208.1701; found: 208.1701.

$[\boldsymbol{\alpha}]_{\boldsymbol{D}}^{\boldsymbol{20}}$: –171 (c= 0.22; $CHCl_3$).

(3*R*,4*R*,9*R*,9a*S*,10*S*)-10-ethyloctahydro-1H-9,3-ethanopyrrolo[1,2-*a*]azepin-11-one ((–)-116)

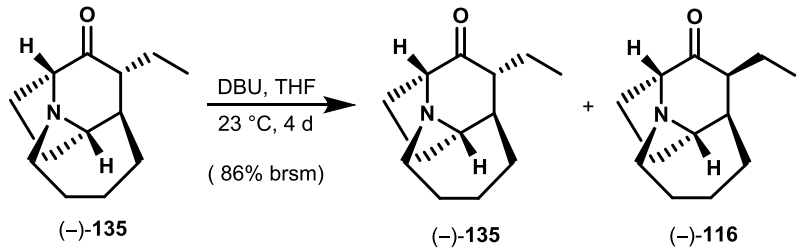

(–)-**135** (235 mg, 1.13 mmol, 1 equiv) was dissolved in tetrahydrofuran (10.0 mL), followed by the addition of 1,8-diazabicyclo[5.4.0]undec-7-ene (0.41 mL, 3.40 mmol, 3 equiv). The resulting reaction mixture was stirred for four days at ambient temperature, before the addition of saturated ammonium chloride solution (10.0 mL) quenched the reaction. The phases were separated and the aqueous layer was extracted with dichloromethane. The combined organic layers were dried over magnesium sulfate and the solvent was removed under reduced pressure. The two isomers were separated by flash column chromatography on silica gel (4% methanol in dichloromethane) to afford 228 mg (86%, based on recovered starting material) of (–)-**116** as colorless oil.

TLC (4% methanol in dichloromethane): $R_f = 0.34$ ($KMnO_4$).

^{1}H NMR (400 MHz, $CDCl_3$): δ = 3.52 (d, *J*=6.8 Hz, 1H), 3.29 (dt, *J* = 13.0, 3.6 Hz, 1H), 3.20 (d, *J*=7.1 Hz, 1H), 2.69 (td, *J*=12.9, 3.0 Hz, 1H), 2.64 – 2.58 (m, 1H), 2.54 (q, *J* = 7.7, 5.6 Hz, 1H), 2.28 – 2.18 (m, 1H), 1.93 – 1.70 (m, 7H), 1.62 – 1.50 (m, 1H), 1.35 – 1.09 (m, 3H), 0.86 (t, *J* = 7.4 Hz, 3H) ppm. **^{13}C NMR** (125 MHz, $CDCl_3$): δ = 211.9, 70.7, 59.1, 52.5, 48.9, 46.8, 30.2, 29.2, 28.1, 26.9, 25.8, 17.7, 12.3 ppm.

IR (Diamond-ATR, neat) $\tilde{\nu}_{max}$**:** 2928, 2873, 1698, 1450, 1376, 1237, 1207, 1151, 1088, 969, 943, 910, 821, 792, 731cm^{-1}.

HRMS (ESI, *m/z*): calcd for $(C_{13}H_{21}NO)^+$ $[M+H]^+$: 208.1701; found: 208.1701.

$[\boldsymbol{\alpha}]_{\boldsymbol{D}}^{\boldsymbol{20}}$: –76.0 (c = 0.60; CH_2Cl_2).

(2'*R*,3*R*,4*R*,9*R*,9a*S*,10*S*)-10-ethyl-4'-methyleneoctahydro-1H,3'H-spiro[9,3-ethanopyrrolo[1,2-*a*]azepine-11,2'-furan]-5'(4'*H*)-one (144)

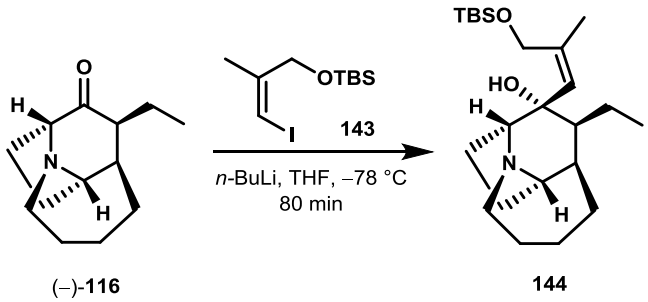

(–)-**116** **144**

n-Butyllithium (2.5 M in hexane, 0.24 mL, 7 equiv) was added dropwise to a solution of vinyl iodide **143**[47] (256 mg, 820 µmol, 10 equiv) in tetrahydrofuran (0.17 mL) at –78 °C. After stirring for 60 min, ketone (–)-**116** (17.0 mg, 82.0 µmol, 1 equiv) in tetrahydrofuran (0.05 mL) was added dropwise. The solution was stirred for another 20 min at –78 °C, before the addition of distillated water and dichloromethane quenched the reaction. The phases were separated and the aqueous layer was extracted with dichloromethane. The combined organic layers were dried over magnesium sulfate and the solvent removed under reduced pressure. The crude material was used in the next step without further purification.

(+)-Parvineostemonine (53)

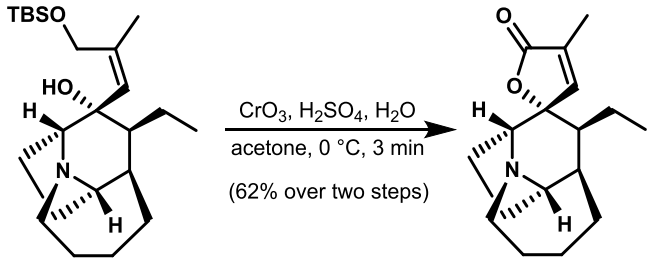

144 parvineostemonine (+)-**53**

Crude tertiary amine **144** (1 equiv) was dissolved in acetone (57.0 mL) and cooled to 0 °C, followed by the dropwise addition of Jones reagent (1.50 M, 2.70 mL, 7 equiv). Thin layer chromatography revealed full conversion of starting material after 3 min. The reaction was quenched with isopropyl alcohol and diluted with 1 M sodium hydroxide solution and dichloromethane. The phases were separated and the aqueous layer was extracted with dichloromethane. The combined organic layers were dried over magnesium sulfate and the solvent was removed under reduced pressure. The crude material was purified by flash column chromatography on silica gel (4% methanol in dichloromethane) to afford 14.0 mg (62% over two steps) of the desired natural product (+)-parvineostemonine (**53**) as a white solid.

TLC (10% methanol in dichloromethane): $R_f = 0.38$ ($KMnO_4$).

^{1}H NMR (400 MHz, $CDCl_3$): δ = 6.88 (d, *J*=1.5 Hz, 1H), 3.71 (d, *J*=6.8 Hz, 1H), 3.60 (td, *J* = 12.8, 3.9 Hz, 1H), 3.12 (dt, *J* = 12.5, 3.7 Hz, 1H), 2.97 (d, *J* = 6.9 Hz, 1H), 2.02 – 1.92 (m, 4H), 1.92 (d, *J* = 1.5 Hz, 3H), 1.90 – 1.85 (m, 3H), 1.77 – 1.61 (m, 3H), 1.60 – 1.48 (m, 1H), 1.41 – 1.22 (m, 3H), 1.07 – 0.94 (m, 1H), 0.80 (t, *J* = 7.4 Hz, 3H) ppm. **^{13}C NMR** (125 MHz, $CDCl_3$): δ = 174.3, 153.1, 130.6, 89.7, 66.2, 57.0, 46.7, 38.4, 38.1, 28.5, 27.4, 27.2, 24.3, 17.3, 11.9, 10.8 ppm.

IR (Diamond-ATR, neat) $\tilde{\nu}_{max}$: 2961, 2877, 1758, 1661, 1449, 1382, 1329, 1232, 1135, 1082, 997, 906, 761, 731 cm^{-1}.

HRMS (ESI, *m*/*z*): calcd for $(C_{17}H_{25}NO_2)^+$ $[M+H]^+$: 276.1964, found: 276.1964.

$[\boldsymbol{\alpha}]_{\boldsymbol{D}}^{\boldsymbol{20}}$: +18 (c = 0.01, MeOH).

Supplementary Table S1: ^{1}H data comparison of synthetically prepared (+)-parvineostemonine and the reported natural product.

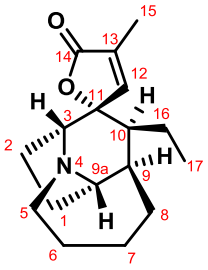

53

IR: (Y. Ye *et al.*)[22] 1735, 1458, 1248 cm^{-1}. (J. Tu *et al.*)[24] 2923, 1747, 997, 731 cm^{-1}. (this work): 2961, 2877, 1758, 1661, 1449, 1382, 1329, 1232, 1135, 1082, 997, 906, 761, 731 cm^{-1}.

^{1}H NMR-data

Nr.	Isolation:[22] [ppm] (400 MHz, $CDCl_3$)	Literature:[24] Synthetic material [ppm] (400 MHz, $CDCl_3$)	This work: Synthetic material (400 MHz, $CDCl_3$)
1	1.55, m; 2.06, m	1.58–1.52 (m, 1H), 2.10–1.94 (m, 1H)	1.60-1.48 (m, 1), 2.02-1.92 (m, 1H)
2	1.67, m; 1.94, m	1.78–1.64 (m, 1 H), 2.10–1.94 (m, 1H)	1.77-1.61 (m, 1H), 2.02-1.92 (m, 1H)
3	2.97 (bd, J = 6.9 Hz)	2.99–2.97 (d, J = 6.8 Hz, 1 H)	2.97 (d, J = 6.9 Hz, 1H)
4	-	-	-
5	3.12, m; 3.61, m	3.15–3.11 (ddd, J = 12.0, 3.2, 3.2 Hz, 1H), 3.66–3.59 (dt, J = 12.8, 3.6 Hz, 1 H)	3.12 (dt, J = 12.5, 3.7 Hz, 1H), 3.60 (td, J = 12.8, 3.9 Hz, 1H)
6	1.75, m; 1.89, m	1.78–1.64 (m, 1 H), 1.89–1.81 (m, 1H),	1.77-1.61 (m, 1H), 1.90-1.85 (m, 1H)
7	1.71, m; 2.02, m	1.78–1.64 (m, 1 H), 2.10–	1.77-1.61 (m, 1H),

		1.94 (m, 1H)	2.02-1.92 (m, 1H)
8	1.34, m; 1.87, m	1.39–1.23 (m, 1H), 1.89–1.81 (m, 3H),	1.41-1.22 (m, 1H), 1.90–1.85 (m, 1H)
9	1.81, m	1.89–1.81 (m, 1H)	1.90–1.85 (m, 1H)
9a	3.72 (bd, *J* = 6.9 Hz)	3.73–3.72 (d, *J* = 6.8 Hz, 1H),	3.71 (d, *J* = 6.8 Hz, 1H)
10	1.98, m	2.10–1.94 (m, 1H)	2.02-1.92 (m, 1H)
11	-	-	-
12	6.88, (d, *J* = 1.4)	6.88–6.87 (d, *J* = 1.6 Hz, 1H)	6.88 (d, *J* = 1.5 Hz, 1H)
13	-	-	-
14	-	-	-
15	1.92 (d, *J* = 1.4)	1.92–1.91 (d, *J* = 1.2 Hz, 3 H)	1.92 (d, *J* = 1.5 Hz, 3H)
16	1.01, m; 1.26, m	1.04–0.98 (m, 1 H), 1.39–1.23 (m, 1H),	1.07-0.94 (m, 1H), 1.41-1.22 (m, 1H)
17	0.80 (t, *J* = 7.4)	0.82–0.78 ppm (t, *J* = 7.2 Hz, 3H)	0.80 (t, *J* = 7.4 Hz, 3H)

Supplementary table S2: ^{13}C data comparison synthetically prepared (+)-parvineostemonine and the reported natural product.

Nr.	Isolation:[22] [ppm] (100 MHz, $CDCl_3$)	Literature:[24] Synthetic material [ppm] (100 MHz, $CDCl_3$)	This work: Synthetic material (125 MHz, $CDCl_3$)
1	28.2	28.1	28.5
2	27.1	26.9	27.2
3	66.2	66.0	66.2

4	-	-	-
5	46.6	46.5	46.7
6	28.3	28.2	28.5
7	24.2	24.0	24.3
8	27.3	27.1	27.4
9	38.4	38.2	38.4
9a	57.0	56.9	57.0
10	38.1	37.9	38.1
11	89.6	89.4	89.7
12	153.0	152.8	153.1
13	130.6	130.6	130.6
14	174.2	174.0	174.3
15	10.7	10.6	10.8
16	17.2	17.1	17.3
17	11.9	11.7	11.9

Minor regioisomer:

(1*R*,2*S*,3*S*,5*R*)-2-allyl-8-cinnamyl-3-ethyl-8-azaspiro[bicyclo[3.2.1]octane-6,2'-[1,3]dithiolan]-4-one (120)

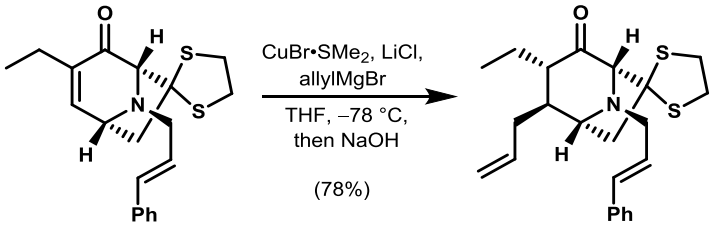

133 120

$CuBr{\cdot}SMe_2$ (64.0 mg, 0.31 mmol, 1 equiv) and dry lithium chloride (27.0 mg, 5.04 mmol, 1.8 equiv) were placed into a flame dried Schlenk flask and treated as described by Lipshutz et al.[44] Tetrahydrofuran (1.50 mL) was added and the resulting reaction mixture was cooled to –78 °C. Allylmagnesium bromide solution (1.0 M in diethyl ether, 0.55 mL, 5.04 mmol, 1.8 equiv) was then added to the solution, followed by immediate dropwise addition of Michael acceptor **133** (100 mg, 280 µmol, 0.9 equiv). The solution was then allowed to stir for 10 minutes, before the addition of 2 M sodium hydroxide at –78 °C quenched the reaction. The mixture was allowed to stir for one hour at ambient temperature, before the mixture was transferred to a separation funnel. Ethyl acetate was added, as well as neat sodium chloride, and the aqueous phase was extracted with ethyl acetate. The combined organic layers were then washed with saturated aqueous sodium chloride solution, followed by drying over magnesium sulfate. The solvent was removed under reduced pressure and the obtained crude oil was purified *via* flash column chromatography on silica gel (10% ethyl acetate in petroleum ether) to yield 87 mg of **120** (78%) as a clear oil.

TLC (10% ethyl acetate in petroleum ether): $R_f = 0.29$ (UV, $KMnO_4$).

^{1}H NMR (400 MHz, $CDCl_3$): δ = 7.40–7.35 (m, 2H), 7.31 (t, *J* = 7.5 Hz, 2H), 7.26–7.19 (m, 1H), 6.55 (d, *J* = 16.0 Hz, 1H), 6.18 (dt, *J* = 15.7, 6.5 Hz, 1H), 5.73 (dddd, *J* = 16.8, 10.4, 8.1, 6.0 Hz, 1H), 5.03–4.90 (m, 2H), 3.80–3.77 (m, 1H), 3.65–3.57 (m, 1H), 3.54–3.43 (m, 3H), 3.36–3.28 (m, 3H), 2.98 (dd, *J* = 14.9, 7.3 Hz, 1H), 2.28–2.12 (m, 3H), 2.06 (q, *J* = 6.0 Hz, 1H), 1.86–1.74 (m, 1H), 1.73–1.60 (m, 1H), 1.39 (dt, *J* = 8.1, 5.9 Hz, 1H), 1.01 (t, *J* = 7.5 Hz, 3H) ppm. **^{13}C NMR** (100 MHz, $CDCl_3$): δ = 207.1, 137.0, 136.3, 133.0, 128.7 (2C), 127.6, 127.3, 126.4 (2C), 117.6, 84.7, 67.9, 62.4, 55.4, 49.9, 46.8, 43.1, 40.5, 40.4, 39.9, 25.0, 12.7 ppm.

IR (Diamond-ATR, neat) $\tilde{\nu}_{max}$**:** 2961, 2928, 1713, 1449, 1375, 1250, 1194, 1113, 1061, 968, 917 cm^{-1}.

$[\alpha]_D^{20}$: –16.0 (c = 0.14, $CDCl_3$).

HRMS (ESI, *m/z*): calcd for $[C_{23}H_{29}NOS_2)^+$ $[M+H]^+$: 400.1769; found: 400.1766.

(3*R*,4*S*,9*S*,9a*R*,10*S*)-10-ethyl-1,3,5,8,9,9a-hexahydrospiro[9,3-ethanopyrrolo[1,2-*a*]azepine-2,2'-[1,3]dithiolan]-11-one (136)

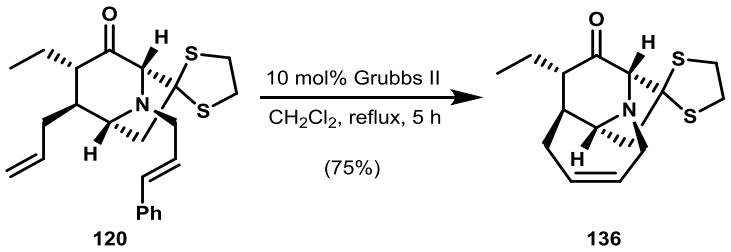

120 136

Bisolefin **120** (141 mg, 353 µmol, 1 equiv) was dissolved in degassed dichloromethane (18.0 mL) and Grubbs II catalyst (35.0 mg, 35.3 µmol, 0.1 equiv) was added in dichloromethane (17.0 mL). The reaction mixture was heated to reflux for 5 h. The solvent was then evaporated and the crude remains were subjected to flash column chromatography on silica gel (11% ethyl acetate in petroleum ether) to obtain 78.0 mg (75%) of olefin **136** as a white solid.

TLC (10% ethyl acetate in petroleum ether): R_f = 0.23 (UV, $KMnO_4$).

^{1}H-NMR (400 MHz, $CDCl_3$): δ = 5.75–5.62 (m, 2H), 3.89 (d, *J* = 17.1 Hz, 1H), 3.63 (dd, *J* = 17.1, 5.8 Hz, 1H), 3.55 (d, *J* = 7.2 Hz, 1H), 3.43–3.31 (m, 2H), 3.31–3.21 (m, 2H), 3.19–3.10 (m, 1H), 2.98 (dd, *J* = 14.7, 7.9 Hz, 1H), 2.45 (d, *J* = 15.0 Hz, 1H), 2.39–2.35 (m, 1H), 2.31–2.27 (m, 1H), 2.25–2.20 (m, 1H), 2.00–1.83 (m, 2H), 1.73–1.62 (m, 1H), 1.02 (t, *J* = 7.0 Hz, 3H) ppm. **^{13}C-NMR** (100 MHz, $CDCl_3$): δ = 212.9, 130.7 (2C), 82.8, 69.2, 62.2, 53.2, 48.8, 47.0, 43.4, 40.5, 39.1, 36.2, 30.4, 13.1 ppm.

IR (Diamond-ATR, neat) $\tilde{\nu}_{max}$**:** 2959, 2922, 2874, 1695, 1456, 1437, 1425, 1319, 1279, 1184, 1163, 1128, 976, 818 cm^{-1}.

$[\alpha]_D^{20}$: –106 (c= 0.11; $CHCl_3$).

HRMS (ESI, *m/z*): calcd for $[C_{15}H_{21}NOS_2)^+$ $[M+H]^+$: 296.1143; found: 296.1141.

(3*S*,4*S*,9*S*,9a*R*,10*S*)-10-ethyloctahydro-1H-9,3-ethanopyrrolo[1,2-a]azepin-11-one ((+)-135)

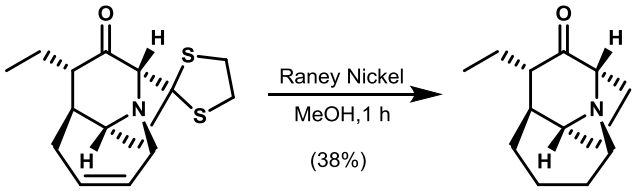

136 (+)-**135**

An aqueous dispersion of Raney nickel in water (3 pipettes) was washed three times with methanol, and the waste solvent was discarded. Dithiolane **136** (53.0 mg, 0.18 μmol) was added in methanol (5.00 mL), and the reaction mixture was stirred for 1 h at ambient temperature. Raney nickel was then filtered off, and the solvent was removed under reduced pressure. The crude oil was subjected to flash column chromatography on silica gel (4% methanol in dichloromethane) to give 14.0 mg (38%) of amine (+)-**135** as clear oil.

$[\boldsymbol{\alpha}]_{\boldsymbol{D}}^{\mathbf{20}}$: +129 (c = 0.10; $CHCl_3$). For more data see enantiomer (–)-**135**.

2.1.1 ^{1}H and ^{13}C NMR Spectra

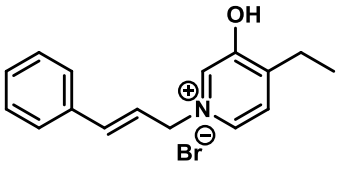

121

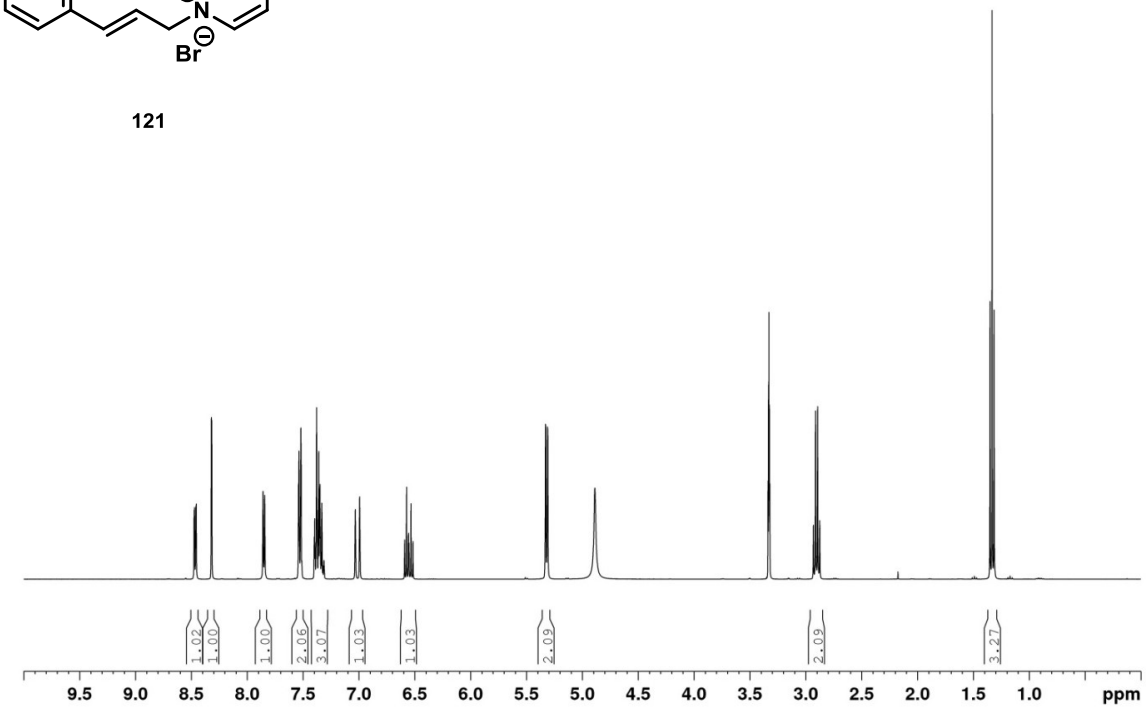

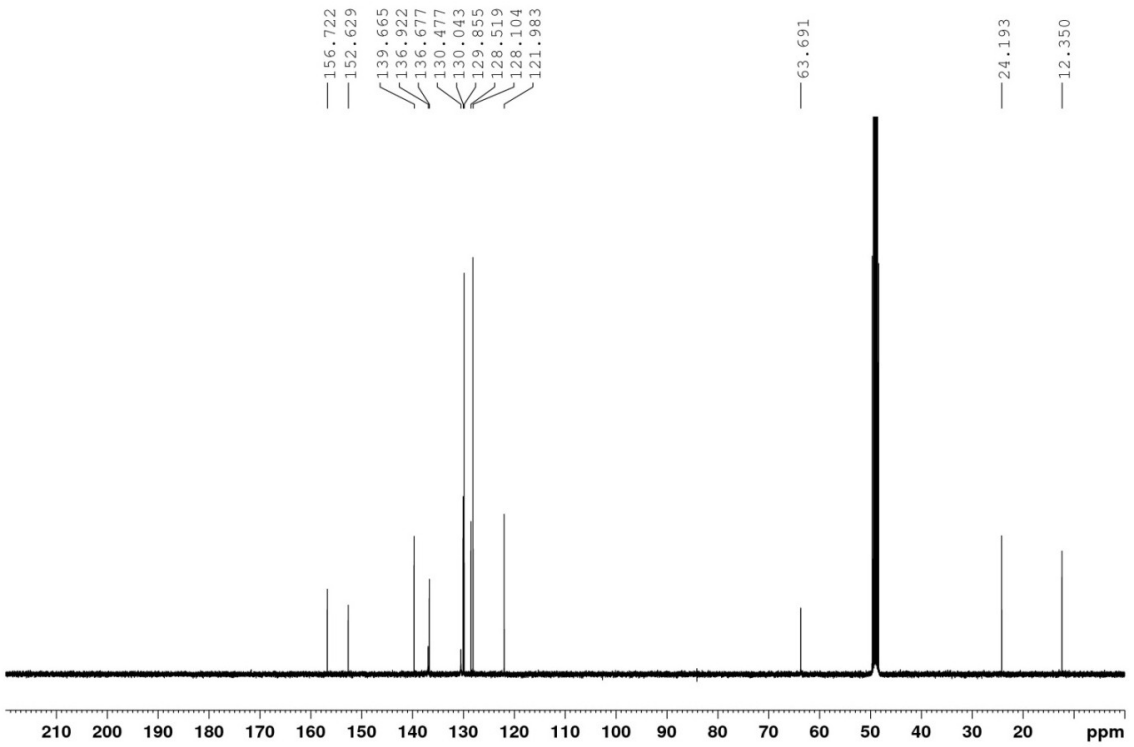

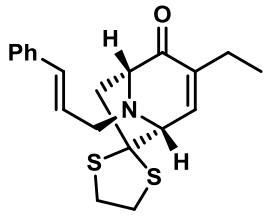
Ph
H
O
N
S
S
H

132

2.05
2.09
1.03
1.00
1.01
1.02
1.03
1.01
3.25
0.95
2.15
1.05
1.19
1.93
3.19
9.5 9.0 8.5 8.0 7.5 7.0 6.5 6.0 5.5 5.0 4.5 4.0 3.5 3.0 2.5 2.0 1.5 1.0 0.5 ppm

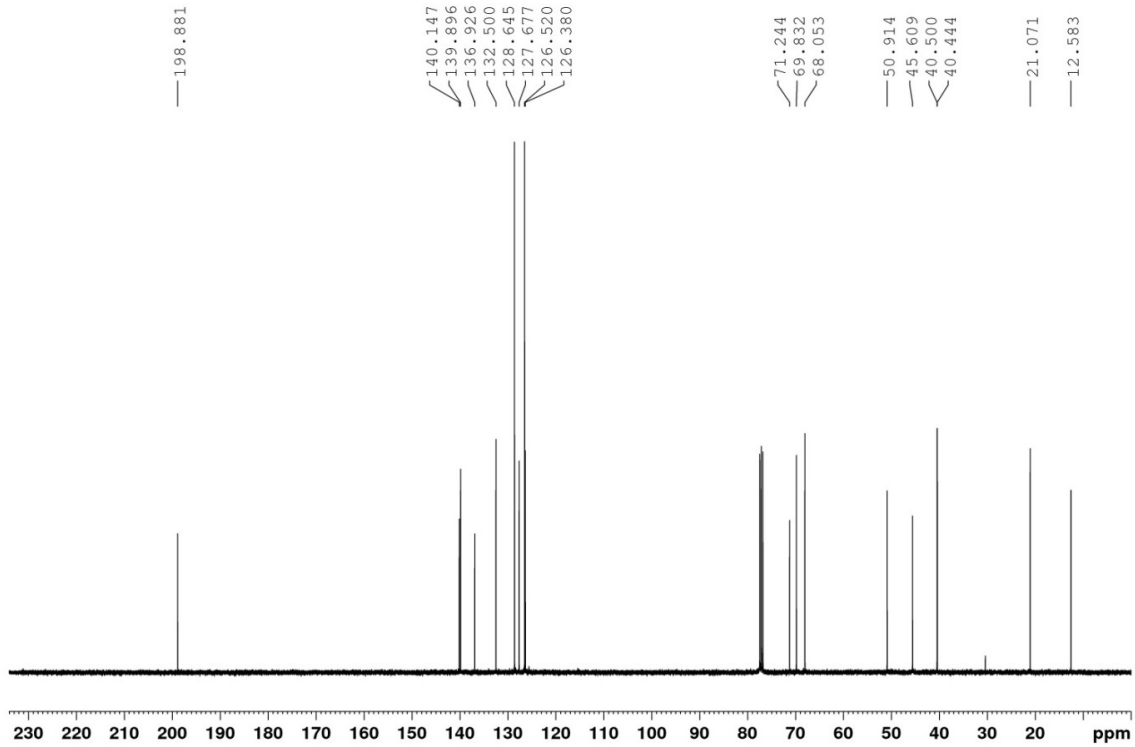
198.881
140.147
139.896
136.926
132.500
128.645
127.677
126.520
126.380
71.244
69.832
68.053
50.914
45.609
40.500
40.444
21.071
12.583
230 220 210 200 190 180 170 160 150 140 130 120 110 100 90 80 70 60 50 40 30 20 ppm

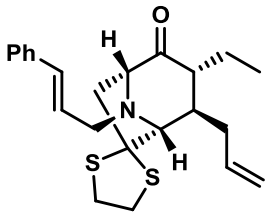
Ph
H
O
N
S
S
H

117

2.00
2.02
1.01
1.01
1.01
1.00
2.02
5.19
1.08
1.85
0.99
2.00
1.07
1.99
2.13
3.01
9.5 9.0 8.5 8.0 7.5 7.0 6.5 6.0 5.5 5.0 4.5 4.0 3.5 3.0 2.5 2.0 1.5 1.0
ppm

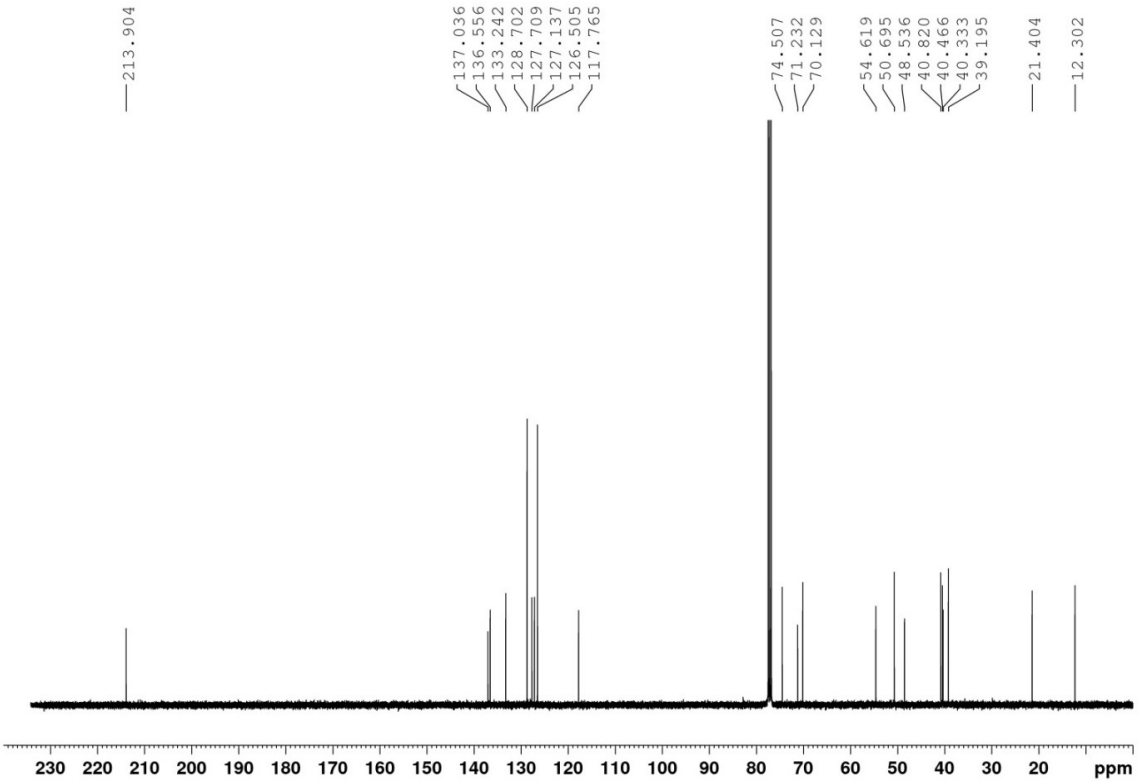
213.904
137.036
136.556
133.242
128.702
127.709
127.137
126.505
117.765
74.507
71.232
70.129
54.619
50.695
48.536
40.820
40.466
40.333
39.195
21.404
12.302
230 220 210 200 190 180 170 160 150 140 130 120 110 100 90 80 70 60 50 40 30 20
ppm

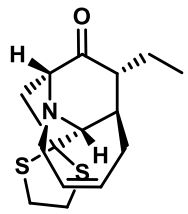
O
H
N
S
S
H

134

2.00
0.97
1.01
5.01
1.02
2.00
3.01
0.97
2.07
3.00
9.5 9.0 8.5 8.0 7.5 7.0 6.5 6.0 5.5 5.0 4.5 4.0 3.5 3.0 2.5 2.0 1.5 1.0 0.5
f1 (ppm)

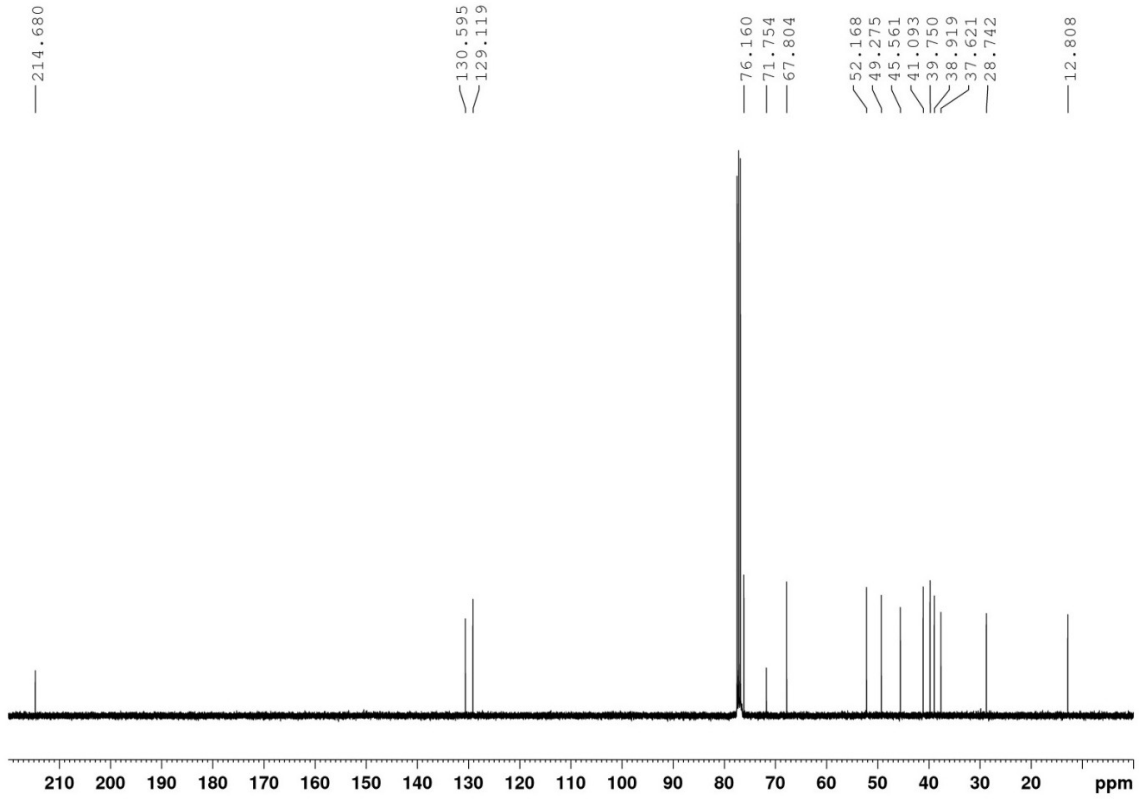
214.680
130.595
129.119
76.160
71.754
67.804
52.168
49.275
45.561
41.093
39.750
38.919
37.621
28.742
12.808
210 200 190 180 170 160 150 140 130 120 110 100 90 80 70 60 50 40 30 20 ppm

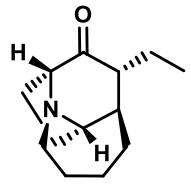
O
H
N
H

(–)-**135**

0.94
0.92
0.95
1.00
1.18
1.25
3.12
8.84
1.25
2.95
9.5 9.0 8.5 8.0 7.5 7.0 6.5 6.0 5.5 5.0 4.5 4.0 3.5 3.0 2.5 2.0 1.5 1.0
ppm

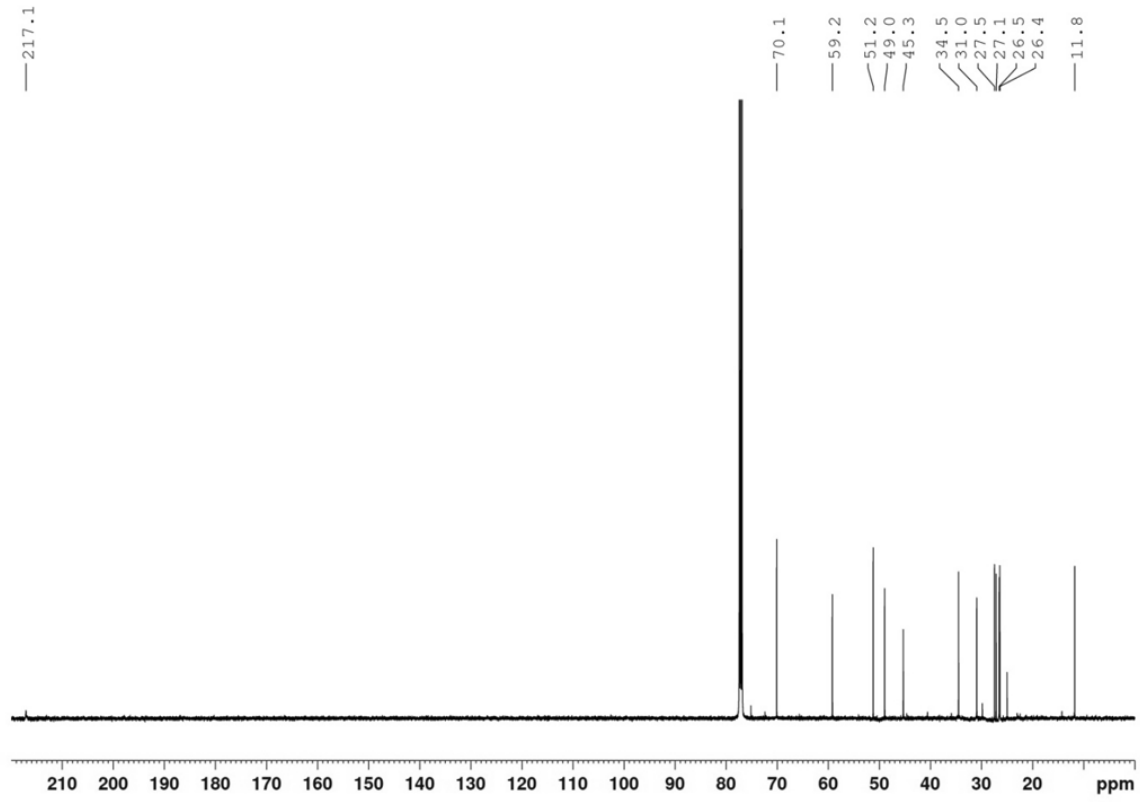
217.1
70.1
59.2
51.2
49.0
45.3
34.5
31.0
27.5
27.1
26.5
26.4
11.8
210 200 190 180 170 160 150 140 130 120 110 100 90 80 70 60 50 40 30 20
ppm

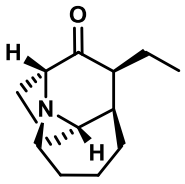
O
H
N
H

(−)-**116**

1.00
1.06
0.97
1.07
1.06
1.07
1.12
1.14
6.73
1.23
3.33
3.14
9.5 9.0 8.5 8.0 7.5 7.0 6.5 6.0 5.5 5.0 4.5 4.0 3.5 3.0 2.5 2.0 1.5 1.0 0.5 0.0 -0.5 -1.0 -1.5 -2.
f1 (ppm)

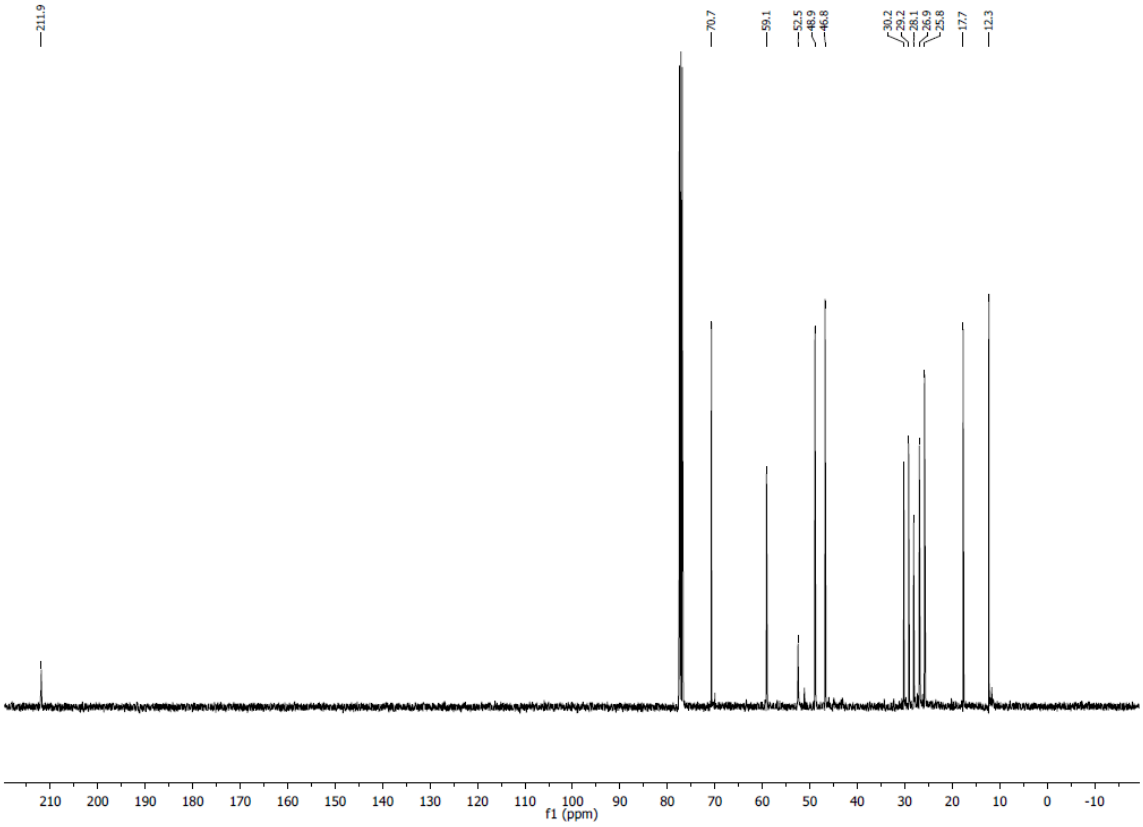
211.9
70.7
59.1
52.5
48.9
46.8
30.2
29.2
28.1
26.9
25.8
17.7
12.3
210 200 190 180 170 160 150 140 130 120 110 100 90 80 70 60 50 40 30 20 10 0 -10
f1 (ppm)

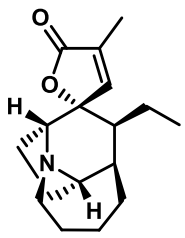
O
O
H
N
H

(+)-**53**

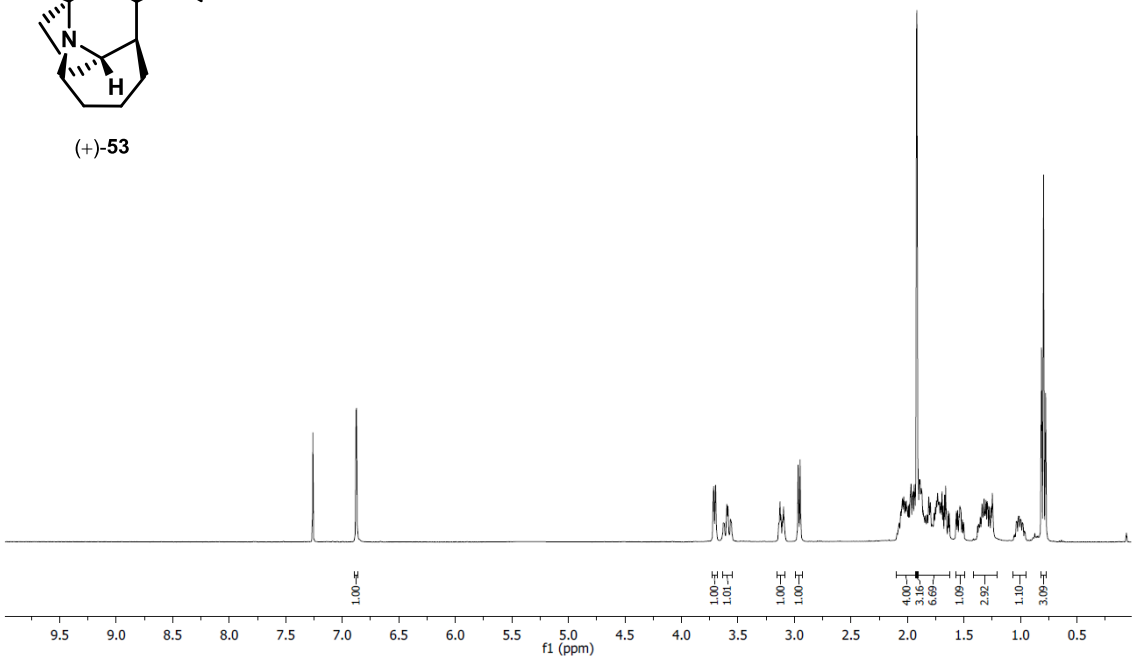
1.00
1.00
1.01
1.00
1.00
4.00
3.18
6.69
1.09
2.92
1.10
3.09
9.5 9.0 8.5 8.0 7.5 7.0 6.5 6.0 5.5 5.0 4.5 4.0 3.5 3.0 2.5 2.0 1.5 1.0 0.5
f1 (ppm)

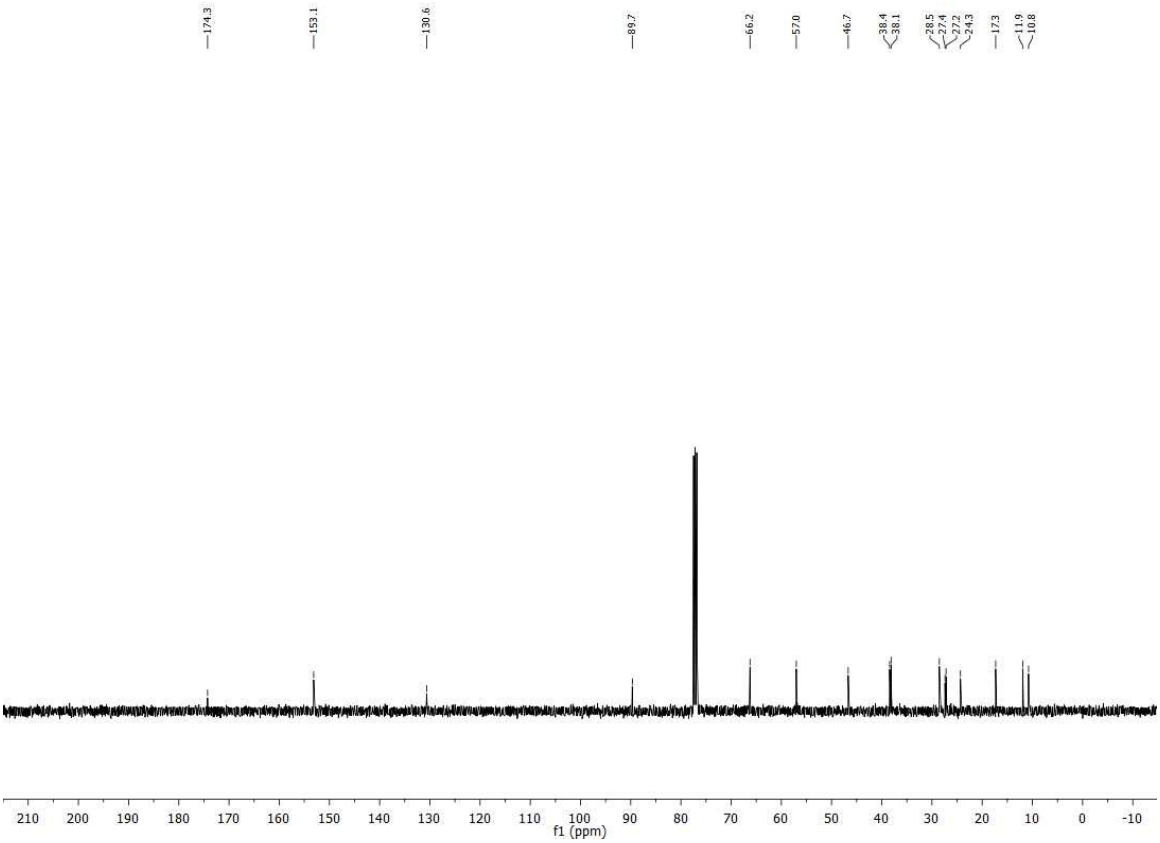
174.3
153.1
130.6
89.7
66.2
57.0
46.7
38.4
38.1
28.5
27.4
27.2
24.3
17.3
11.9
10.8
210 200 190 180 170 160 150 140 130 120 110 100 90 80 70 60 50 40 30 20 10 0 -10
f1 (ppm)

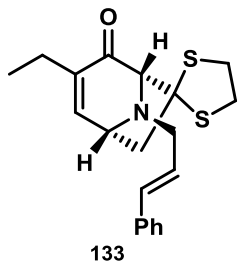
O
H
S
S
N
H
Ph

133

9.5 9.0 8.5 8.0 7.5 7.0 6.5 6.0 5.5 5.0 4.5 4.0 3.5 3.0 2.5 2.0 1.5 1.0 ppm
2.04 2.13 1.09 1.00 1.03 1.04 1.02 0.97 4.45 1.14 1.10 1.02 1.03 2.05 3.16

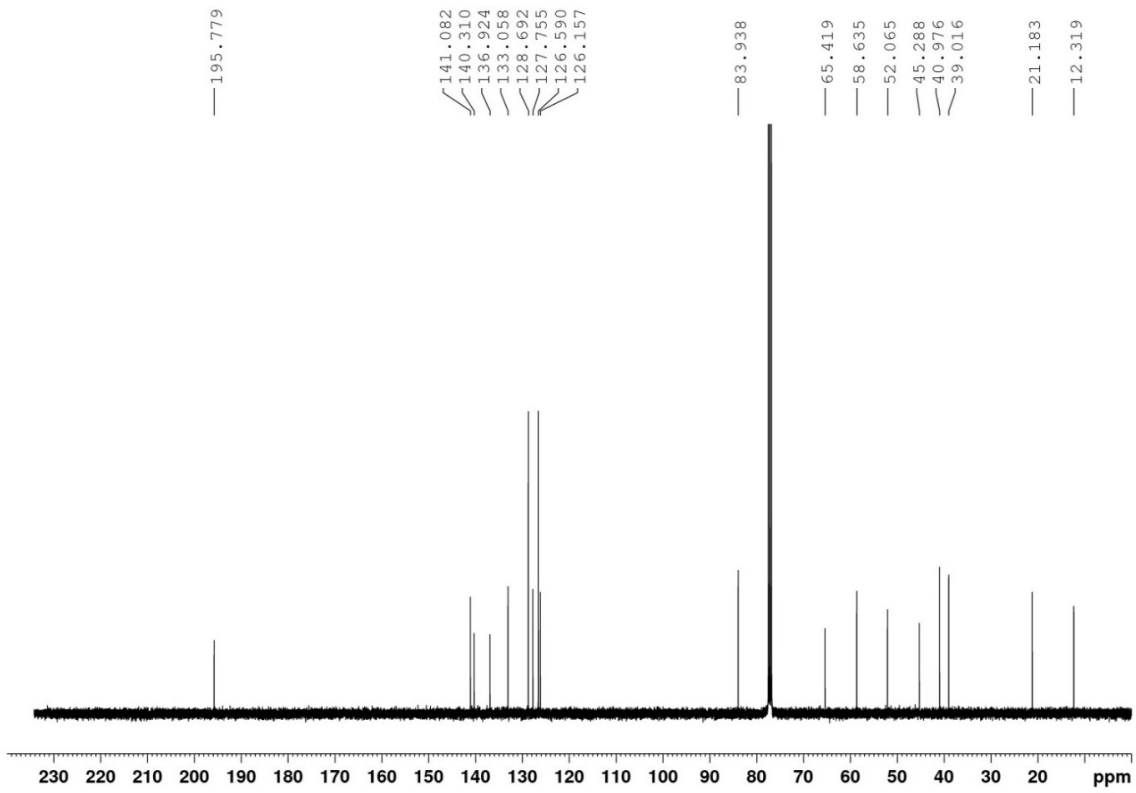
195.779
141.082
140.310
136.924
133.058
128.692
127.755
126.590
126.157
83.938
65.419
58.635
52.065
45.288
40.976
39.016
21.183
12.319
230 220 210 200 190 180 170 160 150 140 130 120 110 100 90 80 70 60 50 40 30 20 ppm

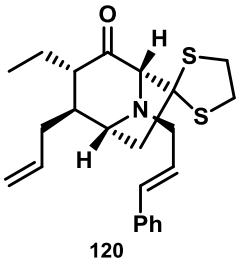
O
H
S
S
N
H
Ph

120

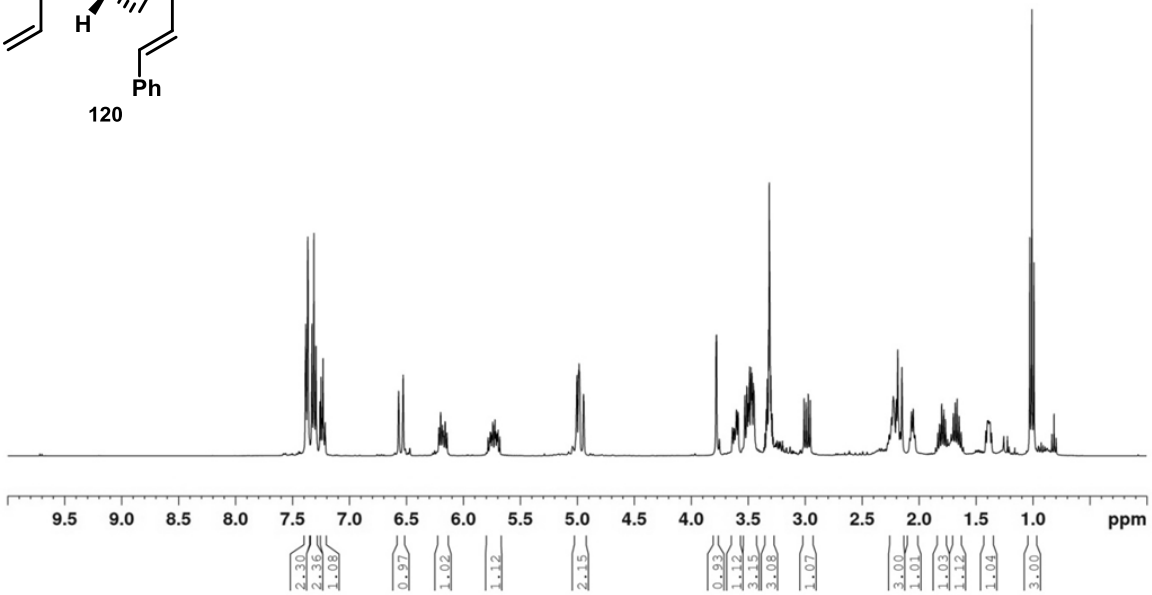
9.5 9.0 8.5 8.0 7.5 7.0 6.5 6.0 5.5 5.0 4.5 4.0 3.5 3.0 2.5 2.0 1.5 1.0 ppm
2.30
2.36
1.08
0.97
1.02
1.12
2.15
0.93
1.12
3.15
3.08
1.07
3.00
1.01
1.03
1.12
1.04
3.00


207.1
137.0
136.3
133.0
128.7
127.6
127.3
126.4
117.6
84.7
67.9
62.4
55.4
49.9
46.8
43.1
40.5
40.4
39.9
25.0
12.7

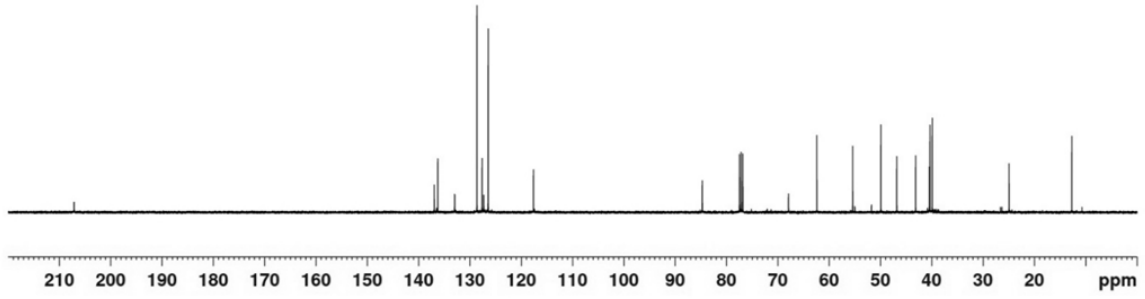
210 200 190 180 170 160 150 140 130 120 110 100 90 80 70 60 50 40 30 20 ppm

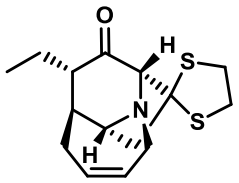
O
H
S
N
S
H

136

9.5 9.0 8.5 8.0 7.5 7.0 6.5 6.0 5.5 5.0 4.5 4.0 3.5 3.0 2.5 2.0 1.5 1.0 ppm
2.00
0.99
1.16
0.95
2.18
1.97
1.12
1.02
1.04
1.15
1.15
1.00
2.12
1.24
3.10

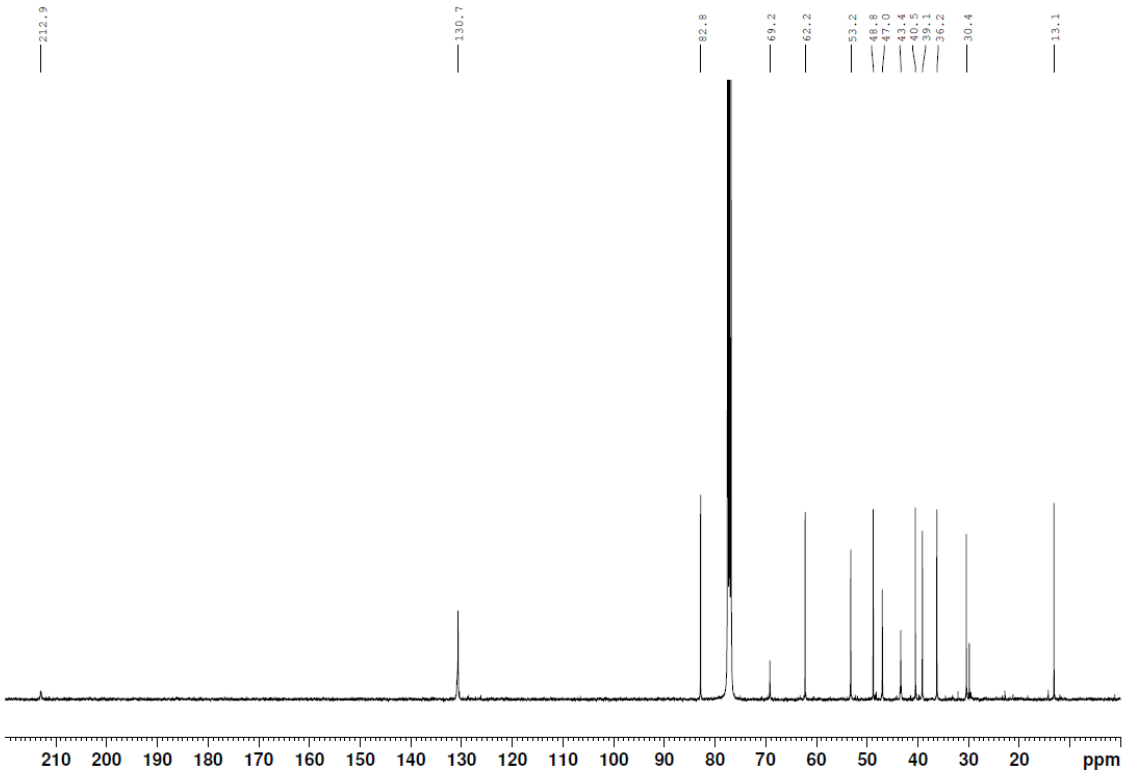
212.9
130.7
82.8
69.2
62.2
53.2
48.8
47.0
43.4
40.5
39.1
36.2
30.4
13.1
210 200 190 180 170 160 150 140 130 120 110 100 90 80 70 60 50 40 30 20 ppm

2.2 The Pepluacetal Project

(1*R*,3*R*,4*R*,6*S*)-4,7,7-Trimethylbicyclo[4.1.0]heptan-3-ol (269)

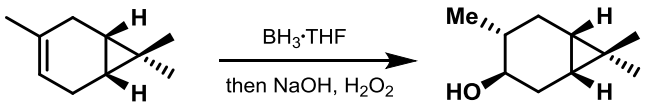

(+)-3-carene (**172**) (87%) **269**

(+)-3-Carene (**172**) (10.0 g, 73.4 mmol, 1 equiv) was dissolved in tetrahydrofuran (61.0 mL) and cooled to 0 °C. Borane tetrahydrofuran complex solution (1 M in THF, 132 mL, 1.8 equiv) was added dropwise and the resulting solution was stirred at 0 °C. After 4 h the reaction mixture was allowed to warm to ambient temperature and was stirred for 16 h. After full consumption of starting material, the reaction mixture was cooled to 0 °C and a premixed solution of water (38.0 mL), hydrogen peroxide (30 wt%, 23.0 mL) and aqueous sodium hydroxide solution (3 M, 23.0 mL) was added slowly. The resulting reaction mixture was stirred at 60 °C. After 3 h the reaction mixture was diluted with saturated aqueous sodium chloride solution and the aqueous layer was extracted with diethyl ether. The combined organic layers were dried over magnesium sulfate, filtered and the filtrate was concentrated under reduced pressure. The crude material was purified by flash column chromatography on silica gel (7% to 10% ethyl acetate in petroleum ether) to yield **269** as a colorless oil (9.85 g, 87%). The obtained data were in full agreement with those values reported in literature.[96]

(1*R*,4*R*,6*S*)-4,7,7-Trimethylbicyclo[4.1.0]heptan-3-one (270)

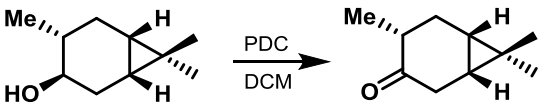

269 (82%) **270**

Alcohol 269 (26.6 g, 172 mmol, 1 equiv) was dissolved in 450 mL dichloromethane and cooled to 0 °C. Pyridinium dichromate (129 g, 344 mmol, 2 equiv) was added in one portion and the resulting reaction mixture was warmed to ambient temperature. After 12 h, the mixture was diluted with saturated aqueous sodium chloride solution and filtered over Celite. The filtrate was extracted with dichloromethane. The combined organic layers were dried over magnesium sulfate, filtered and the filtrate was concentrated under reduced pressure. Purification by flash column chromatography on silica gel (10% ethyl acetate in petroleum ether) yielded ketone **270**

as a colorless oil (21.5 g, 82%). The obtained data were in full agreement with those values reported in the literature.[96]

Trimethyl(((1*S*,4*R*,6*S*)-4,7,7-trimethylbicyclo[4.1.0]hept-2-en-3-yl)oxy)silane (265)

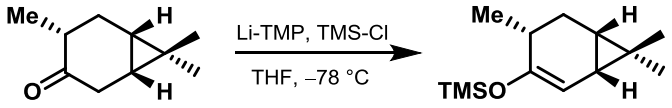

270 265

2,2,6,6-tetramethyl piperidine (25.0 mL, 148 mmol, 1.2 equiv) was dissolved in tetrahydrofuran (250 mL) and cooled to –78 °C. *n*-Butyl lithium (2.5 M in hexanes, 54.3 mL, 1.1 equiv) was added dropwise and the resulting yellow solution was stirred at –78 °C for 15 min. Ketone **270** (18.7 g, 123 mmol, 1 equiv) was dissolved in tetrahydrofuran (47 mL) and added dropwise. The reaction mixture was stirred at –78 °C for 30 min. Trimethylsilyl chloride (31.3 mL, 247 mmol, 2 equiv) was added dropwise and the reaction mixture was stirred at –78 °C. After 45 min, the solution was diluted with water at –78 °C and the reaction mixture was allowed to warm to ambient temperature. The aqueous layer was extracted with diethyl ether. The combined organic layers were washed with saturated aqueous sodium chloride solution, dried over magnesium sulfate, filtered and the filtrate was concentrated under reduced pressure. The obtained yellow oil was used without further purification in the next step.

Methyl (*R*)-3-((1*S*,3*R*)-3-formyl-2,2-dimethylcyclopropyl)-2-methylpropanoate (264)

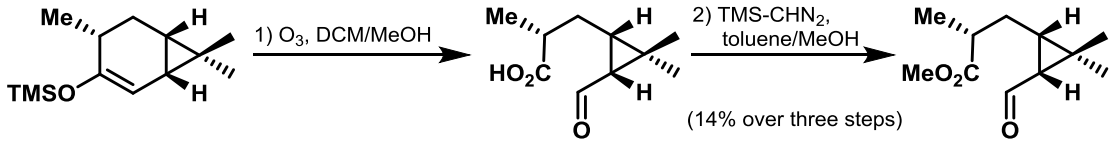

265 389 264

Crude trimethylsilyl enol ether **265** (27.0 g, 120 mmol, 1 equiv) was dissolved in dichloromethane (450 mL) and methanol (50.0 mL). The resulting solution was cooled to −78 °C and ozonized. After full consumption of starting material, the reaction mixture was quenched with thiourea (18.3 g, 240 mmol, 2 equiv), warmed to ambient temperature and for 90 min. The solvents were removed under reduced pressure and the residue was dissolved in diethyl ether. The organic layer was extracted with aqueous sodium hydroxide solution (1 M). The combined aqueous layers were acidified with aqueous hydrogen chloride solution (2 M) until pH = 3. The

aqueous layer was extracted with diethyl ether, the combined organic layers were dried over magnesium sulfate, filtered and concentrated under reduced pressure, yielding crude carboxylic acid **389** (3.09 g, 16.8 mmol) as a colorless oil.

Crude carboxylic acid **389** (3.09 g, 16.8 mmol, 1 equiv) was dissolved in toluene/methanol (84.0 mL, 3/1, 0.2 M) and cooled to 0 °C. Trimethylsilyl diazomethane (2 M in hexanes, 12.6 mL, 1.5 equiv) was added. The resulting yellow mixture was warmed to ambient temperature and stirred overnight. After full consumption of starting material, the reaction mixture was concentrated under reduced pressure and purified by flash column chromatography on silica gel (10% ethyl acetate in petroleum ether). Methyl ester **264** was obtained as a yellow oil (3.09 g, 13% over three steps). The obtained data data were in full agreement with those values reported in literature.[96]

Methyl (*R*)-2-methyl-3-((triisopropylsilyl)oxy)propanoate (271)

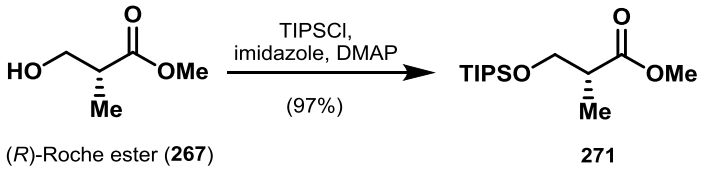

(*R*)-Roche ester (**267**) **271**

Methyl (*R*)-3-hydroxy-2-methylpropanoate (**267**) (2.34 mL, 21.2 mmol, 1 equiv) was dissolved in dimethylformamide (21.2 mL) and cooled to 0 °C. *N,N*-Dimethylpyridin-4-amine (258 mg, 2.12 mmol, 0.1 equiv), 1*H*-imidazole (1.44 g, 21.2 mmol, 1 equiv) and triisopropylsilyl chloride (4.94 mL, 23.3 mmol, 1.1 equiv) were added in one portion. The reaction mixture was stirred at 0 °C. After 30 min, the reaction mixture was allowed to warm to ambient temperature. After 12 h, the solution was diluted with water and diethyl ether. The aqueous layer was extracted with diethyl teher. The combined organic layers were dried over magnesium sulfate, filtered and the filtrate was concentrated under reduced pressure. Purification by flash column chromatography on silica gel (2% ethyl acetate in petroleum ether) yielded methyl ester **271** as a colorless oil (5.64 g, 97%). The obtained data were in full agreement with those values reported in literature.[126]

For the corresponding (*S*)-isomer, the same conditions were applied and the same results were obtained.

(*S*)-2-Methyl-3-((triisopropylsilyl)oxy)propan-1-ol (272)

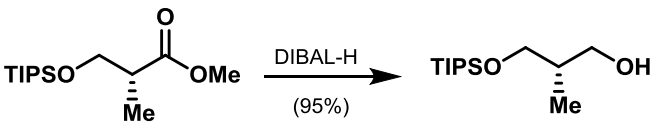

271 272

Methyl ester **271** (5.41 g, 19.7 mmol, 1 equiv) was dissolved in dichloromethane (200 mL) and cooled to –78 °C. Diisobutylaluminium hydride (1 M in hexanes, 118 mL, 6 eq) was added dropwise and the reaction mixture was stirred at −78 °C. After 90 min, the solution was diluted with saturated aqueous potassium sodium tartrate solution at −78 °C and the reaction mixture was allowed to warm to ambient temperature. After 2 h, the solution was extracted with diethyl ether, the combined organic layers were washed with saturated aqueous sodium chloride solution, dried over magnesium sulfate, filtered and the filtrate was concentrated under reduced pressure. Alcohol **272** was obtained as a colorless oil (4.61 g, 95%) after purification by flash column chromatography on silica gel (10% ethyl acetate in petroleum ether). The obtained characterization data were in full agreement with those reported in literature.[142]

For the corresponding (*S*)-isomer, the same conditions were applied and the same results were obtained.

(*R*)-(3-Iodo-2-methylpropoxy)triisopropylsilane (273)

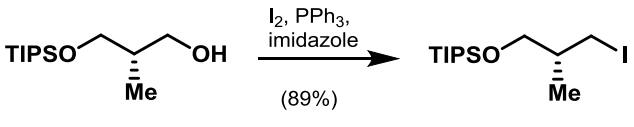

272 273

In a Schlenk flask covered in aluminum foil alcohol **272** (2.34 g, 9.94 mmol, 1 equiv) was dissolved in dichloromethane (31.6 mL) and the solution was cooled to 0 °C. Triphenylphosphine (3.61 g, 14.2 mmol, 1.5 equiv) and 1*H*-imidazole (0.970 g, 14.2 mmol. 1.5 equiv) were added in one portion. Iodine (3.61 g, 14.2 mmol, 1.5 equiv) was added and the reaction mixture was allowed to warm to ambient temperature. After 12 h, the solution was diluted with water and dichloromethane. The layers were separated and the aqueous layer was extracted with dichloromethane. The combined organic layers were washed with brine, dried over magnesium sulfate, filtered and the filtrate was concentrated under reduced pressure. Purification by flash column chromatography on silica gel (2% ethyl acetate in petroleum ether) yielded alkyl iodide

273 as a violet oil (3.15 g, 89%). The obtained data were in full agreement with those values reported in literature.[143]

For the corresponding (*S*)-isomer, the same conditions were applied and the same results were obtained.

(*S*)-(2-methyl-3-((triisopropylsilyl)oxy)propyl)triphenylphosphonium (280)

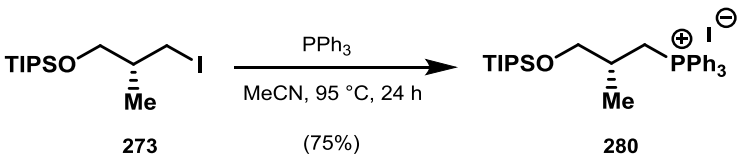

273 (75%) **280**

To a solution of alkyl iodide **273** (7.10 g, 19.9 mmol, 1 equiv) in acetonitrile (20.0 mL) was added triphenylphosphine (4.50 g, 19.9 mmol, 1 equiv) and the resulting reaction mixture was stirred at reflux. After 12 h, the crude material was recrystallized with petroleum ether to afford **280** as a white solid (9.23 g, 75%).

TLC (100% ethyl acetate): R_f = 0.22 (CAM, UV).

IR (Diamond-ATR, neat) $\tilde{\nu}_{max}$: 2955, 2930, 2860, 1417, 1246, 1203, 1142, 1077 cm^{-1}.

^{1}H NMR (400 MHz, $CHCl_3$) δ = 7.91 (ddd, *J* = 12.6, 7.2, 1.7 Hz, 6H), 7.80 (td, *J* = 7.3, 1.7 Hz, 3H), 7.71 (ddd, *J* = 8.9, 7.0, 3.4 Hz, 6H), 3.90 (ddd, *J* = 15.7, 12.4, 9.0 Hz, 1H), 3.67 (m, 3H), 2.18 (m, 1H), 1.03 (m, 21H), 0.87 (d, *J* = 6.8 Hz, 3H) ppm.**^{13}C NMR** (100 MHz, $CDCl_3$) δ = 135.3, 133.9, 130.8, 68.3, 32.3, 18.2, 17.9, 17.6, 12.0 ppm.

HRMS (ESI, *m*/*z*): calcd for $(C_{31}H_{44}OPSiI)^+$ $[M+H_2O]^+$: 636.2049; found: 636.2055.

$[\alpha]_D^{20}$ = −21.4 (c = 0.05, $CHCl_3$).

Melting area: 130-150 °C.

The same conditions were applied and the same yields were obtained for isomer **(*S*)-(2-methyl-3-((triisopropylsilyl)oxy)propyl)triphenylphosphonium (305)**

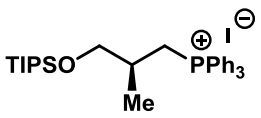

305

TLC (100% ethyl acetate): R_f = 0.22 (CAM, UV).

IR (Diamond-ATR, neat) $\tilde{\nu}_{max}$: 2955, 2930, 2860, 1417, 1246, 1203, 1142, 1077 cm^{-1}.

^{1}H NMR (400 MHz, $CHCl_3$) δ = 7.94 – 7.85 (m, 6H), 7.84 – 7.77 (m, 3H), 7.75 – 7.67 (m, 6H), 3.92 – 3.74 (m, 1H), 3.71 – 3.58 (m, 3H), 2.25 – 2.11 (m, 1H), 1.14 – 1.05 (m, 3H), 1.02 (dd, *J* = 6.6, 4.1 Hz, 18H), 0.85 (dd, *J* = 6.8, 2.0 Hz, 3H) ppm. **^{13}C NMR** (100 MHz, $CDCl_3$) δ = 135.3, 133.9, 130.8, 68.1, 32.2, 24.8, 18.2, 12.0 ppm.

HRMS (ESI, *m*/*z*): calcd for $(C_{31}H_{44}OPSiI)^+$ $[M+H_2O]^+$: 636.2049; found: 636.2055.

$[\alpha]_D^{20}$ = +112.7 (c = 0.05, $CHCl_3$).

Methyl (*R*)-3-((1*S*,3*R*)-2,2-dimethyl-3-vinylcyclopropyl)-2-methylpropanoate (281)

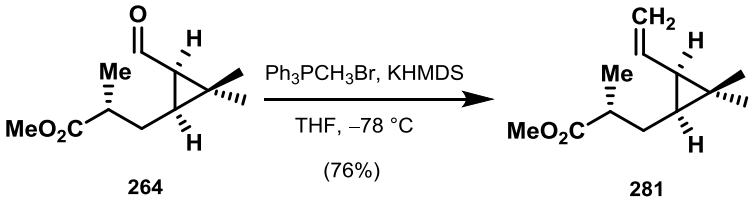

264 **281**

A solution of methylphosphonium bromide (234 mg, 656 µmol, 1.3 equiv) in tetrahydrofuran (3.50 mL) was cooled to –78 °C and stirred for 10 min. Then, a solution of potassium bis(trimethylsilyl)amide (KHMDS) (0.7 M in toluene, 793 µL, 555 µmol, 1.1 equiv) was added dropwise. The reaction mixture was stirred for 30 min at –78 °C, then allowed to warm to room temperature and stirred for another 30 min. The suspension was added with a cannula within 20 min to a solution of methyl ester **264** (100 mg, 504 µmol, 1 equiv) in tetrahydrofuran (2.00 mL) at –78 °C. After 2 h at –78 °C, the reaction mixture was allowed to warm to 0 °C and poured into diethyl ether and water. The phases were separated and the aqueous layer was extracted with ethyl acetate. The combined organic layers were dried over magnesium sulfate, filtered and concentrated. The residue was purified by flash column chromatography on silica gel (2% ethyl acetate in petroleum ether) to afford alkene **281** (75.4 mg, 76%) as a colorless oil.

TLC (2% ethyl acetate in petroleum ether): R_f = 0.46 (UV, KMnO4).

^{1}H NMR ($CDCl_3$, 400 MHz): δ = 5.50 (dt, *J* = 16.9, 10.1 Hz, 1H), 5.12 (ddd, *J* = 16.9, 2.2, 0.6 Hz, 1H), 5.00 (ddd, *J* = 10.3, 2.3, 0.6 Hz, 1H), 3.66 (s, 3H), 2.47 (h, *J* = 7.0 Hz, 1H), 1.80 – 1.68 (m, 1H), 1.48 (dt, *J* = 14.1, 7.7 Hz, 1H), 1.34 – 1.22 (m, 1H), 1.17 (d, *J* = 7.0 Hz, 3H), 1.07 (s, 3H), 1.00 (s, 3H), 0.72 (ddd, *J* = 8.9, 7.8, 6.5 Hz, 1H). **^{13}C NMR** ($CDCl_3$, 100 MHz): δ = 177.2, 135.5, 115.3, 51.7, 39.9, 31.4, 29.3, 28.9, 28.3, 21.4, 16.8, 15.7 ppm.

IR (Diamond-ATR, neat) $\tilde{\nu}_{max}$: 2947, 1737, 1632, 1457, 1435, 1376, 1250, 1194, 1163, 1121, 1055, 988 cm^{-1}.

HRMS (ESI, *m*/*z*) calcd for $(C_{12}H_{20}O_2)^+$ $[M+H]^+$: 197.1536; found: 197.1533.

$[\boldsymbol{\alpha}]_{\boldsymbol{D}}^{\boldsymbol{20}}$ = –63.3 (c = 0.025, $CHCl_3$).

1,3-Dimethyl-1,3,2-diazaphospholidine 2-oxide (294)

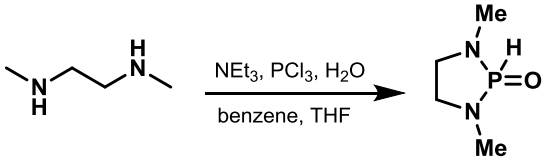

293 **294**

N,N'-Dimethyl ethylenediamine (**293**) (6.89 mL, 64.0 mmol, 1 equiv) and dry triethyl amine (35.7 mL, 256 mmol, 4 equiv) were dissolved in dry benzene/tetrahydrofuran (150 mL, 1/1, 0.42 M) and cooled to 0 °C. Phosphorus trichloride (5.58 mL, 64.0 mmol, 1 equiv) was added dropwise. The reaction mixture was allowed to warm to ambient temperature. After 45 min, the reaction mixture was cooled to 0 °C and water (1.15 mL, 64.0 mmol, 1 equiv) was added. The reaction was allowed to warm to ambient temperature and after 3.5 h the mixture was filtered over magnesium sulfate. The filter cake was washed with dry tetrahydrofuran and the filtrate was concentrated under reduced pressure. Phosphonamide **294** (8.65 g, 100% crude) was collected as yellow oil, which was used in the next step without further purification. The obtained data were in full agreement with those values reported in literature.[112]

(*R*)-1,3-Dimethyl-2-(2-methyl-3-((triisopropylsilyl)oxy)propyl)-1,3,2-diaza-phospholidine 2-oxide (295)

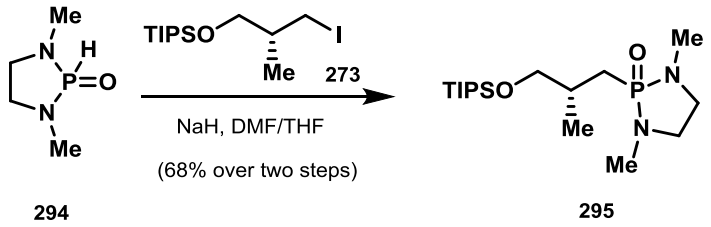

294 **295**

Iodide **273** (2.87 g, 8.05 mmol, 1 equiv) and **294** (4.32 g, 32.2 mmol, 4 equiv) were dissolved in dimethylformamide (40 mL, 0.2 M) and cooled to 0 °C. Sodium hydride (60% in mineral oil, 1.13 g, 28.2 mmol, 2.5 equiv) was added portion wise. The reaction mixture was warmed to ambient temperature. After 18 h saturated aqueous ammonium chloride solution was added and the aqueous layer was extracted with ethyl acetate. The combined organic layers were washed with saturated aqueous sodium chloride solution, dried over magnesium sulfate, filtered and the filtrate was concentrated under reduced pressure. The crude material was purified by flash column chromatography on silica gel (ethyl acetate, to 11% ethanol in ethyl acetate) phosphonamide **295** was obtained as a colorless oil (1.98 g, 68%).

TLC (11% methanol in ethyl acetate): R_f = 0.51 (CAM).

IR (Diamond-ATR, neat) $\tilde{\nu}_{max}$: 3389, 2942, 2864, 1463, 1382, 1225, 1155, 1092, 1033, 941 cm^{-1}.

^{1}H NMR (400 MHz, $CDCl_3$) δ = 3.52 (ddd, *J* = 9.4, 5.7, 2.4 Hz, 1H), 3.44 (dd, *J* = 9.4, 6.9 Hz, 1H), 3.27 – 3.15 (m, 2H), 3.14 – 3.02 (m, 2H), 2.66 (dd, *J* = 9.5, 4.7 Hz, 6H), 2.19 (ddd, *J* = 17.2, 15.8, 3.5 Hz, 1H), 1.97 – 1.70 (m, 1H), 1.58 (td, *J* = 15.7, 8.9 Hz, 1H), 1.18 – 1.02 (m, 21H), 1.00 (d, *J* = 6.7 Hz, 3H) ppm. **^{13}C NMR** (100 MHz, $CDCl_3$) δ = 68.9, 48.4, 48.2, 32.2, 32.0, 30.6, 29.4, 18.2, 12.1 ppm. **^{31}P NMR** (162 MHz, $CDCl_3$) δ = 42.22 (s, 1P) ppm.

HRMS (ESI, *m*/*z*): calcd for $(C_{17}H_{39}N_2O_2PSi)^+$ $[M+H]^+$: 363.2518; found: 363.2519.

$[\boldsymbol{\alpha}]_{\boldsymbol{D}}^{\boldsymbol{23}}$ = −5.25 (c = 0.02, $CHCl_3$).

(*R*)-2-((2-Methyl-3-((triisopropylsilyl)oxy)propyl)thio)benzo[*d*]thiazole (276)

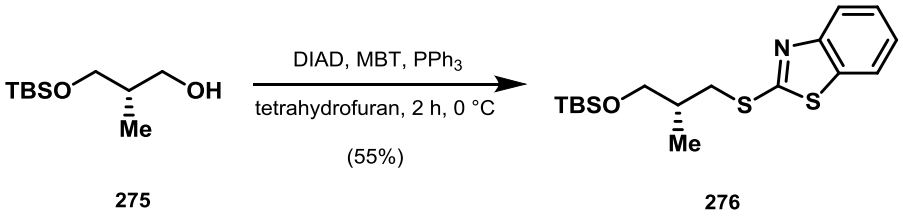

275 276

Tertbutyldimethyl azodicarboxylate (2.02 mL, 10.3 mmol, 1.08 equiv) was dissolved in anhydrous tetrahydrofuran (60 mL) and cooled to 0 °C. A solution of alcohol **275** (2.34 g, 9.49 mmol, 1 equiv), triphenylphosphine (2.74 g, 10.4 mmol, 1.1 equiv) and mercaptobenzothiazole (1.68 g, 10.1 mmol, 1.06 equiv) in anhydrous tetrahydrofuran (40 mL) was added and the reaction mixture was stirred at 0 °C for 2 h. Saturated aqueous sodium bicarbonate solution was added, and the mixture was filtered over Celite. The filtrate was extracted with diethyl ether. The combined organic layers were dried over magnesium sulfate, filtered and the filtrate was concentrated under reduced pressure. Purification by flash column chromatography on silica gel (7% ethyl acetate in petroleum ether) yielded **276** as a colorless oil (2.05 g, 55%). The obtained data were in full agreement with those values reported in literature.[99]

(*R*)-2-((2-Methyl-3-((triisopropylsilyl)oxy)propyl)sulfonyl)benzo[*d*]thiazole (277)

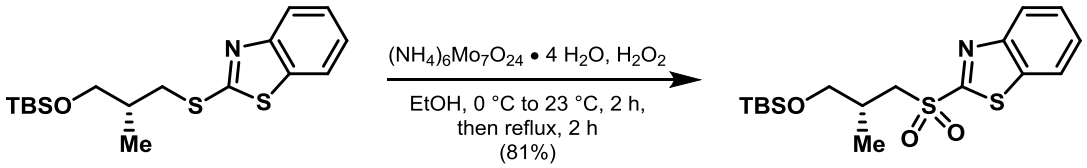

276 277

A solution of sulfide **276** (1.00 g, 2.53 mmol, 1 equiv) in ethanol (10 mL) was added to ammonium heptamolybdate tetrahydrate (625 mg, 0.505 mmol, 0.2 equiv) in a 30wt% hydrogen peroxide solution (2.00 mL, 19.6 mmol, 7.75 equiv) at 0 °C. The reaction mixture was allowed to warm to ambient temperature. After 2 h, hydrogen peroxide solution (1.00 mL, 8.90 mmol, 3.87 equiv) was added and the reaction mixture was heated to reflux. After 2 h, the solution was diluted with saturated aqueous sodium chloride solution and diethyl ether. The aqueous layer was extracted with diethyl ether. The combined organic layers were dried over magnesium sulfate, filtered and the filtrate was concentrated under reduced pressure. Purification by flash column chromatography on silica gel (ethyl acetate) yielded **277** as a pale-yellow oil (986 mg, 81%). The obtained data were in full agreement with those values reported in literature.[99]

Methyl (*R*)-3-((1*S*,3*R*)-2,2-dimethyl-3-((*S*,*E*)-3-methyl-4-((triisopropylsilyl)oxy)but-1-en-1-yl)cyclopropyl)-2-methylpropanoate (278)

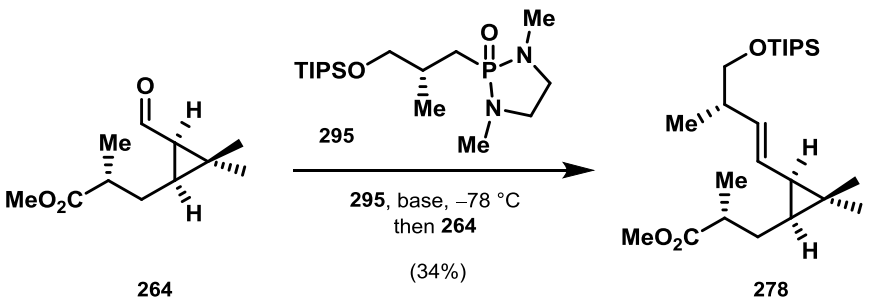

Phosphonamide **295** (40.6 mg, 112 µmol, 2.22 equiv) was dissolved in anhydrous tetrahydrofuran (0.32 mL, 0.35 M) and cooled to −78 °C. *n*-Butyl lithium (2.5 M in hexanes, 0.04 mL, 0.09 mmol, 1.88 equiv) was added dropwise and the resulting solution was stirred at −78 °C for 3 h. Subsequently, methyl ester **264** (10.0 mg, 50.4 µmol, 1.00 equiv) in tetrahydrofuran (0.5 mL) was added dropwise. The resulting reaction mixture was stirred at −78 °C for 90 min. Acetic acid and saturated aqueous ammonium chloride solution was added at −78 °C and the reaction mixture was allowed to warm to ambient temperature. After 2 h, the layers were separated, and the aqueous layer was extracted with dichloromethane. The combined organic layers were dried over magnesium sulfate, filtered and the filtrate was concentrated under reduced pressure. Purification by flash column chromatography on silica gel (2% ethyl acetate in petroleum ether) yielded (*E*)-olefin **278** as a colorless oil (7.03 mg, 34%).

TLC (5% ethyl acetate in petroleum ether): R_f = 0.45 (CAM).

IR (Diamond-ATR, neat) $\tilde{\nu}_{max}$: 2942, 2866, 1740, 1462, 1377, 1162, 1094 cm^{-1}.

^{1}H NMR (400 MHz, $CDCl_3$) δ = 5.48 (dd, *J* = 15.3, 7.3 Hz, 1H), 5.14 (dd, *J* = 15.4, 9.6 Hz, 1H), 3.66 (s, 3H), 3.56 (dd, *J* = 9.5, 6.1 Hz, 1H), 3.45 (dd, *J* = 9.4, 7.0 Hz, 1H), 2.47 (q, *J* = 7.0 Hz, 1H), 2.38 – 2.25 (m, 1H), 1.72 (dt, *J* = 14.2, 6.5 Hz, 1H), 1.48 – 1.39 (m, 2H), 1.27 – 1.19 (m, 2H), 1.16 (d, *J* = 7.0 Hz, 3H), 1.07 – 1.04 (m, 21H), 0.99 (d, *J* = 6.8 Hz, 3H), 0.97 (s, 3H), 0.63 (td, *J* = 8.4, 6.2 Hz, 1H) ppm. **^{13}C NMR** (100 MHz, $CDCl_3$) δ = 177.4, 134.7, 126.1, 68.9, 51.7, 40.3, 39.9, 30.2, 29.3, 29.0, 27.6, 20.7, 18.2, 17.1, 16.1, 15.8, 12.1 ppm.

HRMS (ESI, *m*/*z*): calcd for $(C_{24}H_{46}O_3Si)^+$ $[M+H_2O+H]^+$: 429.3216; found: 429.3214.

$[\alpha]_D^{23}$ = –40.75 (c = 0.02, $CHCl_3$).

(*R*)-1-((1*S*,3*R*)-2,2-dimethyl-3-((*S*,*E*)-3-methyl-4-((triisopropylsilyl)oxy)but-1-en-1-yl)cyclopropyl)propan-2-ol (296)

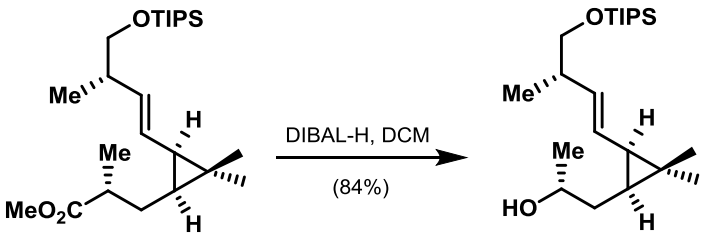

278 296

Methyl ester **278** (190 mg, 462 µmol, 1 equiv) was dissolved in dichloromethane (4.60 mL) and cooled to –78 °C. Diisobutylaluminium hydride (1 M in hexanes, 2.77 mL, 6 equiv) was added dropwise and the reaction mixture was stirred at −78 °C. After 90 min, the solution was diluted with saturated aqueous potassium sodium tartrate solution at −78 °C and the reaction mixture was allowed to warm to ambient temperature. After 2 h, the solution was extracted with diethyl ether, the combined organic layers were washed with saturated aqueous sodium chloride solution, dried over magnesium sulfate, filtered and the filtrate was concentrated under reduced pressure. Alcohol **296** was obtained as a colorless oil (148 mg, 84%) after purification by flash column chromatography on silica gel (10% ethyl acetate in petroleum ether).

TLC (20% ethyl acetate in petroleum ether): R_f = 0.5 (CAM).

IR (Diamond-ATR, neat) $\tilde{\nu}_{max}$: 3388, 2942, 2865, 1464, 1096, 882 cm^{-1}.

^{1}H NMR (400 MHz, $CDCl_3$) δ = 5.50 (dd, *J* = 15.3, 7.4 Hz, 1H), 5.19 (ddd, *J* = 15.3, 9.7, 1.1 Hz, 1H), 3.55 (dd, *J* = 9.4, 6.2 Hz,), 3.46 (dd, *J* = 9.4, 6.9 Hz, 1H), 2.39 – 2.27 (m, 1H), 1.70 – 1.61 (m, 1H), 1.41 – 1.31 (m, 2H), 1.28 – 1.18 (m, 3H), 1.10 (m, 1H), 1.07 (m, 21H), 0.99 (d, *J* = 6.7 Hz, 3H), 0.97 (s, 3H), 0.95 (d, *J* = 6.9 Hz, 3H), 0.65 (dt, *J* = 8.9, 6.8 Hz, 1H) ppm. **^{13}C NMR** (100 MHz, $CDCl_3$) δ = 134.7, 126.6, 100.0, 68.8, 68.0, 40.3, 36.8, 30.1, 29.0, 28.4, 28.3, 20.6, 18.2, 17.9, 17.0 15.8, 12.1 ppm.

HRMS (ESI, *m*/*z*): calcd for $(C_{22}H_{44}O_2Si)^+$ $[M+H]^+$: 369.3189; found: 369.3191.

$[\alpha]_D^{20}$ = –50.31 (c = 0.01, $CHCl_3$).

(*R*)-3-((1*S*,3*R*)-2,2-dimethyl-3-((*S*,*E*)-3-methyl-4-((triisopropylsilyl)oxy)but-1-en-1-yl)cyclopropyl)-2-methylpropanal (260)

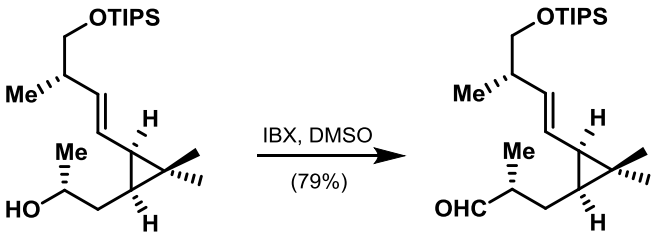

296 260

Alcohol **296** (149 mg, 389 µmol, 1 equiv) was dissolved in dimethyl sulfoxide (3.00 mL) and 2-iodoxybenzoic acid (545 mg, 1.95 mmol, 5 equiv) was added. The resulting reaction mixture was stirred for 1 h at ambient temperature. Subsequently, diethyl ether was added and the suspension was filtered through a short plug of Celite. The filter cake was rinsed with diethyl ether and the filtrate was concentrated. The crude product was purified by flash column chromatography on silica gel (5% ethyl acetate in petroleum ether) to afford **260** (117 mg, 79%) as a colorless oil.

TLC (10% ethyl acetate in petroleum ether): R_f = 0.77 (CAM).

IR (Diamond-ATR, neat) $\tilde{\nu}_{max}$: 2941, 2893, 2965, 1729, 1460, 1378, 1247, 1093, 1067, 1013 cm^{-1}.

^{1}H NMR (400 MHz, $CDCl_3$) δ = 9.63 (d, *J* = 1.85 Hz, 1H), 5.50 (dd, *J* = 15.2, 7.5 Hz, 1H), 5.11 (ddd, *J* = 15.3, 9.8, 1.1 Hz, 1H), 3.53 (dd, J = 15.7, 6.3 Hz, 1H), 3.45 (dd, J = 16.3, 6.9 Hz, 1H), 2.43-2-25 (m, 2H), 1.73 (dt, J = 14.4, 6.8 Hz, 1H), 1.47 – 1.37 (m, 2H), 1.27-1.21 (m, 2H), 1.11 (d, *J* = 7.0 Hz, 3H), 1.06 – 1.04 (m, 22H), 0.99 (s, 3H), 0.98 (d, *J* = 6.8 Hz, 3H), 0.67 (dt, *J* = 8.9, 7.1 Hz, 1H) ppm. **^{13}C NMR** (100 MHz, $CDCl_3$) δ = 205.5, 135.3, 125.7, 68.8, 47.1, 40.3, 30.1, 28.9, 27.4, 26.1, 20.7, 18.2, 17.1, 15.7, 13.4, 12.1 ppm.

HRMS (ESI, *m*/*z*): calcd for $(C_{23}H_{44}O_2Si)^+$ $[M+MeCN]^+$: 421.3376; found: 421.3380.

$[\alpha]_D^{23}$ = –58.2 (c = 0.05, $CHCl_3$).

(1*R*/*S*,2*R*)-3-((1*S*,3*R*)-2,2-dimethyl-3-((*S*,*E*)-3-methyl-4-((triisopropylsilyl)oxy)but-1-en-1-yl)cyclopropyl)-2-methyl-1-(8-methyl-1,4-dioxaspiro[4.4]non-6-en-6-yl)propan-1-ol (297a/297b)

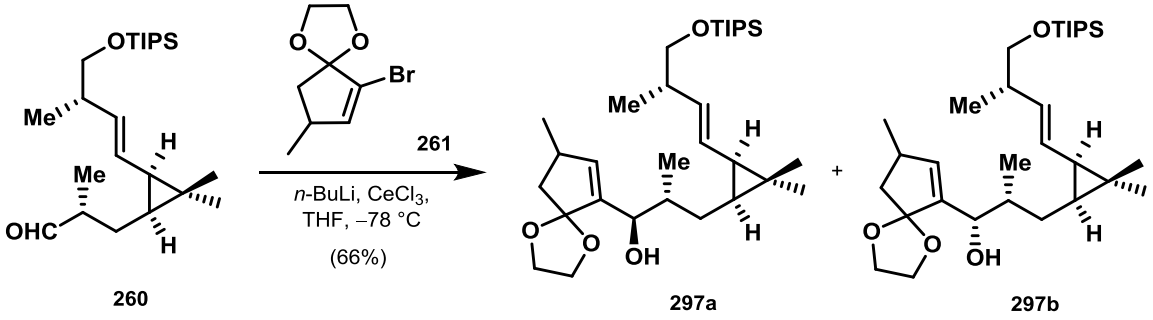

Vinyl bromide **261** (115 mg, 525 µmol, 2 equiv) was dissolved in tetrahydrofuran (1.05 mL) and cooled to –78 °C. *n*-BuLi (2.5 M in pentane, 420 µL, 4 equiv) was added dropwise, followed by the addition of $CeCl_3$ (129 mg, 525 µmol, 2 equiv). The resulting reaction mixture was stirred at –78 °C. After 60 min, aldehyde **260** (100 mg, 262 µmol, 1 equiv) in tetrahydrofuran (524 µL) was added. After 3 h, the reaction was diluted with saturated aqueous ammonium chloride solution. The layers were separated and the aqueous layer was extracted with diethyl ether. The combined organic layers were washed with saturated aqueous sodium chloride solution, the washed solution was dried over magnesium sulfate and the dried solution was filtered. The filtrate was concentrated under reduced pressure. The crude product was purified by flash column chromatography on silica gel (10% ethyl acetate in petroleum ether) to afford an inseparable mixture of both diastereomers of **297** (1:1) (90.0 mg, 66%) as a colorless oil.

TLC (20% ethyl acetate in petroleum ether): R_f = 0.53 (CAM).

IR (Diamond-ATR, neat) $\tilde{\nu}_{max}$: 3504, 2942, 2866, 1461, 1376, 1209, 1121, 1093, 1067, 1014 cm^{-1}.

^{1}H NMR (400 MHz, $CDCl_3$) δ = 5.90 (d, *J* = 14.6 Hz, 1H), 5.44 (ddd, *J* = 15.2, 12.2, 7.6 Hz, 1H), 5.19 (ddd, *J* = 14.8, 9.7, 4.6 Hz, 1H), 4.19 (d, *J* = 4.2 Hz, 1H), 4.04 – 3.88 (m, 5H), 3.55 (ddt, *J* = 9.0, 5.6, 2.7 Hz, 1H), 3.43 (td, *J* = 10.0, 7.1 Hz, 1H), 2.76 – 2.69 (m, 1H), 2.31 (td, *J* = 6.9, 2.1 Hz, 1H), 2.27 (dd, *J* = 13.5, 7.5 Hz, 1H), 1.83 (m, 2H), 1.58 (s, 2H), 1.56 (dd, *J* = 13.7, 5.1 Hz, 1H), 1.22 – 1.16 (m, 1H), 1.08 (d, *J* = 6.8 Hz, 6H), 1.05 (d, *J* = 5.3 Hz, 21H), 0.98 (d, *J* = 6.7 Hz, 3H), 0.96 (d, *J* = 5.1 Hz, 3H), 0.95 (d, *J* = 6.8 Hz, 2H), 0.88 (d, *J* = 6.7 Hz, 2H), 0.67 (ddd, *J* = 16.0, 9.2, 6.8 Hz, 1H) ppm.

HRMS (ESI, *m*/*z*): calcd for $(C_{31}H_{56}O_4Si)^+$ $[M+H]^+$: 521.4026; found: 521.4021.

(2*R*)-3-((1*S*,3*R*)-2,2-dimethyl-3-((*S*,*E*)-3-methyl-4-((triisopropylsilyl)oxy)but-1-en-1-yl)cyclopropyl)-2-methyl-1-(8-methyl-1,4-dioxaspiro[4.4]non-6-en-6-yl)propan-1-one (259)

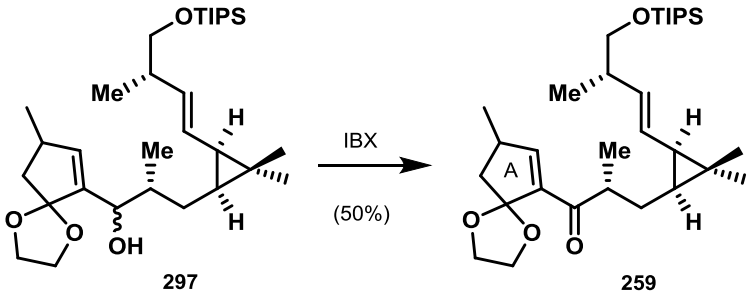

A 1:1 mixture of alcohols **297** (90.0 mg, 173 µmol, 1 equiv) was dissolved in dimethylsulfoxide (2.16 mL) and 2-iodoxybenzoic acid (96.8 mg, 346 µmol, 2 equiv) was added. The resulting reaction mixture was stirred for 1 h at ambient temperature. Subsequently, diethyl ether was added and the suspension was filtered through a short plug of Celite. The filter cake was rinsed with diethyl ether and the filtrate was concentrated. The crude product was purified by flash column chromatography on silica gel (10% ethyl acetate in petroleum ether) to afford **259** (44.9 mg, 50%) as a colorless oil.

TLC (10% ethyl acetate in petroleum ether): R_f = 0.51 (CAM).

IR (Diamond-ATR, neat) $\tilde{\nu}_{max}$: 2926, 2866, 1677, 1459, 1376, 1210, 1156, 1094, 1024 cm^{-1}.

^{1}H NMR (400 MHz, $CDCl_3$) δ = 6.84 (dd, *J* = 5.7, 2.4 Hz, 1H), 5.46 (dd, *J* = 15.4, 8.04, 1H), 5.13 (dd, *J* = 14.8, 9.3, 1H), 4.27 – 4.18 (m, 2H), 3.99 – 3.95 (m, 1H), 3.94 – 3.90 (m, 1H), 3.47 (dd, *J* = 9.5, 6.1 Hz, 1H), 3.45 (dd, *J* = 9.5, 6.1 Hz, 1H), 3.09 – 3.02 (m, 1H), 2.88 – 2.79 (m, 1H), 2.36 (dd, *J* = 13.7, 7.6 Hz, 1H), 2.33 – 2.26 (m, 1H), 1.76 – 1.71 (m, 1H), 1.71 – 1.66 (m, 1H), 1.16 (d, *J* = 7.1 Hz, 3H), 1.11 (dd, *J* = 6.8, 3.5 Hz, 3H), 1.06 – 1.03 (m, 24H), 0.98 (d, *J* = 6.7 Hz, 3H), 0.97 (s, 3H), 0.69 – 0.62 (m, 1H) ppm. **^{13}C NMR** (150 MHz, $CDCl_3$) δ = 202.5, 153.7, 142.0, 143.7, 126.5, 118.5, 68.9, 66.2, 65.9, 45.9, 42.9, 40.5, 35.2, 32.1, 30.2, 29.9, 29.3, 29.0, 27.9, 27.8, 22.8, 21.0, 19.9, 18.2, 17.2, 16.6, 15.9, 12.2 ppm.

HRMS (ESI, *m*/*z*): calcd for $(C_{31}H_{54}O_4Si)^+$ $[M]^+$: 518.3791; found: 518.3797.

$[\boldsymbol{\alpha}]_{\boldsymbol{D}}^{\boldsymbol{23}}$ = –53.6 (c = 0.05, $CHCl_3$).

2-((1*R*,3*S*)-2,2-dimethyl-3-(2-oxopropyl)cyclopropyl)acetaldehyde (309)

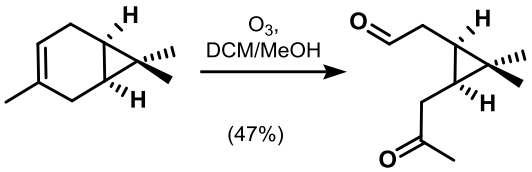

(+)-3-carene (**172**) **309**

(+)-3-Carene (**172**) (19 g, 139 mmol, 1 equiv) was dissolved in a mixed solvent of dichloromethane and methanol (556 mL, 7:1, 0.25 M). The resulting reaction mixture was cooled to –78 °C and treated with ozone until full consumption of 172. Thiourea (21.2 g, 278 mmol, 2.0 equiv) was added at –78 °C and the mixture was stirred for two hours at ambient temperature. Methanol was evaporated off and the residue was dissolved in diethyl ether. The organic layer was washed with saturated aqueous sodium chloride solution, dried over magnesium sulfate, filtered and the filtrated was concentrated. The crude product was purified by flash column chromatography on silica gel (33% ethyl acetate in petroleum ether) to yield aldehyde **309** (11.0 g, 47%) as a colorless oil. The obtained data were in full agreement with those values reported in the literature.[96]

1-((1*S*,3*R*)-3-(2,2-dimethoxyethyl)-2,2-dimethylcyclopropyl)propan-2-one (310)

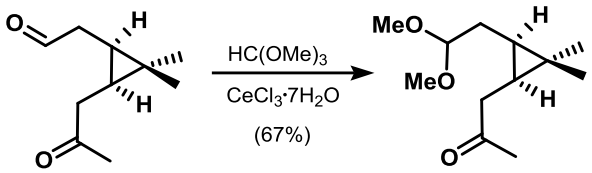

309 **310**

To a solution of aldehyde **309** (11.6 g, 68.9 mmol, 1 equiv.) and $CeCl_3$•7H2O (28.2 g, 114 mmol, 1.1 equiv.) in methanol (181 mL) was added trimethyl orthoformate (53.0 mL, 484 mmol, 7 equiv.) and the resulting reaction mixture was stirred at ambient temperature. After 30 min, the reaction was quenched with saturated sodium bicarbonate solution. Methanol was evaporated off and the residue was extracted three times with diethyl ether. The combined organic layers were washed with aqueous sodium chloride solution and dried over magnesium sulfate. After filtration the filtrate was concentrated and the crude product was further purified by flash column chromatography on silica gel (25% ethyl acetate in petroleum ether). The product was obtained in 67% yield (9.89 g) as colorless oil. The obtained data were in full agreement with those values reported in the literature.[96]

((3-((1*S*,3*R*)-3-(2,2-dimethoxyethyl)-2,2-dimethylcyclopropyl)prop-1-en-2-yl)oxy)trimethylsilane (305)

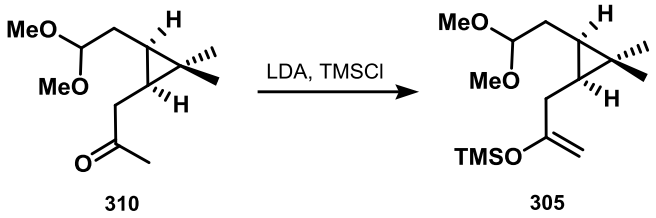

310 305

n-Butyllithium (2.51 M in *n*-hexane, 4.10 mL, 10.3 mmol, 1.1 equiv) was added dropwise to a solution of diisopropylamine (1.57 mL, 11.2 mmol, 1.2 equiv) in tetrahydrofuran (28 mL) at –78 °C. After 5 min, the cooling bath was removed, and the reaction mixture was allowed to warm to ambient temperature. After 20 min, the solution was cooled to –78 °C and a solution of **310** (2.00 g, 9.33 mmol, 1 equiv) in tetrahydrofuran (18.6 mL) was added. After 1 h, TMS-Cl (2.38 mL, 18.6 mmol, 2 equiv) was added dropwise. After 2 h, the reaction was diluted with saturated aqueous ammonium chloride solution. The layers were separated and the aqueous layer was extracted with diethyl ether. The combined organic layers were washed with saturated aqueous sodium chloride solution, the washed solution was dried over magnesium sulfate and the dried solution was filtered. The filtrate was concentrated. The crude product was obtained as slight yellow oil (98% crude) and used in the next step without further purification. The obtained data were in full agreement with those values reported in the literature.[96]

(1*S*,7*R*)-5-methoxy-8,8-dimethylbicyclo[5.1.0]octan-3-one (311)

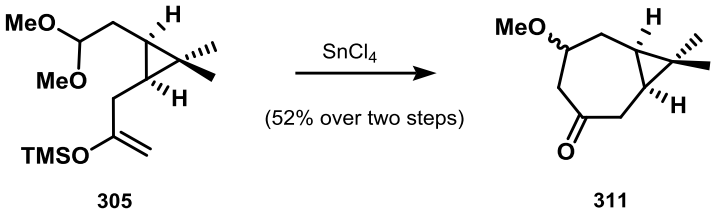

305 311

$SnCl_4$ (1 M in DCM, 7.00 mL, 10.1 mmol, 1.2 equiv) was dissolved in acetonitrile (54 mL) and cooled to –20 °C. Enol ether **305** (2.40 g, 8.37 mmol, 1 equiv) dissolved in acetonitrile (21 mL) was added dropwise. After 10 min, the reaction was diluted with water and diethyl ether. The layers were separated and the aqueous layer was extracted with diethyl ether. The combined organic layers were dried over magnesium sulfate, the dried solution was filtered and the filtrate was concentrated. The crude product was purified by flash column chromatography on silica gel (10% ethyl acetate in petroleum ether) and obtained **311** in 52% (792 mg) yield over two steps. The obtained data were in full agreement with those values reported in the literature.[96]

(1*S*,7*R*)-8,8-dimethylbicyclo[5.1.0]oct-4-en-3-one (304)

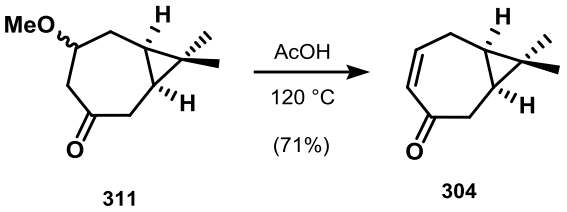

311 304

A solution of seven-membered ring ketone **311** (3.59 g, 19.7 mmol, 1 equiv) in 126 mL acetic acid was stirred at reflux. After 6 h acetic acid was evaporated off and the residue was dissolved diethyl ether. The solution was washed with saturated aqueous sodium carbonate. The washed organic layer was dried over magnesium sulfate, filtered and the filtrate was concentrated. The residue was purified by flash column chromatography on silica gel (10% ethyl acetate in petroleum ether) to yield **304** (2.10 mg, 71%) as a colorless oil. The obtained data were in full agreement with those values reported in the literature.[96]

Trimethyl(((1*S*,5*R*,7*R*)-5,8,8-trimethylbicyclo[5.1.0]oct-3-en-3-yl)oxy)silane (312)

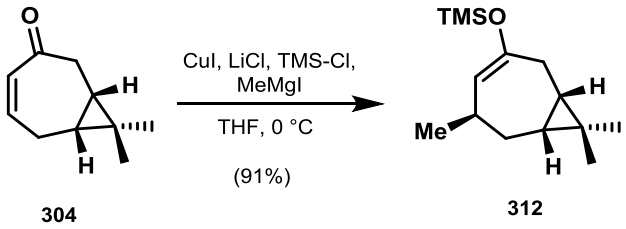

304 312

In a Schlenk flask LiCl (26.0 mg, 0.665 mmol, 0.2 equiv) and CuI (63.0 mg, 0.332 mmol, 0.1 equiv) were dissolved in tetrahydrofuran (3.00 mL). After stirring for 20 min, the reaction mixture was cooled to 0 °C and enone **304** (500 mg, 3.32 mmol, 1 equiv) in tetrahydrofuran (3.00 mL) and TMS-Cl (0.46 mL, 3.66 mmol, 1.1 equiv) were added successively. After 10 min, MeMgI (1.33 mL, 3.99 mmol, 1.2 equiv) was added. After 30 min, the reaction mixture was poured into saturated sodium bicarbonate solution. The aqueous layer was extracted with diethyl ether and the combined organic layers were dried over magnesium sulfate. It was filtered and the filtrate was concentrated. The crude product (**312**) was obtained as colorless oil (91% crude) and used in the next step without further purification. The obtained data were in full agreement with those values reported in the literature.[96]

(1*S*,4*S*,5*R*,7*R*)-4-hydroxy-5,8,8-trimethylbicyclo[5.1.0]octan-3-one (313)

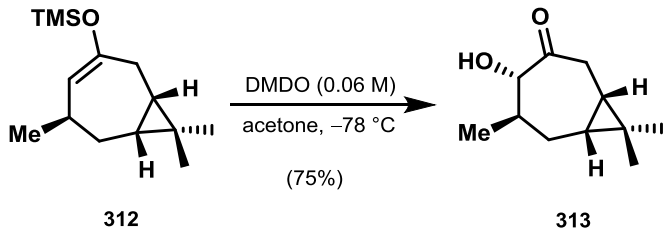

312 313

Crude enol ether **312** (500 mg, 3.32 mmol, 1 equiv) was dissolved in acetone (6.64 mL) and cooled to –78 °C. Freshly prepared dimethyldioxirane (83.0 mL, 0.06 M in acetone, 1.5 equiv) was added and the resulting solution was stirred for 12 h at –78 °C. The solvent was evaporated off and the residue was purified by flash column chromatography on silica gel (20% ethyl acetate in petroleum ether). α-hydroxy ketone **313** was obtained as colorless oil, in 75% yield (453 mg) over two steps.

TLC (20% ethyl acetate in petroleum ether): R_f = 0.5 (CAM).

IR (Diamond-ATR, neat) $\tilde{\nu}_{max}$: 3437, 2955, 1702, 1456, 1377, 1068, 1052, 987 cm^{-1}.

^{1}H NMR (400 MHz, $CDCl_3$) δ = 4.42 (dd, *J* = 8.5, 6.5 Hz, 1H), 3.25 (d, *J* = 6.5 Hz, 1H), 2.77 (dd, *J* = 19.8, 7.9 Hz, 1H), 2.22 (dd, *J* = 19.9, 9.4, 1H), 1.72 – 1.60 (m, 2H), 1.28 (d, *J* = 6.8 Hz, 3H), 1.24 – 1.13 (m, 1H), 1.10 (s, 3H), 0.99 (s, 3H), 0.99 (m, 1H), 0.79 – 0.72 (m, 1H) ppm. **^{13}C NMR** (200 MHz, $CDCl_3$) δ = 214.3, 80.5, 40.0, 36.0, 28.7, 27.0, 21.6, 20.4, 19.4, 19.2, 14.9 ppm.

HRMS (ESI, *m*/*z*): calcd for $(C_{11}H_{18}O_2)^+$ $[M+MeCN]^+$: 223.1572; found: 223.1571.

$[\alpha]_D^{23}$ = +44.06 (c = 0.015, $CHCl_3$).

(1*S*,4*S*,5*R*,7*R*)-4-((tert-butyldimethylsilyl)oxy)-5,8,8-trimethylbicyclo[5.1.0]octan-3-one (315)

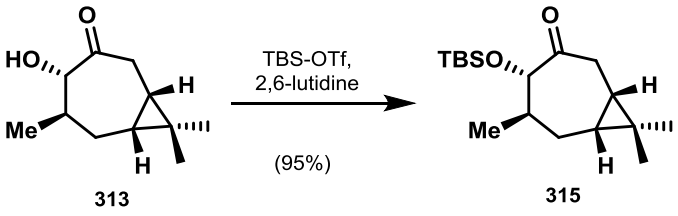

313 315

To a cooled solution of α-hydroxy ketone **313** (100 mg, 0.548 mmol, 1 equiv) and 2,6-lutidine (0.120 mL, 1.10 mmol, 2 equiv) in dichloromethane was added dropwise TBS-OTf (0.180 mL, 0.823 mmol, 1.5 equiv) at –5 °C. After 10 min, the reaction was diluted with water and dichloromethane and the layers were separated. The aqueous layer was extracted with dichloromethane and the combined organic layers were dried over magnesium sulfate, filtered and the filtrate was concentrated. The crude product was purified by flash column

chromatography on silica gel (5% ethyl acetate in petroleum ether). **315** was obtained as colorless oil (154 mg, 95%).

TLC (10% ethyl acetate in petroleum ether): R_f = 0.72 (CAM).

IR (Diamond-ATR, neat) $\tilde{\nu}_{max}$: 2954, 2858, 2930, 1713, 1461, 1252, 1085 cm^{-1}.

^{1}H NMR (400 MHz, $CDCl_3$) δ = 3.97 (dd, *J* = 4.9, 1.7 Hz, 1H), 2.63 (dd, *J* = 12.1, 10.7 Hz, 1H), 2.25 (ddd, *J* = 12.1, 7.1, 1.7 Hz, 1H), 2.00-1.91 (m, 1H), 1.67 (d, *J* = 3.4 Hz, 1H), 1.65 (dd, *J* = 3.4, 1.4 Hz, 1H), 1.07 (s, 3H), 1.05 (s, 3H), 0.95 (d, *J* = 7.3 Hz, 3H), 0.88 (s, 9H), 0.65 (q, *J* = 8.9 Hz, 1H), 0.49 (ddd, *J* = 10.7, 9.0, 7.1 Hz, 1H), 0.03 (s, 3H), -0.01 (s, 3H) ppm. **^{13}C NMR** (100 MHz, $CDCl_3$) δ = 209.3, 83.3, 38.0, 33.4, 28.8, 25.8, 23.5, 22.5, 21.6, 20.2, 28.1, 15.3, 14.5, –4.9, –5.0 ppm.

HRMS (ESI, *m*/*z*): calcd for $(C_{17}H_{32}O_2Si)^+$ $[M]^+$: 296.2172; found: 296.2171.

$[\alpha]_D^{24}$ = +96.78 (c = 0.028, $CHCl_3$).

(1*R*,4*S*,5*R*,7*R*)-4-((tert-butyldimethylsilyl)oxy)-5,8,8-trimethylbicyclo[5.1.0]oct-2-en-3-yl trifluoromethanesulfonate (316)

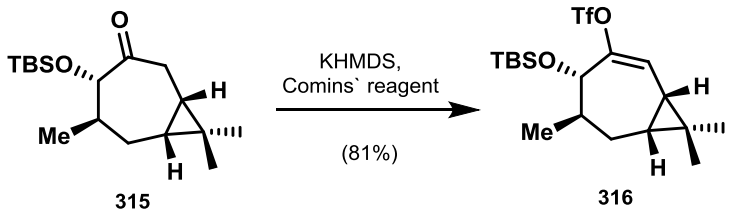

To a cooled solution of silyl ether **315** (281 mg, 0.947 mmol, 1 equiv) in tetrahydrofuran (4.72 mL) at –78 °C was added KHMDS (2.20 mL, 0.5 M in toluene, 1.2 equiv). After 45 min, Comins` reagent (446 mg, 1.13 mmol, 1.2 equiv) was added and stirring was continued for 60 min. The reaction was diluted with saturated aqueous ammonium chloride solution and diethyl ether. The layers were separated and the aqueous layer was extracted with diethyl ether. The combined organic layers were dried over magnesium sulfate, filtered and the filtrate was concentrated. The crude product was purified by flash column chromatography on silica gel (2% ethyl acetate in petroleum ether). Vinyl triflate **316** was obtained as colorless oil (329 mg, 81%).

TLC (100% petroleum ether): R_f = 0.47 (CAM, UV).

IR (Diamond-ATR, neat) $\tilde{\nu}_{max}$: 2934, 1417, 1246, 1205, 1142, 1080 cm^{-1}.

^{1}H NMR (400 MHz, $CDCl_3$) δ = 5.73 (d, *J* = 3.8 Hz, 1H), 4.28 (dd, *J* = 6.1, 1.3 Hz, 1H), 1.97 – 1.81 (m, 2H), 1.66 (ddd, *J* = 14.9, 7.8, 4.3 Hz, 1H), 1.15 (d, *J* = 7.1 Hz, 3H), 1.12 (s, 3H), 1.11 –

1.03 (m, 2H), 1.02 (s, 3H), 0.90 (s, 9H), 0.09 (s, 3H), 0.06 (s, 3H). **^{13}C NMR** (100 MHz, $CDCl_3$) δ = 149.8, 120.8, 76.1, 35.6, 28.1, 25.8, 23.5, 23.4, 23.3, 21.4, 18.2, 16.2, 15.9, –4.8, –4.9 ppm.

HRMS (ESI, *m*/*z*): calcd for $(C_{18}H_{31}F_3O_4SSi)^+$ $[M+H_2O+H]^+$: 447.1848; found: 447.1850.

$[\alpha]_D^{24} = -47.35$ (c = 0.02, $CHCl_3$).

(1*S*,4*S*,5*R*,7*R*)-4-((tert-butyldimethylsilyl)oxy)-N-methoxy-N,5,8,8-tetramethylbicyclo[5.1.0]oct-2-ene-3-carboxamide (317)

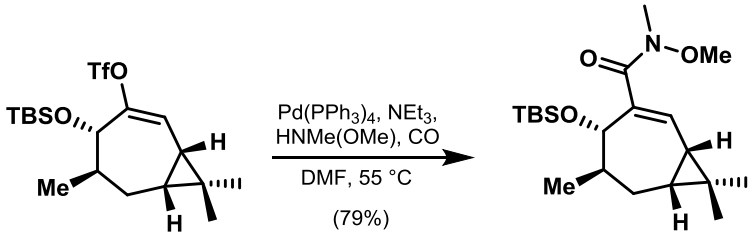

316 317

To a solution of vinyl triflate **316** (200 mg, 0.466 mmol, 1 equiv) in dimethylformamide (9.33 mL) was added $Pd(PPh_3)_4$ (107 mg, 0.0932 mmol, 0.2 equiv), freshly distilled triethylamine (0.2 mL, 1.39 mmol, 3 equiv) and *N*,*O*-dimethylhydroxylamine (260 mg, 2.65 mmol, 5.7 equiv). The reaction was warmed to 55 °C. An atmosphere of carbon monoxide was maintained by charging the mixture with a stream of carbon monoxide gas using a stainless steel needle for 1 min and vigorous stirring of the suspension was then continued under carbon monoxide atmosphere at 55 °C. After 18 h, carbon monoxide gas was released from the flask and the reaction mixture was diluted with saturated aqueous ammonium chloride solution and diethyl ether. The layers were separated and the aqueous layer was extracted with diethyl ether. The combined organic layers were washed with saturated aqueous sodium chloride solution, the washed solution was dried over magnesium sulfate, the dried solution was filtered and the filtrate was concentrated. The residue was purified by flash column chromatography on silica gel (10% ethyl acetate in petroleum ether) to yield **317** (135 mg, 79%) as a colorless oil.

TLC (14% ethyl acetate in petroleum ether): R_f = 0.6 (CAM, UV).

IR (Diamond-ATR, neat) $\tilde{\nu}_{max}$: 2953, 2982, 2857, 1659, 1461, 1376, 1250, 1091, 1044 cm^{-1}.

^{1}H NMR (400 MHz, $CDCl_3$) δ = 5.83 (d, *J* = 3.35 Hz, 1H), 4.55 (d, *J* = 6.04, 1H), 3.63 (s, 3H), 3.22 (s, 3H), 2.02 – 1.91 (m, 1H), 1.80 – 1.69 (m, 1H), 1.64 (ddd, *J* = 14.6, 7.2, 4.1 Hz, 1H), 1.14 (d, *J* = 7.07, 3H), 1.10 (s, 3H), 1.03 (s, 3H), 0.04 (s, 3H), 0.00 (s, 3H) ppm. **^{13}C NMR** (100 MHz,

$CDCl_3$) δ = 171.1, 139.1, 129.4, 75.8, 60.9, 35.9, 28.2, 26.8, 25.9, 24.6, 23.2, 20.6, 18.0, 17.1, 16.3, −4.4, −4.8 ppm.

HRMS (ESI, *m*/*z*): calcd for $(C_{20}H_{37}NO_3Si)^+$ $[M+H]^+$: 368.2621; found: 368.2630.

$[\alpha]_D^{24}$ = −6.8 (c = 0.05, $CHCl_3$).

(*S*)-1-((1*S*,4*S*,5*R*,7*R*)-4-((tert-butyldimethylsilyl)oxy)-5,8,8-trimethylbicyclo[5.1.0]oct-2-en-3-yl)-3-methyl-4-((triisopropylsilyl)oxy)butan-1-one (343)

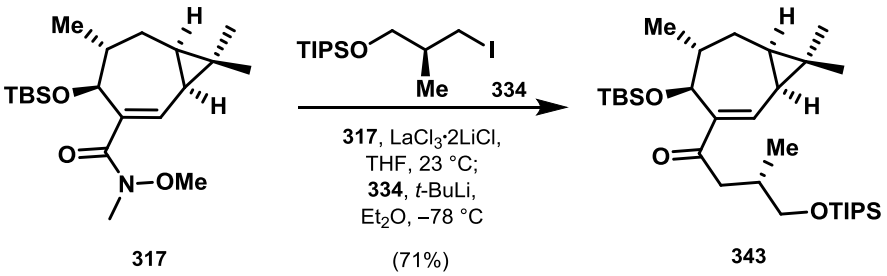

Alkyl iodide **334** (318 mg, 1.01 mmol, 3 equiv) was dissolved in diethyl ether and cooled to –78 °C. *t*-BuLi (1.06 mL, 1.9 M solution in pentane, 6 equiv) was added dropwise and it was stirred for 30 min. Weinreb amide **317** (124 mg, 337 µmol, 1 equiv) was dissolved in tetrahydrofuran (2.2 mL), a solution of $LaCl_3$•2LiCl (1.70 mL, 0.6 M in THF, 3 equiv) was added at ambient temperature. After 30 min, the solution was added to lithiated alkyl iodide **334** and the resulting reaction mixture was stirred at –78 °C for 10 min. After warming to –40 °C and stirring for additional 10 min, the solution was diluted with saturated aqueous ammonium chloride solution and the layers were separated. The aqueous layer was extracted with diethyl ether, the combined organic layers were washed with saturated aqueous sodium chloride solution and the washed solution was dried over magnesium sulfate. The dried solution was filtered and the filtrate was concentrated. The crude product was purified by flash column chromatography on silica gel (2% ethyl acetate in petroleum ether) to afford **343** (128 mg, 71%) as a colorless oil.

TLC (1.6% ethyl acetate in petroleum ether): R_f = 0.70 (CAM, UV).

IR (Diamond-ATR, neat) $\tilde{\nu}_{max}$: 2954, 2866, 2325, 1666, 1642, 1462, 1382, 1252, 1066, 1049 cm^{-1}.

^{1}H NMR (400 MHz, $CDCl_3$) δ = 6.66 (d, *J* = 4.6 Hz, 1H), 4.69 (dd, *J* = 5.9, 0.8 Hz, 1H), 3.53 (dd, *J* = 9.5, 5.3 Hz, 1H), 3.45 (dd, *J* = 9.5, 7.0 Hz, 1H), 2.93 (dd, *J* = 15.5, 4.2 Hz, 1H), 2.28 (dd, *J* = 15.5, 9.2 Hz, 1H), 2.19 – 2.08 (m, 1H), 2.01 – 1.90 (m, 2H), 1.20 (dd, *J* = 8.18, 4.5 Hz, 1H), 1.16 (s, 3H), 1.07-1.05 (m, 23H), 1.03 (s, 3H), 0.87 (d, *J* = 6.7 Hz, 3H), 0.82 (s, 9H), 0.06 (s, 3H), -0.03 (s, 3H) ppm. **^{13}C NMR** (100 MHz, $CDCl_3$) δ = 203.3, 142.2, 139.0, 72.7, 68.4, 43.3, 36.4, 33.8, 28.7, 28.6, 26.0, 24.7, 23.4, 22.8, 18.2, 16.8, 16.2, 15.9, 12.2, –4.5, –4.9 ppm.

HRMS (ESI, *m*/*z*): calcd for $(C_{31}H_{60}O_3Si_2)^+$ $[M+H]^+$: 537.4159; found: 537.4160.

$[\alpha]_D^{20}$ = –52.62 (c = 0.016, $CHCl_3$).

(*S*)-4-hydroxy-1-((1*S*,4*S*,5*R*,7*R*)-4-hydroxy-5,8,8-trimethylbicyclo[5.1.0]oct-2-en-3-yl)-3-methylbutan-1-one (344)

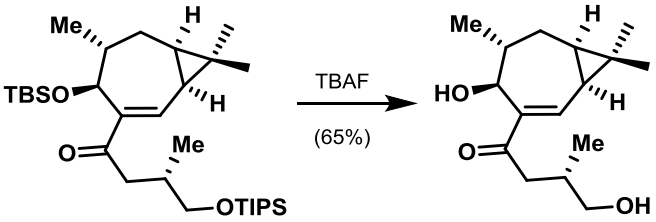

343 **344**

Tetrabutylammonium fluoride (1 M in THF, 730 µL, 730 µmol, 4 equiv) was added dropwise to a solution of TBS ether **343** (98.0 mg, 182 µmol, 1 equiv) in tetrahydrofuran (5.10 mL) at ambient temperature. After 3 h, the solution was diluted with saturated aqueous sodium bicarbonate solution. The layers were separated and the aqueous layer was extracted with diethyl ether. The combined organic layers were washed with saturated aqueous sodium chloride solution, the washed solution was dried over magnesium sulfate and the dried solution was filtered. The filtrate was concentrated. The crude product was purified by flash column chromatography on silica gel (50% ethyl acetate in petroleum ether) to afford **344** (22.2 mg, 65%) as a colorless oil.

TLC (50% ethyl acetate in petroleum ether): R_f = 0.48 (CAM, UV).

IR (Diamond-ATR, neat) $\tilde{\nu}_{max}$: 3404, 2952, 2917, 2870, 1638, 1454, 1377, 1218, 1042 cm^{-1}.

^{1}H NMR (400 MHz, $CDCl_3$) δ = 6.67 (d, *J* = 2.9 Hz, 1H), 4.41 (t, *J* = 8.0 Hz, 1H), 3.85 (d, *J* = 8.8 Hz, 1H), 3.55 (dd, *J* = 10.7, 5.1 Hz, 1H), 3.41 (dd, *J* = 10.7, 6.9 Hz, 1H), 2.82 (dd, *J* = 15.8, 6.7 Hz, 1H), 2.56 (dd, *J* = 15.8, 6.7 Hz, 1H), 2.27-2.16 (m, 1H), 1.98 (s, 1H), 1.98 (s, 1H), 1.86 – 1.73 (m, 1H), 1.64 (ddd, *J* = 14.6, 6.1, 2.6 Hz, 1H), 1.34 – 1.23 (m, 3H), 1.17 (d, *J* = 7.0 Hz, 3H), 1.14 (s, 3H), 0.97 (s, 3H), 0.94 (d, *J* = 6.9 Hz, 3H) ppm. **^{13}C NMR** (100 MHz, $CDCl_3$) δ = 205.3, 143.7, 140.1, 75.6, 67.8, 42.3, 35.7, 33.1, 28.2, 26.3, 22.3, 21.8, 17.6, 17.2, 16.1 ppm.

HRMS (ESI, *m*/*z*): calcd for $(C_{16}H_{26}O_3)^+$ $[M+H_2O]^+$: 284.1988; found: 284.1986.

$[\alpha]_D^{24}$ = –123.7 (c = 0.05, $CHCl_3$).

(*S*)-2-methyl-4-oxo-4-((1*S*,5*R*,7*R*)-5,8,8-trimethyl-4-oxobicyclo[5.1.0]oct-2-en-3-yl)butanal (345)

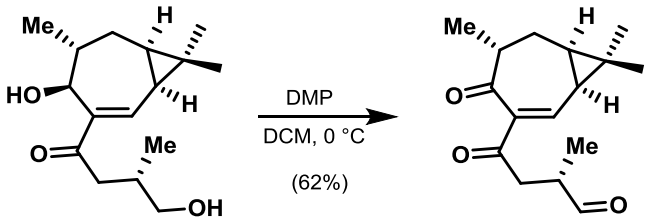

344 **345**

Dess–Martin periodinane (397 mg, 937 µmol, 2.5 equiv) was added to a solution of alcohol **344** (100 mg, 375 µmol, 1 equiv) in dichloromethane (468 µL) at 0 °C. The suspension was then allowed to warm to ambient temperature. After 3 h, diethyl ether was added and the suspension was filtered through a short plug of Celite. The filter cake was rinsed with diethyl ether and the filtrate was concentrated. The crude product was purified by flash column chromatography on silica gel (10% ethyl acetate in petroleum ether) to afford **345** (61.0 mg, 62%) as a colorless oil.

TLC (33% ethyl acetate in petroleum ether): R_f = 0.41 (CAM, UV).

IR (Diamond-ATR, neat) $\tilde{\nu}_{max}$: 2931, 1725, 1688, 1600, 1457, 1378, 1263, 1200, 1135 cm^{-1}.

^{1}H NMR (400 MHz, $CDCl_3$) δ = 9.69 (d, *J* = 0.7 Hz, 1H), 6.98 (dd, *J* = 2.6, 0.7 Hz, 1H), 3.17 (dd, *J* = 17.8, 7.1 Hz, 1H), 3.00 – 2.90 (m, 1H), 2.71 – 2.63 (m, 1H), 2.53 (dd, *J* = 17.9, 5.6 Hz, 1H), 1.90 (ddd, *J* = 14.9, 6.2, 3.3 Hz, 1H), 1.78 (ddd, *J* = 15.0, 10.8, 4.4 Hz, 1H), 1.35 (d, *J* = 8.2, 2.6 Hz, 1H), 1.32 (d, *J* = 7.1 Hz, 4H), 1.22 – 1.18 (m, 1H), 1.17 (s, 4H), 1.15 (d, *J* = 7.4 Hz, 3H), 1.05 (s, 3H) ppm. **^{13}C NMR** (100 MHz, $CDCl_3$) δ = 207.9, 203.5, 197.0, 144.4, 143.4, 46.1, 41.9, 40.9, 28.1, 27.1, 26.7, 24.9, 24.0, 15.7, 15.0, 13.7 ppm.

HRMS (ESI, *m*/*z*): calcd for $(C_{16}H_{22}O_3)^+$ $[M+H_2O]^+$: 280.1675; found: 280.1678.

$[\alpha]_D^{23}$ = –56.35 (c = 0.015, $CHCl_3$).

***N*'-((1*S*,4*S*,5*R*,7*R*,*E*)-4-((tert-butyldimethylsilyl)oxy)-5,8,8-trimethylbicyclo[5.1.0]octan-3-ylidene)-4-methylbenzenesulfonohydrazide (355)**

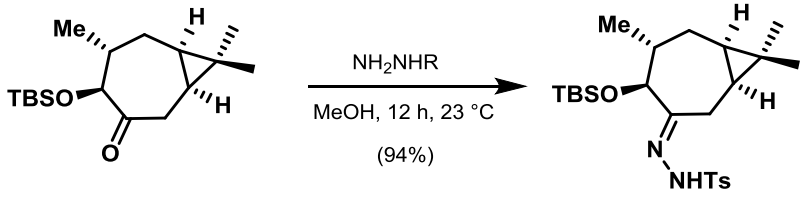

315 **355**

Ketone **315** (134 mg, 452 µmol, 1 equiv) was dissolved in methanol (220 µL) and *p*-toluenesulfonyl hydrazide (101 mg, 0.542 mmol, 1.2 equiv) was added. The resulting reaction mixture was stirred at ambient temperature for 12 h. The solvent was removed under reduced pressure and the crude product was purified by flash column chromatography on silica gel (10% ethyl acetate in petroleum ether) to afford **355**(206 mg, 94%) as a white foam.

TLC (1% ethyl acetate in petroleum ether): R_f = 0.3 (CAM, UV).

IR (Diamond-ATR, neat) $\tilde{\nu}_{max}$: 3220, 2954, 2929, 2858, 1599, 1462, 1389, 1358, 1340, 1252, 1168, 1083, 1021 cm^{-1}.

^{1}H NMR (400 MHz, $CDCl_3$) δ = 7.80 (d, *J* = 8.2 Hz, 2H), 7.47 (s, 1H), 7.26 (d, *J* = 8.4 Hz, 2H), 4.01 (d, *J* = 3.5 Hz, 1H), 2.40 (s, 3H), 2.29 (dd, *J* = 14.4, 4.7 Hz, 1H), 2.04-1.96 (m, 1H), 1.89-1.78 (m, 1H), 1.66 – 1.58 (m, 2H), 0.99 (d, *J* = 1.6 Hz, 3H), 0.77 (s, 4H), 0.64 (d, *J* = 7.3 Hz, 1H), 0.42 – 0.32 (m, 1H), –0.09 (s, 1H), –0.26 (s, 1H) ppm. **^{13}C NMR** (100 MHz, $CDCl_3$) δ = 144.0, 129.6, 128.1, 79.2, 38.1, 28.8, 25.8, 22.8, 22.4, 21.7, 21.3, 20.2, 18.0, 15.0, 14.5, –5.0, –5.1 ppm.

HRMS (ESI, *m*/*z*): calcd for $(C_{24}H_{40}N_2O_3SSi)^+$ $[M+MeCN]^+$: 505.2794; found: 505.2800.

$[\alpha]_D^{22}$ = +182.2 (c = 0.05, $CHCl_3$).

(1*S*,5*R*,7*R*)-5,8,8-trimethylbicyclo[5.1.0]octan-3-one (362)

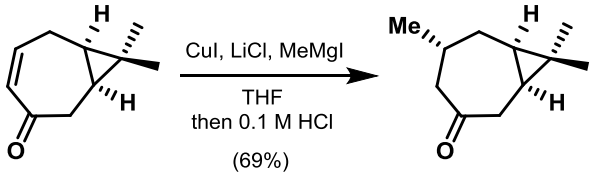

304 **362**

In a Schlenk flask LiCl (28.1 mg, 664 µmol, 0.2 equiv) and CuI (63.2 mg, 332 µmol, 0.1 equiv) were dissolved in tetrahydrofuran (3.32 mL). After stirring for 20 min the reaction mixture was cooled to 0 °C and unsaturated ketone **304** (500 mg, 3.32 mmol, 1 equiv) in tetrahydrofuran

(0.66 mL) was added. After 10 min a solution of MeMgI (3 M in diethyl ether, 1.33 mL, 1.2 equiv) was added dropwise. After 30 min, the reaction mixture was diluted with 0.1 M hydrogen chloride solution and the layers were separated. The aqueous layer was extracted with diethyl ether. The combined organic layers were washed with saturated aqueous sodium chloride solution, the washed solution was dried over magnesium sulfate and the dried solution was filtered. The filtrate was concentrated. The crude product was purified by flash column chromatography on silica gel (10% ethyl acetate in petroleum ether) to afford **362** (38.1 mg, 69%) as a colorless oil. The obtained data were in full agreement with those values reported in the literature.[96]

2,4,6-triisopropyl-*N*'-((1*S*,5*R*,7*R*,*Z*)-5,8,8-trimethylbicyclo[5.1.0]octan-3-ylidene)benzenesulfonohydrazide (363)

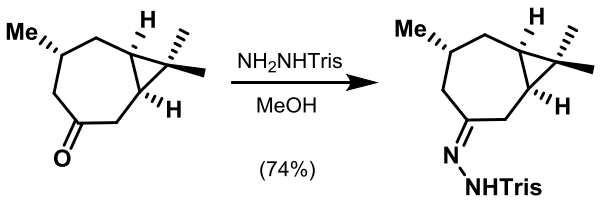

362 **363**

Ketone **362** (100 mg, 601 µmol, 1 equiv) was dissolved in methanol (60 µL) and 2,4,6-triisopropylbenzenesulfonyl hydrazide (215 mg, 721 µmol, 1.2 equiv) was added. The resulting reaction mixture was stirred at ambient temperature for 12 h. The solvent was removed under reduced pressure and the crude product was purified by flash column chromatography on silica gel (10% ethyl acetate in petroleum ether) to afford **363** (199 mg, 74%) as a white foam.

TLC (1% ethyl acetate in petroleum ether): R_f = 0.43 (CAM, UV).

IR (Diamond-ATR, neat) $\tilde{\nu}_{max}$: 3225, 2955, 2868, 1599, 1565, 1460, 1426, 1380, 1323, 1257, 1164, 1152, 1024 cm^{-1}.

^{1}H NMR (400 MHz, $CDCl_3$) δ = 7.15 (s, 2H), 4.28 – 4.17 (m, 2H), 2.97 – 2.82 (m, 1H), 2.58 (dd, *J* = 17.1, 7.0 Hz, 1H), 2.33 (dd, *J* = 12.5, 8.2 Hz, 0.5H), 2.18 (dd, *J* = 12.6, 5.5, 0.5H), 2.01 – 1.88 (m, 1H), 1.86 – 1.51 (m, 3H), 1.29 – 1.22 (m, 18H), 1.06 (s, 2H), 1.02 (d, *J* = 9.1 Hz, 2H), 0.98 (s, 3H), 0.85 (d, *J* = 6.9 Hz, 2H), 0.71 – 0.50 (m, 3H) ppm. **^{13}C NMR** (100 MHz, $CDCl_3$) δ = 159.6, 153.2, 151.4, 131.6, 123.8, 43.3, 34.3, 31.3, 30.1, 28.8, 28.2, 25.4, 25.0, 23.7, 21.7, 20.2, 19.6, 19.4, 15.0 ppm.

HRMS (ESI, *m*/*z*): calcd for $(C_{26}H_{42}N_2O_2S)^+$ $[M+MeCN+H_2O]^+$: 488.32; found: 488.32.

$[\alpha]_D^{20}$ = +99.1 (c = 0.01, $CHCl_3$).

(1*R*,5*R*,7*R*)-5,8,8-trimethylbicyclo[5.1.0]oct-2-en-3-yl trifluoromethanesulfonate (371)

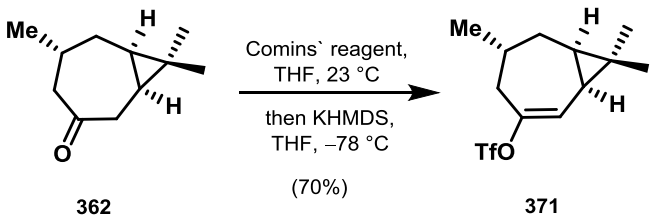

362 371

To a solution of ketone **362** (200 mg, 1.20 mmol, 1 equiv) in tetrahydrofuran (600 µL) was added *N*,*N*-bis(trifluoromethylsulfonyl)-5-chloro-2-pyridylamine (Comins` reagent) (567 mg, 1.44 mmol, 1.2 equiv) and the resulting reaction mixture was cooled to –78 °C. A solution of KHMDS (0.5 M in toluene, 2.88 mL, 1.2 equiv) was added dropwise. After 1 h, the solution was diluted with saturated aqueous ammonium chloride solution. The layers were separated and the aqueous layer was extracted with diethyl ether. The combined organic layers were washed with saturated aqueous sodium chloride solution, the washed solution was dried over magnesium sulfate and the dried solution was filtered. The filtrate was concentrated. The crude product was purified by flash column chromatography on silica gel (10% ethyl acetate in petroleum ether) to afford **371** (250 mg, 70%) as a colorless oil.

TLC (100% petroleum ether): R_f = 0.45 (CAM, UV).

IR (Diamond-ATR, neat) $\tilde{\nu}_{max}$: 2956, 1414, 1245, 1203, 1141, 1061, 1021 cm^{-1}.

^{1}H NMR (400 MHz, $CDCl_3$) δ = 6.15 (t, *J* = 2.0 Hz, 1H), 3.05 – 2.96 (m, 1H), 2.38 (dd, *J* = 14.8, 5.8 Hz, 1H), 1.98 – 1.88 (m, 1H), 1.61 (ddd, *J* = 14.5, 5.6, 2.2 Hz, 1H), 1.37 – 1.25 (m, 2H), 1.04 (s, 6H), 0.97 (s, 3H), 0.71 (ddd, *J* = 11.4, 8.6, 5.6 Hz, 1H) ppm. **^{13}C NMR** (100 MHz, $CDCl_3$) δ = 137.7, 99.7, 49.0, 29.1, 28.3, 28.1, 26.4, 20.7, 20.6, 19.4, 16.1 ppm.

HRMS (ESI, *m*/*z*): calcd for $(C_{12}H_{17}F_3O_3S)^+$ $[M+MeCN]^+$: 339.1116; found: 339.1120.

$[\alpha]_D^{23}$ = +11.95 (c = 0.06, $CHCl_3$).

(1*R*,5*R*,7*R*)-3-iodo-5,8,8-trimethylbicyclo[5.1.0]oct-2-ene (372)

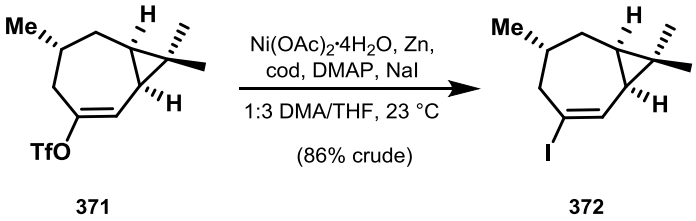

371 372

A Schlenk flask was charged with $Ni(OAc)_2$•$4H_2O$ (25.0 mg, 100 µmol, 0.1 equiv), Zn (13.2 mg, 201 µmol, 0.2 equiv), NaI (754 mg, 603 µmol, 6 equiv) and COD (2.00 µL, 201 µmol, 0.2 equiv).

Anhydrous dimethylacetamide (1.33 mL) and tetrahydrofuran (2.67 mL) were added (0.25 M overall), resulting in a color change to bright yellow. Enol triflate **371** (300 mg, 1.01 mmol, 1 equiv) was added and the resulting reaction mixture was stirred at ambient temperature. After 14 h, the solution was diluted with saturated aqueous ammonium chloride solution. The layers were separated and the aqueous layer was extracted with diethyl ether. The combined organic layers were washed with saturated aqueous sodium chloride solution, the washed solution was dried over magnesium sulfate and the dried solution was filtered. The filtrate was concentrated. The crude product **372** was obtained as volatile colorless oil (85% crude) and was used in the next step without further purification.

(1*R*,3*R*,6*R*,*Z*)-3,6-dimethyl-7-((triisopropylsilyl)oxy)-1-((1*S*,5*R*,7*R*)-5,8,8-trimethylbicyclo[5.1.0]oct-2-en-3-yl)hept-4-en-1-ol (364) and (1*S*,3*R*,6*R*,*Z*)-3,6-dimethyl-7-((triisopropylsilyl)oxy)-1-((1*S*,5*R*,7*R*)-5,8,8-trimethylbicyclo[5.1.0]oct-2-en-3-yl)hept-4-en-1-ol (364a)

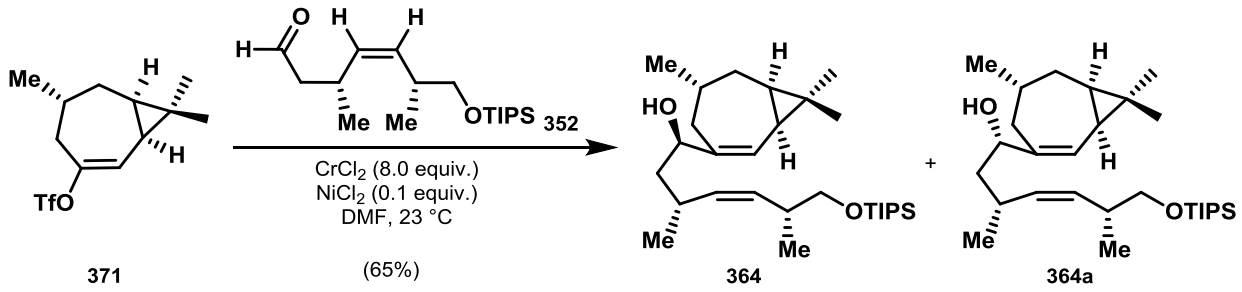

Vinyl triflate **371** (200 mg, 669 µmol, 1 equiv) and side chain **352** (25.0 mg, 335 µmol, 0.1 equiv) were dissolved in degassed dimethylsulfoxide (830 µL). The solution was added to a mixture of $CrCl_2$ (329 mg, 5.35 mmol, 8 equiv) and $NiCl_2$ (430 µg, 66.9 µmol, 0.1 equiv) in degassed dimethylsulfoxide (1.67 µL) and the resulting reaction mixture was stirred at ambient temperature. After 24 h, the reaction was diluted with saturated aqueous ammonium chloride solution. The layers were separated and the aqueous layer was extracted with diethyl ether. The combined organic layers were washed with saturated aqueous sodium chloride solution, the washed solution was dried over magnesium sulfate and the dried solution was filtered. The filtrate was concentrated. The crude product was purified by flash column chromatography on silica gel (5% ethyl acetate in petroleum ether) to afford a 1:1 mixture of both isomers **364** and **364a** (201 mg, 65%) as a colorless oil.

364:

TLC (10% ethyl acetate in petroleum ether): R_f = 0.54 (CAM).

IR (Diamond-ATR, neat) $\tilde{\nu}_{max}$: 3369, 2954, 2925, 2866, 2160, 1459, 1378, 1104, 1066, 1015 cm^{-1}.

^{1}H NMR (400 MHz, $CDCl_3$) δ = 5.38 (s, 1H), 5.13 (qd, *J* = 10.9, 9.0 Hz, 2H), 3.98 (dd, *J* = 9.0, 4.4 Hz, 1H), 3.52 (dd, *J* = 9.3, 5.8 Hz, 1H), 3.42 (dd, *J* = 9.4, 7.1 Hz, 1H), 2.74 – 2.55 (m, 2H), 2.17 (dt, *J* = 24.4, 13.0 Hz, 1H), 2.05 (dd, *J* = 13.3, 6.0 Hz, 1H), 1.79 – 1.63 (m, 1H), 1.54 – 1.47 (m, 2H), 1.25 (s, 3H), 1.06 – 1.04 (m, 26H), 0.99 (d, *J* = 4.7 Hz, 3H), 0.96 (d, *J* = 1.8 Hz, 3H), 0.93 (s, 3H), 0.71 – 0.63 (m, 1H) ppm. **^{13}C NMR** (100 MHz, $CDCl_3$) δ = 144.2, 136.4, 132.1, 121.9, 75.8, 68.5, 43.3, 35.6, 33.1, 29.9, 28.0, 24.9, 22.3, 22.0, 20.2, 18.2, 17.7, 16.1, 12.0 ppm.

HRMS (ESI, *m*/*z*): calcd for $(C_{29}H_{54}O_2Si)^+$ $[M+MeCN+H]^+$: 503.4237; found: 504.4236.

$[\alpha]_D^{24}$ = –31.7 (c = 0.01, $CHCl_3$).

364a:

TLC (10% ethyl acetate in petroleum ether): R_f = 0.45 (CAM).

IR (Diamond-ATR, neat) $\tilde{\nu}_{max}$: 3369, 2954, 2925, 2866, 2160, 1459, 1378, 1104, 1066, 1015 cm^{-1}.

^{1}H NMR (400 MHz, $CDCl_3$) δ = 5.38 (s, 1H), 5.22 (dd, *J* = 20.6, 10.6 Hz, 1H), 5.13 (dd, *J* = 20.4, 9.5 Hz, 1H), 4.02 (t, *J* = 6.8 Hz, 1H), 3.52 (dd, *J* = 9.4, 5.7 Hz, 1H), 3.41 (dd, *J* = 9.5, 7.54 Hz, 1H), 2.67 – 2.58 (m, 1H), 2.55 – 2.45 (m, 1H), 2.21 (dt, *J* = 24.4, 13.0 Hz, 1H), 1.94 (dd, *J* = 13.3, 6.0 Hz, 1H), 1.79 – 1.66 (m, 1H), 1.54 – 1.49 (m, 2H), 1.45 – 1.38 (m, 1H), 1.25 (s, 3H), 1.24 – 1.18 (m, 2H), 1.10 – 1.07 (m, 1H), 1.05 (s, 21H), 1.04 – 1.03 (m, 2H), 0.98 (d, *J* = 2.75 Hz, 3H), 0.95 (s, 3H), 0.69 – 0.63 (m, 1H) ppm. **^{13}C NMR** (100 MHz, $CDCl_3$) δ = 144.3, 136.4, 132.1, 121.9, 75.8, 68.5, 43.3, 35.6, 33.1, 29.9, 28.0, 24.9, 22.3, 22.0, 20.2, 18.2, 17.7, 16.1, 12.1 ppm.

HRMS (ESI, *m*/*z*): calcd for $(C_{29}H_{54}O_2Si)^+$ $[M+MeCN+H]^+$: 503.4237; found: 504.4237.

$[\alpha]_D^{23}$ = –11.9 (c = 0.015, $CHCl_3$).

(3*R*,6*R*,*Z*)-3,6-dimethyl-7-((triisopropylsilyl)oxy)-1-((1*S*,5*R*,7*R*)-5,8,8-trimethylbicyclo[5.1.0]oct-2-en-3-yl)hept-4-en-1-one (373)

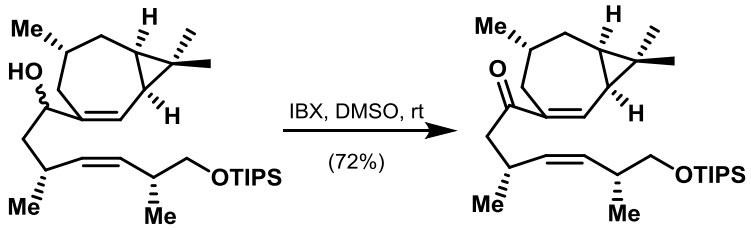

364 373

Alcohol **364** (100 mg, 216 µmol, 1 equiv) was dissolved in dimethylsulfoxide (2.16 mL) and 2-iodoxybenzoic acid (121 mg, 432 µmol, 2 equiv) was added. The resulting reaction mixture was stirred for 1 h at ambient temperature. Subsequently, diethyl ether was added and the suspension was filtered through a short plug of Celite. The filter cake was rinsed with diethyl ether and the filtrate was concentrated. The crude product was purified by flash column chromatography on silica gel (5% ethyl acetate in petroleum ether) to afford **373** (71.6 mg, 72%) as a colorless oil.

TLC (5% ethyl acetate in petroleum ether): R_f = 0.48 (CAM, UV).

IR (Diamond-ATR, neat) $\tilde{\nu}_{max}$: 2925, 1865, 1729, 1667, 1615, 1459, 1378, 1247, 1178, 1103, 1067, 1014 cm^{-1}.

^{1}H NMR (400 MHz, $CDCl_3$) δ = 6.61 (d, *J* = 2.2 Hz, 1H), 5.15 (t, *J* = 10.7, 9.6, 1H), 5.09 (t, *J* = 10.7, 9.7, 1H), 3.51 (dd, *J* = 9.4, 6.0 Hz, 1H), 3.43 (dd, *J* = 9.4, 6.9 Hz, 1H), 3.01 (dq, *J* = 9.0, 6.7 Hz, 1H), 2.68 (dd, *J* = 13.2, 5.9 Hz, 1H), 2.66 – 2.61 (m, 1H), 2.56 (dd, *J* = 7.0, 2.0 Hz, 2H), 2.04 (t, *J* = 12.7, 10.9, 1H), 1.74-1.69 (m, 1H), 1.29-1.28 (m, 1H), 1.13 (s, 3H), 1.09 – 1.07 (m, 1H), 1.07 – 1.02 (m, 24H), 0.99 (s, 3H), 0.97 (d, *J* = 6.7 Hz, 3H), 0.94 (d, *J* = 6.7 Hz, 3H), 0.88 – 0.87 (m, 1H), 0.83-0.81 (m, 1H) ppm. **^{13}C NMR** (200 MHz, $CDCl_3$) δ = 200.7, 144.4, 139.2, 134.8, 132.2, 68.6, 45.0, 35.5, 31.1, 30.1, 29.9, 28.3, 28.2, 26.4, 22.0, 21.7, 20.8, 19.5, 18.2, 17.8, 16.2, 12.1 ppm.

HRMS (ESI, *m*/*z*): calcd for $(C_{29}H_{52}O_2Si)^+$ $[M+H]^+$: 461.3815; found: 461.3820.

$[\alpha]_D^{20}$ = –22.7 (c = 0.05, $CHCl_3$).

(*R*)-3-(1,3-dithian-2-yl)-2-methylpropan-1-ol (349)

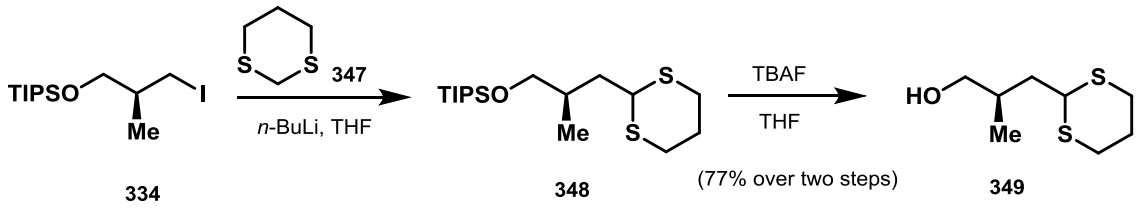

1,3-Dithiane **347** (3.70 mL, 9.25 mmol, 1.1 equiv) was dissolved in tetrahydrofuran (46.0 mL) and cooled to –78 °C. *n*-BuLi (2.5 M in hexane, 7.20 mL, 1.1 equiv) was added dropwise and the reaction was warmed to 0 °C. After 20 min, a solution of alkyl iodide **334** (3.00 g, 8.42 mmol, 1 equiv) in tetrahydrofuran (42.0 mL) was added at 0 °C. After 45 min, the reaction was diluted with saturated aqueous ammonium chloride solution and diethyl ether. The layers were separated and the aqueous layer was extracted with diethyl ether. The combined organic layers were dried over magnesium sulfate and the dried solution was filtered and the filtrate was concentrated. The product was used in the next step without further purification.

Tetrabutylammonium fluoride (1 M in THF, 10.8 mL, 10.8 mmol, 1.2 equiv) was added dropwise to a solution of to alkylated dithiane **348** (3.14 g, 9.01 mmol, 1 equiv) in tetrahydrofuran (45.0 mL) at 0 °C. After 3 h, the solution was diluted with saturated aqueous ammonium chloride solution. The layers were separated and the aqueous layer was extracted with ethyl acetate. The combined organic layers were washed with saturated aqueous sodium chloride solution, the washed solution was dried over magnesium sulfate and the dried solution was filtered. The filtrate was concentrated. The crude product was purified by flash column chromatography on silica gel (20% ethyl acetate in petroleum ether) to afford **349** (1.25 g, 77% over two steps) as a colorless oil.

TLC (25% ethyl acetate in petroleum ether): R_f = 0.42 (CAM).

IR (Diamond-ATR, neat) $\tilde{\nu}_{max}$: 3394, 2897, 1421, 1274 cm^{-1}.

^{1}H NMR (400 MHz, $CDCl_3$) δ = 4.14 (dd, *J* = 8.3, 6.5 Hz, 1H), 3.51 (d, *J* = 5.8 Hz, 2H), 2.94 – 2.78 (m, 4H), 2.17 – 2.08 (m, 1H), 2.06 – 1.95 (m, 1H), 1.93 – 1.80 (m, 2H), 1.58 (ddd, *J* = 14.2, 7.9, 6.5 Hz, 1H), 0.97 (d, *J* = 6.7 Hz, 3H) ppm. **^{13}C NMR** (100 MHz, $CDCl_3$) δ = 67.9, 45.5, 39.2, 33.0, 30.6, 30.5, 26.1, 16.8 ppm.

HRMS (ESI, *m*/*z*): calcd for $(C_8H_{16}OS_2)^+$ $[M+H]^+$: 193.0721; found: 193.0718.

$[\alpha]_D^{24}$ = +9.09 (c = 0.033, $CHCl_3$).

(*R*)-3-(1,3-dithian-2-yl)-2-methylpropanal (350)

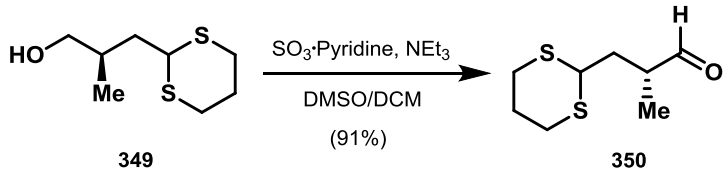

349 350

Alcohol **349** (1.37 g, 7.12 mmol, 1 equiv) was dissolved in dimethyl sulfoxide (23.7 mL) and dichloromethane (48 mL) and cooled to 0 °C. Sulfur trioxide pyridine complex (2.27 g, 14.2 mmol, 2 equiv) and triethylamine (4.00 mL, 28.5 mmol, 4 equiv) were added and the reaction was warmed to ambient temperature. After 30 min, the reaction mixture was diluted with saturated aqueous ammonium chloride solution. The layers were separated and the aqueous layer was extracted with diethyl ether. The combined organic layers were washed with saturated aqueous sodium chloride solution, the washed solution was dried over magnesium sulfate and the dried solution was filtered. The filtrate was concentrated. The crude product was purified by flash column chromatography on silica gel (25% ethyl acetate in petroleum ether) to afford **350** (1.23 g, 91%) as a colorless oil.

TLC (25% ethyl acetate in petroleum ether): R_f = 0.76 (CAM).

IR (Diamond-ATR, neat) $\tilde{\nu}_{max}$: 2901, 1720, 1421, 1275 cm^{-1}.

^{1}H NMR (400 MHz, $CDCl_3$) δ = 9.67 (d, *J* = 1.2 Hz, 1H), 4.07 (t, *J* = 7.5 Hz, 1H), 2.87 – 2.81 (m, 4H), 2.75 (qd, *J* = 7.0, 1.3 Hz, 1H), 2.25 (dt, *J* = 14.7, 6.9 Hz, 1H), 2.16 – 2.07 (m, 1H), 1.94 – 1.82 (m, 1H), 1.75 (dt, *J* = 14.1, 7.0 Hz, 1H), 1.16 (d, *J* = 7.2 Hz, 3H) ppm. **^{13}C NMR** (100 MHz, $CDCl_3$) δ = 203.6, 44.8, 43.6, 36.0, 30.1, 25.9, 13.8 ppm.

HRMS (ESI, *m*/*z*): calcd for $(C_8H_{14}OS_2)^+$ $[M]^+$: 190.0486; found: 190.0496.

$[\alpha]_D^{23}$ = +26.53 (c = 0.032, $CHCl_3$).

(((2*R*,5*R*,*Z*)-6-(1,3-dithian-2-yl)-2,5-dimethylhex-3-en-1-yl)oxy)triisopropylsilane (351)

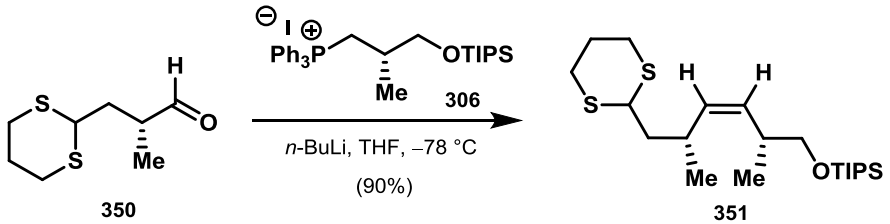

350 351

Phosphonium salt **306** (1.43 g, 2.30 mmol, 1.2 equiv) was dissolved in tetrahydrofuran (11.5 mL) and cooled to –78 °C. *n*-BuLi (2.5 M in hexane, 0.84 mL, 1.1 equiv) was added dropwise and the reaction was warmed to 0 °C. After 30 min, the solution was cooled to –78 °C and aldehyde **350** (366 mg, 1.92 mmol, 1 equiv) in tetrahydrofuran (9.40 mL) was added. After 30 min, the solution

was diluted with saturated aqueous ammonium chloride solution. The layers were separated and the aqueous layer was extracted with diethyl ether. The combined organic layers were washed with saturated aqueous sodium chloride solution, the washed solution was dried over magnesium sulfate and the dried solution was filtered. The filtrate was concentrated. The crude product was purified by flash column chromatography on silica gel (5% ethyl acetate in petroleum ether) to afford **351** (696 mg, 90%) as a colorless oil.

TLC (5% ethyl acetate in petroleum ether): R_f = 0.56 (CAM).

IR (Diamond-ATR, neat) $\tilde{\nu}_{max}$: 2942, 2864, 1461, 1102, 1014 cm^{-1}.

^{1}H NMR (400 MHz, $CDCl_3$) δ = 5.27 (t, *J* = 20.2, 10.7, 1H), 5.07 (t, *J* = 20.7, 10.3, 1H), 3.95 (dd, *J* = 9.6, 5.0 Hz, 1H), 3.66 (dd, *J* = 9.3, 4.9 Hz, 1H), 3.44 (dd, *J* = 9.3, 7.3 Hz, 1H), 2.91 – 2.76 (m, 4H), 2.14 – 2.04 (m, 1H), 1.92 – 1.79 (m, 1H), 1.71 (ddd, *J* = 13.9, 9.7, 5.1 Hz, 1H), 1.60 (td, *J* = 9.3, 4.7 Hz, 1H), 1.08 – 1.04 (m, 20H), 1.00 (d, *J* = 6.7 Hz, 3H), 0.97 (d, *J* = 6.7 Hz, 3H) ppm. **^{13}C NMR** (100 MHz, $CDCl_3$) δ = 134.3, 133.2, 68.4, 45.5, 42.9, 35.2, 30.6, 30.2, 29.4, 26.3, 21.7, 18.2, 18.1, 12.1 ppm.

HRMS (ESI, *m/z*): calcd for $(C_{21}H_{42}OS_2Si)^+$ $[M+H]^+$: 403.2525; found: 403.2530.

$[\alpha]_D^{24}$ = –23.08 (c = 0.035, $CHCl_3$).

(3*S*,6*S*,*Z*)-3,6-dimethyl-7-((triisopropylsilyl)oxy)hept-4-enal (352)

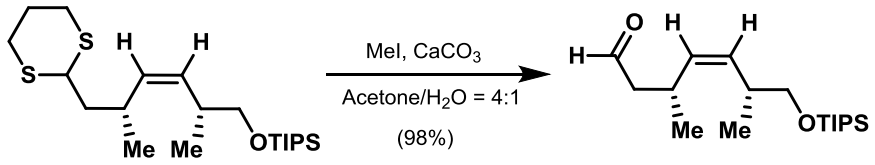

351 352

Olefin **351** (774 mg, 1.92 mmol, 1 equiv), MeI (2.40 mL, 38.4 mmol, 20 equiv) and $CaCO_3$ (2.88 g, 28.8 mmol, 15 equiv) were dissolved in acetone (28.5 mL) and water (9.5 mL). The resulting reaction mixture was stirred at 60 °C. After 3 h, the mixture was diluted with saturated aqueous ammonium hydroxide solution and diethyl ether. The layers were separated and the aqueous layer was extracted with diethyl ether. The combined organic layers were dried over magnesium sulfate and the dried solution was filtered. The filtrate was concentrated. The crude product was purified by flash column chromatography on silica gel (5% ethyl acetate in petroleum ether) to afford **352** (588 mg, 98%) as a colorless oil.

TLC (5% ethyl acetate in petroleum ether): R_f = 0.80 (CAM).

IR (Diamond-ATR, neat) $\tilde{\nu}_{max}$: 2943, 2866, 1727, 1462, 1103, 1013 cm^{-1}.

^{1}H NMR (400 MHz, $CDCl_3$) δ = 9.70 (t, *J* = 2.3 Hz, 1H), 5.21 (dd, *J* = 6.7, 2.2 Hz, 2H), 3.54 (dd, *J* = 9.5, 6.0 Hz, 1H), 3.47 (dd, *J* = 9.4, 6.7 Hz, 1H), 3.07 (td, *J* = 6.8, 2.1 Hz, 1H), 2.68 (td, *J* = 6.5, 2.2 Hz, 1H), 2.37 (dt, *J* = 6.9, 1.9 Hz, 2H), 1.07-1.04 (m, 21H), 1.03 (d, *J* = 3.2 Hz, 3H), 0.99 (d, *J* = 6.7 Hz, 3H) ppm. **^{13}C NMR** (100 MHz, $CDCl_3$) δ = 202.6, 133.8, 133.0, 68.3, 51.2, 35.5, 27.5, 21.5, 18.2, 17.9, 12.1 ppm.

HRMS (ESI, *m*/*z*): calcd for $(C_{18}H_{36}O_2Si)^+$ $[M+MeCN]^+$: 353.2750; found: 353.2755.

$[\alpha]_D^{24}$ = –44.93 (c = 0.029, $CHCl_3$).

2.2.1 ^{1}H and ^{13}C NMR Spectra

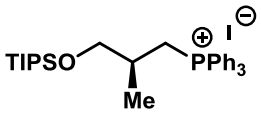

305

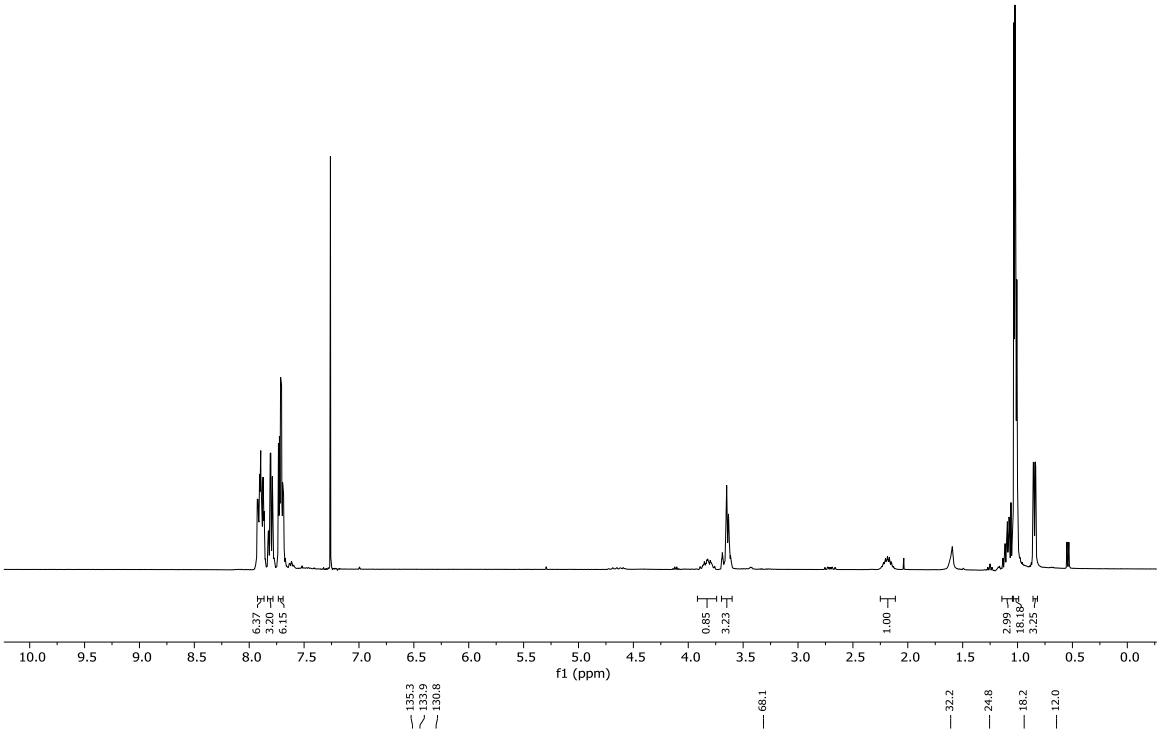

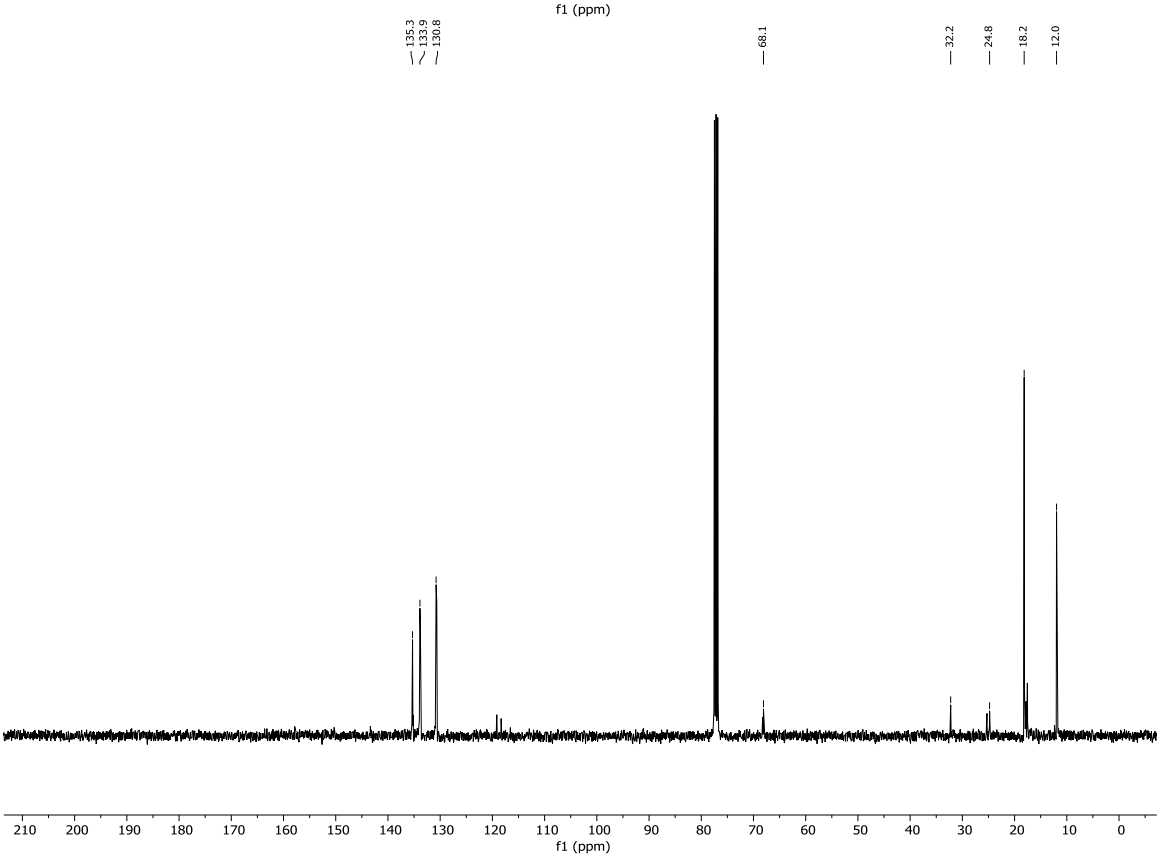

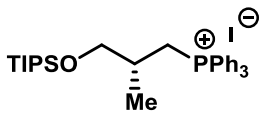
TIPSO
PPh3
I
Me

280

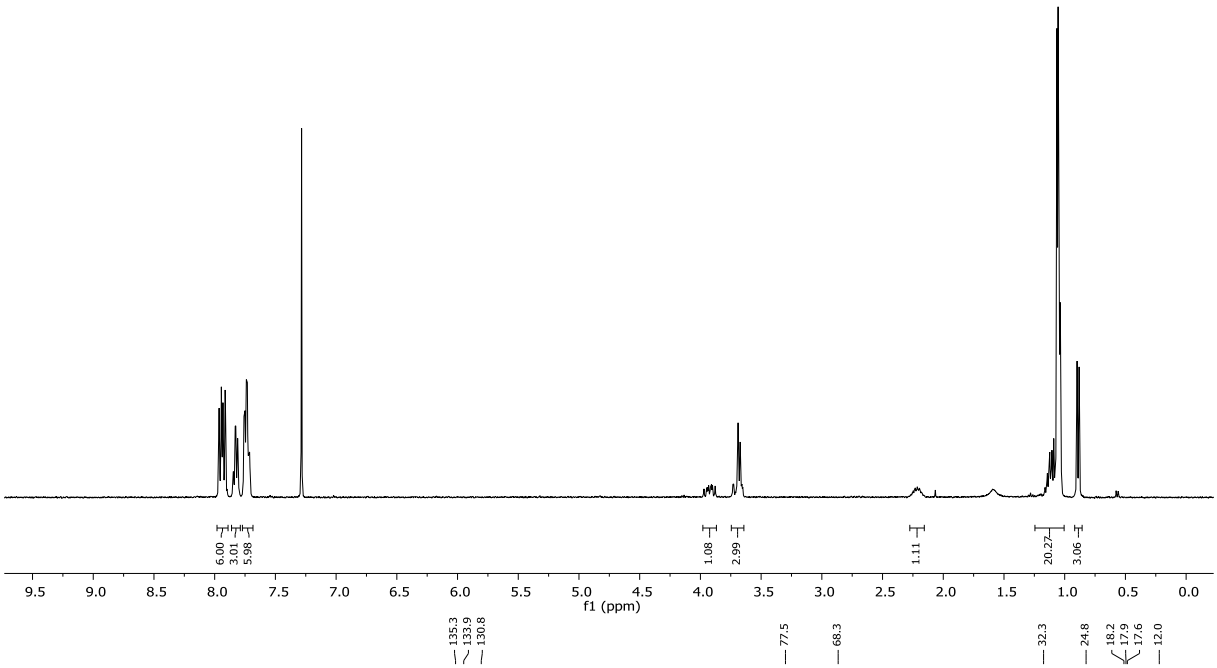
6.00
3.01
5.98
1.08
2.99
1.11
20.27
3.06
f1 (ppm)
135.3
133.9
130.8
77.5
68.3
32.3
24.8
18.2
17.9
17.6
12.0

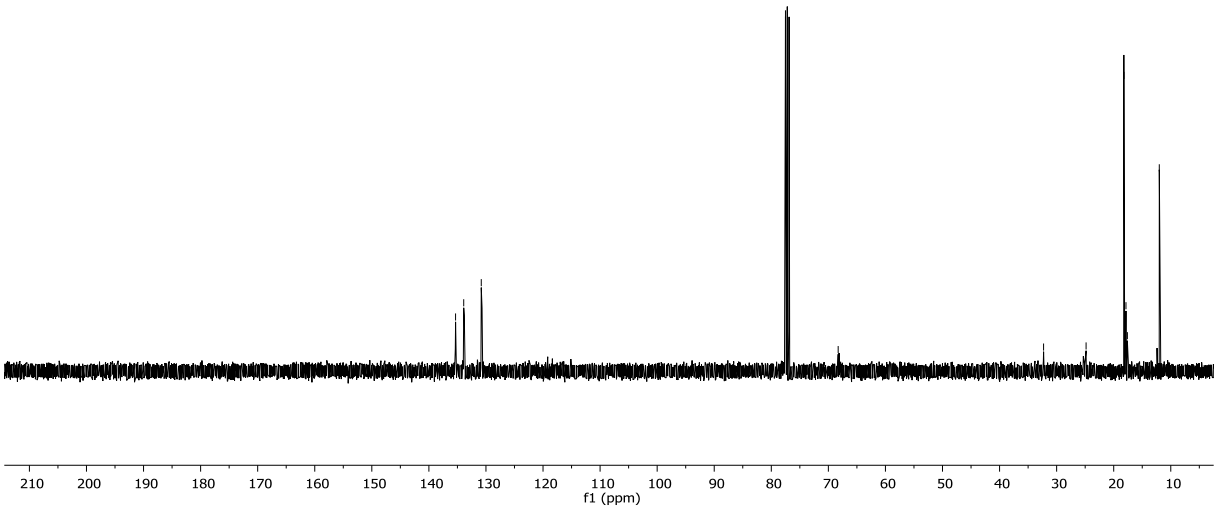
f1 (ppm)

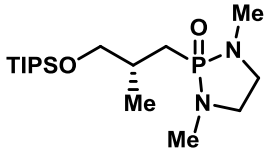
TIPSO
Me
O
P
N
Me
N
Me

295

0.95
0.96
1.88
1.92
6.00
0.93
0.93
0.91
21.00
3.41
9.5 9.0 8.5 8.0 7.5 7.0 6.5 6.0 5.5 5.0 4.5 4.0 3.5 3.0 2.5 2.0 1.5 1.0 0.5 0.0
f1 (ppm)

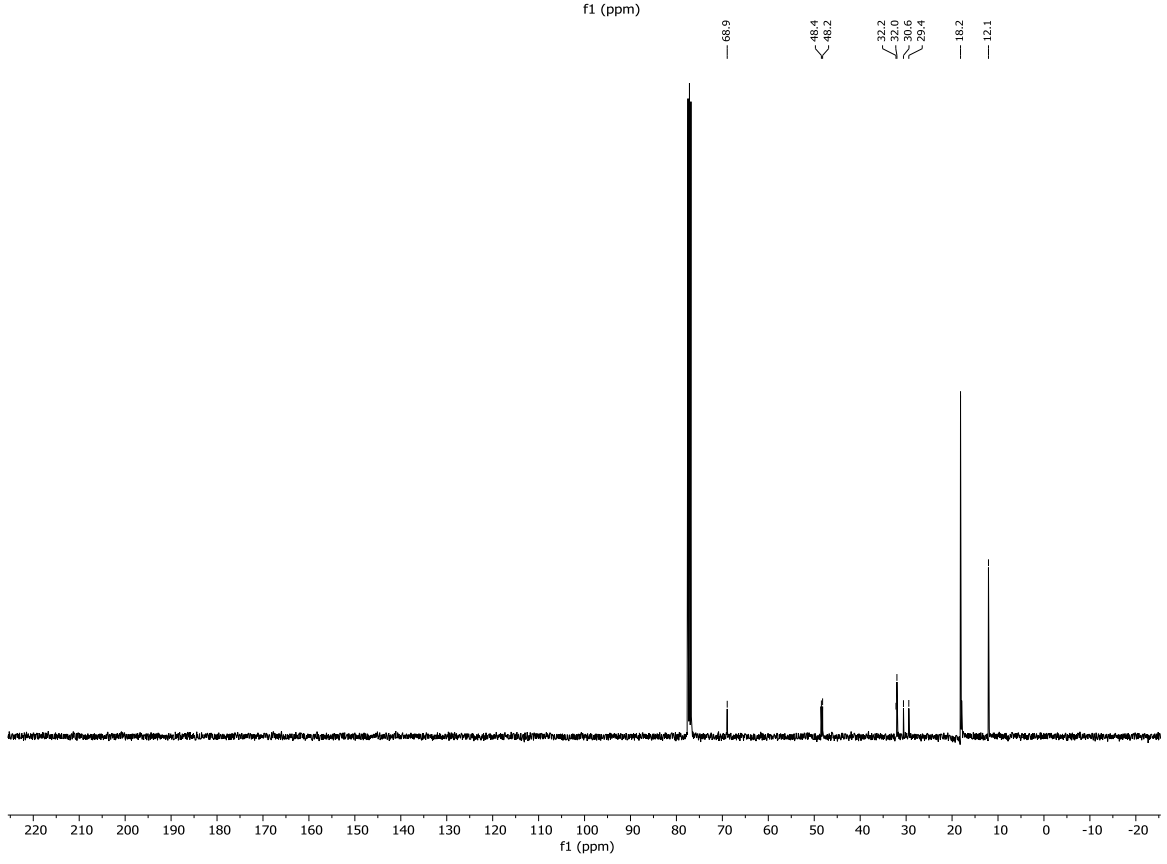
68.9
48.4
48.2
32.2
32.0
30.6
29.4
18.2
12.1
220 210 200 190 180 170 160 150 140 130 120 110 100 90 80 70 60 50 40 30 20 10 0 -10 -20
f1 (ppm)

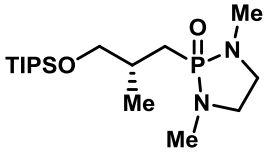
TIPSO
O
P
N
Me
Me
N
Me

295, ^{31}P-NMR

42.2
200
180
160
140
120
100
80
60
40
20
0
-20
-40
-60
-80
-100
-120
-140
-160
-180
-20
f1 (ppm)

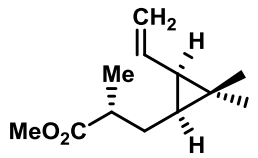
CH2
H
Me
MeO2C
H

281

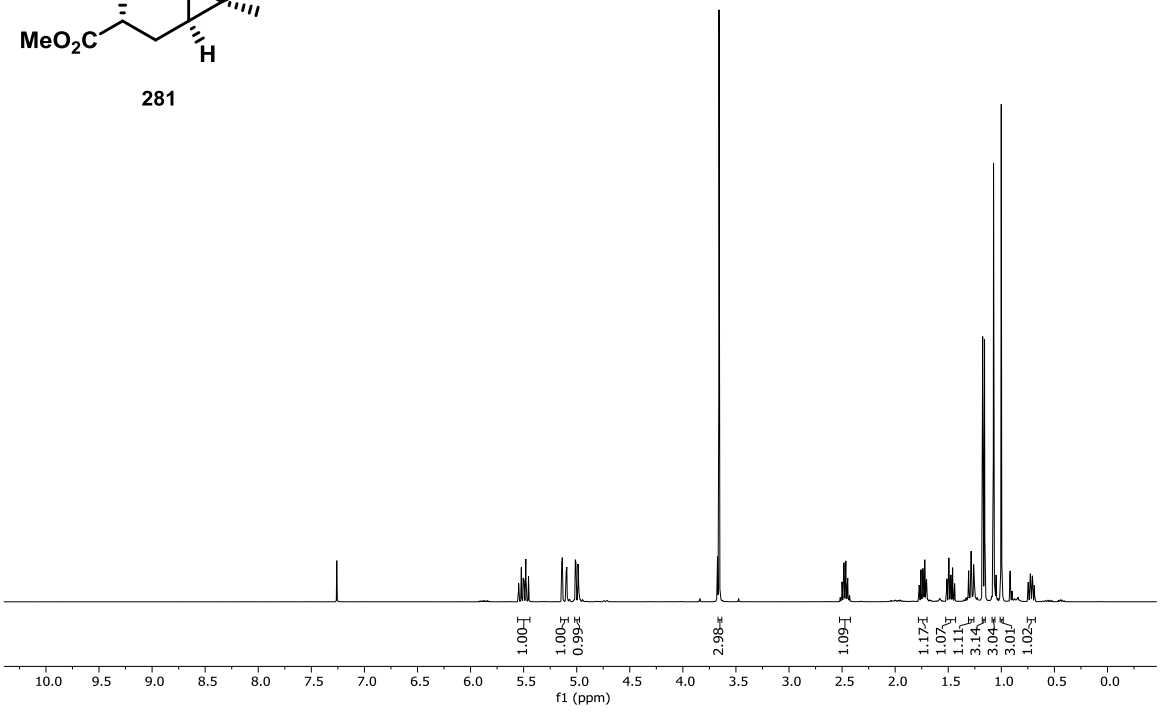
1.00
1.00
0.99
2.98
1.09
1.17
1.07
1.11
3.14
3.04
3.01
1.02
10.0 9.5 9.0 8.5 8.0 7.5 7.0 6.5 6.0 5.5 5.0 4.5 4.0 3.5 3.0 2.5 2.0 1.5 1.0 0.5 0.0
f1 (ppm)

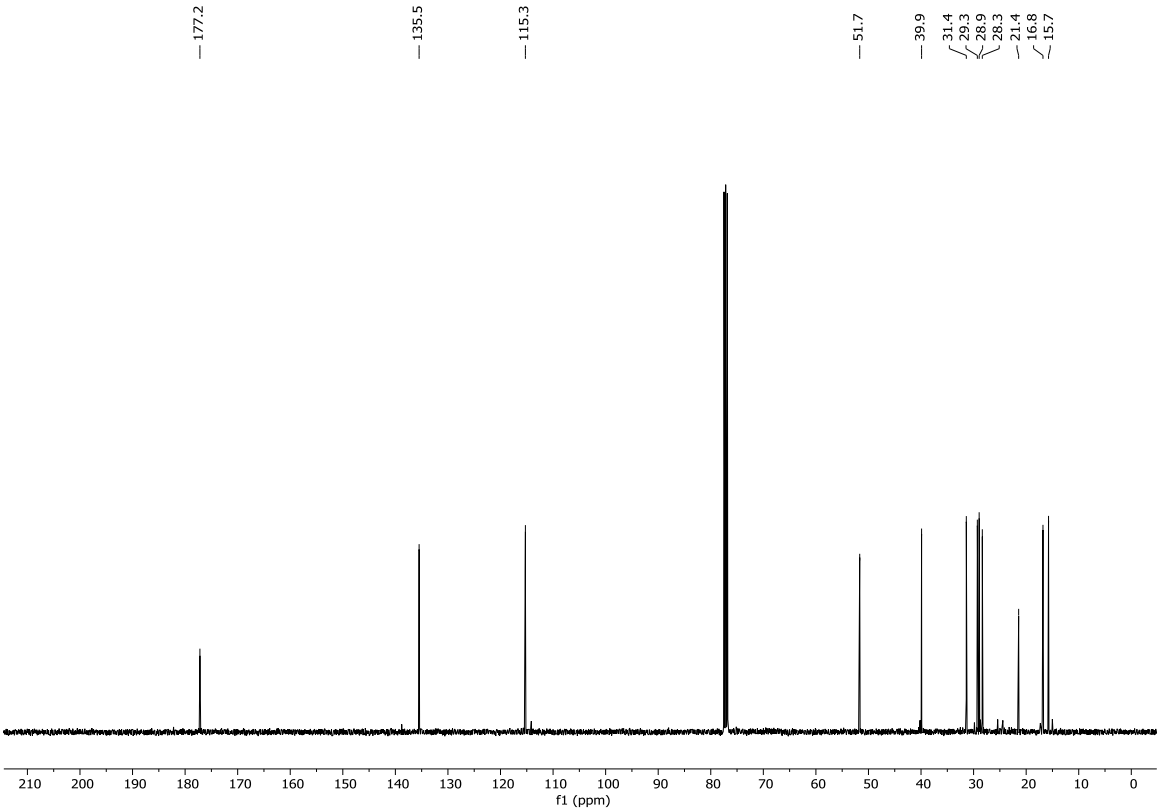
177.2
135.5
115.3
51.7
39.9
31.4
29.3
28.9
28.3
21.4
16.8
15.7
210 200 190 180 170 160 150 140 130 120 110 100 90 80 70 60 50 40 30 20 10 0
f1 (ppm)

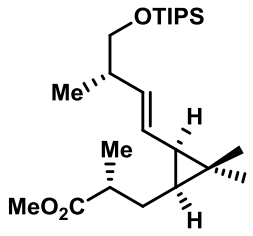
OTIPS
Me
H
Me
MeO2C
H

278

1.09
1.07
3.00
1.00
1.00
1.06
1.17
1.03
1.94
1.55
2.97
1.10
21.16
3.12
3.09
1.14
f1 (ppm)
177.4
134.7
126.1
68.9
51.7
40.3
39.9
30.2
29.3
29.0
27.6
20.7
18.2
17.1
16.7
15.8
12.1

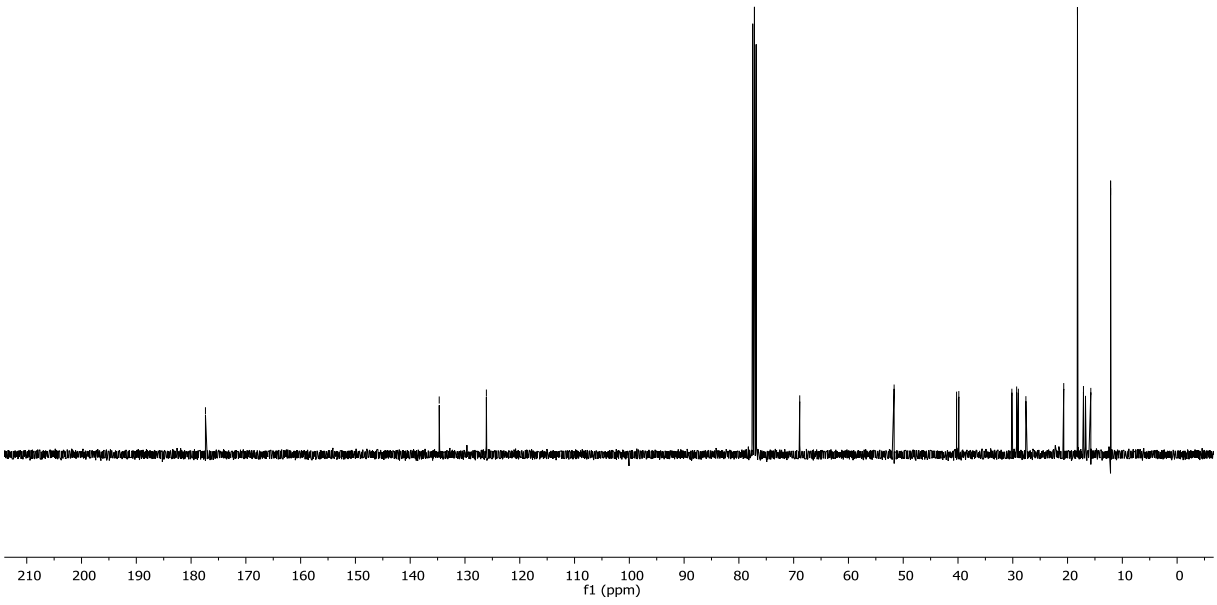
f1 (ppm)

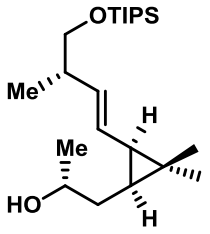
OTIPS
Me
H
Me
HO
H

296

1.00
1.01
1.16
1.13
1.04
1.11
2.20
2.93
1.18
20.86
3.36
3.13
3.06
0.89
10.0 9.5 9.0 8.5 8.0 7.5 7.0 6.5 6.0 5.5 5.0 4.5 4.0 3.5 3.0 2.5 2.0 1.5 1.0 0.5 0.0
f1 (ppm)
134.7
126.6
100.1
68.9
68.1
40.3
36.9
30.1
29.0
28.4
28.4
20.6
18.2
17.2
17.0
15.9
12.2

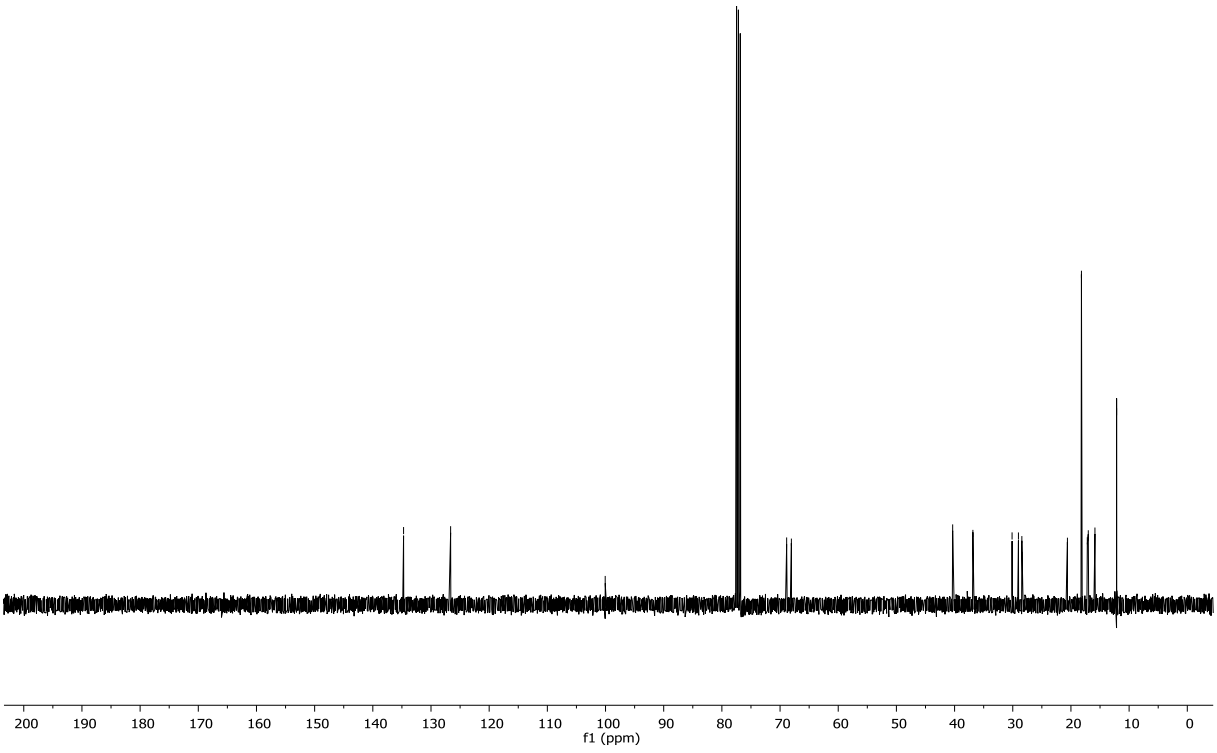
200 190 180 170 160 150 140 130 120 110 100 90 80 70 60 50 40 30 20 10 0
f1 (ppm)

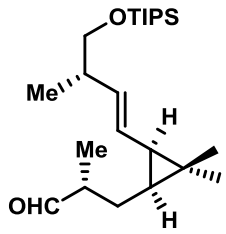
OTIPS
Me
H
Me
OHC
H

260

1.00
1.13
1.15
1.13
1.11
2.37
1.16
1.83
1.87
3.41
21.61
6.36
1.12
11.0 10.5 10.0 9.5 9.0 8.5 8.0 7.5 7.0 6.5 6.0 5.5 5.0 4.5 4.0 3.5 3.0 2.5 2.0 1.5 1.0 0.5 0.0
f1 (ppm)
205.5
135.3
125.7
68.8
47.1
40.3
30.1
28.9
27.4
26.1
20.7
18.2
17.1
15.7
13.4
12.1
220 210 200 190 180 170 160 150 140 130 120 110 100 90 80 70 60 50 40 30 20 10 0
f1 (ppm)

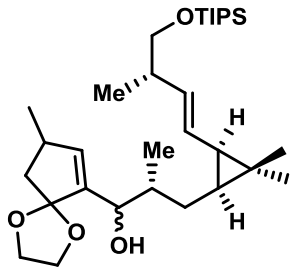
OTIPS
Me
H
Me
O
O
OH
H

297

1.00
0.93
1.01
0.56
4.58
1.05
1.01
0.95
2.60
1.37
1.98
0.60
2.50
5.02
20.83
3.32
3.14
1.84
1.82
1.04
10.0 9.5 9.0 8.5 8.0 7.5 7.0 6.5 6.0 5.5 5.0 4.5 4.0 3.5 3.0 2.5 2.0 1.5 1.0 0.5 0.0
f1 (ppm)

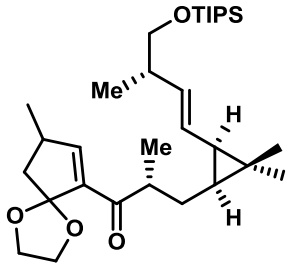
OTIPS
Me
H
Me
H
O
O
O

259

1.00
0.95
0.94
2.13
2.18
0.93
1.08
1.07
1.10
1.08
0.94
1.14
0.97
3.10
3.08
24.14
6.06
1.00
10.0 9.5 9.0 8.5 8.0 7.5 7.0 6.5 6.0 5.5 5.0 4.5 4.0 3.5 3.0 2.5 2.0 1.5 1.0 0.5 0.0
f1 (ppm)

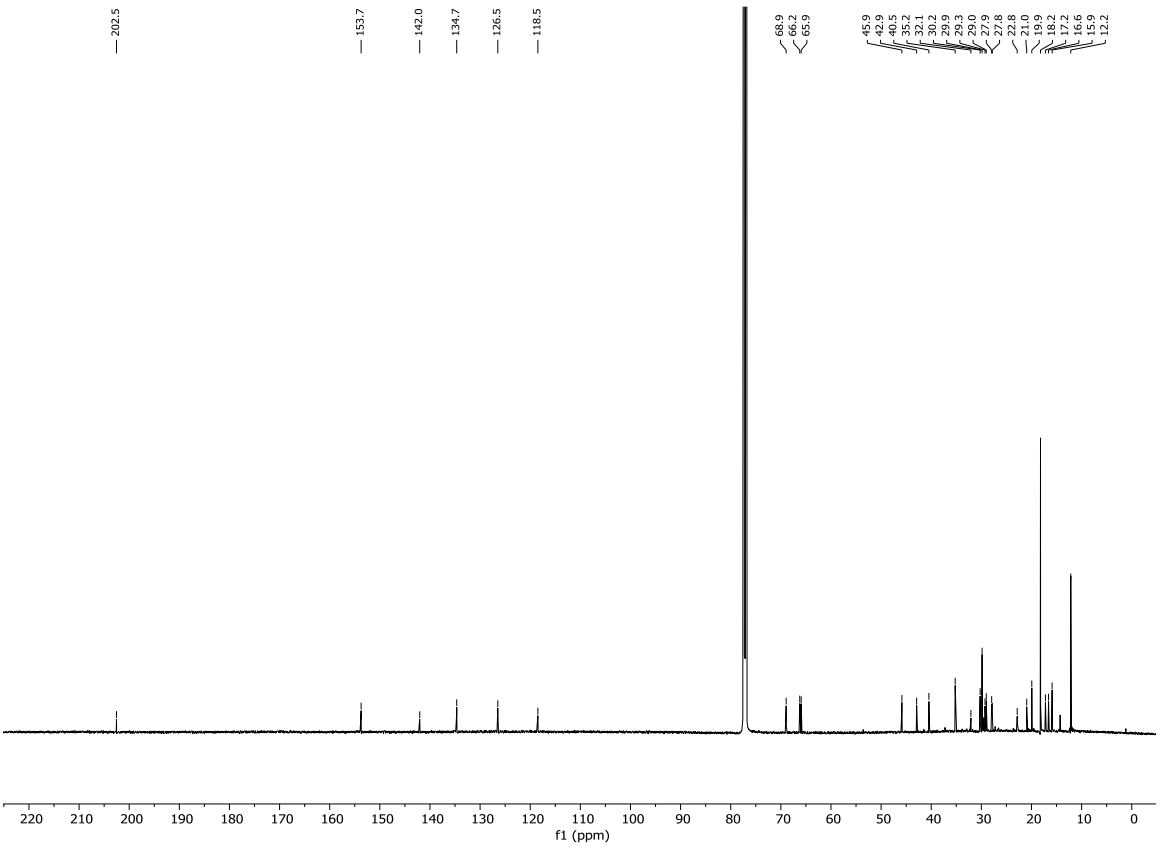
202.5
153.7
142.0
134.7
126.5
118.5
68.9
66.2
65.9
45.9
42.9
40.5
35.2
32.1
30.2
29.9
29.3
29.0
27.9
27.8
22.8
21.0
19.9
18.2
17.2
16.6
15.9
12.2
220 210 200 190 180 170 160 150 140 130 120 110 100 90 80 70 60 50 40 30 20 10 0
f1 (ppm)

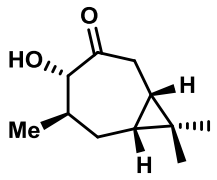
O
HO
H
Me
H

313

1.00
1.00
1.07
1.07
2.11
3.11
1.16
3.04
0.95
3.10
0.51
1.12
10.0 9.5 9.0 8.5 8.0 7.5 7.0 6.5 6.0 5.5 5.0 4.5 4.0 3.5 3.0 2.5 2.0 1.5 1.0 0.5 0.0
f1 (ppm)

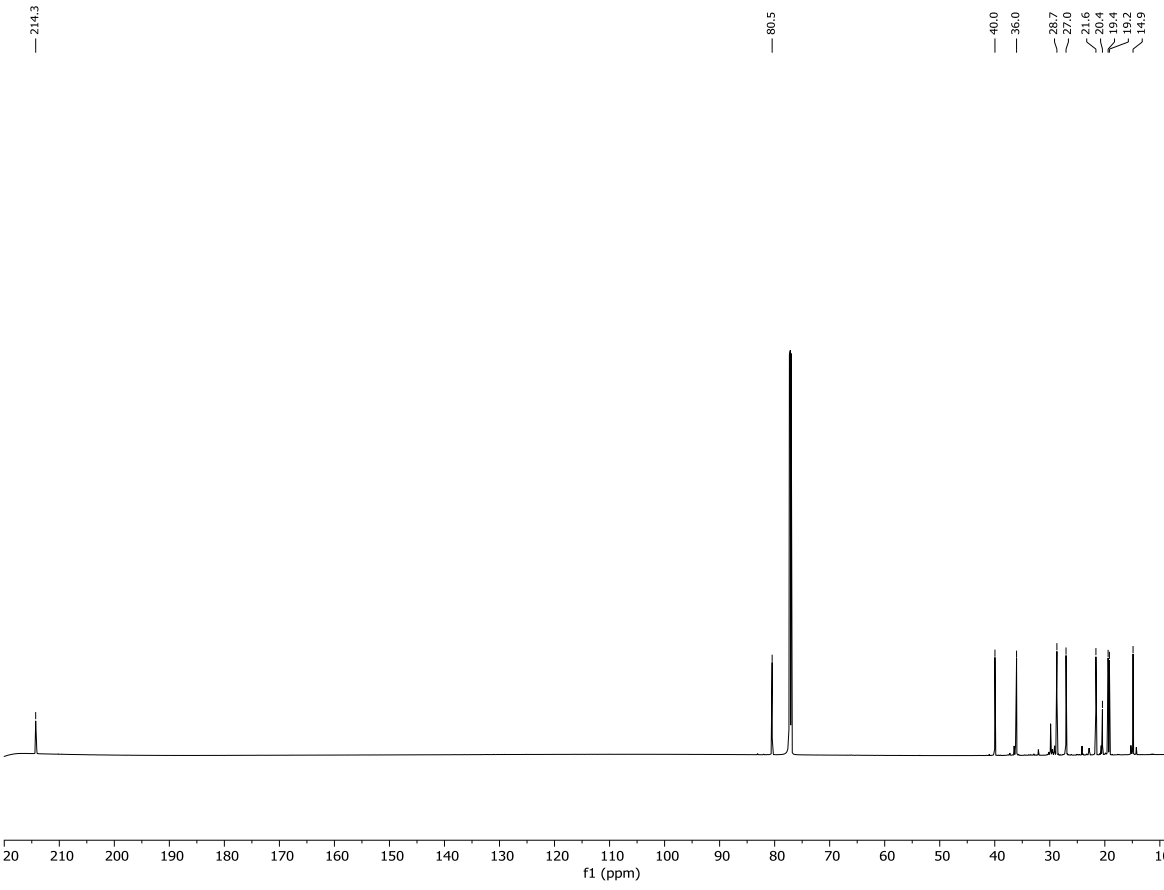
214.3
80.5
40.0
36.0
28.7
27.0
21.6
20.4
19.4
19.2
14.9
20 210 200 190 180 170 160 150 140 130 120 110 100 90 80 70 60 50 40 30 20 10
f1 (ppm)

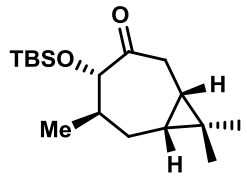
O
TBSO
H
Me
H

315

1.00
0.97
0.97
0.98
0.80
0.96
2.91
3.04
3.03
9.15
1.19
1.04
3.26
3.17
10.0 9.5 9.0 8.5 8.0 7.5 7.0 6.5 6.0 5.5 5.0 4.5 4.0 3.5 3.0 2.5 2.0 1.5 1.0 0.5 0.0
f1 (ppm)

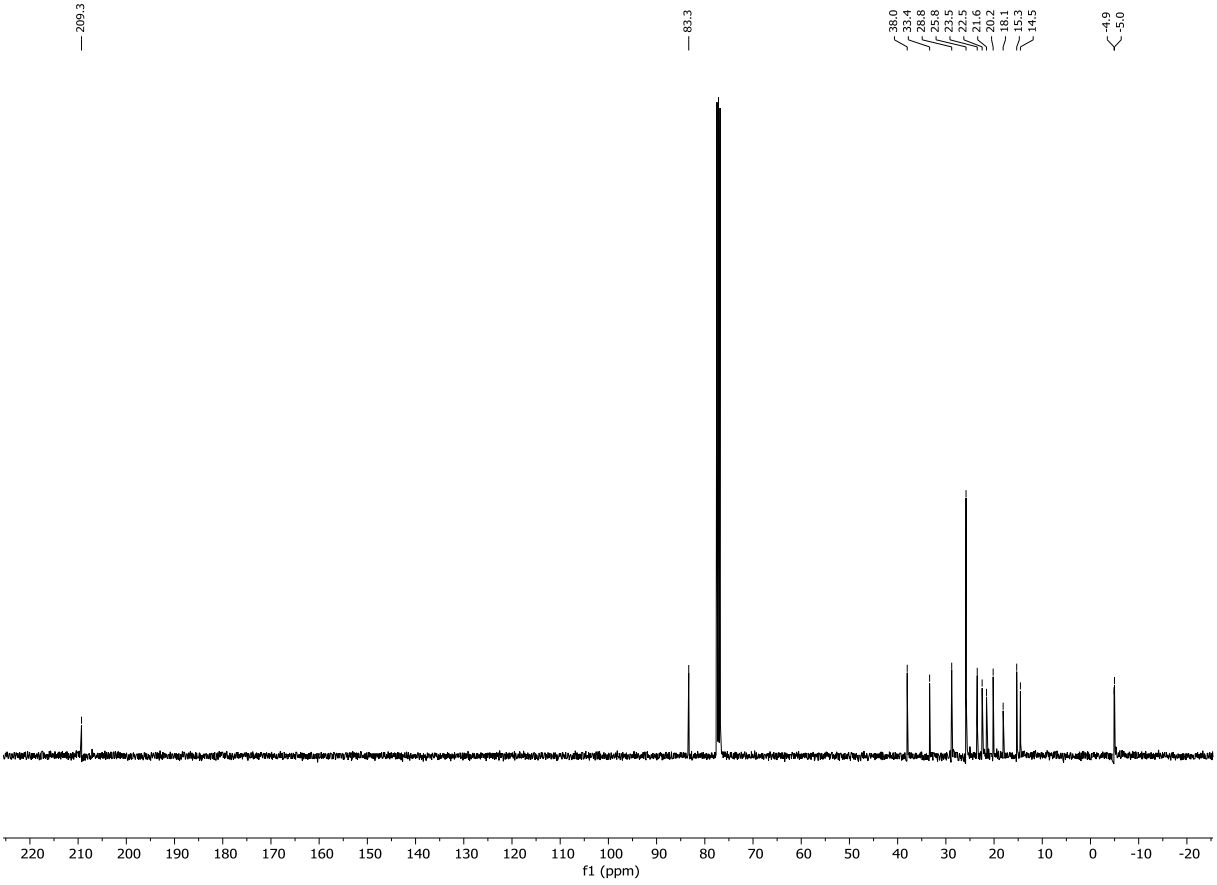
209.3
83.3
38.0
33.4
28.8
25.8
23.5
22.5
21.6
20.2
18.1
15.3
14.5
-4.9
-5.0
220 210 200 190 180 170 160 150 140 130 120 110 100 90 80 70 60 50 40 30 20 10 0 -10 -20
f1 (ppm)

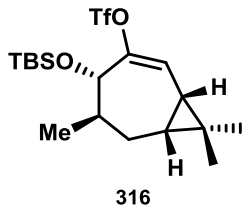
TfO
TBSO
H
Me
H

316

1.00
1.05
2.11
1.17
3.05
3.18
2.08
3.03
9.09
3.06
3.08
10.0 9.5 9.0 8.5 8.0 7.5 7.0 6.5 6.0 5.5 5.0 4.5 4.0 3.5 3.0 2.5 2.0 1.5 1.0 0.5 0.0
f1 (ppm)
149.8
120.8
76.1
35.6
28.1
25.8
23.5
23.4
23.3
21.4
18.2
16.2
15.9
-4.8
-4.9

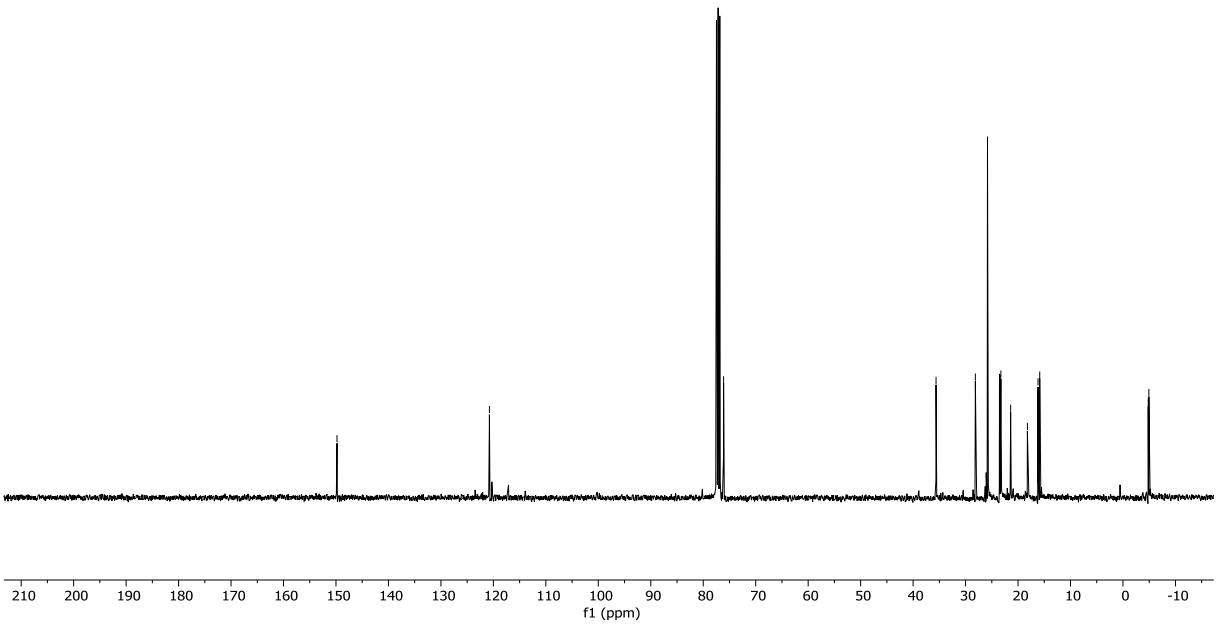
210 200 190 180 170 160 150 140 130 120 110 100 90 80 70 60 50 40 30 20 10 0 -10
f1 (ppm)

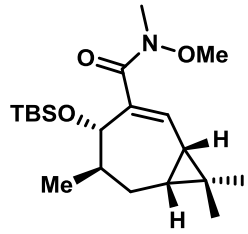
O
N
OMe
TBSO
H
Me
H

317

1.00
1.02
3.00
3.00
1.11
1.19
1.08
3.25
3.02
3.06
9.11
3.04
3.02
10.0 9.5 9.0 8.5 8.0 7.5 7.0 6.5 6.0 5.5 5.0 4.5 4.0 3.5 3.0 2.5 2.0 1.5 1.0 0.5 0.0
f1 (ppm)

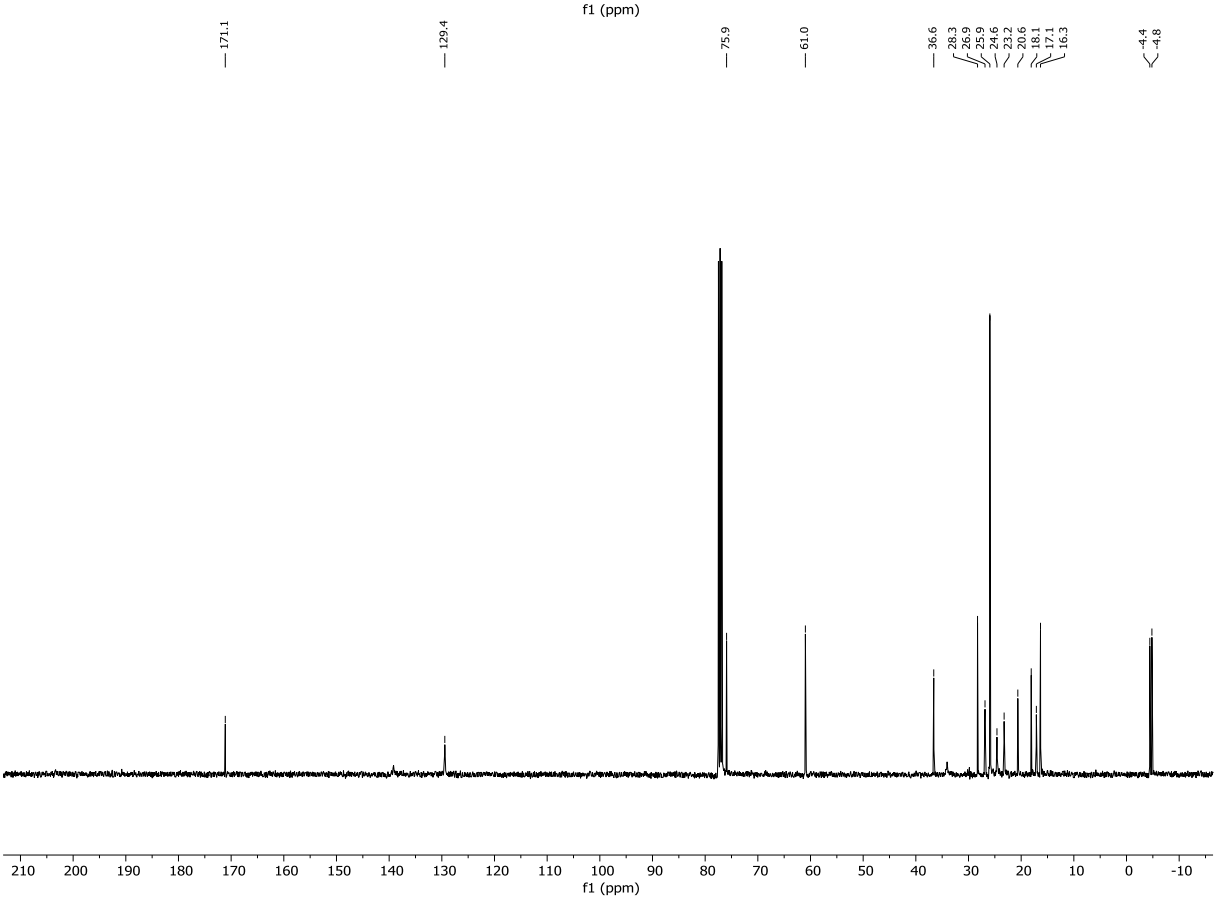
171.1
129.4
75.9
61.0
36.6
28.3
26.9
25.9
24.6
23.2
20.6
18.1
17.1
16.3
-4.4
-4.8
210 200 190 180 170 160 150 140 130 120 110 100 90 80 70 60 50 40 30 20 10 0 -10
f1 (ppm)

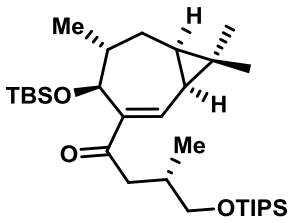
Me
H
TBSO
H
O
Me
OTIPS

343

1.00
0.92
1.42
1.14
0.94
0.95
0.89
2.17
0.89
1.65
2.91
23.38
3.04
2.74
3.05
9.65
3.45
2.96
10.0 9.5 9.0 8.5 8.0 7.5 7.0 6.5 6.0 5.5 5.0 4.5 4.0 3.5 3.0 2.5 2.0 1.5 1.0 0.5 0.0 -0.5
f1 (ppm)

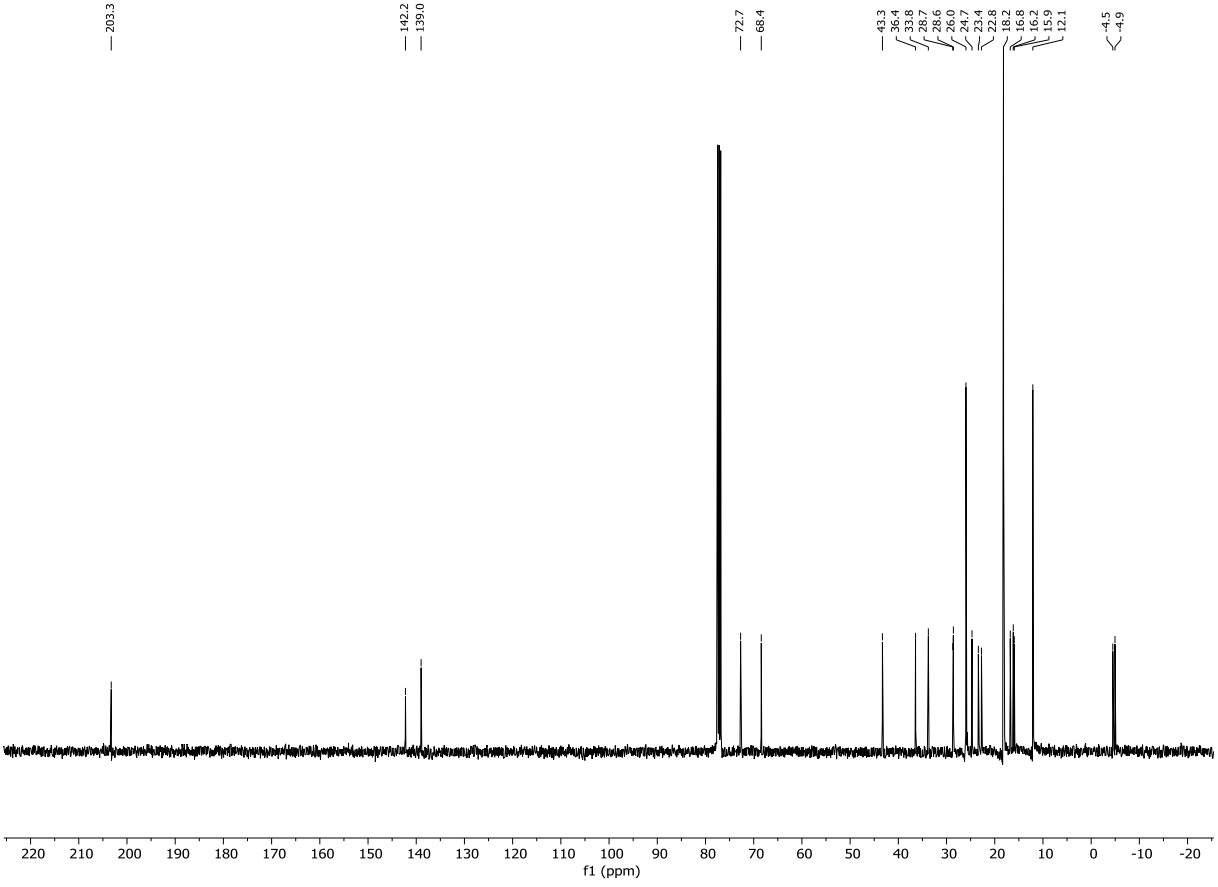
203.3
142.2
139.0
72.7
68.4
43.3
36.4
33.8
28.7
28.6
26.0
24.7
23.4
22.8
18.2
16.8
16.2
15.9
12.1
-4.5
-4.9
220 210 200 190 180 170 160 150 140 130 120 110 100 90 80 70 60 50 40 30 20 10 0 -10 -20
f1 (ppm)

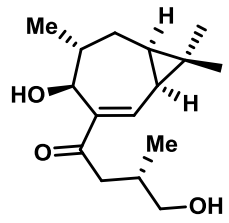
Me
H
HO
H
O
Me
OH

344

1.00
1.02
0.90
1.01
1.04
1.02
1.00
1.05
0.74
1.15
1.09
2.20
3.09
3.07
3.04
3.04
0.90
10.0 9.5 9.0 8.5 8.0 7.5 7.0 6.5 6.0 5.5 5.0 4.5 4.0 3.5 3.0 2.5 2.0 1.5 1.0 0.5 0.0
f1 (ppm)

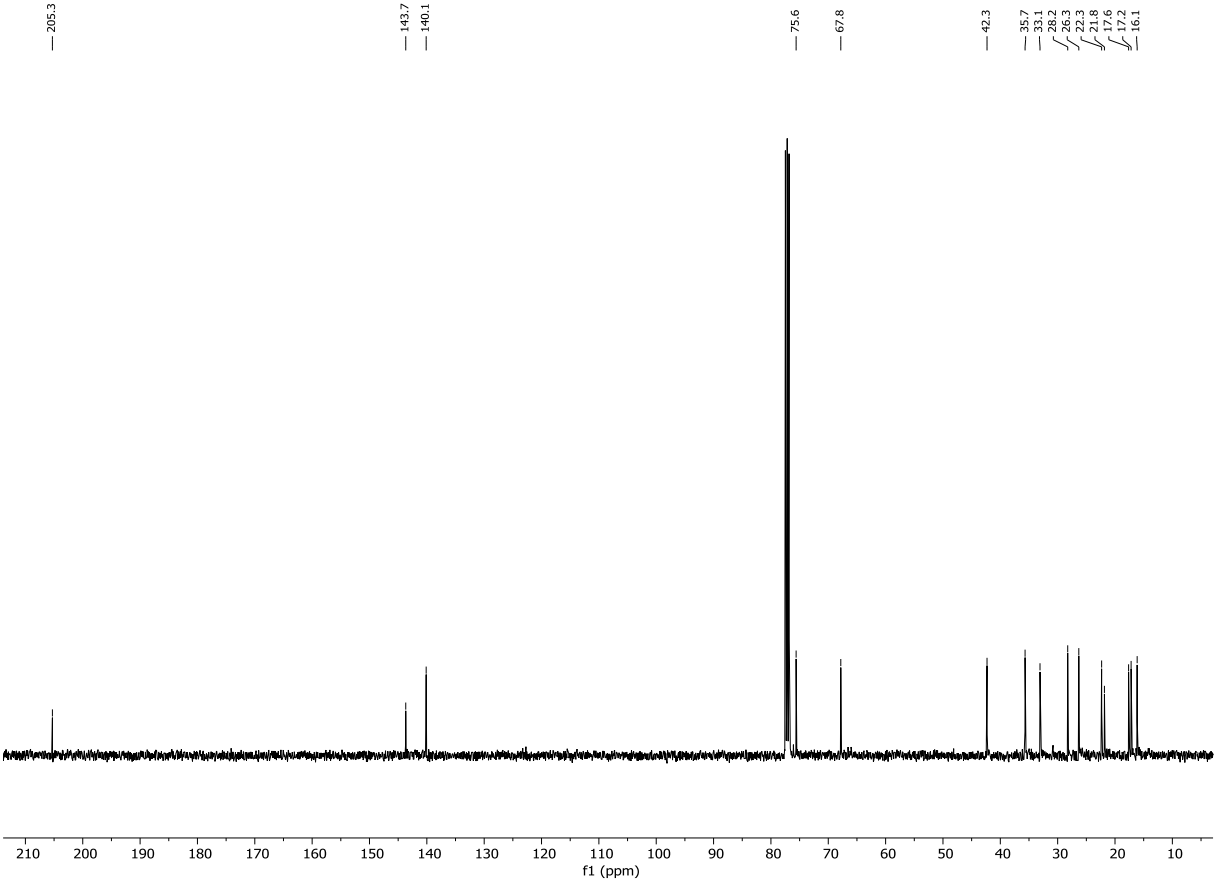
205.3
143.7
140.1
75.6
67.8
42.3
35.7
33.1
28.2
26.3
22.3
21.8
17.6
17.2
16.1
210 200 190 180 170 160 150 140 130 120 110 100 90 80 70 60 50 40 30 20 10
f1 (ppm)

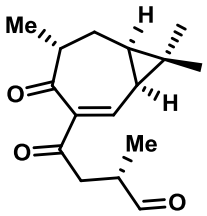
Me
H
O
H
O
Me
O

354

1.00
1.05
1.12
1.10
1.14
1.14
1.15
1.17
1.18
3.14
0.89
3.12
3.25
3.06
11.0 10.5 10.0 9.5 9.0 8.5 8.0 7.5 7.0 6.5 6.0 5.5 5.0 4.5 4.0 3.5 3.0 2.5 2.0 1.5 1.0 0.5 0.0
f1 (ppm)
207.9
203.5
197.0
144.4
143.4
46.1
41.9
40.9
28.1
27.1
26.7
24.9
24.0
15.7
15.0
13.7

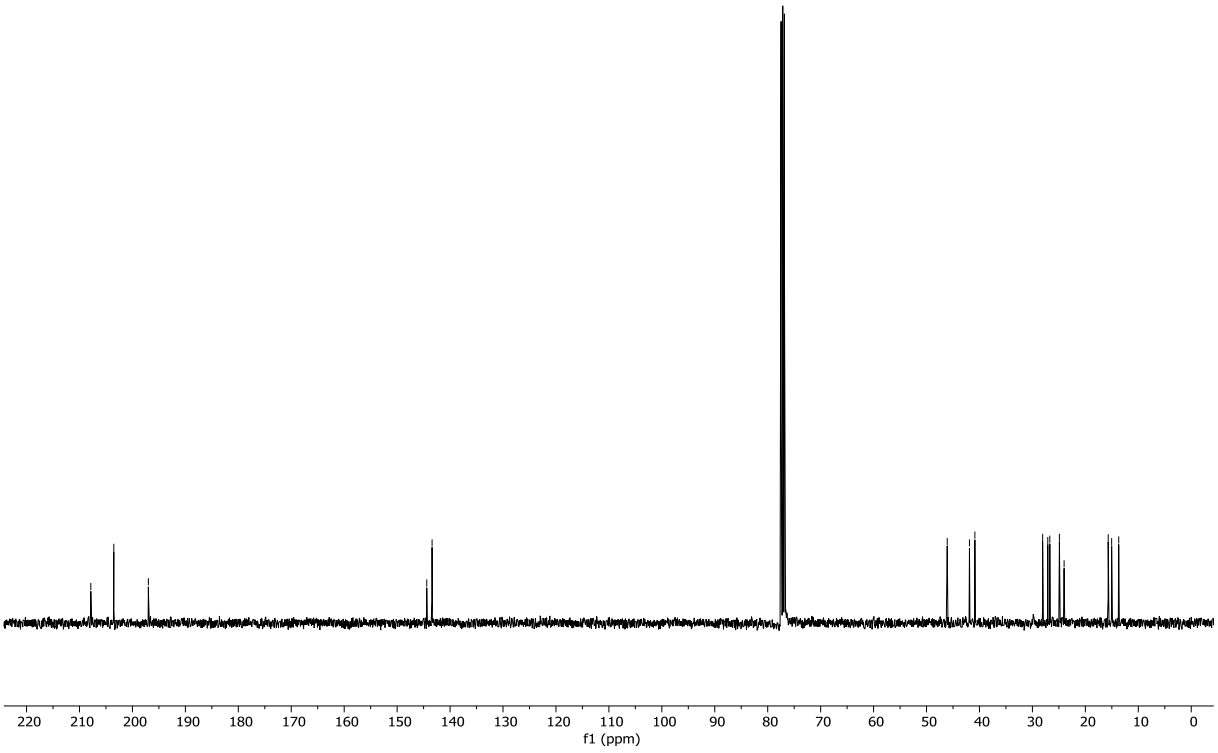
220 210 200 190 180 170 160 150 140 130 120 110 100 90 80 70 60 50 40 30 20 10 0
f1 (ppm)

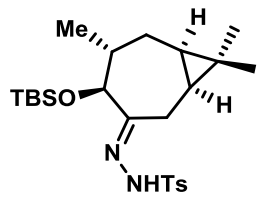
Me
H
TBSO
H
N
NHTs

355

2.09
0.80
2.14
0.85
3.06
1.08
1.18
1.04
2.37
6.15
9.03
3.00
2.03
2.91
3.00
10.0 9.5 9.0 8.5 8.0 7.5 7.0 6.5 6.0 5.5 5.0 4.5 4.0 3.5 3.0 2.5 2.0 1.5 1.0 0.5 0.0 -0.5
f1 (ppm)

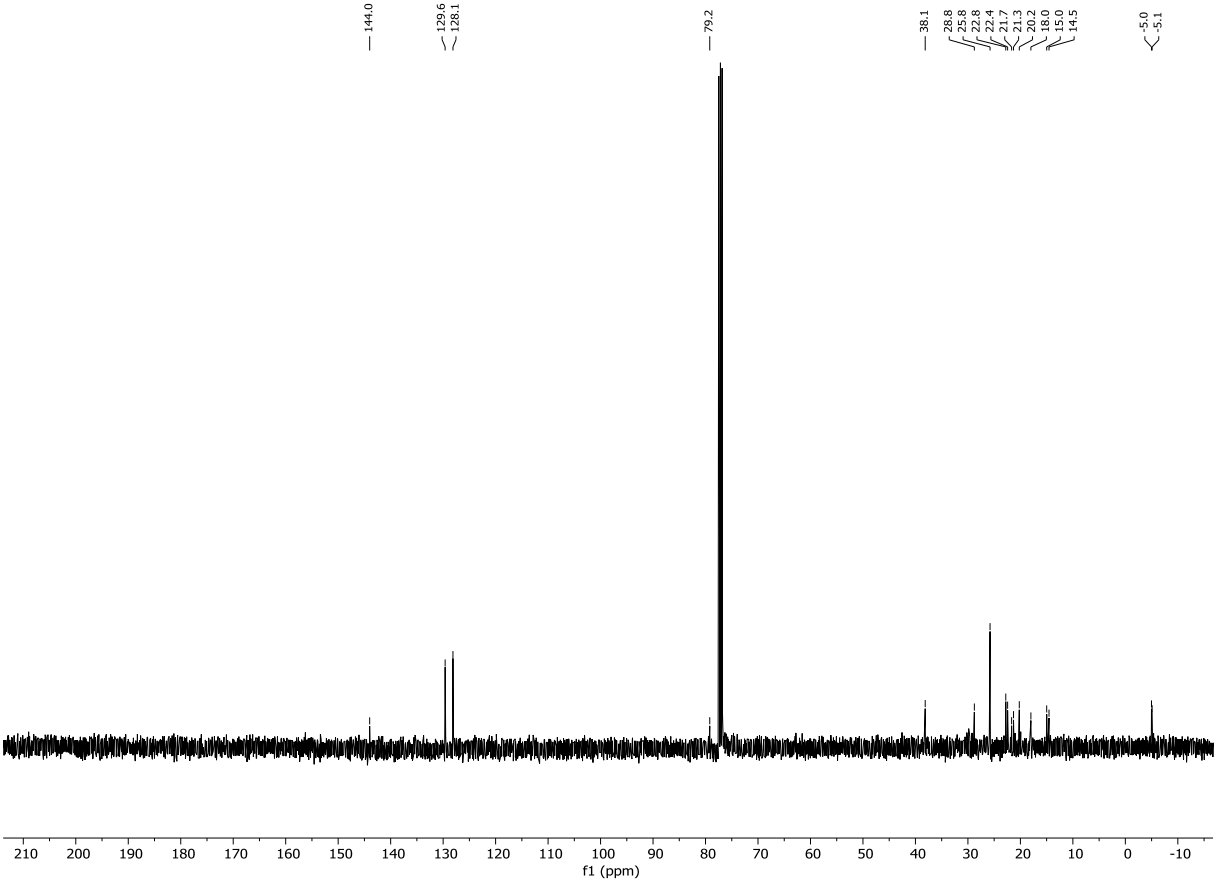
144.0
129.6
128.1
79.2
38.1
28.8
25.8
22.8
22.4
21.7
21.3
20.2
18.0
15.0
14.5
-5.0
-5.1
210 200 190 180 170 160 150 140 130 120 110 100 90 80 70 60 50 40 30 20 10 0 -10
f1 (ppm)

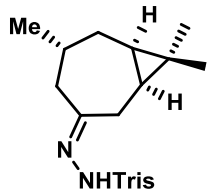
Me
H
H
N
NHTris

363

2.07
2.08
1.00
0.95
0.59
0.60
0.73
2.94
18.12
1.89
1.69
3.10
1.96
3.02
10.0 9.5 9.0 8.5 8.0 7.5 7.0 6.5 6.0 5.5 5.0 4.5 4.0 3.5 3.0 2.5 2.0 1.5 1.0 0.5 0.0
f1 (ppm)

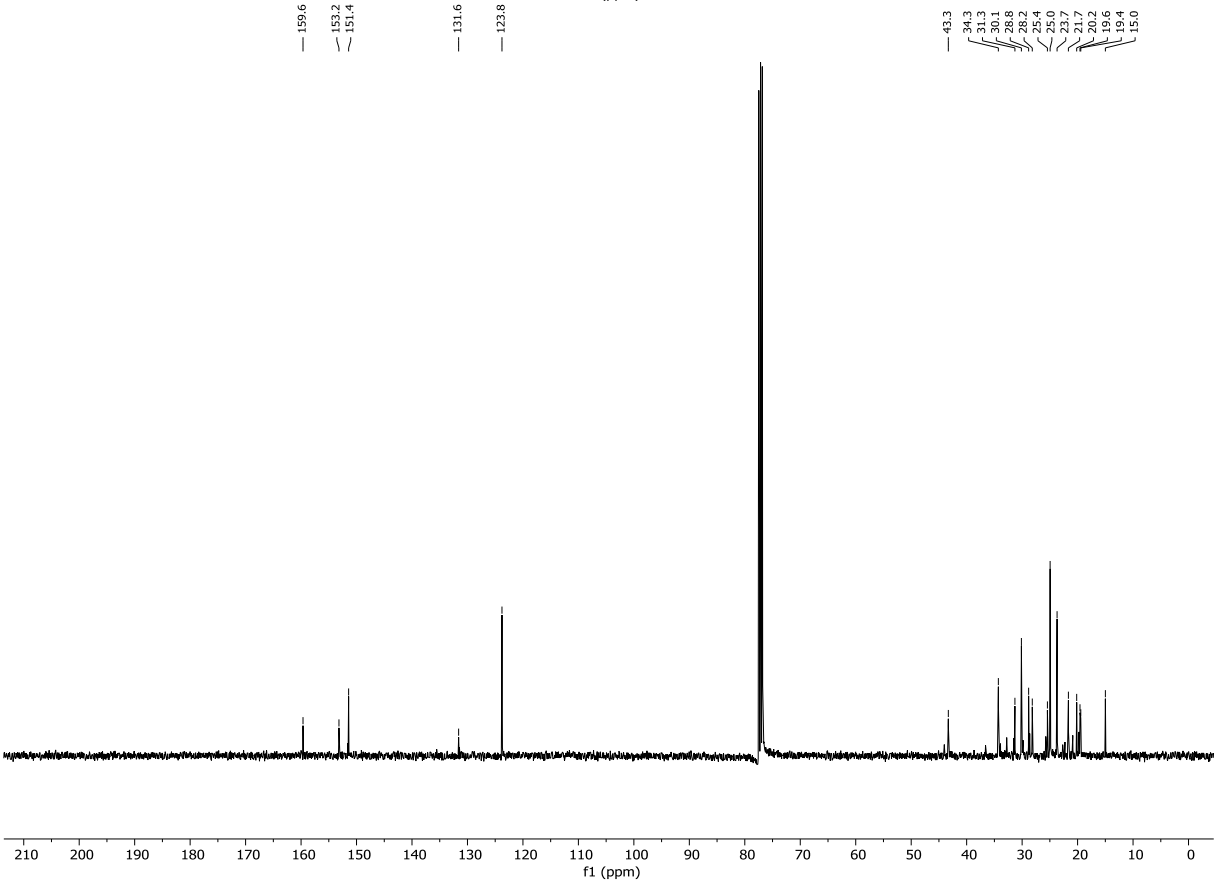
159.6
153.2
151.4
131.6
123.8
43.3
34.3
31.3
30.1
28.8
28.2
25.4
25.0
23.7
21.7
20.2
19.6
19.4
15.0
210 200 190 180 170 160 150 140 130 120 110 100 90 80 70 60 50 40 30 20 10 0
f1 (ppm)

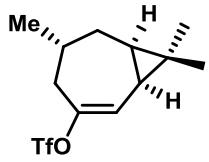
Me
H
H
TfO

371

1.00
1.13
1.13
1.17
1.22
2.14
6.00
3.13
1.13
10.0 9.5 9.0 8.5 8.0 7.5 7.0 6.5 6.0 5.5 5.0 4.5 4.0 3.5 3.0 2.5 2.0 1.5 1.0 0.5 0.0
f1 (ppm)

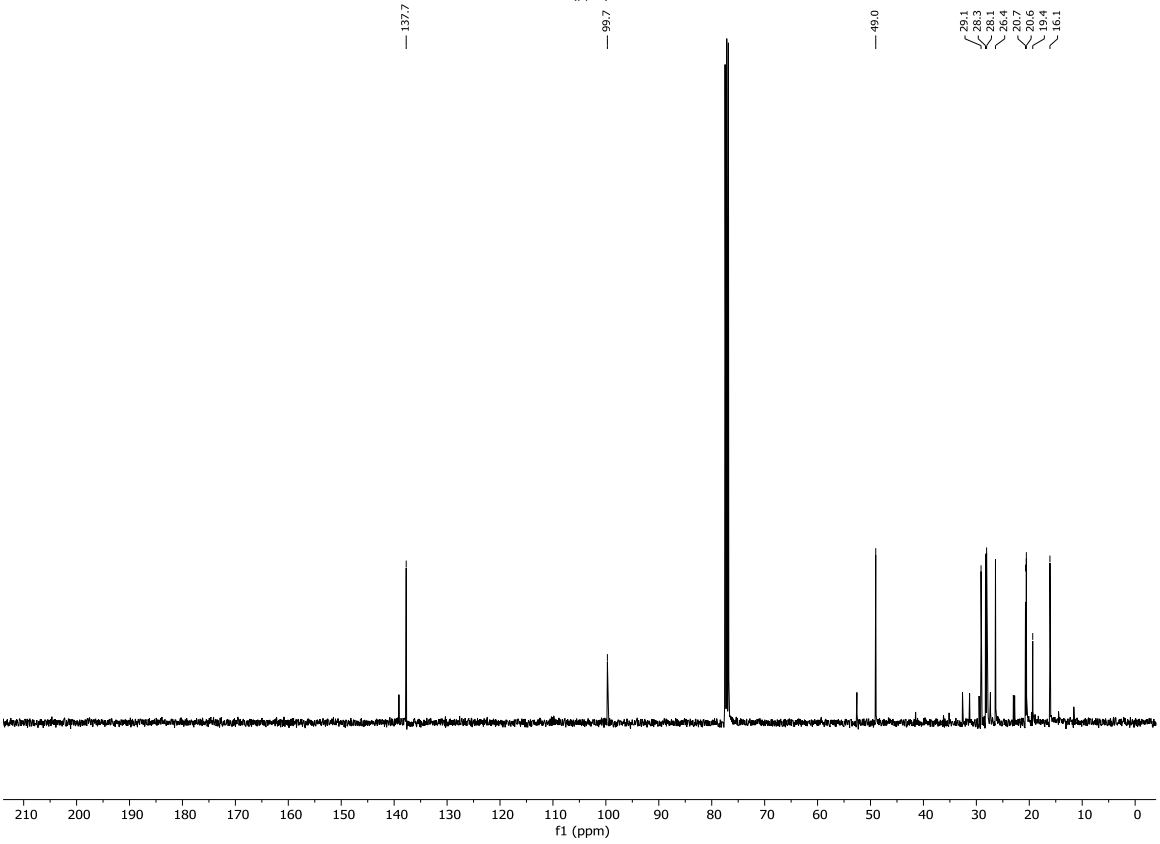
137.7
99.7
49.0
29.1
28.3
28.1
26.4
20.7
20.6
19.4
16.1
210 200 190 180 170 160 150 140 130 120 110 100 90 80 70 60 50 40 30 20 10 0
f1 (ppm)

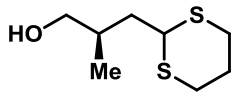
HO
Me
S
S

349

1.01
2.00
4.05
1.00
1.05
2.03
1.08
3.00
10.0 9.5 9.0 8.5 8.0 7.5 7.0 6.5 6.0 5.5 5.0 4.5 4.0 3.5 3.0 2.5 2.0 1.5 1.0 0.5 0.0
f1 (ppm)

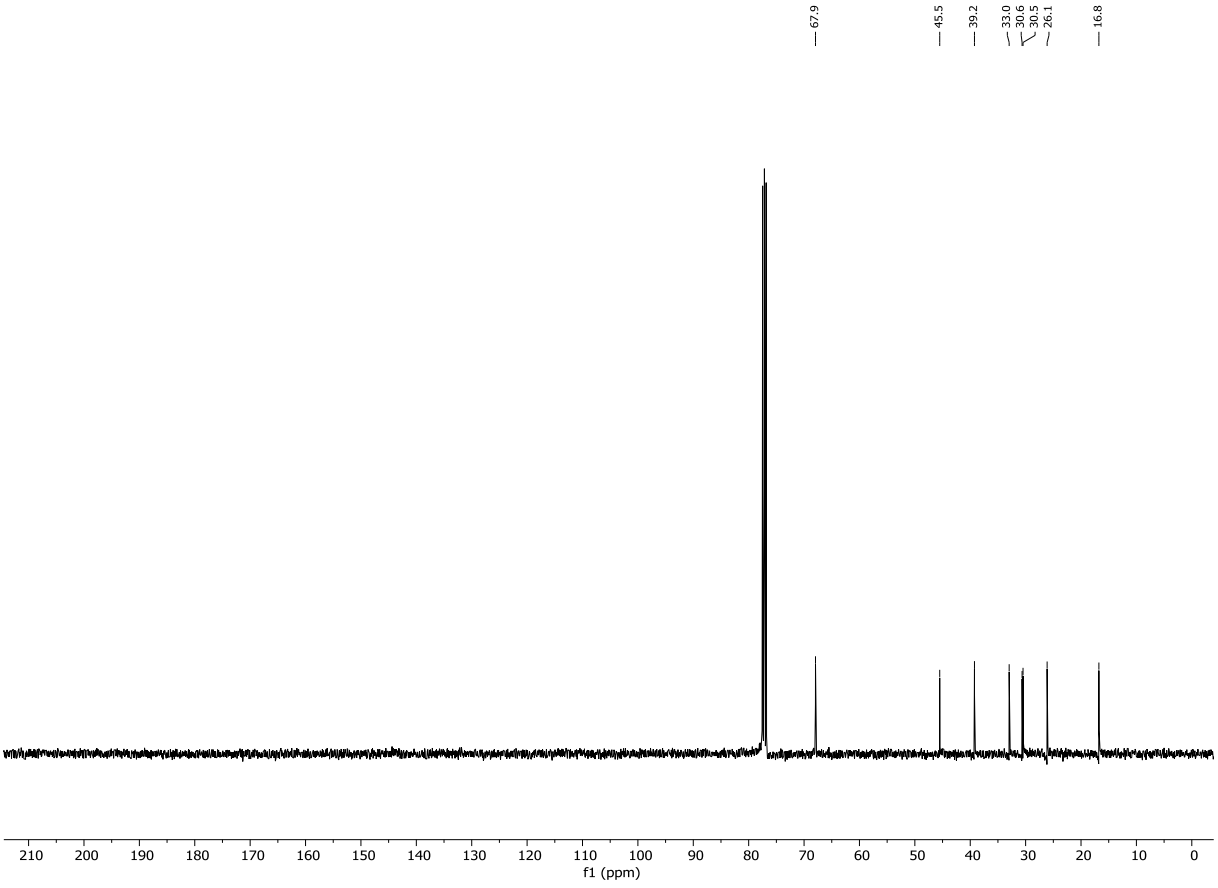
67.9
45.5
39.2
33.0
30.6
30.5
26.1
16.8
210 200 190 180 170 160 150 140 130 120 110 100 90 80 70 60 50 40 30 20 10 0
f1 (ppm)

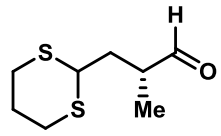
H
S
O
S
Me

350

1.00
1.00
4.03
1.02
1.04
1.07
1.06
1.04
3.10
10.0 9.5 9.0 8.5 8.0 7.5 7.0 6.5 6.0 5.5 5.0 4.5 4.0 3.5 3.0 2.5 2.0 1.5 1.0 0.5 0.0
f1 (ppm)
203.6
44.8
43.6
36.0
30.1
30.1
25.9
13.8

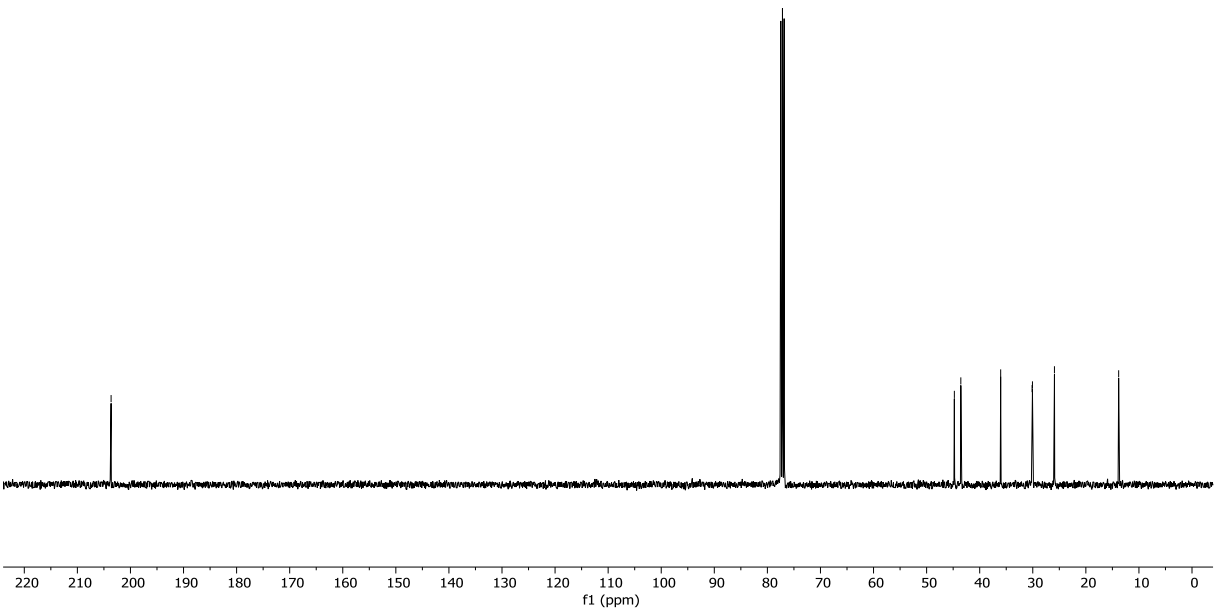
220 210 200 190 180 170 160 150 140 130 120 110 100 90 80 70 60 50 40 30 20 10 0
f1 (ppm)

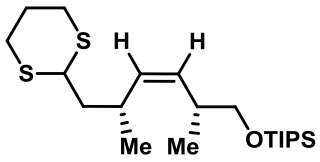
S
H
H
S
Me
Me
OTIPS

351

1.00
0.94
1.01
0.93
1.03
5.44
1.03
1.01
0.98
1.03
21.15
3.33
3.18
10.0 9.5 9.0 8.5 8.0 7.5 7.0 6.5 6.0 5.5 5.0 4.5 4.0 3.5 3.0 2.5 2.0 1.5 1.0 0.5 0.0
f1 (ppm)

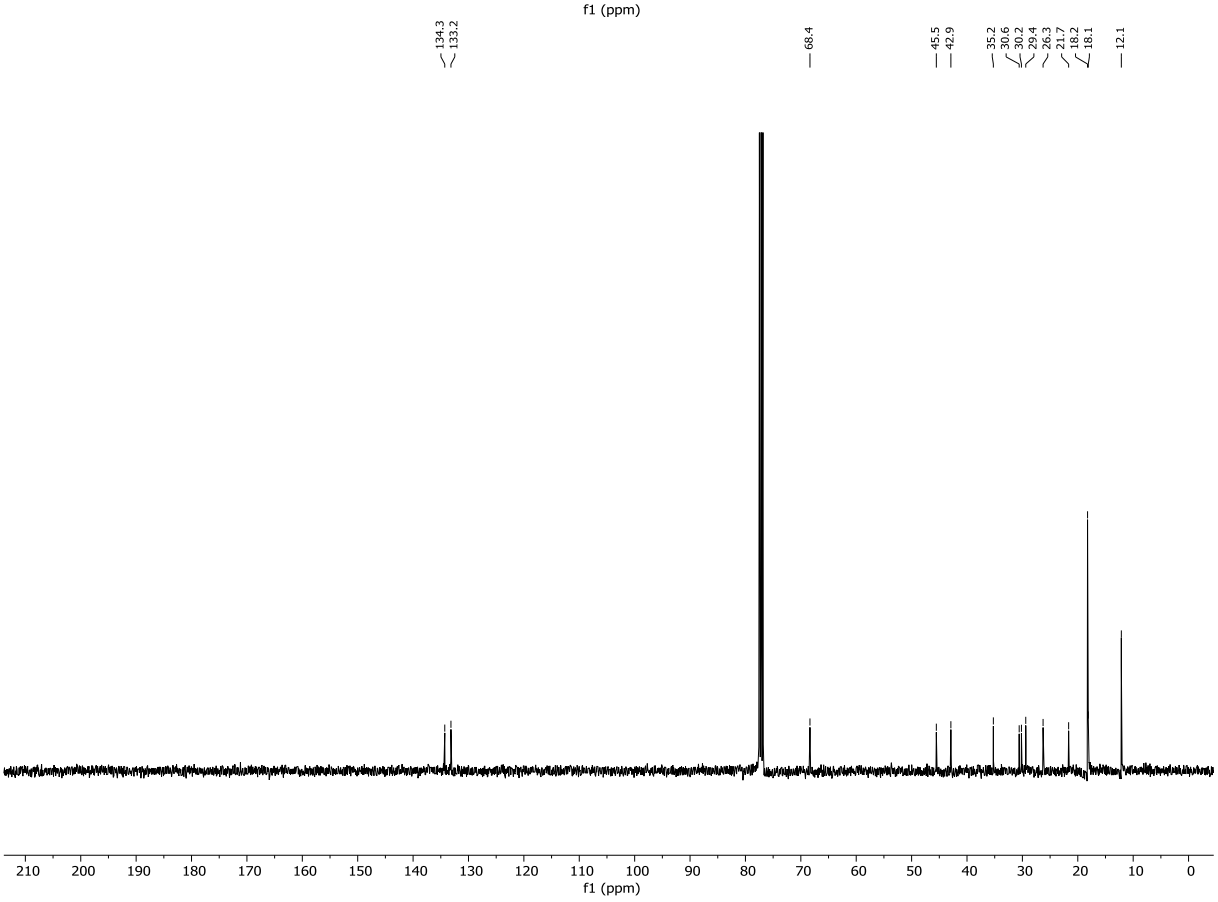
134.3
133.2
68.4
45.5
42.9
35.2
30.6
30.2
29.4
26.3
21.7
18.2
18.1
12.1
210 200 190 180 170 160 150 140 130 120 110 100 90 80 70 60 50 40 30 20 10 0
f1 (ppm)

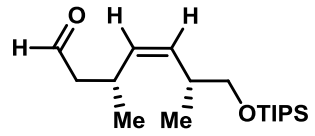
O
H
H
H
Me
Me
OTIPS

352

1.00
2.01
1.17
1.18
1.05
1.19
2.17
21.16
3.15
3.03
11.0 10.5 10.0 9.5 9.0 8.5 8.0 7.5 7.0 6.5 6.0 5.5 5.0 4.5 4.0 3.5 3.0 2.5 2.0 1.5 1.0 0.5 0.0
f1 (ppm)

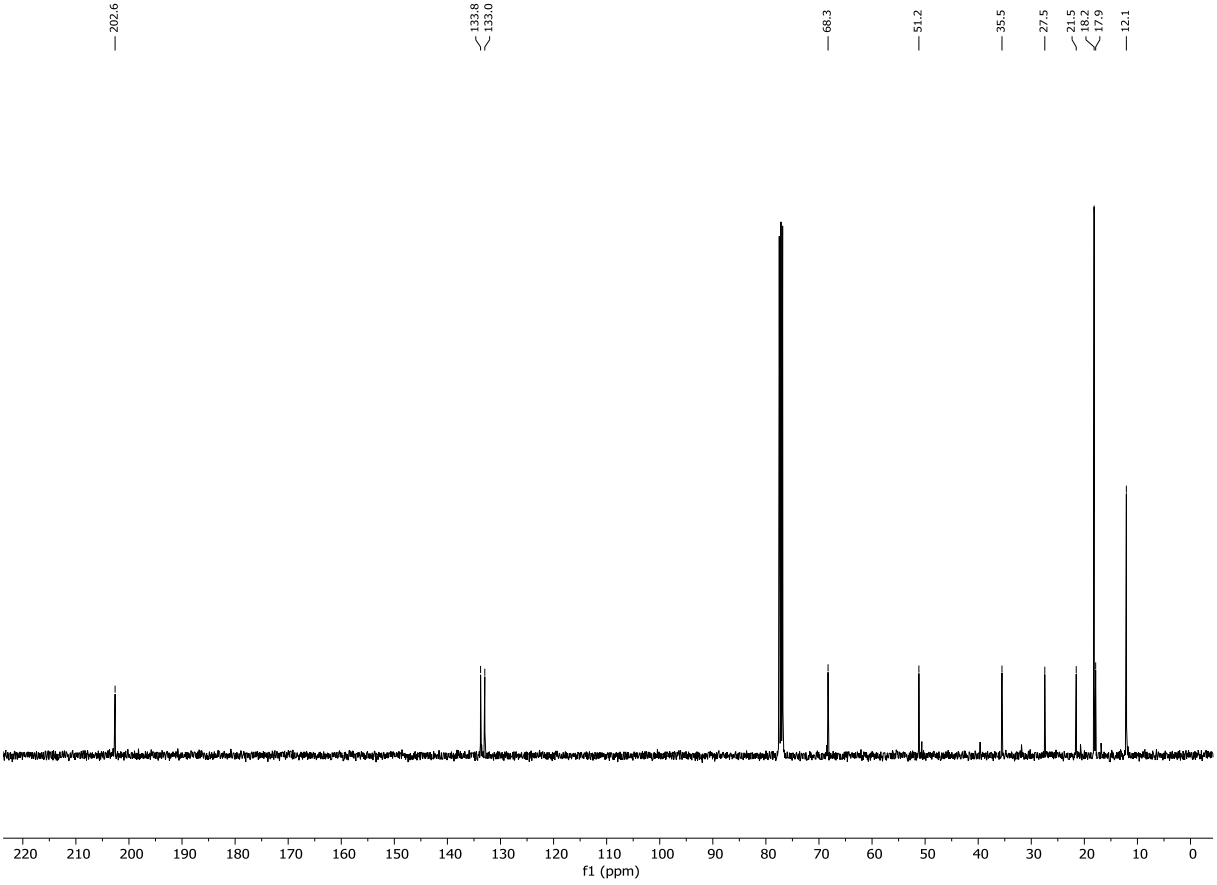
202.6
133.8
133.0
68.3
51.2
35.5
27.5
21.5
18.2
17.9
12.1
220 210 200 190 180 170 160 150 140 130 120 110 100 90 80 70 60 50 40 30 20 10 0
f1 (ppm)

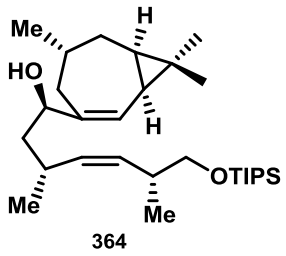
Me
H
HO
H
OTIPS
Me
Me

364

1.00
0.97
0.99
0.96
1.05
0.98
0.98
0.96
0.99
1.01
1.35
2.06
1.28
3.28
1.94
1.20
2.13
2.90
3.05
3.15
0.92
10.0 9.5 9.0 8.5 8.0 7.5 7.0 6.5 6.0 5.5 5.0 4.5 4.0 3.5 3.0 2.5 2.0 1.5 1.0 0.5 0.0
f1 (ppm)
144.3
136.4
132.1
121.9
75.8
68.5
43.3
35.6
33.1
29.9
28.0
24.9
22.3
22.0
20.2
18.2
17.7
16.1
12.1
210 200 190 180 170 160 150 140 130 120 110 100 90 80 70 60 50 40 30 20 10 0 -10
f1 (ppm)

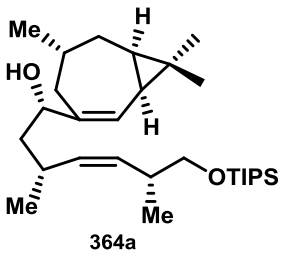
Me
H
HO
H
OTIPS
Me
Me

364a

1.00
1.04
0.97
0.92
1.11
1.13
2.10
1.01
1.15
1.17
2.22
3.29
2.06
26.21
3.08
2.92
2.91
1.08
f1 (ppm)

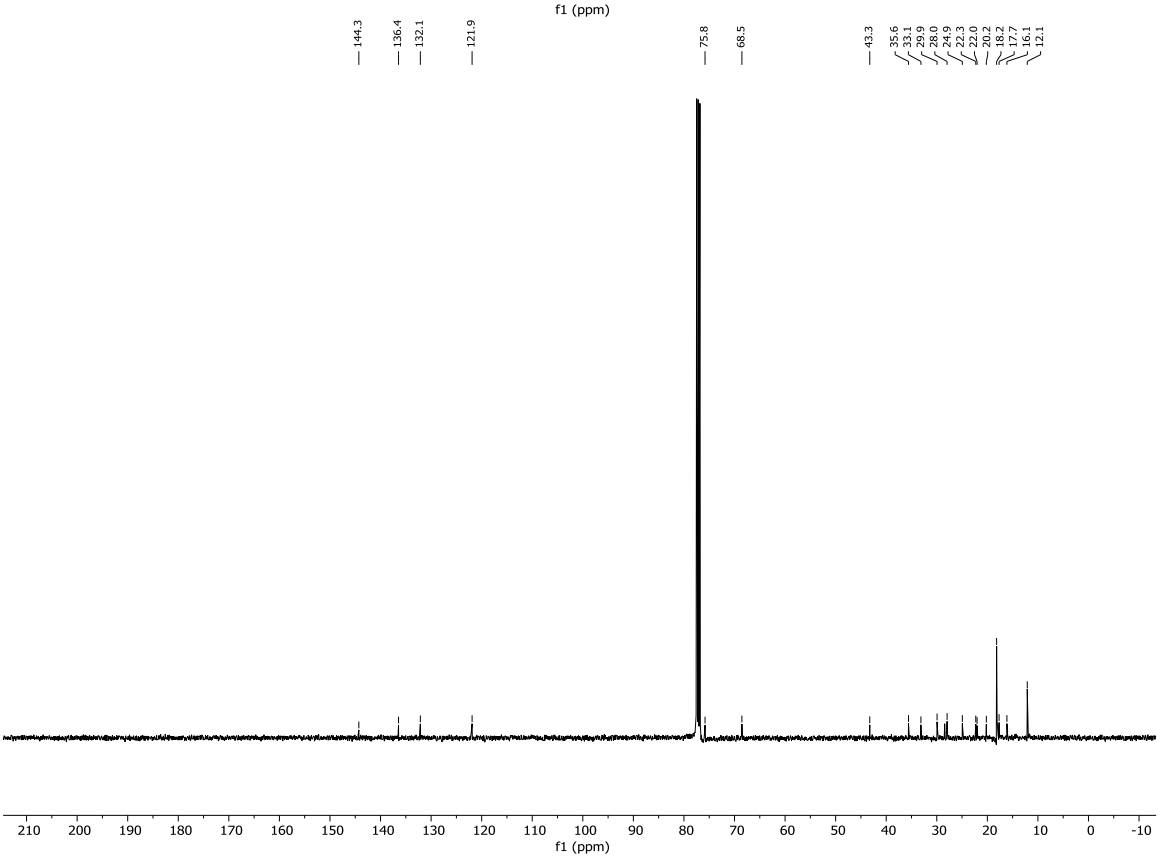
144.3
136.4
132.1
121.9
75.8
68.5
43.3
35.6
33.1
29.9
28.0
24.9
22.3
22.0
20.2
19.2
17.7
16.1
12.1
f1 (ppm)

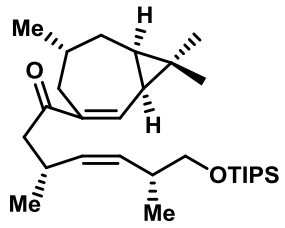
Me
H
O
H
OTIPS
Me
Me

373

0.94
0.92
0.92
1.01
1.01
1.00
0.99
1.03
2.01
1.09
1.12
1.13
3.08
2.14
24.02
3.05
3.09
3.06
1.06
1.05
10.0 9.5 9.0 8.5 8.0 7.5 7.0 6.5 6.0 5.5 5.0 4.5 4.0 3.5 3.0 2.5 2.0 1.5 1.0 0.5 0.0
f1 (ppm)

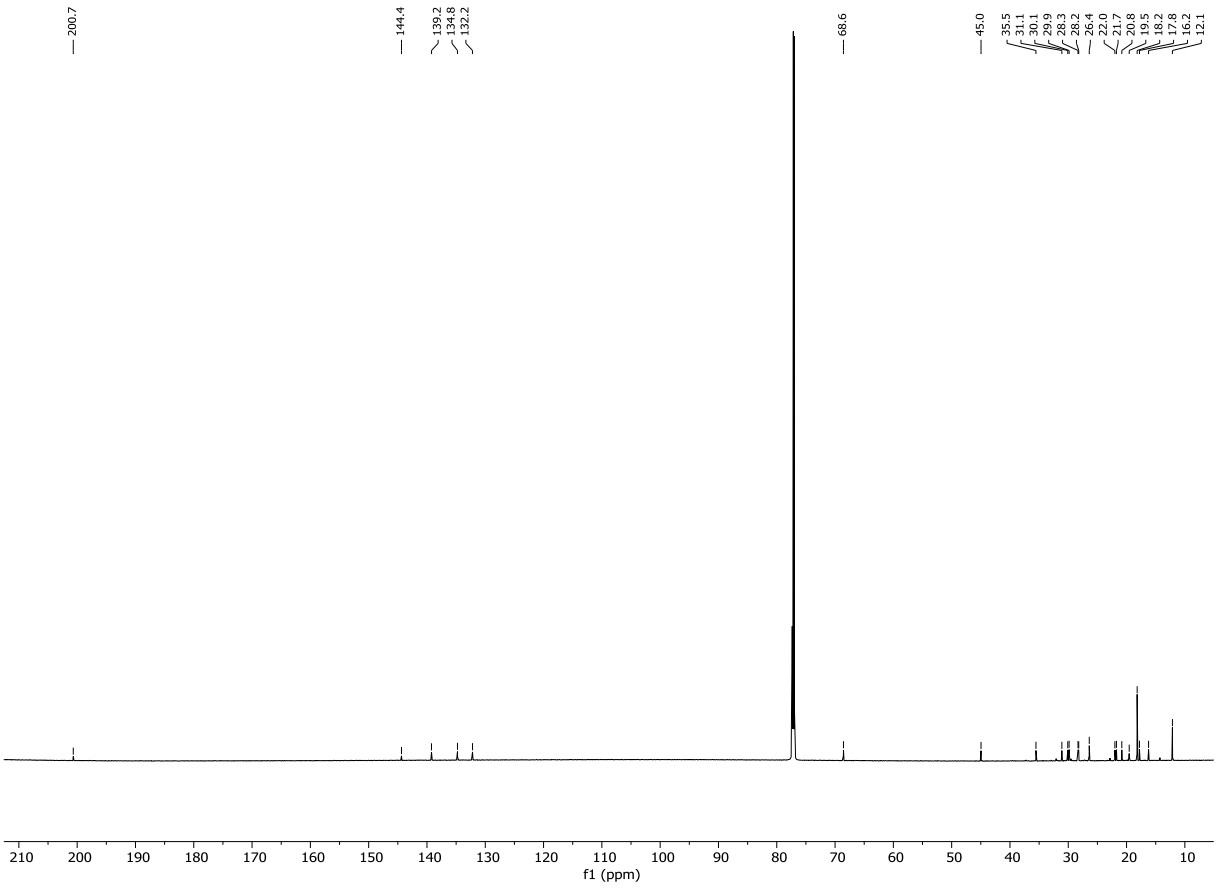
200.7
144.4
139.2
134.8
132.2
68.6
45.0
35.5
31.1
30.1
29.9
28.3
28.2
26.4
22.0
21.7
20.8
19.5
18.2
17.8
16.2
12.1
210 200 190 180 170 160 150 140 130 120 110 100 90 80 70 60 50 40 30 20 10
f1 (ppm)

3 Single Crystal X-ray Analysis

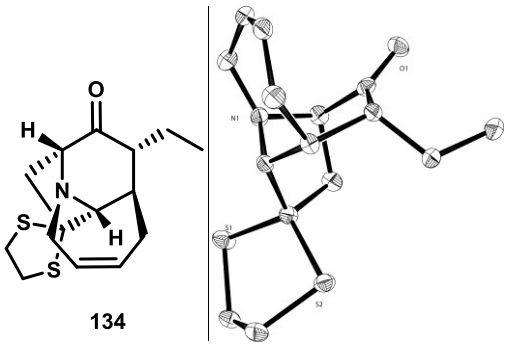

134

Table 21. Crystallographic data for olefin 134.

Empirical formula	$C_{15}H_{21}NOS_2$
Formula weight	295.46
Temperature	100(2) K
Wavelength	0.71073 Å
Crystal system	Orthorhombic
Space group	$P2_12_12_1$
Unit cell dimensions	a = 9.3373(10) Å
	b = 12.3300(16) Å
	c = 12.4027(19) Å
Volume	1427.9(3) $Å^3$
Z	4
Density (calculated)	1.374 Mg/m^3
Absorption coefficient	0.365 mm^{-1}
F(000)	632
Crystal size	0.450 x 0.236 x 0.160 mm^3
Theta range for data collection	2.329 to 27.353°.
Index ranges	-12<=h<=10, -15<=k<=15, -15<=l<=15
Reflections collected	18221
Independent reflections	3198 [R(int) = 0.1371]
Completeness to theta = 25.242°	100.0 %
Absorption correction	Integration
Max. and min. transmission	0.9482 and 0.9048
Refinement method	Full-matrix least-squares on F^2

Data / restraints / parameters	3198 / 0 / 173
Goodness-of-fit on F^2	0.971
Final R indices [I>2sigma(I)]	R1 = 0.0346, wR2 = 0.0762
R indices (all data)	R1 = 0.0402, wR2 = 0.0774
Absolute structure parameter	-0.02(6)
Extinction coefficient	n/a
Largest diff. peak and hole	0.322 and -0.224 e.Å^{-3}

Computing details:

Data collection: Bruker APEX2; cell refinement: Bruker SAINT; data reduction: Bruker SAINT; program used to solve structure: SHELXS97 (Sheldrick, 2008); program(s) used to refine structure: SHELXL2014/7 (Sheldrick, 2014).
CCDC number: 1874543.

Table 22. Atomic coordinates (x10^4) and equivalent isotropic displacement parameters (Å^{2}x 10^3) for olefin 134. U(eq) is defined as one third of the trace of the orthogonalized U^{ij} tensor.

	x	y	z	U(eq)
C(1)	9872(3)	2424(2)	2879(2)	18(1)
C(2)	8703(3)	1534(2)	3012(2)	20(1)
C(3)	7272(3)	2153(2)	2851(2)	18(1)
C(9)	9028(3)	3375(2)	2377(2)	15(1)
C(4)	6657(3)	4142(2)	3009(2)	24(1)
C(5)	6016(3)	4523(2)	1954(2)	25(1)
C(6)	6657(3)	4654(2)	1012(2)	24(1)
C(7)	8186(3)	4389(2)	717(2)	22(1)
C(8)	8740(3)	3302(2)	1154(2)	17(1)
C(10)	7707(3)	2377(2)	807(2)	17(1)
C(11)	6732(3)	1991(2)	1706(2)	18(1)
C(12)	8525(3)	1431(2)	258(2)	20(1)
C(13)	7577(3)	534(2)	-183(3)	26(1)
C(14)	12378(3)	2565(3)	4064(2)	25(1)
C(15)	12751(3)	2664(2)	2879(3)	27(1)
N(1)	7723(2)	3281(2)	3031(2)	18(1)
O(1)	5582(2)	1561(2)	1526(2)	24(1)
S(1)	10505(1)	2894(1)	4216(1)	25(1)

Table 23. Bond lengths [Å] and angles [°] for olefin 134.

C(1)-C(9)	1.544(4)
C(1)-C(2)	1.557(4)
C(1)-S(2)	1.812(3)
C(1)-S(1)	1.854(3)
C(2)-C(3)	1.552(4)
C(3)-N(1)	1.470(3)
C(3)-C(11)	1.520(4)
C(9)-N(1)	1.468(3)
C(9)-C(8)	1.543(3)
C(4)-N(1)	1.455(4)
C(4)-C(5)	1.514(4)
C(5)-C(6)	1.323(4)
C(6)-C(7)	1.509(4)
C(7)-C(8)	1.536(4)
C(8)-C(10)	1.554(4)
C(10)-C(11)	1.516(4)
C(10)-C(12)	1.552(4)
C(11)-O(1)	1.218(3)
C(12)-C(13)	1.519(4)
C(14)-C(15)	1.516(4)
C(14)-S(1)	1.805(3)
C(15)-S(2)	1.803(3)
C(9)-C(1)-C(2)	102.7(2)
C(9)-C(1)-S(2)	117.79(19)
C(2)-C(1)-S(2)	111.36(19)
C(9)-C(1)-S(1)	106.60(18)
C(2)-C(1)-S(1)	110.44(17)

S(2)-C(1)-S(1)	107.70(14)
C(3)-C(2)-C(1)	104.1(2)
N(1)-C(3)-C(11)	111.2(2)
N(1)-C(3)-C(2)	101.5(2)
C(11)-C(3)-C(2)	109.9(2)
N(1)-C(9)-C(8)	113.2(2)
N(1)-C(9)-C(1)	98.1(2)
C(8)-C(9)-C(1)	116.1(2)
N(1)-C(4)-C(5)	120.9(2)
C(6)-C(5)-C(4)	128.5(3)
C(5)-C(6)-C(7)	128.0(3)
C(6)-C(7)-C(8)	115.0(2)
C(7)-C(8)-C(9)	110.8(2)
C(7)-C(8)-C(10)	109.5(2)
C(9)-C(8)-C(10)	115.1(2)
C(11)-C(10)-C(12)	112.5(2)
C(11)-C(10)-C(8)	113.5(2)
C(12)-C(10)-C(8)	111.6(2)
O(1)-C(11)-C(10)	122.1(2)
O(1)-C(11)-C(3)	121.4(2)
C(10)-C(11)-C(3)	116.5(2)
C(13)-C(12)-C(10)	114.8(2)
C(15)-C(14)-S(1)	107.8(2)
C(14)-C(15)-S(2)	106.7(2)
C(4)-N(1)-C(9)	120.0(2)
C(4)-N(1)-C(3)	119.4(2)
C(9)-N(1)-C(3)	103.19(19)
C(14)-S(1)-C(1)	98.37(13)
C(15)-S(2)-C(1)	96.90(13)

Table 24. Anisotropic displacement parameters for olefin 134. The anisotropic displacement factor exponent takes the form: $-2\pi^2[h^2 a^{*2}U^{11} + ... + 2 h k a^* b^* U^{12}]$

	U^{11}	U^{22}	U^{33}	U^{23}	U^{13}	U^{12}
C(1)	17(1)	24(1)	12(1)	-2(1)	0(1)	0(1)
C(2)	20(1)	20(1)	21(1)	3(1)	-2(1)	-2(1)
C(3)	18(1)	20(1)	17(1)	2(1)	3(1)	-3(1)
C(9)	14(1)	17(1)	16(1)	-2(1)	0(1)	-2(1)
C(4)	22(1)	25(1)	25(1)	-7(1)	2(1)	4(1)
C(5)	21(1)	17(1)	37(2)	-7(1)	-6(1)	4(1)
C(6)	26(2)	14(1)	32(2)	0(1)	-11(1)	1(1)
C(7)	25(2)	18(1)	25(1)	5(1)	-4(1)	-1(1)
C(8)	18(1)	17(1)	14(1)	1(1)	1(1)	-3(1)
C(10)	16(1)	16(1)	17(1)	-1(1)	-2(1)	0(1)
C(11)	17(1)	13(1)	23(1)	1(1)	1(1)	2(1)
C(12)	18(1)	21(1)	21(1)	-5(1)	1(1)	1(1)
C(13)	23(2)	20(2)	34(2)	-8(1)	0(1)	2(1)
C(14)	18(1)	28(2)	29(1)	-3(1)	-8(1)	2(1)
C(15)	16(1)	32(2)	32(2)	-4(1)	3(1)	-3(1)
N(1)	17(1)	19(1)	18(1)	-3(1)	3(1)	-2(1)
O(1)	16(1)	28(1)	28(1)	-3(1)	0(1)	-5(1)
S(1)	19(1)	40(1)	16(1)	-4(1)	-2(1)	1(1)
S(2)	17(1)	26(1)	20(1)	-2(1)	1(1)	3(1)
C(1)	17(1)	24(1)	12(1)	-2(1)	0(1)	0(1)
C(2)	20(1)	20(1)	21(1)	3(1)	-2(1)	-2(1)

Table 25. Torsion angles [°] for olefin 134.

C(9)-C(1)-C(2)-C(3)	-13.8(2)
S(2)-C(1)-C(2)-C(3)	-140.82(19)
S(1)-C(1)-C(2)-C(3)	99.6(2)
C(1)-C(2)-C(3)-N(1)	-18.7(2)
C(1)-C(2)-C(3)-C(11)	99.1(2)
C(2)-C(1)-C(9)-N(1)	41.1(2)
S(2)-C(1)-C(9)-N(1)	163.92(17)
S(1)-C(1)-C(9)-N(1)	-75.03(19)
C(2)-C(1)-C(9)-C(8)	-79.7(3)
S(2)-C(1)-C(9)-C(8)	43.1(3)
S(1)-C(1)-C(9)-C(8)	164.14(18)
N(1)-C(4)-C(5)-C(6)	-38.8(4)
C(4)-C(5)-C(6)-C(7)	4.3(5)
C(5)-C(6)-C(7)-C(8)	42.7(4)
C(6)-C(7)-C(8)-C(9)	-73.9(3)
C(6)-C(7)-C(8)-C(10)	54.0(3)
N(1)-C(9)-C(8)-C(7)	79.6(3)
C(1)-C(9)-C(8)-C(7)	-168.0(2)
N(1)-C(9)-C(8)-C(10)	-45.2(3)
C(1)-C(9)-C(8)-C(10)	67.2(3)
C(7)-C(8)-C(10)-C(11)	-103.3(2)
C(9)-C(8)-C(10)-C(11)	22.2(3)
C(7)-C(8)-C(10)-C(12)	128.4(2)
C(9)-C(8)-C(10)-C(12)	-106.1(3)
C(12)-C(10)-C(11)-O(1)	-77.0(3)
C(8)-C(10)-C(11)-O(1)	155.2(2)

C(12)-C(10)-C(11)-C(3)	102.2(3)
C(8)-C(10)-C(11)-C(3)	-25.7(3)
N(1)-C(3)-C(11)-O(1)	-129.3(3)
C(2)-C(3)-C(11)-O(1)	119.1(3)
N(1)-C(3)-C(11)-C(10)	51.6(3)
C(2)-C(3)-C(11)-C(10)	-60.1(3)
C(11)-C(10)-C(12)-C(13)	55.7(3)
C(8)-C(10)-C(12)-C(13)	-175.4(2)
S(1)-C(14)-C(15)-S(2)	-49.4(2)
C(5)-C(4)-N(1)-C(9)	54.6(4)
C(5)-C(4)-N(1)-C(3)	-74.3(3)
C(8)-C(9)-N(1)-C(4)	-68.5(3)
C(1)-C(9)-N(1)-C(4)	168.5(2)
C(8)-C(9)-N(1)-C(3)	67.4(2)
C(1)-C(9)-N(1)-C(3)	-55.7(2)
C(11)-C(3)-N(1)-C(4)	66.4(3)
C(2)-C(3)-N(1)-C(4)	-176.8(2)
C(11)-C(3)-N(1)-C(9)	-69.9(3)
C(2)-C(3)-N(1)-C(9)	47.0(2)
C(15)-C(14)-S(1)-C(1)	30.2(2)
C(9)-C(1)-S(1)-C(14)	-127.81(19)
C(2)-C(1)-S(1)-C(14)	121.3(2)
S(2)-C(1)-S(1)-C(14)	-0.51(17)
C(14)-C(15)-S(2)-C(1)	44.8(2)
C(9)-C(1)-S(2)-C(15)	97.3(2)
C(2)-C(1)-S(2)-C(15)	-144.4(2)
S(1)-C(1)-S(2)-C(15)	-23.19(17)

4 References

[1] D. J. Newman, G. M. Cragg, *J. Nat. Prod.* **2016**, *79*, 629–661.

[2] G. A. Cordell, M. Lou Quinn-Beattie, N. R. Farnsworth, *Phyther. Res.* **2001**, *15*, 183–205.

[3] K. Suzuki, *J. Pharm. Soc. Jpn*. **1934**, *54*, 573-579.

[4] H. Greger, *Structural Classification and Biological Activities of Stemona Alkaloids*, Springer Netherlands, **2019**.

[5] W. Chanmahasathien, C. Ampasavate, H. Greger, P. Limtrakul, *Phytomedicine* **2011**, *18*, 199–204.

[6] B. Brem, C. Seger, T. Pacher, O. Hofer, S. Vajrodaya, H. Greger, *J. Agric. Food Chem.* **2002**, *50*, 6383–6388.

[7] R. A. Pilli, G. B. Rosso, M. da C. Ferreira de Oliveira, *Nat. Prod. Rep.* **2010**, *27*, 1908–1937.

[8] F. P. Wang, Q. H. Chen, *Nat. Prod. Commun.* **2014**, *9*, 1809–1822.

[9] H. Greger, *Planta Med.* **2006**, *72*, 99–113.

[10] R. W. Jiang, P. M. Hon, Y. Zhou, Y. M. Chan, Y. T. Xu, H. X. Xu, H. Greger, P. C. Shaw, P. P. H. But, *J. Nat. Prod.* **2006**, *69*, 749–754.

[11] S. Kongkiatpaiboon, J. Schinnerl, S. Felsinger, V. Keeratinijakal, S. Vajrodaya, W. Gritsanapan, L. Brecker, H. Greger, *J. Nat. Prod.* **2011**, *74*, 1931–1938.

[12] J. Schinnerl, B. Brem, P. P. H. But, S. Vajrodaya, O. Hofer, H. Greger, *Phytochemistry* **2007**, *68*, 1417–1427.

[13] S.-L. Li, R.-W. Jiang, P.-M. Hon, L. Cheng, H.-X. Xu, H. Greger, P. P.-H. But, P.-C. Shaw, *Biomed. Chromatogr.* **2007**, *21*, 1088–1094.

[14] C. Seger, K. Mereiter, E. Kaltenegger, T. Pacher, H. Greger, O. Hofer, *Chem. Biodivers.* **2004**, *1*, 265–279.

[15] H. Greger, J. Schinnerl, S. Vajrodaya, L. Brecker, O. Hofer, *J. Nat. Prod.* **2009**, *72*, 1708–1711.

[16] S. G. Pyne, A. T. Ung, A. Jatisatienr, P. Mungkornasawakul, *Maejo Int. J. Sci. Technol.* **2007**, *1*, 157–165.

[17] R. A. Pilli, G. B. Rosso, M. da C. Ferreira de Oliveira, *The Alkaloids*, Academic Press, **2005**.

[18] H. Shinozaki, M. Ishida, *Brain Res.* **1985**, *334*, 33–40.

[19] K. Sakata, K. Aoki, C. F. Chang, A. Sakurai, S. Tamura, S. Murakosm, *Agric. Biol. Chem.* **1978**, *42*, 457–463.

[20] S. Jiwajinda, N. Hirai, K. Watanabe, V. Santisopasri, N. Chuengsamarnyart, K. Koshimizu, H. Ohigashi, *Phytochemistry* **2001**, *56*, 693–695.

[21] B. Rinner, V. Siegl, P. Pürstner, T. Efferth, B. Brem, H. Greger, R. Pfragner, *Anticancer Res.* **2004**, *24*, 495–500.

[22] Y. Y. C. Q. Ke, Z. S. He, Y. P. Yang, *Chinese Chem. Lett.* **2003**, 173–175.

[23] J. E. Antoline, R. P. Hsung, J. Huang, Z. Song, G. Li, V. Uni, R. Hall, A. V Highland, *Org. Lett.* **2007**, *9*, 1275–1278.

[24] Z. H. Chen, J. M. Tian, Z. M. Chen, Y. Q. Tu, *Chem. - An Asian J.* **2012**, *7*, 2199–2202.

[25] C. K. G. Gerlinger, T. Gaich, *Chem. - A Eur. J.* **2019**, *25*, 10782–10791.

[26] S. B. Jones, B. Simmons, A. Mastracchio, D. W. C. MacMillan, *Nature* **2011**, *475*, 183–188.

[27] R. M. Wilson, S. J. Danishefsky, *J. Org. Chem.* **2007**, *72*, 4293–4305.

[28] E. Poupon, B. Nay, Eds. , *Biomimetic Organic Synthesis*, WILEY VCH Verlag, **2011**.

[29] C. K. G. Gerlinger, S. Krüger, T. Gaich, *Chem. - A Eur. J.* **2018**, *24*, 3994–3997.

[30] S. Krüger, T. Gaich, *Angew. Chem. Int. Ed. Engl.* **2015**, *54*, 315–317.

[31] H. Rebmann, C. K. G. Gerlinger, T. Gaich, *Chem. - A Eur. J.* **2018**, *25*, 2704–2707.

[32] V. K. Aggarwal, J. Drabowicz, R. S. Grainger, Z. Gültekin, M. Lightowler, P. L. Spargo, *J. Org. Chem.* **1995**, *60*, 4962–4963.

[33] A. P. Kozikowski, G. L. Araldi, R. G. Ball, *J. Org. Chem.* **1997**, *62*, 503–509.

[34] V. K. Aggarwal, R. S. Grainger, G. K. Newton, P. L. Spargo, A. D. Hobson, H. Adams, *Org. Biomol. Chem.* **2003**, *1*, 1884–1893.

[35] M. J. Sung, H. I. Lee, Y. Chong, J. K. Cha, *Org. Lett.* **1999**, *1*, 2017–2019.

[36] M. P. Smith, C. George, A. P. Kozikowski, *Tetrahedron Lett.* **1988**, *39*, 197–200.

[37] M. E. Jung, Z. Longmei, P. Tangsheng, Z. Huiyan, L. E. Yan, S. U. Jingyu, *J. Org. Chem.* **1992**, *57*, 3528–3530.

[38] Y. Zhang, L. S. Liebeskind, *J. Am. Chem. Soc.* **2006**, *128*, 465–472.

[39] E. R. Ashley, E. G. Cruz, B. M. Stoltz, *J. Am. Chem. Soc.* **2003**, *125*, 15000–15001.

[40] K. M. Peese, D. Y. Gin, *J. Am. Chem. Soc.* **2006**, *128*, 8734–8735.

[41] N. K. Garg, D. D. Caspi, B. M. Stoltz, *J. Am. Chem. Soc.* **2005**, *127*, 5970–5978.

[42] F. J. Sardina, M. H. Howard, M. Morningstar, H. Rapoport, *J. Org. Chem.* **1990**, *55*, 5025–5033.

[43] S. Krüger, Dissertation: The 3-Oxidopyridinium [5+2] Cycloaddition in the Total Synthesis of Alkaloids and Developement of a Diazo Insertion Based Strategy for the Formation of Hexahydrocyclohepta[b]indoles, Hannover, **2016**.

[44] B. H. Lipshutz, C. Hackmann, *J. Org. Chem.* **1994**, *59*, 7437.

[45] P. Knochel, M. C. P. Yeh, S. C. Berk, J. Talbert, *J. Org. Chem.* **1988**, *53*, 2390–2392.

[46] A. Krasovskiy, P. Knochel, *Angew. Chemie* **2004**, *116*, 3396–3399.

[47] D. J. Del Valle, M. J. Krische, *J. Am. Chem. Soc.* **2013**, *135*, 10986–10989.

[48] A. Vasas, J. Hohmann, *Chem. Rev.* **2014**, *114*, 8579–8612.

[49] J. T. Mwine, P. van Damme, *J. Med. Plants Res.* **2011**, *5*, 652–662.

[50] G. L. WEBSTER, *Bot. J. Linn. Soc.* **1987**, *94*, 3–46.

[51] R. E. SCHULTES, *Bot. J. Linn. Soc.* **1987**, *94*, 79–95.

[52] R. J. Schmidt, *Bot. J. Linn. Soc.* **1987**, *94*, 221–230.

[53] J. S. Dickschat, *Angew. Chemie* **2019**, *131*, 16110–16123.

[54] D. Luo, R. Callari, B. Hamberger, S. G. Wubshet, M. T. Nielson, J. Andersen-Ranberg, B. M. Hallstrom, F. Cozzi, H. Heider, B. Lindberg-Moller, et al., *Oxidation and Cyclization of Casbene in the Biosynthesis of Euphorbia Factors from Mature Seeds of Euphorbia Lathyris L*, Proceedings Of The National Academy Of Sciences Of The United States Of America, **2016**.

[55] M. L. Jorgensen, S. J. McKerrall, C. A. Kuttruff, F. Ungeheuer, J. Felding, P. S. Baran, *Science* **2013**, *341*, 878–882.

[56] A. J. King, G. D. Brown, A. D. Gilday, E. Forestier, T. R. Larson, I. A. Graham, *ChemBioChem* **2016**, 1593–1597.

[57] J. H. Wang, Y. J. Zhou, X. Bai, P. He, *Mol. Cells* **2011**, *32*, 451–457.

[58] H. Luo, A. Wang, *Can. J. Physiol. Pharmacol.* **2006**, *84*, 959–965.

[59] C. Valente, M. Pedro, A. Duarte, M. S. J. Nascimento Maria, P. M. Abreu, M. J. U. Ferreira, *J. Nat. Prod.* **2004**, *67*, 902–904.

[60] Q. W. Shi, X. H. Su, H. Kiyota, *Chem. Rev.* **2008**, *108*, 4295–4327.

[61] J. Hohmann, F. Evanics, G. Dombi, J. Molnár, P. Szabó, *Tetrahedron* **2001**, *57*, 211–215.

[62] S. Ghosh, M. Karin, *Cell* **2002**, *109*, 81–96.

[63] M. O. Fatope, L. Zeng, J. E. Ohayaga, G. Shi, J. L. McLaughlin, *J. Med. Chem.* **1996**, *39*, 1005–1008.

[64] Q. Le Dang, Y. H. Choi, G. J. Choi, K. S. Jang, M. S. Park, N. J. Park, C. H. Lim, H. Kim, L. H. Ngoc, J. C. Kim, *J. Asia. Pac. Entomol.* **2010**, *13*, 51–54.

[65] G. Sanchez-Duffhues, M. Q. Vo, M. Perez, M. A. Calzado, S. Moreno, G. Appendino, E. Munoz, *Curr. Drug Targets* **2012**, *12*, 348–356.

[66] I. Kissin, A. Szallasi, *Curr. Top. Med. Chem.* **2011**, *11*, 2159–2170.

[67] E. Hecker, *Cancer Res.* **1968**, *28*, 2338–2349.

[68] K. Tanino, K. Onuki, K. Asano, M. Miyashita, T. Nakamura, Y. Takahashi, I. Kuwajima, *J. Am. Chem. Soc.* **2003**, *125*, 1498–1500.

[69] A. Nickel, T. Maruyama, H. Tang, P. D. Murphy, B. Greene, N. Yusuff, J. L. Wood, *J. Am. Chem. Soc.* **2004**, *126*, 16300–16301.

[70] K. Watanabe, Y. Suzuki, K. Aoki, A. Sakakura, K. Suenaga, H. Kigoshi, *J. Org. Chem.* **2004**, *69*, 7802–7808.

[71] I. Kuwajima, K. Tanino, *Chem. Rev.* **2005**, *105*, 4661–4670.

[72] A. B. Smith, M. A. Guaciaro, S. R. Schow, P. M. Wovkulich, B. H. Toder, T. W. Hall, *J. Am. Chem. Soc.* **1981**, *103*, 219–222.

[73] A. B. Smith, B. D. Dorsey, T. Maeda, M. S. Malamas, M. Visnick, *J. Am. Chem. Soc.* **1986**, *108*, 3110–3112.

[74] J. Jakupovic, T. Morgenstern, M. Bittner, M. Silva, *Phytochemistry* **1998**, *47*, 1601–1609.

[75] ukwildflowers.com (17.01.2020), photograph and copyright by Peter Llewellyn.

[76] L. S. Wan, Y. Nian, C. J. Ye, L. D. Shao, X. R. Peng, C. A. Geng, Z. L. Zuo, X. N. Li, J. Yang, M. Zhou, et al., *Org. Lett.* **2016**, *18*, 2166–2169.

[77] L. S. Wan, Y. Nian, X. R. Peng, L. D. Shao, X. N. Li, J. Yang, M. Zhou, M. H. Qiu, *Org. Lett.* **2018**, *20*, 3074–3078.

[78] *Flora of China*, Sciene Press: Beijing, **1990**, *44*, 111.

[79] J. Xuan, Z. Liu, A. Zhu, P. Rao, L. Yu, H. Ding, *Angew. Chemie - Int. Ed.* **2017**, *56*, 8898–8901.

[80] P. G. Sammes, *Tetrahedron* **1976**, *32*, 405–422.

[81] C. Liebermann, *Berichte der Dtsch. Chem. Gesellschaft* **1877**, *10*, 2177–2179.

[82] S. Poplata, A. Tröster, Y. Q. Zou, T. Bach, *Chem. Rev.* **2016**, *116*, 9748–9815.

[83] G. Ciamician, P. Silber, *Berichte der Dtsch. Chem. Gesellschaft* **1908**, *41*, 1071–1080.

[84] G. Büchi, I. M. Goldman, *J. Am. Chem. Soc.* **1957**, *79*, 4741–4748.

[85] G. O. Schenck, W. Hartmann, S. -P Mannsfeld, W. Metzner, C. H. Krauch, *Chem. Ber.* **1962**, *95*, 1642–1647.

[86] P. E. Eaton, *J. Am. Chem. Soc.* **1962**, *84*, 2454–2455.

[87] W. Horspool, F. Lenci, Eds. , *Handbook of Organic Photochemistry and Photobiology*, CRC Press LLC, **2004**.

[88] R. G. Salomon, *Tetrahedron* **1983**, *39*, 485–575.

[89] B. Sylvie Le, P. Jean-Pierre, P. Olivier, *Tetrahedron Lett.* **1992**, *34*, 635–638.

[90] M. C. Pirrung, *J. Am. Chem. Soc.* **1981**, *103*, 82–87.

[91] M. Birch, G. Pattenden, *J. Chem. Soc. Chem. Commun.* **1980**, 1195–1197.

[92] T. Bach, A. Spiegel, *Synlett* **2002**, 1305–1307.

[93] A. Jana, S. Mondal, S. Ghosh, *Org. Biomol. Chem.* **2015**, *13*, 1846–1859.

[94] A. B. Smith, *J. Org. Chem.* **1987**, *52*, 5280–5283.

[95] L. Yu, H. Hu, F. Nan, S. Key, M. Medica, Z. H. Park, *J. Org. Chem.* **2011**, *76*, 1448–1451.

[96] K. Yamakawa, *Chem. Pharm. Bull.* **1984**, *32*, 1401–1410.

[97] M. M. Hansen, C. F. Bertsch, A. R. Harkness, B. E. Huff, D. R. Hutchison, V. V. Khau, M. E. LeTourneau, M. J. Martinelli, J. W. Misner, B. C. Peterson, et al., *J. Org. Chem.* **1998**, *63*, 775–785.

[98] M. Julia, J. M. Paris, *Tetrahedron Lett.* **1973**, *14*, 4833–4836.

[99] K. Prantz, J. Mulzer, *Chem. - A Eur. J.* **2010**, *16*, 485–506.

[100] P. R. Blakemore, W. J. Cole, P. J. Kocieński, A. Morley, *Synlett* **1998**, 26–28.

[101] P. Liu, E. N. Jacobsen, *J. Am. Chem. Soc.* **2001**, *123*, 10772–10773.

[102] P. R. Blakemore, *J. Chem. Soc. Perkin 1* **2002**, *2*, 2563–2585.

[103] M. Schlosser, K. F. Christmann, *Angew. Chemie* **1966**, 115–116.

[104] H. B. Tuong, B. Schaub, M. Schlosser, *Tetrahedron Lett.* **1985**, *26*, 311–314.

[105] D. M. Hodgson, T. Arif, *Org. Lett.* **2010**, *12*, 4204–4207.

[106] J. S. Oh, B. H. Kim, Y. G. Kim, *Tetrahedron Lett.* **2004**, *45*, 3925–3928.

[107] J. M. Lukesh, W. A. Donaldson, *Chem. Commun. (Camb).* **2005**, 110–112.

[108] D. F. Taber, P. V. Joshi, K. Kanai, *J. Org. Chem.* **2004**, *69*, 2268–2271.

[109] S. Teufel, Masterthesis: Synthetic Approach toward the " Euphorbia Lathyrane Diterpene " Skeleton, University of Konstanz, **2018**.

[110] E. J. Corey, G. T. Kwiatkowski, *J. Am. Chem. Soc.* **1966**, *88*, 5652–5656.

[111] T. Focken, S. Hanessian, *Beilstein J. Org. Chem.* **2014**, *10*, 1848–1877.

[112] T. Focken, X. Mi, R. Oza, B. Chen, D. Ritson, R. Beaudegnies, S. Hanessian, *J. Org. Chem.* **2010**, *75*, 5601–5618.

[113] E. J. Corey, D. E. Cane, *J. Org. Chem.* **1969**, *34*, 3053–3057.

[114] D. J. Rawlinson, G. Sosnovsky, *Synthesis* **1972**, *1*, 1–28.

[115] M. T. Reetz, A. Kindler, *J. Organomet. Chem.* **1995**, *502*, 5–7.

[116] A. J. Frontier, S. Raghavan, S. J. Danishefsky, *J. Am. Chem. Soc.* **2000**, *122*, 6151–6159.

[117] G. M. Rubottom, J. M. Gruber, *J. Org. Chem.* **1978**, *43*, 1599–1602.

[118] C. F. Thompson, T. F. Jamison, E. N. Jacobsen, *J. Am. Chem. Soc.* **2001**, *123*, 9974–9983.

[119] L. Zhu, C. Zhou, W. Yang, S. He, G. J. Cheng, X. Zhang, C. S. Lee, *J. Org. Chem.* **2013**, *78*, 7912–7929.

[120] S. Stanković, J. H. Espenson, *J. Org. Chem.* **1998**, *63*, 4129–4130.

[121] W. Adam, L. Hadjiarapoglou, V. Jäger, J. Klicić, B. Seidel, X. Wang, *Chem. Ber.* **1991**, *124*, 2361–2368.

[122] D. L. Comins, A. Dehghani, *Tetrahedron Lett.* **1992**, *33*, 6299–6302.

[123] V. P. Baillargeon, J. K. Stille, *J. Am. Chem. Soc.* **1986**, *108*, 452–461.

[124] J. Huang, L. Fang, J. Gong, C. Li, Z. Yang, *Tetrahedron* **2015**, *71*, 3720–3733.

[125] A. Deagostino, P. Larini, E. G. Occhiato, L. Pizzuto, C. Prandi, P. Venturello, *J. Org. Chem.* **2008**, *73*, 1941–1945.

[126] G. Sabitha, R. Srinivas, J. S. Yadav, *Synthesis* **2011**, 1484–1488.

[127] K. J. Lee, W. S. Lee, H. Yun, Y. J. Hyun, C. D. Seo, C. W. Lee, H. S. Lim, *Org. Lett.* **2016**, *18*, 3678–3681.

[128] L. A. Paquette, R. Guevel, S. Sakamoto, I. H. Kim In Ho, J. Crawford, *J. Org. Chem.* **2003**, *68*, 6096–6107.

[129] M. B. Herbert, R. H. Grubbs, *Angew. Chemie - Int. Ed.* **2015**, *54*, 5018–5024.

[130] B. K. Keitz, K. Endo, P. R. Patel, M. B. Herbert, R. H. Grubbs, *J. Am. Chem. Soc.* **2012**, *134*, 693–699.

[131] A. Krasovskiy, F. Kopp, P. Knochel, *Angew. Chemie - Int. Ed.* **2006**, *45*, 497–500.

[132] R. H. Shapiro, M. J. Heath, *J. Am. Chem. Soc.* **1967**, *89*, 5734–5735.

[133] R. J. Sharpe, J. S. Johnson, *J. Org. Chem.* **2015**, *80*, 9740–9766.

[134] Y. Okude, S. Hirano, T. Hiyama, H. Nozaki, *J. Am. Chem. Soc.* **1977**, *35*, 114.

[135] A. Gil, F. Albericio, M. Álvarez, *Chem. Rev.* **2017**, *117*, 8420–8446.

[136] D. P. Stamos, X. C. Sheng, S. S. Chen, Y. Kishi, *Tetrahedron Lett.* **1997**, *38*, 6355–6358.

[137] J. L. Hofstra, K. E. Poremba, A. M. Shimozono, S. E. Reisman, *Angew. Chemie - Int. Ed.* **2019**, *58*, 14901–14905.

[138] W. D. Wulff, G. A. Peterson, W. E. Bauta, K. S. Chan, K. L. Faron, S. R. Gilbertson, R. W. Kaesler, D. C. Yang, C. K. Murray, *J. Org. Chem.* **1986**, *51*, 277–279.

[139] B. Li, M. Driess, J. F. Hartwig, *J. Am. Chem. Soc.* **2014**, *136*, 6586–6589.

[140] L. You, X. T. Liang, L. M. Xu, Y. F. Wang, J. J. Zhang, Q. Su, Y. H. Li, B. Zhang, S. L. Yang, J. H. Chen, et al., *J. Am. Chem. Soc.* **2015**, *137*, 10120–10123.

[141] P. A. Bonvallet, E. M. Todd, Y. S. Kim, R. J. McMahon, *J. Org. Chem.* **2002**, *67*, 9031–9042.

[142] K. Komatsu, K. Tanino, M. Miyashita, *Angew. Chemie* **2004**, *116*, 4441–4445.

[143] A. M. Szpilman, D. M. Cereghetti, N. R. Wurtz, J. M. Manthorpe, E. M. Carreira, *Angew. Chemie - Int. Ed.* **2008**, *47*, 4335–4338.

5 List of Figures

6 List of Schemes

7 List of Tables

8 Acknowledgements

An erster Stelle möchte ich mich bei Prof. Dr. Tanja Gaich bedanken. Für die Aufnahme in deine Arbeitsgruppe und dass ich die letzten Jahre unglaublich viel lernen durfte. Danke, dass du mir stets die Freiheit gegeben hast mich weiter zu entwickeln, immer hinter mir gestanden hast und mich mit deiner schier unerschöpflichen Begeisterung für die Chemie immer wieder aufs Neue motiviertest. Ich konnte nicht nur fachlich, sondern auch menschlich vieles von dir lernen, danke dafür.

Mein Dank gilt ebenfalls meinem zweiten Betreuer dieser Doktorarbeit, Herrn Prof. Dr. Andreas Marx. Für die Übernahme des Prüfungsvorsitzes möchte ich herzlich Herrn Prof. Dr. Rainer Winter danken.

Für geduldiges Korrekturlesen dieser Arbeit möchte ich mich besonders bei Cedric Hugelshofer, Magnus Pfaffenbach und Michael Breunig bedanken.

Als ich nach Konstanz gekommen bin, wurde ich von den „alten Gaichis“ herzlich aufgenommen. Magnus Pfaffenbach danke ich für die Aufnahme im Bosslabor und für viele lehrreiche Weisheiten. Sebastian Krüger für dieses spannende Projekt, alle Unterstützung und gute Musik. Konstantin Samarin und Darius Schwarzer danke ich für die täglich gute Laune und die besondere musikalische Untermalung des Laboralltags. Christian Leitner für sein geradezu unerschöpfliches Wissen, Michael Breunig für seine unvergleichliche Art, Misha Kabdulov für lustige Anekdoten und Birte Schröder. Ich danke euch allen für eure Freundschaft und die schöne gemeinsame Zeit.

Mit der Zeit wuchs die Arbeitsgruppe zu den „neuen Gaichis“. Bei euch allen möchte ich mich besonders bedanken. Die tolle Arbeitsatmosphäre, zahlreiche und schöne AG-Ausflüge und dass ihr es immer wieder geschafft habt mich zu lustigen Abenden und allen möglichen Partys zu überreden, welche über so manchen Laborfrust hinweg geholfen haben. Danke an Heiko Rebmann, Simone Zanella, Johannes Bayer, Maximilian Häfner, Paul Gamerdinger, Lisa Rosenbaum, Till Vogel, Yevhenii Sokolenko, Lukas Holz, Wenbo Huang, Fabian Schneider, Po Yuan, Jun Tian, Benedikt Maier und Philipp Bruttel.

Während meiner Doktorarbeit durfte ich die Projekte einiger talentierter und motivierter Studenten betreuen: Hannah Baehr, Markus Kufleitner, Arne Aerts, Jochen Bohnacker, Philipp Bruttel und Johannes Zinngisser. Besonderer Dank geht hier an Sophia Teufel und Valentin Bruder, welche nicht nur einen wichtigen Beitrag zu dieser Dissertation geleistet haben, sondern auch den Laboralltag mit viel positiver Energie und guter Musik füllten.

Dem NMR-Team, bestehend aus Anke Friemel und Ulrich Haunz, möchte ich ganz herzlich für viele extra Messungen und vor allem für die Hilfe beim Interpretieren einiger kniffliger NMR´s danken.

Ohne die Mitarbeiter, die uns im Hintergrund organisatorisch unterstützen, wäre keine Doktorarbeit denkbar. Danke Thomas Huhn, für jegliche Hilfe am Computer, lustige und ausschweifende Diskussionen während den Mittagspausen und dein stets sonniges Gemüt. Danke Angelika Früh, für deine tolle Unterstützung bezüglich allem was das Labor und Praktikum angeht und für dein immer offenes Ohr, dass du für mich hattest. Danke an Malin Bein, für deine Organisation und deine immer zuverlässige Hilfe bei allerlei Messungen. Danke auch an Milena Quentin, für all deine Unterstützung und Organisation der Arbeitsgruppe.

Ein ganz besonderer Dank geht an meine Freunde außerhalb des Labors: Florentine Hartmann, Christina Kaufmann, Alina Demmel, Sophia Teufel, Marisa Ferch, Alice Zimmermann, Julia Bumba und Lara Weisheit. Danke, dass ihr mich die letzten vier Jahre begleitet und es in schwierigen und oft frustrierenden Zeiten immer wieder geschafft habt, mich auf eure besondere Weise aufzubauen, abzulenken und zu motivieren. Ich verdanke euch sehr viel.

Meiner Familie möchte ich von ganzem Herzen für die unermüdliche Unterstützung in jeglicher Hinsicht in den letzten Jahren danken. Besonders meinem Bruder Roland und seiner Frau Polina, meinem Vater Richard und vor allem auch meiner Tante Johanna und meiner Cousine Hermina. Mein größter Dank jedoch, gilt meiner Mutter. Dafür, dass du in jeder Situation die richtigen Worte findest um mich zum Lachen zu bringen und wieder aufzumuntern. Danke, dass du uneingeschränkt hinter (fast) jeder meiner Entscheidungen stehst und ich immer auf dich zählen kann.

Zuletzt gilt mein Dank dir, Marcel. Es war eine intensive Zeit, mit vielen Erlebnissen, zahlreichen tollen Erinnerungen, aber auch einigen Phasen des Zweifels und des Frusts. Danke, dass du mich trotz allem während der letzten zehn Jahre meiner Ausbildung begleitet hast. Danke dass du mir immer den Rücken frei gehalten und mir vor allem immer wieder den Mut gegeben hast weiterzumachen.

„Und dann muss man ja auch noch Zeit haben, einfach dazusitzen und vor sich hin zu schauen.“

Astrid Lindgren